STRUCTURAL STUDIES OF CRYSTALS WITH INTERACTING COMPONENTS

Miss Weenawan Somphon

A Thesis Submitted in Partial Fulfillment of the Requirements for

the Degree of Doctor of Philosophy in Chemistry

Suranaree University of Technology

Academic Year 2004

ISBN 974-533-422-7

การศึกษาโครงสร้างผลึกที่มีองค์ประกอบซึ่งมีอันตรกิริยาต่อกัน

นางสาววีนาวรรณ สมผล

วิทยานิพนธ์นี้เป็นส่วนหนึ่งของการศึกษาตามหลักสูตรปริญญาวิทยาศาสตรดุษฎีบัณฑิต

สาขาวิชาเคมี

มหาวิทยาลัยเทคโนโลยีสุรนารี

ปีการศึกษา 2547

ISBN 974-533-422-7

STRUCTURAL STUDIES OF CRYSTALS WITH INTERACTING COMPONENTS

Suranaree University of Technology has approved this thesis submitted in partial fulfillment of the requirements for the Degree of Doctor of Philosophy.

Thesis Examining Committee

(Asst. Prof. Dr. Malee Tangsathitkulchai)

Chairperson

(Assoc. Prof. Dr. Kenneth J. Haller)

Member (Thesis Advisor)

(Prof. Dr. A. David Rae)

Member

(Assoc. Prof. Dr. Ian D. Williams)

Member

(Dr. Sutham Srilomsak)

Member

(Assoc. Prof. Dr. Sarawut Sujitjorn)

Vice Rector for Academic Affairs

(Assoc. Prof. Dr. Prasart Suebka)

Dean of Institute of Science

วีนาวรรณ สมผล : การศึกษาโครงสร้างผลึกที่มีองค์ประกอบซึ่งมีอันตรกิริยาต่อกัน (STRUCTURAL STUDIES OF CRYSTALS WITH INTERACTING COMPONENTS) อาจารย์ที่ปรึกษา : รองศาสตราจารย์ ดร. เค็นเนท เจ. แฮลเลอร์, 262 หน้า. ISBN 974-533-422-7

วิทยานิพนธ์ฉบับนี้ได้รวบรวมการยอมรับและการสืบสาวของโครงสร้างผลึกที่มีปัญหาซึ่งต้องการแบบจำลองนวัตกรรม เพื่อสามารถพอที่จะนำมาอธิบายโครงสร้าง และทำให้สละสลวยขึ้น โครงสร้างที่ศึกษา ได้แก่ ความสมมาตรเทียม ความไม่เป็นระเบียบของผลึก ผลึกเชิงคู่ โครงสร้างสารผลึก โครงสร้างที่มีการกลำ้ การแพร่กระเจิง และสถานภาคเฟส การแยกปัญหาให้ชัดเจนขึ้นอยู่กับความยากของปัญหา ที่ต้องการความพึงพอใจของวิธีข้อมูลทางโครงสร้างคือการกระจายตัวในข้อมูลการกระเจิงเลี้ยวเบน และใช้วิธีการทำให้สละสลวยซึ่งตัวแปรเสริมต้องเป็นที่ยอมรับเป็นความสำคัญ และสิ่งเหล่านั้นเป็นสิ่งเล็กน้อยที่ทำให้เกิดผลสำเร็จบนแบบรูปการเลี้ยวเบนแสง

โครงสร้างผลึกที่มีพฤติกรรมของปรากฏการณ์ชนิดที่น่าสนใจศึกษา ในการหาโครงสร้างที่น่าเชื่อถือในระหว่างผลเฉลยโครงสร้างและการทำให้ชัดเจนและเชื่อถือได้ ได้แก่ (i) โครงสร้างสารผลึก $[SnCl_2(C_2H_4COOH)(C_2H_4COO)]^-\cdot[C_{12}H_9N_2]^+$, (ii) ความสมมาตรเทียมและระบบการสะท้อนที่ไม่คมชัดใน $[Mg(H_2O)_6](NO_3)_2\cdot 2HMT\cdot 4H_2O$, (iii) การสะท้อนที่พิเศษของ $PS(C_2H_5)_3$, (v) โครงสร้างเชิงคู่รวมไปถึงการเหลื่อมลำ้บางส่วนและอย่างสมบูรณ์ของความเข้มในการเลี้ยวเบนแสงใน $[M(H_2O)_6]I_2\cdot 2HMT\cdot 4H_2O]$, เมื่อ M = Ni และ Mn, (v) โครงสร้างการกลำ้ที่ได้สัดส่วนกันของ $\{[Cu(bipy)]_2SO_4\cdot TPA\}_n$, และ (vi) โครงสร้างที่อุณหภูมิสูง ต่ำ ซึ่งเหมาะสมในการเปลี่ยนแปลงอันดับที่เป็นระเบียบ-ไม่เป็นระเบียบของผลึกของ $[Ag(bipy)NO_3]_n$ และเหตุผลสำหรับการสังเกตการแพร่กระเจิงของรูปแบบที่ไม่เป็นระเบียบ

สาขาวิชาเคมี
ปีการศึกษา 2547

ลายมือชื่อนักศึกษา W. Sumphon
ลายมือชื่ออาจารย์ที่ปรึกษา Kenneth J. Haller

WEENAWAN SOMPHON : STRUCTURAL STUDIES OF CRYSTALS WITH INTERACTING COMPONENTS. THESIS ADVISOR : ASSOC. PROF. KENNETH J. HALLER, Ph.D. 262 PP. ISBN 974-533-422-7

STRUCTURE MODULATION/POLYMORPHISM/POLYTYPISM/ TWINNING PHASE TRANSITION/SUPRAMOLECULAR STRUCTURE

This thesis is focused on the recognition and investigation of problem crystal structures that require innovative modeling for adequate structure description and refinement. The structures studied were associated with pseudo symmetry, disorder, twinning, polytypes, structure modulation, diffuse scattering, and phase transitions. Resolution of the inherent difficulties required an appreciation of how structural information is distributed in diffraction data and used refinement techniques that recognized which parameters are important and those that had little effect on the diffraction pattern.

Crystal structures that exhibited phenomena which posed particular challenges during structure solution and refinement were (i) the polytypism of $[SnCl_2(C_2H_4CO_2H)(C_2H_4CO_2)]^-\cdot[C_{12}H_9N_2]^+$, (ii) the pseudo symmetry and systematically weak reflections in $[Mg(H_2O)_6](NO_3)_2\cdot 2HMT\cdot 4H_2O$, (iii) the extra reflections of $PS(C_2H_5)_3$, (iv) the twinning including partial and perfect overlap of diffraction intensities in $[M(H_2O)_6]I_2\cdot 2HMT\cdot 4H_2O]$, where M = Ni and Mn, (v) the commensurately modulated structure of $\{[Cu(bipy)]_4(SO_4)_2\cdot 2(TPA)\}_n$, and (vi) the high and low temperature structures involved in an order-disorder transformation of crystallized $[Ag(bipy)NO_3]_n$ and the reason for the observed diffuse scattering of the disordered form.

School of Chemistry

Academic Year 2004

Student's Signature W. Somphon

Advisor's Signature Kenneth J. Haller

ACKNOWLEDGEMENTS

Firstly, I would like to express my gratitude to my supervisor, Assoc. Prof. Dr. Kenneth J. Haller for his guidance and patience during this research. In doing research with him, his expertise in chemistry and crystallography has helped to elevate my understanding of technical issues to higher levels. I am indebted not just for his scientific contribution but also for his motivating words, day after day, his help, the opportunities he has created, and his friendship.

I am extremely grateful to my coadvisor, Prof. Dr. A. David Rae for his constant enthusiasm and guidance and for all his intensive proofreading of this thesis and his continuous streams of ideas which opened many avenues for study. He is an excellent crystallographer and taught me deep advance crystallography. Thanks to his least squares refinement program, RAELS.

I also appreciate and admire to Annas Rae, his wife, for her help in taking care of me while I was in Australia, and thank her for her special role as a stand-in mother figure. I also thank Prof. Dr. Ray Withers for organizing the solid state group at The Research School of Chemistry, The Australian National University.

I have been fortunate to have a great thesis committee consisting of excellent scholars with diverse backgrounds. I am thankful to the members of my committee, Asst. Prof. Dr. Malee Tangsathitkulchai (chairperson) and Dr. Sutham Srilomsak, for their invaluable contributions which increased the quality of my writing. I would also like to thank the staff of Suranaree University of Technology's School of Chemistry.

I am most grateful to The Royal Golden Jubilee (RGJ) Ph.D. Scholarship Program of The Thailand Research Fund for giving me the opportunity to pursue a Ph.D. degree, and especially for the resources to work at The Research School of Chemistry, The Australian National University with Prof. Dr. A. David Rae. I am also grateful to them for the additional support of my Ph.D. research provided by an RGJ Basic Research Grant.

I wish to express my special thanks to The Asian Crystallographic Association for Young Scientist Financial Support grants to support my attendance at the AsCA'01 meeting in Bangalore, India and the AsCA'04 meeting in Hong Kong, China and to MacScience for a registration support award for AsCA'01. Thanks to The International Union of Crystallography for a Bursary Award for travel support to attend the XIX Congress and General Assembly of the IUCr in Geneva, Switzerland. Also thanks to The Oxford Cryosystems Low Temperature for selecting my work for the best poster prize from The Asian Crystallographic Association Meeting, AsCA'04 in Hong Kong, China.

I would like to thank The Research School of Chemistry for use of their equipment and support, and Dr. Allison Edwards and Dr. Tony Willis of the X-ray crystallography unit, and Pam Cohen and Christopher Delfs of the computer unit for their help during my two visits at The Australian National University.

Thanks are also owed to Prof. Dr. A. L. Spek at the Laboratory of Crystal and Structural Chemistry, Bijvoet Center for Biomolecular Research, Utrecht University, The Netherlands, for training and discussion about state-of-the-art crystal structure, validation methods, and software, especially the newest developments from Utrecht, and about solution of structures with nonroutine diffraction patterns, and how to use

this technology in Thailand. I also thank Bruker Nonius Company for inviting me to Delft for preliminary training in use of the new EvalCCD integration software.

Thanks to Assoc. Prof. Dr. Ian D. Williams for providing a stimulating problem, for his hospitality during a visit to his laboratory at the Department of Chemistry, Hong Kong University of Science and Technology, Hong Kong, and especially for serving on my thesis committee.

Special thanks to Dr. Lasse Norén and Miss Valeska Ting at the Australian National University for their help with my thesis, for being the best friends, and for their warmth toward me throughout.

Finally, I would like to thank all the members of our research group (especially Ms. Nongnaphat Khosavithitkul, Ms. Samroeng Krachodnok, Ms. Saiphon Chanpaka, Mr. Kittipong Chainok, and Mr. Winya Dungkaew) and other chemistry friends for their friendship and help. I thank my mother for her love and for understanding me.

My apologies to the others who I have not mentioned by name, I am indebted to them for the many ways they helped me.

Weenawan Somphon

CONTENTS

CONTENTS (Continued)

CONTENTS (Continued)

CONTENTS (Continued)

CONTENTS (Continued)

LIST OF TABLES

LIST OF TABLES (Continued)

LIST OF TABLES (Continued)

LIST OF TABLES (Continued)

LIST OF TABLES (Continued)

LIST OF TABLES (Continued)

LIST OF FIGURES

LIST OF FIGURES (Continued)

LIST OF FIGURES (Continued)

LIST OF ABBREVIATIONS

a, b, c	Unit cell axial lengths in direct space
a, b*, c**	Unit cell axial lengths in reciprocal lattice
a, b, c	Unit cell vectors of the direct space
a*, b*, c*	Unit cell vectors of the reciprocal lattice
ADPs	anisotropic displacement parameters
bipy	4,4′-bipyridine
C	C centered lattice
CSD	Cambridge Structural Database
d	Space between the lattice planes in crystal
1D	One-dimension
2D	Two-dimension
3D	Three-dimension
EvalCCD	data reduction software from Bruker Nonius
F	F centered lattice
F_{obs}	Amplitude of structure observed and calculate
F_{hkl}	The structure factor
f	Atomic scattering factor
Gof	estimated standard deviation of an observation of unit weight, or goodness of fit

LIST OF ABBREVIATIONS (Continued)

h, k, l	Miller indices to identify a family of planes or reflection
HMT	Hexamethylenetetramine
I	Intensity of light
P	Primitive
phen	1,10-phenanthroline
$phenH^{+}$	1,10-Phenanthrolin-1-ium
$phenH_2^{2+}$	1,10-Phenanthrolin-1,10-diium
RAELS	least squares structure refinement package
R	Conventional discrepancy index = $\sum\|(\|F_o\|-\|F_c\|)\|/\sum\|F_o\|$
S	estimated standard deviation of an observation of unit weight, or goodness of fit
T	Temperature
TL	libration
TLX	libration with refinable origin
TPA	terephthalic acid or 1,4-dicarboxylic acid
θ	Bragg angle or scattering angle
λ	wavelength of x-radiation
μ	linear absorption coefficient
ρ	electron density
α, β, γ	Angle between unit cell axes in direct space
$\alpha^*, \beta^*, \gamma^*$	Angle between unit cell axes in reciprocal space

LIST OF ABBREVIATIONS (Continued)

δ	Phase angle
wR	The weighted R-factor
U	atomic displacement factor
Z	Number of formula mass unit in the unit cell

CHAPTER I

GENERAL INTRODUCTION

1.1 Introduction

Crystal engineers and supramolecular chemists are interested in materials chemistry and structural reactivity of the solid state (Schmidt, 1971; Desiraju, 1989). The goal is to control the formation of the crystal structure and therefore the properties of the solids. This may be done by rational design of supramolecular structures to systematically create molecular architecture (Desiraju, 1997; 1995; 2003). Crystal engineering attempts to obtain order out of the seemingly random facts concerning molecular orientations in crystals (Atwood, Davies, Vögtle & Lehn, 1996). Currently, this means that a wide variety of supramolecular aggregates have been created and their crystal packing patterns and supramolecular structures have been characterized by X-ray diffraction and other solid state analytical techniques.

Supramolecular chemists are also interested in the design and creation of specific supramolecular structures. As the field has developed, researchers have begun to determine what types of properties and functions supramolecular aggregates exhibit and how these properties and functions differ from those of the individual molecules that comprise the assemblies. Supramolecular synthons are the smallest units which contain all the information inherent in directing the process of assembling the molecules into the supramolecular structure. They are made up of spatial

arrangements of potential intermolecular interactions that are realized in crystals and are significant in crystal engineering (Reddy, Craig & Desiraju, 1996; Reddy, Ovchinnikov, Shishkin, Struchkov & Desiraju, 1996). A necessary first step in engineering any crystalline framework is to choose appropriate synthons. Coordination chemistry provides the crystal engineer with a wealth of data from which to make these choices. External influences on the assembly process, such as electrochemical direction of hydrogen bonding (Ge, Lilienthal & Smith, 1996) have also been identified.

Knowledge of the various intermolecular interactions such as charge transfer interactions, electrostatic interactions, dipole-dipole interactions, hydrogen bonding, van der Waals attractions, halogen-halogen interactions, and the various π-π contact interactions that govern the extended structure of organic solids and coordination compounds is important (Desiraju, 1996; Biradha & Zaworotko, 1998; Langley, Hulliger, Thaimattam & Desiraju, 1998; Alshahateet, Rahman, Bishop, Craig & Scudder, 2002; Choudhury, Urs, Row & Nagarajan, 2002).

Weak noncovalent interactions, often called nonbonding interactions, play a crucial role in determining the three-dimensional structures of large molecules and aggregates (Stone & Tsuzuki, 1997, Kelly, Skakle, Wardell, Wardell, Low & Glidewell, 2002; Mathew, Paul, Shivasankar, Choudhury & Rao, 2002; Chen, Cheng, Zhao, Yan, Liao & Jiang, 2003). A clear understanding of the weak intermolecular interactions and the way in which they coexist in crystals is a key aspect of crystal engineering since the weak intermolecular interactions are essential to correct prediction of the structure and material properties of an assembly.

Hydrogen bonds have been studied in depth because they provide viable approaches toward the design of molecular solids with specific supramolecular architectures and functions (Lewis, Yang & Stern, 1996; Thaimattam, Sharma, Clearfield & Desiraju, 2001). They are much weaker than the covalent bonds which hold organic molecules together. Hydrogen bonds involve hydrogen donor and hydrogen acceptor groups, the strength of the bond depending on the electronegativity of the donor and acceptor atoms. Strong donors and acceptors form strong hydrogen bonds (*e.g.* O−H···O and other classical hydrogen bonds), weak donors and strong acceptors form intermediate strength hydrogen bonds (*e.g.* C−H···O), and weak donors and weak acceptors form weak hydrogen bonds (*e.g.* C−H···π).

Van der Waals forces are weak electrostatic forces created by fluctuating charge distributions, which induce temporary dipoles that create weak attractive forces between atoms. These induced interactions are quite weak with interaction energies comparable to the weakest hydrogen bond interactions. The distinction between hydrogen bonds and van der Waals interactions is their directional characteristics. Hydrogen bonds are inherently directional with linear or close to linear geometries about the H atom favored. In contrast, van der Waals contacts are nondirectional with interaction energies depending primarily on distance (Steiner & Desiraju, 1998).

Dipole-dipole interactions are receiving increasing attention for their importance in the stabilization of the packing of small organic molecules in a supramolecular structure. Among the dipole-dipole interactions are the $O(\delta^-)\cdots C(\delta^+)$ carbonyl-carbonyl interactions (Allen, Baalham, Lommerse & Raithby, 1998; Chainok, 2004) and the $O(\delta^-)\cdots C(\delta^+)$ ether-carbonyl interaction (Phothikanith, 2004).

1.2 Nature of the Problem

The majority of organic molecules, as evidenced by the prevalence of recrystallization as a purification technique, pack as pure single component crystals. Of the numerous packing options, the correct one is often associated with a distinctly lower free energy (Atwood, Davies, Vögtle & Lehn, 1996). Cocrystallization has been studied for many decades, often as a way to explore intermolecular interactions. Early examples of relevance to this thesis are cocrystals of hexamethylenetetramine (HMT) with various other components ($MnCl_2 \cdot 2HMT \cdot 2H_2O$, Tang & Sturdivant, 1952; HMT:$\{HO_2C(CH_2)_{n-2}CO_2H\}$ ($5 \leq n \leq 13$), Gaillard, Paciorek, Schenk & Chapuis, 1996; Gaillard, Chapuis, Dusek & Petříček, 1998; Hostettler, Birkedal, Gardon, Chapuis, Schwarzenbach & Bonin, 1999; Gardon, Schönleber, Chapuis, Hostettler & Bonin, 2001; Bonin, Welberry, Hostettler, Gardon, Birkedal, Chapuis, Möchli, Ogle & Schenk, 2003; Gardon, Pinheiro & Chapuis, 2003; Pinheiro, Gardon & Chapuis, 2003).

Cocrystals of triphenylphosphine oxide with organic compounds have also been of interest. Etter and Baures (1988) found that addition of triphenylphosphine oxide to the mother liquor of several organic compounds that crystallized as fine needles led to an energetically preferred multicomponent crystal of more suitable habit. Cocrystallization has proven to be a particularly fruitful way to create new materials and supramolecular assemblies. Cooperative intermolecular interactions control the arrangements of the constituents of these cocrystals. Electron donor-acceptor attractions between organic groups to control the structure of crystal lattices have led to the use of donor-acceptor based molecular recognition phenomena for crystal engineering of hexamethylenetetramine cocrystals (Mak, Tse, Chong & Mok,

1977; Mak & Lau, 1978; Mak, Yu & Lam, 1978). The design of engineered cocrystalline organic solids implies control over molecular packing and this necessitates a detailed analysis of the intermolecular interactions of individual component structure motifs in cocrystals (Coupar, Glidewell & Ferguson, 1997; Low, López, Mascarós, Domingo, Godino, Garzón, Gutiérrez, Melguizo, Ferguson & Glidewell, 2000). Cocrystals, almost by definition, exhibit supramolecular structures, and examples of one-, two-, and three-dimensional types are known (Boldog, Rusanov, Chernega, Sieler & Domasevitch, 2001; Khlobystov, Blake, Champness, Lemenovskii, Majouga, Zyk & Schröder, 2001; Wang, Bei, Yang, Lu & Wang, 2002).

Most of the structures are well-behaved from an X-ray crystallographic point of view, and can be solved and refined using standard refinement techniques (MacLean, Glidewell, Ferguson, Gregson & Lough, 1999; Glidewell, Ferguson, Gregson & Campana, 2000; Glidewell, Low & Wardell, 2000; Gregson, Glidewell, Ferguson & Lough, 2000; Shan, Bond & Jones, 2002). However, some structures exhibit phenomena which pose particular challenges during structure solution and/or refinement. Pseudo symmetry is a common cause of problems (Scheidt, Cheng, Haller, Mislankar, Rae, Reddy, Song, Orosz, Reed, Cukiernik & Marchon, 1993; Quirós, 1994; Ng & Rae, 2000), as is disorder (Mahmoud & Wallwork, 1979; Haller, Rae, Heerdegen, Hockless & Welberry, 1995; Yaghi & Li, 1995; Yaghi, Li & Groy, 1997), twinning (Li, Petříček, Cisarova & Coppens, 1995; Schaefer, Marsh, Rodriguez & Bazan, 1996; Haller, Rae, Bygott, Hockless, Geue, Ralph & Sargeson, 1999), structure modulation (Kan & Moss, 1992; Haller & Rae, 1993; Weber, Boysen, Frey & Neder, 1997), and stacking faults (Gardon, Pinheiro & Chapuis, 2003).

Polymorphism and polytypism are also of interest. Polymorphism refers to substantially different structures whereas polytypism refers to structures containing essentially identical building units assembled in alternative fashions, for example different stackings of the same sort of layer. Twinning and stacking faults are commonly associated with polytypism. Phase transformations occur when crystal structures change as a function of temperature, pressure, or other thermodynamic parameters. The phase change may result in some difficulty for structure solution or refinement as it may cause twinning and/or disorder (Chaudhary, 1993; Hostettler, Birkedal, Gardon, Chapuis, Schwarzenbach & Bonin, 1999), and the creation of superstructures (Gaillard, Paciorek, Schenk & Chapuis, 1996; Gaillard, Chapuis, Dusek & Petříčer, 1998), which can result in diffuse scattering (Ishii, 2000). Composition change by chemical replacement may result in similar problems.

The structure determination of small molecule crystals by single crystal X-ray crystallography is the most convenient method for obtaining an accurate three-dimensional structure of a compound. However, some crystals have features which cause difficulties during the refinement process. When these features are not recognized or are not taken into account the refined structures do not accurately represent reality. Since the structures of these less well refined crystals are included in databases such as the Cambridge Structure Database (CSD) and ultimately used as "a true answer" in theoretical modeling methods, this can cause problems. Revision of some published crystal structures may thus be necessary. Changes of space groups from lower to higher symmetry to give better models have been published (Marsh & Herbstein, 1983; Baur, 1986; Marsh & Herbstein, 1988; Marsh, Kapon, Hu & Herbstein, 2002; Clemente & Marzotto, 2003). Failing to recognize a symmetry

operation does not necessarily hurt a refinement though it does create unnecessary variables. The use of an incorrect symmetry element will always do some damage. Pseudo symmetry may isolate data fitting problems to specific classes of reflections.

1.3 Categories of Problem Structures

An ideal crystal would have exact three-dimensional repetition of identical unit cells with exactly the same arrangement of atoms and molecules in each unit cell. In real crystals this is often not the case. The diffraction pattern from a real crystal contains the effects of departure from an idealized structure. This can result in overlapped reflections, weak satellite reflections (commensurate or incommensurate), diffuse scattering, anisotropic mosaicity, and poor data reflections.

This thesis focuses on the recognition and investigation of a variety of nonideal crystal structure types related to the phenomenological problems noted above and used crystals formed by cocrystallization. Many of the structures presented challenges during structure solution and refinement. Problems involved pseudo symmetry, weak spots, occupational disorder, large thermal motions, twinning including partial and perfect overlap of diffraction intensities, structure modulation, stacking faults, diffuse scattering, phase transitions, and polytypic structures.

The program RAELS (Rae, 2000) was used to control the refinement of crystal structures displaying disordered and/or largely librating solvent molecules or ligands. This program has useful features for such refinements. Atoms can be described using refinable local coordinates relative to refinable orthonormal axial systems. Atomic displacement parameters can be described using refinable *TL* and *TLX* models to describe rigid body motions. Constraints and restraints can be used to

impose more rational models and control refinement pathways by decreasing the effective number of refinable variables. Wrong choices however do not help. Many structure modulations can be regarded as the results of interacting substructures. Symmetry elements lost because of the coexistence of these substructures can provide mechanisms for twinning, stacking faults, and polytypism.

Chapter III reports the supramolecular structure of $[SnCl_2(C_2H_4COOH)(C_2H_4COO)]^-\cdot[C_{12}N_2H_9]^+$. The Sn atom has pseudo octahedral coordination by two *cis* Cl atoms, two C atoms, and two O atoms *trans* to the chlorine atoms. The crystal packing has a three-dimensional network of interactions consisting of strong and weak hydrogen bonds. A mechanism is identified for the creation of twins, stacking faults, and polytypes.

Chapters IV and V report on structures containing hexamethylenetetramine (HMT) molecules cocrystallized with inorganic salts and ten water molecules. Chapter IV describes the pseudo symmetric $[Mg(H_2O)_6](NO_3)_2\cdot 2HMT\cdot 4H_2O$ structure and chapter V describes the isomorphic and partially twinned crystals of $[M(H_2O)_6]I_2\cdot 2HMT\cdot 4H_2O$, where M = Ni and Mn. These structures can be described using substructures of different symmetry that contain the true symmetry as a subgroup. This identifies a mechanism for stacking faults and twinning.

Chapter VI reports the multiply twinned, modulated, and disordered crystal structure of triethylphosphine sulfide, $SP(C_2H_5)_3$.

Chapter VII reports the structure of the $\{[Cu(bipy)]_2SO_4\cdot TPA\}_n$ coordination polymer formed by solvothermal synthesis from copper sulfate pentahydrate, 4,4′-bipyridyl (bipy), and terephthalic acid (TPA). The structure can be described as

commensurate displacive modulation of a parent structure with a stacking fault leaving a residual 1:1 disorder of the structure.

Chapter VIII reports the polymeric $[Ag(bipy)NO_3]_n$ structure. This structure undergoes a reversible order-disorder transformation at about 150 K. The high temperature phase (> 150 K) is orthorhombic (*Fddd*) and disordered, and shows diffuse scattering. The layers of diffuse scattering essentially disappear at low temperature (< 150 K) and an ordered structure (monoclinic, *C*2/*c*) results. The phase transition to the ordered structure creates twinned crystals and splits twin related reflections.

1.4 References

Allen, F. H., Baalham, C. A., Lommerse, J. P. M. and Raithby, P. R. (1998). Carbonyl-carbonyl interactions can be competitive with hydrogen bonds. **Acta Crystallographica** B54: 320-329.

Alshahateet, S. F., Rahman, A. N. M. M., Bishop, R., Craig, D. C. and Scudder, M. L. (2002). Interlocking molecular grid lattices involving weak assembly forces. **CrystEngComm** 4(97): 585-590.

Atwood, J. L., Davies, J. E. D., Vögtle, F. and Lehn, J. (1996). *Comprehensive Supramolecular Chemistry*, **Elsevier Science Ltd.**, vol. 6: 1-20.

Baur, W. H. (1986). How to avoid unnecessarily low symmetry in crystal structure determinations. **Acta Crystallographica** B42: 95-111.

Biradha, K. and Zaworotko, M. J. (1998). A supramolecular analogue of cyclohexane sustained by aromatic C−H···π interactions: Complexes of 1,3,5-

trihydroxybenzene with substituted pyridines. **Journal of the American Chemical Society** 120(25): 6431-6432.

Boldog, I., Rusanov, E. B., Chernega, A. N., Sieler, J. and Domasevitch, K. V. (2001). One- and two-dimensional coordination polymers of 3,3′,5,5′-tetramethyl-4,4′-bipyrazolyl, a new perspective crystal engineering module. **Polyhedron** 20(9-10): 887-897.

Bonin, M., Welberry, T. R., Hostettler, M., Gardon, M., Birkedal, H., Chapuis, G., Möchli, P., Ogle, C. A. and Schenk, K. J. (2003). Urotropin azelate: A rather unwilling co-crystal. **Acta Crystallographica** B59: 77-89.

Chainok, K. (2004). M. Sc. Thesis, Suranaree University of Technology.

Chaudhary, S. K. (1993). Impurity- and temperature-dependent structural transformations in polytypic crystals of CdI_2, PbI_2 and $CdBr_2$. **Acta Crystallographica** B49: 454-458.

Chen, X.-Y., Cheng, P., Zhao, B., Yan, S.-P., Liao, D.-Z. and Jiang, Z.-H. (2003). A novel coordination polymer with dicyanamide ligand: Multi-dimensional architecture stabilized by hydrogen bonding. **Journal of Molecular Structure** 655(1): 179-184.

Choudhury, A. R., Urs, U. K., Row, T. N. G. and Nagarajan, K. (2002). Weak interactions involving organic fluorine: A comparative study of the crystal packing in substituted isoquinolines. **Journal of Molecular Structure** 605(1): 71-77.

Clemente, D. A. and Marzotto, A. (2003). 22 Space-group changes. **Acta Crystallographica** B59: 43-50.

Coupar, P. I., Glidewell, C. and Ferguson, G. (1997). Crystal engineering using bisphenols and trisphenols. Complexes with hexamethylenetetramine (HMTA): strings, multiple helices and chains-of-rings in the crystal structures of the adducts of HMTA with 4,4′-thiodiphenol (1/1), 4,4′-sulfonyldiphenol (1/1), 4,4′-isopropylidenediphenol (1/1), 1,1,1-tris(4-hydroxyphenyl)ethane (1/2) and 1,3,5-trihydroxybenzene (2/3). **Acta Crystallographica** B53: 521-533.

Desiraju, G. R. (1989). *Crystal Engineering: The Design of Organic Solids*. **Elsevier,** Amsterdam.

Desiraju, G. R. (1995). Supramolecular synthons in crystal engineering−a new organic synthesis. **Angewandte Chemie International Edition in English** 34(21): 2311-2327.

Desiraju, G. R. (1996). The C−H···O hydrogen bond: Structural implications and supramolecular design. **Accounts of Chemical Research** 29(9): 441-449.

Desiraju, G. R. (1997). Designer crystals: Intermolecular interactions, network structures and supramolecular synthons. **Chemical Communications** (16): 1475-1482.

Desiraju, G. R. (2003). Crystal engineering. From molecules to materials. **Journal of Molecular Structure** 656: 5-15.

Etter, M. C. and Baures, P. W. (1988). Triphenylphosphine oxide as a crystallographic aid. **Journal of the American Chemical Society** 110(2): 639-640.

Gaillard, V. B., Chapuis, G., Dusek, M. and Petříček, V. (1998). Hexamethylenetetramine sebacate, an incommensurate structure with large

nonsinusoidal modulations: Comparison of two refinement strategies. **Acta Crystallographica** A54: 31-43.

Gaillard, V. B., Paciorek, W., Schenk, K. and Chapuis, G. (1996). Hexamethylenetetramine suberate, a strongly anharmonic modulated structure. **Acta Crystallographica** B52: 1036-1047.

Gardon, M., Pinheiro, C. B. and Chapuis, G. (2003). Structural phases of hexamethylenetetramine-pimelic acid (1/1): A unified description based on a stacking model. **Acta Crystallographica** B59: 527-536.

Gardon, M., Schönleber, A., Chapuis, G., Hostettler, M. and Bonin, M. (2001). The lock-in-phase in the urotropine–sebacic acid system. **Acta Crystallographica** C57: 936-938.

Ge, Y., Lilienthal, R. R. and Smith, D. K. (1996). Electrochemically-controlled hydrogen bonding selective recognition of urea and amide derivatives by simple redox-dependent receptors. **Journal of the American Chemical Society** 118(16): 3976-3977.

Glidewell, C., Ferguson, G., Gregson, R. M. and Campana, C. F. (2000). Supramolecular chemistry of amine-phenol adducts; novel three-dimensional framework structures in adducts of bis(2-aminoethyl)amine with 4,4′-sulfonyldiphenol, 1,1,1-tris(4-hydroxyphenyl)-ethane and 3,5-dihydroxy benzoic acid, and in the methanol-solvated adduct of tris(2-aminoethyl)-amine with 4,4′-biphenol. **Acta Crystallographica** B56: 68-84.

Glidewell, C., Low, J. N. and Wardell, J. L. (2000). Conformational preferences and supramolecular aggregation in 2-nitrophenylthiolates: disulfides and thiosulfonates. **Acta Crystallographica** B56: 893-905.

Gregson, R. M., Glidewell, C., Ferguson, G. and Lough, A. J. (2000). Meso-5,5,7, 12,12,14-hexamethyl-1,4,8,11-tetraazacyclotatradecane as a building block in supramolecular chemistry; salts formed with 2,2′-biphenol, 4,4′-biphenol, 4,4′-thiodiphenol, 4,4′-sulfonyldiphenol, 3- and 4-hydroxybenzoic acids, 3,5-dihydroxybenzoic acid and phenylphosphonic acid; supramolecular structures in zero, one, two and three dimensions. **Acta Crystallographica** B56: 39-57.

Haller, K. J. and Rae, A. D. (1995). The modulated crystal structure of a metalloporphyrin π−cation radical. **Acta Crystallographica** A49: S242.

Haller, K. J., Rae, A. D., Heerdegen, A. P., Hockless, D. C. R. and Welberry, T. R. (1995). The fourfold disordered structures of *p*-chloro-*N*-(*p*-methyl benzylidene)aniline and *p*-methyl-*N*-(*p*-chlorobenzylidene)aniline. **Acta Crystallographica** B51: 187-197.

Haller, K. J., Rae, A. D., Bygott, A. M. T., Hockless, D. C. R., Ralph, S. F., Geue, R. J. and Sargeson, A. M. (1999). Four-component intergrowth structures of the metal-ion cage complexes *fac*-(1,5,9,13,20-pentamethyl-3,7,11,15,18,22-hexa azabicyclo[7.7.7]tricosane)M^{II} diperchlorate hydrate, $[M(C_{22}H_{48}N_6)](ClO_4)_2.xH_2O$, M = Ni, Zn. **Acta Crystallographica** B55: 380-388.

Hostettler, M., Birkedal, H., Gardon, M., Chapuis, G., Schwarzenbach, D. and Bonin, M. (1999). Phase-transition-induced twinning in the 1:1 adduct of hexamethylenetetramine and azelaic acid. **Acta Crystallographica** B55: 448-458.

Ishii, Y. (2000). Anisotropic phasonic diffuse scattering from decagonal quasicrystals. **Materials Science and Engineering** 294-295: 377-380.

Kan, X. B. and Moss, S. C. (1992). Four-dimensional crystallographic analysis of the incommensurate modulation in a $Bi_2Sr_2CaCu_2O_8$ single crystal. **Acta Crystallographica** B48: 122-134.

Kelly, C. J., Skakle, J. M. S., Wardell, J. L., Wardell, S. M. S. V., Low, J. N. and Glidewell, C. (2002). Iodo-nitroarenesulfonamides: Interplay of hard and soft hydrogen bonds, I···O interactions and aromatic π···π stacking interactions. **Acta Crystallographica** B58: 94-108.

Khlobystov, A. N., Blake, A. J., Champness, N. R., Lemenovskii, D. A., Majouga, A. G., Zyk, N. V. and Schröder, M. (2001). Supramolecular design of one-dimensional coordination polymers based on silver(I) complexes of aromatic nitrogen-donor ligands. **Coordination Chemistry Reviews** 222(1): 155-192.

Langley, P. J., Hulliger, J., Thaimattam, R. and Desiraju, G. R. (1998). Supramolecular synthons mediated by weak hydrogen bonding: Forming linear molecular arrays *via* C≡C−H···N≡C and C≡C−H···O_2 N recognition. **New Journal of Chemistry** 12: 1307-1309.

Lewis, F. D., Yang, J.-S. and Stern, C.L. (1996). Crystal structures of secondary arenedicarboxamides. An investigation of arene-hydrogen bonding relationships in the solid state. **Journal of the American Chemical Society** 118(48): 12029-12037.

Li, R., Petříček, V., Cisarova, I. and Coppens, P. (1995). Analysis of the diffraction pattern of a twinned crystal of (3,4;3′,4′-bis(ethylenedioxo)-2,2′,5,5′-tetrathiafulvalene)$_2$·$Ag(CN)_2$. **Acta Crystallographica** B51: 798-802.

Low, J. N., López, M. D., Mascarós, P. A., Domingo, J. C., Godino, M. L., Garzón, R. L., Gutiérrez, M. D., Melguizo, M., Ferguson, G. and Glidewell, C. (2000).

N-(6-Amino-3,4-dihydro-3-methyl-5-nitroso-4-oxopyrimidin-2-yl) derivatives of glycine, valine, serine, threonine and methionine: interplay of molecular, molecular-electronic and supramolecular structures. **Acta Crystallographica** B56: 882-892.

MacLean, E. J., Glidewell, C., Ferguson, G., Gregson, R. M. and Lough, A. J. (1999). Hexamethylenetetramine is a fourfold acceptor of O−H···N hydrogen bonds in its 1:2 adduct with 2,2′-biphenol. **Acta Crystallographica** C55: 1867-1870.

Mahmoud, M. M. and Wallwork, S. C. (1979). The crystal structures of the 1:1 complexes formed by hexamethylenetetramine with hydroquinone and resorcinol. **Acta Crystallographica** B35: 2370-2374.

Mak, T. C. W., Tse, C.-S., Chong, Y.-H. and Mok, F.-C. (1977). Hexamethylenetetramine-hydroquinone (1:1). **Acta Crystallographica** B33: 2980-2982.

Mak, T. C. W. and Lau, O. W. (1978). Preparation and X-ray analysis of a 1:2 adduct of hexamethylenetetramine and thiourea. **Acta Crystallographica** B34: 1290-1294.

Mak, T. C. W., Yu, W.-H. and Lam, Y.-S. (1978). Hexamethylenetetramine-*m*-cresol (1:2). **Acta Crystallographica** B34: 2061-2063.

Marsh, R. E. and Herbstein, F. H. (1983). Some additional changes in space groups of published crystal structures. **Acta Crystallographica** B39: 280-287.

Marsh, R. E. and Herbstein, F. H. (1988). More space-group changes. **Acta Crystallographica** B44: 77-88.

Marsh, R. E., Kapon, M., Hu, S. and Herbstein, F. H. (2002). Some 60 new space-group corrections. **Acta Crystallographica** B58: 62-77.

Mathew, S., Paul, G., Shivasankar, K., Choudhury, A. and Rao, C. N. R. (2002). Supramolecular hydrogen-bonded structures in organic amine squarates. **Journal of Molecular Structure** 641(2-3): 263-279.

Ng, S. W. and Rae, A. D. (2000). A pseudo symmetric triclinic modification of triphenyltin isopropylxanthate. **Acta Crystallographica** C56: e47-e48.

Phothikanith, A. (2004). Ph. D. Thesis, Suranaree University of Technology.

Pinheiro, C. B., Gardon, M. and Chapuis, G. (2003). Structural changes of hexamethylenetetramine and undecanedioic acid co-crystal (HMT-C11) as a function of the temperature. **Acta Crystallographica** C59: 416-427.

Quirós, M. (1994). Silver 2-pyrimidinolate dihydrate, $[Ag(C_4H_3N_2O)].2H_2O$: A case of pseudo symmetry. **Acta Crystallographica** C50: 1236-1239.

Rae, A. D. (2000). *RAELS. A Comprehensive Constrained Least Squares Refinement Program*, Australian National University, Canberra, Australia.

Reddy, D. S., Craig, D. C. and Desiraju, G. R. (1996). Supramolecular synthons in crystal engineering. 4. Structure simplification and synthon interchangeability in some organic diamondoid solids. **Journal of the American Chemical Society** 118(17): 4090-4093.

Reddy, D. S., Ovchinnikov, Y. E., Shishkin, O. V., Struchkov, Y. T. and Desiraju, G. R. (1996). Supramolecular synthons in crystal engineering. 3. Solid state architecture and synthon robustness in some 2,3-dicyano-5,6-dichloro-1,4-dialkoxybenzenes. **Journal of the American Chemical Society** 118(17): 4085-4089.

Schaefer, W. P., Marsh, R. E., Rodriguez, G. and Bazan, G. C. (1996). A tribenzylidenemethane-tantalum compound: Some experiences with ′inversion twinning′. **Acta Crystallographica** B52: 465-470.

Scheidt, W. R., Cheng, B., Haller, K. J., Mislankar, A., Rae, A. D., Reddy, K. V., Song, H., Orosz, R. D., Reed, C. A., Cukiernik, F. and Marchon, J.-C. (1993). Preparation and characterization of singly oxidized metalloporphyrin dimers: $[M(OEP)]_2SbCl_6$, M = Cu, Ni. Photosynthetic special pair models. **Journal of the American Chemical Society** 115(3): 1181-1183.

Schmidt, G. M. J. (1971). Photodimerization in the solid state. **Pure and Applied Chemistry** 27: 687-688.

Shan, N., Bond, A. D. and Jones, W. (2002). Crystal engineering using 4,4′-bipyridyl with di- and tri-carboxylic acids. **Crystal Engineering** 5: 9-24.

Steiner, T. and Desiraju, G. R. (1998). Distinction between the weak hydrogen bond and the van der Waals interaction. **Chemical Communications** (8): 891-892.

Stone, A. J. and Tsuzuki, S. (1997). Intermolecular interactions in strongly polar crystals with layer structures. **The Journal of Physical Chemistry B** 101(49): 10178-10183.

Tang, Y.-C. and Sturdivant, J. H. (1952). The crystal structure of the complex of hexamethylenetetramine with manganese chloride. **Acta Crystallographica** 5: 74-82.

Thaimattam, R., Sharma, C. V. K., Clearfield, A. and Desiraju, G. R. (2001). Diamondoid and square grid networks in the same structure. Crystal engineering with the Iodo···Nitro supramolecular synthon. **Crystal Growth and Design** 1(2): 103-106.

Wang, J., Bei, F. L., Yang, X. J., Lu, L. D. and Wang, X. (2002). Crystal structure of a carboxylate-bridged one-dimensional linear chain polymer N-salicylidene-2-amino-phenylacidato copper(II) complex. **Journal of Molecular Structure** 643(1-3): 129-133.

Weber, T., Boysen, H., Frey, F. and Neder, R. B. (1997). Modulated structure of the composite crystal urea/*n*-heptadecane. **Acta Crystallographica** B53: 544-552.

Yaghi. O. M. and Li, H. (1995). Hydrothermal synthesis of a metal-organic framework containing large rectangular channels. **Journal of the American Chemical Society** 117(41): 10401-10402.

Yaghi, O. M., Li, H. and Groy, T. L. (1997). A molecular railroad with large pores: Synthesis and structure of $Ni(4,4'\text{-bpy})_{2.5}(H_2O)_2(ClO_4)_2 \cdot 1.5(4,4'\text{-bpy}) \cdot 2H_2O$. **Inorganic Chemistry** 36(20): 4292-4293.

CHAPTER II

CONCEPTS AND THEORETICAL BACKGROUND

2.1 Introduction

Single crystal X-ray structure solution and refinement is completely routine for a large fraction of small molecule structures, including most multi-component structures. Clean diffraction patterns showing reflections organized by a reciprocal lattice are used to create structures organized by a lattice describing allowed translations of the contents of a unit cell that describe the translationally repeating unit.

Many problem (*i.e.* nonroutine) structures involve pseudo symmetry, structure modulation, twinning, stacking faults, *etc.* as described in chapter I. This may result in problems such as creating false minima in the least squares refinement (Cotton & Rice, 1978; Marsh & Schomaker, 1979; Rae, Thompson, Withers & Willis, 1990; Rae, Thompson & Withers, 1991; Murphy, Rabinovich & Parkin, 1995; Herbstein & Marsh, 1998; Murphy, Rabinovich, Hascall, Klooster, Koetzle & Parkin, 1998). The nature of many of these problems can be understood by reference to an idealized parent structure of higher symmetry or interacting parent substructures of different symmetries. Another group of nonroutine structures are those for which disorder locates atoms (averaging over different unit cells) too close together for easy refinement. In these cases the diffraction data is often of insufficient quality to refine a conventional fully parameterized structure model with three atomic coordinates and

six atomic displacement parameters for each disordered atom. Determination of a most probable structure must suffice in these cases and use of constrained/restrained refinements, including control of geometry and occupancy, or versatile modeling of thermal groups may be crucial to the success of the structure determination. For structures having dimensionality greater than three, a mathematical description of the extended order is required and thus the standard structure solution/refinement packages are inadequate and specialized programs must be used.

2.2 Nonroutine Indexing of Diffraction Patterns

Pseudo symmetry

The commonest case of pseudo symmetry (meaning approximate but not exact symmetry) occurs when the heavy atoms alone can be described using a higher symmetry space group than that appropriate for the whole structure. Often the repeat of a pseudo symmetry operation would change the size of the unit cell. The effect of pseudo symmetry causes the associated diffraction pattern to approximate the pattern appropriate to the higher symmetry. Intensities as a function of h, k, and l can be a systematic pattern of weak and strong reflections, where the weak reflections arise from breaking the translational symmetry of an idealized parent structure, see Figure 2.1. The strong reflections see a structure averaged using a smaller repeating unit.

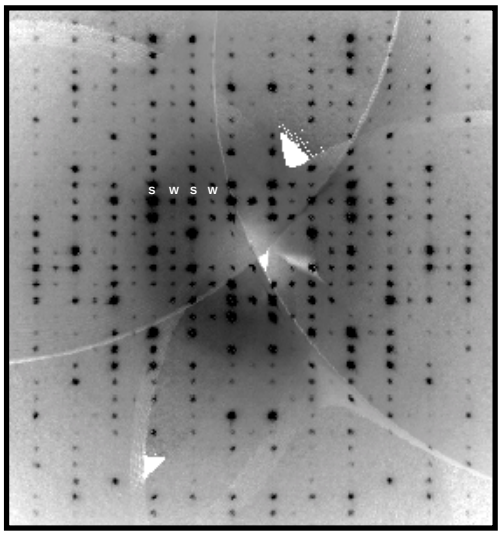

Figure 2.1 Synthetic precession photograph of the 1*kl* reflections in $[Mg(H_2O)_6](NO_3)_2 \cdot 2HMT \cdot 4H_2O$.

Two common categories of pseudo symmetry are pseudo translation symmetry and pseudo centrosymmetry. Pseudo translation symmetry occurs when parts of the crystal structure approximate higher translation symmetry, and is especially relevant to structures containing heavy atoms. When the arrangement of the heavy atoms contributes little to the extra reflections, structures can be difficult to solve. The distinction between alternative models is very much tied up with these extra reflections that should be carefully monitored. Pseudo centrosymmetry refers to structures that approximate exact inversion symmetry. This inversion symmetry might only apply to an individual substructure or the pseudo inversion centers of one substructure might not coincide with those of another substructure. Fourier maps that are phased by an exactly centrosymmetric model show a superimposed image of the true structure and its inversion through the assumed inversion center. By resolving the

disorder one can calculate structure factors for an ordered structure but this is not necessarily easy and all reasonable options should be considered.

The phase reliability of pseudo-centrosymmetric structures was discussed by Rae (1975a). The choice of phases imposed by an initial model tends to be preserved during refinement and false minima are sometime difficult to escape. Alternative starting models must be considered (Rae, Thompson, Withers & Willis, 1990).

Modulated Structures

In a modulated structure atoms suffer from certain occupational (substitutional) and/or positional fluctuations according to a periodic modulation (Zuñiga, Madariaga, Paciorek, Péres-Mato, Ezpeleta & Etxebarria, 1989; Weber, Boysen, Frey & Neder, 1997). Modulated crystal structures often have a longer range periodic variation imposed on a smaller period parent structure. The periodic distortion can sometimes be thought of as the consequence of interacting substructures and this can be used to direct the most appropriate parameter choice. The term modulated structure also includes a lowering of symmetry with no change of unit cell. However, conventional descriptions of space groups may cause confusion. When *Fddd* symmetry is lowered to *F*2/*d* symmetry with no change of cell volume, convention re-describes *F*2/*d* as *C*2/*c* with half the unit cell volume (Chapter VIII). Comparing the volumes of the reduced cells (*i.e.* primitive cells) reveals the true situation. However, the reduced cell of *Fddd* is a primitive cell in one of four orientations related by 222 symmetry and the reduced cell of *F*2/*d* is in one of two orientations.

The presence of periodic distortion is often revealed by the existence of satellite reflections, which are generally weak and distributed about stronger

reflections (main reflections). These reflections can be indexed in terms of a base vector (or vectors) which can be expressed relative to the base vectors describing the diffraction pattern of the parent structure. These extra base vectors define the wave nature of the structure modulation. Structural information for a particular harmonic component of a modulation wave is dominantly contained in a particular set of satellite reflections and this demands specialized refinement techniques as satellite reflections are often weak. Each set of satellite reflections should be individually monitored to make sure the relevant modulation wave is appropriate, in scale, content (detail of the modulation), and overall phase relative to other modulations.

A hierarchical approach to refinement is often used; parameters with the largest effect are refined first. Modulated structures can often be thought to be the consequence of the interaction of two (or more) coexisting substructures, which need not have identical repeat distances for all three dimensions of a crystal. The resulting modulation waves can be commensurate or incommensurate; depending on whether the lattices for the substructures regularly coincide in all 3 dimensions.

Twinning

A twin crystal consists of two or more single crystals of the same species in different orientations (Giacovazzo, Monaco, Artioli, Viterbo, Ferraris, Gilli, Zanotti & Catti, 2002). A twin law describes the relationship between the components and applies to both real and reciprocal space. Copies of the diffraction pattern are reoriented and superimposed with no correlation between them. This presents problems for extracting the diffraction data for a single twin component. Figure 2.2 shows possible forms of crystals with twin domains. There can be two or more orientations of a twin depending on the twin rule (or twin rules).

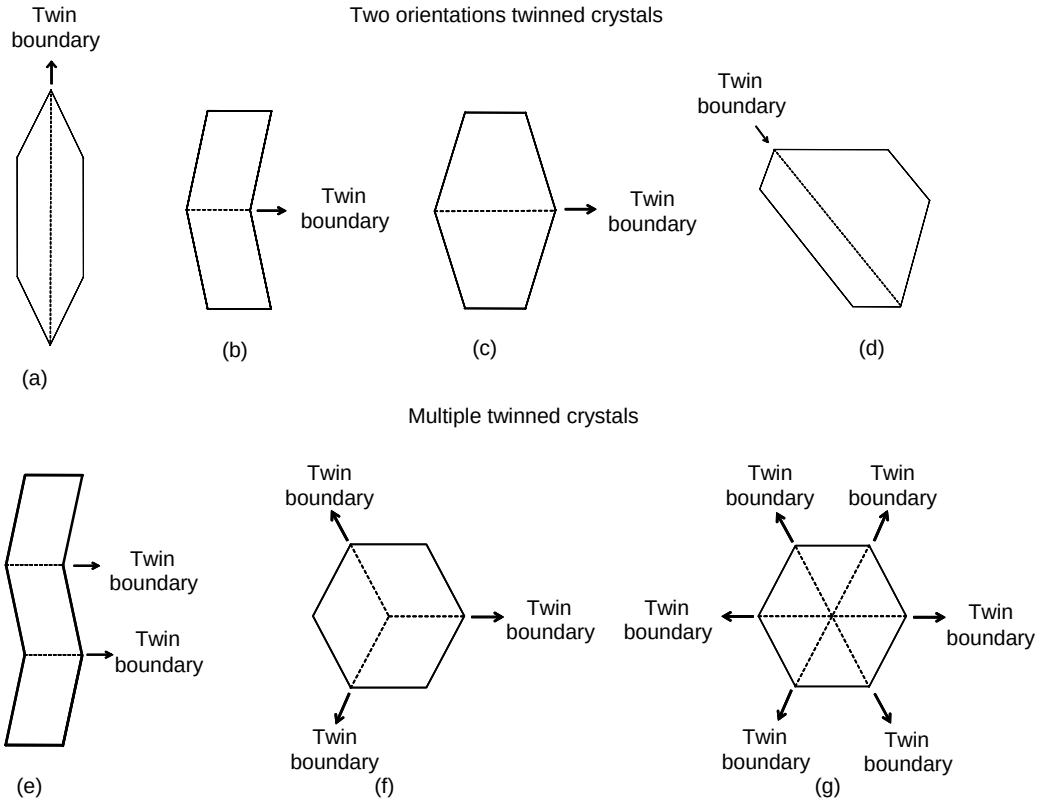

Figure 2.2. 2D illustration showing twin domains. Orthorhombic and monoclinic crystals twinned in two orientations (a-e) and multiple orientations (f-g).

Twinning may occur either during the growth of a crystal or may arise because of a phase transition which lowers the symmetry of the crystal. Sometimes if the crystal is subjected to stress of temperature/pressure conditions different from those under which it was originally formed, two or more intergrown crystals may be formed in a symmetrical fashion displaying one of three type of twinned crystals: contract twins (where the two components are joined at a plane (Yacoot, Moore & Machado, 1998), interpenetrating twins, (where the twinned intergrowth generates an irregular interface between components, Machado, Moore & Yacoot, 1998), or polysynthetic

twins or multiple twins (consisting of three or more components, Sadanaga & Takeuchi, 1961). In many cases twinning may be identified by visual inspection under an optical microscope and the components separated to give a single crystal. In other cases the twinning is not obvious to visual inspection and it may not be possible to find a crystal which is not twinned.

Diffraction patterns from twinned crystals are the non-interacting superposition of the diffraction patterns from the individual twin components. Including twin parameters and a twin rule in the refinement model is essential for the successful structure determination of a twinned crystal. The identification of the likely interface between twin components is desirable.

Four distinct types of diffraction pattern are produced by twinning (Herbst-Irmer & Sheldrick, 1998):

(i) Merohedral twinning (in which the different orientations of both the direct and reciprocal lattice will coincide exactly with one another) may occur in tetragonal, trigonal, hexagonal, and cubic systems (*e.g.*, Bolte, 1994; Boese, Gehrke, Kapon & Herbstein, 2000; Degen & Bolte, 2001; Allan, McGregor, McLachlan, Parsons & Pulham, 2002).

(ii) Pseudo-merohedral twinning involves monoclinic structures with β close to 90° or *a* and *c* almost equal, *e.g.*, Grainger, 1969a; 1969b; van Koningsveld, 1983; Bolte & Ketter, 1998. The reciprocal lattices overlap exactly and twinning is not detectable from the diffraction pattern. For equal amounts of each twin the diffraction symmetry is enhanced.

(iii) Reticular merohedral twinning (sometimes called chameleon twinning) involves obverse/reverse twinning of a rhombohedral structure (Schaefer, Marsh,

Rodriguez & Bazan, 1996). One third of the reflections overlap, giving rise to a characteristic pattern of systematic absences. Some examples of obverse/reverse twinned crystal were refined by Herbst-Irmer & Sheldrick (2002).

(iv) Nonmerohedral twinning occurs when there is limited overlap of the reflections for the two components (*e.g.*, Cooper, Gould, Parson & Watkin, 2002; Flippen-Anderson, Deschamps, George, Folk, Jacobson & Rice, 2002; Lutz & Bakker, 2003). The indexing usually fails at first as both components contribute to the set of trial reflections. This is resolved by separating reflections into separate classes identifying the lattice of the reflections in each class, and relating the sets of reflections by a twin rule or by twin rules. The use of synthetic precession photographs from area detector data often allows the twin rule to be clearly seen. Structure solution should normally be possible but the refinement may well be unsatisfactory because of overlap of some reflections.

To select the correct one of inversion related structures an artificial twinning model can be used (Flack, 1983; Bernardinelli & Flack, 1985). Intensities are described as

$$(1\text{-}x)\, F_c^2(hkl) + x\, F_c^2\, \overline{hkl}$$

where x is the fraction contribution of the inverted component of a twin. If $x = 0$ the first twin component is correct, if $x = 1$ the other component is correct.

In the case of merohedral twinning the intensity of each diffraction spot is the sum of the independent intensities related by the twin rule.

Disorder

In real crystals, parts of the structure are found distributed over a number of positions and orientations. The collected Bragg reflections see an average structure where the averaging is over all unit cells implied by the lattice describing these reflections Knowledge of this average structure is sometimes not enough to understand the properties of the solid state material. Knowledge of the real local environment is required to identify the effect of impurities.

Disorder is not always random. For example whole molecules or planes or columns may be disordered by a symmetry operation of the crystal or by operations that would be symmetry related for a parent structure of higher symmetry (Haller, Rae, Heerdegen, Hockless & Welberry, 1995; Haller, Rae, Bygott, Hockless, Ralph, Geue & Sargeson, 1999). The structure determined from the diffraction intensities is the spatial average of these orientations over the whole crystal. It is useful to distinguish two types of disorder: substitutional disorder (Szabó, Gonzáles-Arias & Szabó, 1980; Le Bas & Doucet, 1997) and positional disorder (Benno & Fritchie, 1973; Hazell, Simonsen, Wernberg, 1986; Wu & Max, 1996; Bose, Rahaman, Mostafa, Walsh, Zaworotko & Ghosh, 2004). Substitutional disorder, which is common in minerals and salt-like crystals, is when the same position of space is occupied by different types of atoms in different unit cells while positional disorder (more common in crystals of molecular compounds) is when an atom or group of atoms has different spatial location in different unit cells.

To model substitutional disorder, the different atomic species are introduced with the same coordinates but with different occupation factors, depending on the fraction of each species. Removing the exact superposition of atoms creates

refinement difficulties. Modeling positional disorder can be quite simple when the disordered atoms do not overlap. However models that exactly overlap some atoms to simplify refinement often produce strange geometry when these atoms are related to the resolved atoms.

In some cases the disorder is dynamic and collecting the data at low temperature can alter the disorder, converting dynamic to static disorder. In the other cases a phase transition orders a disorder. Disorder can be associated with the departure from a Gaussian distribution to describe some atom positions, the shortening of bond lengths from ideal values, and high apparent anisotropic displacement parameters. Inappropriate modeling results in electron density peaks and holes near the affected atoms.

Refinement problems occur when a disorder is not recognized or when the disorder causes atoms to not be clearly resolved in the average structure (Mahmoud & Wallwork, 1974). In many disordered situations the components of a disorder have essentially the same geometry and may have inherent symmetry. This can be used to advantage by controlling the number of variables describing a structure. Geometric knowledge from related structures can also be used. The determination of atom site occupancy is an essential part of the refinement of all disordered structures and linking occupancies to satisfy chemical and cell content requirements is useful. When the disorder is a stacking fault, the effect of the stacking fault can often be effectively described by varying the relative scales of components of the reflection data. For example shifting a layer of structure by 1/2**c** has no effect on *l* even reflections but the intensities of *l* odd reflections are reduced.

Sometimes, it may be difficult or impossible to distinguish between twinning and disorder. An uninformed refinement of a 2-fold disorder, in principle, doubles the number of variables, whereas the refinement of a twin model usually requires only one additional parameter. Refinements using stacking faults and twin models may avoid the need for a more complicated model.

Stacking faults

Stacking faults allow substructures to have alternative origins or orientations. Often this causes effects that can be modeled by changing the scale of reflection intensities or differences in reflection intensities for particular classes of reflections, but not necessarily for all classes of reflections. An approximate structure solution can identify the possibility of a stacking fault, and appropriate modeling can then be used to allow for the effects of such faults.

Polymorphism

Polymorphism is one of the most intriguing phenomena connected with crystal engineering. It has widely recognized practical and utilitarian implications, besides representing a substantial scientific challenge. Polymorphism means "many forms"; it means that a single chemical composition can exist in two or more crystal forms, sometimes with radically different bonding (Feeder & Jones, 1993; Valkonen, 1994; Baggio, Garland & Perec, 2003). Isomorphism implies the same structure for different components (Bats, Ma & Wagner, 2002; Braga, Cojazzi, Emiliani, Maini, Polito, Gobetto & Grepioni, 2002; Gainsford, Chong, Ingham & Tallon, 2002). Phase changes may be regarded as a form of polymorphism and may be central to understanding of crystallization mechanisms (Tolédano, Berry, Brown, Glazer,

Metselaar, Pandey, Perez-Mato, Roth & Abrahams, 2001; Birkedal, Bürgi, Komatsu & Schwarzenbach, 2003).

There are four types of structural transformations: displacive, reconstitutive, order-disorder, and polytrophic. A displacive polymorphism is when the internal arrangement is only slightly changed and no bonds are broken. The process is therefore reversible and instantaneous. Thus, no unstable polymorphs will occur (Steurer & Depmeier, 1989; Meyer, Paciorek, Schenk, Chapuis & Depmeier, 1994; Fütterer, Depmeier & Petříček, 1995). A reconstitutive polymorphism is the extensive rearrangement of the crystal structure and the breaking of atomic bonds and reassembly in a different structure (Grebille, Leligny, Ruyter, Labbé & Raveau, 1996; Daniels, 1998; Ishii, 2000). The rate in this type of transformation may be very low, because of the extensive rearrangement. Thus, unstable polymorphs may exist for long periods of time. Order-disorder polymorphism is common in alloys. The higher temperature forms are more disordered than lower temperature forms (Baudour & Meinnel, 1982; Herbstein & Samson, 1994; Matsumoto & Mizuguchi, 2001; Usman, Chantrapromma & Fun, 2001).

Polytypism is a special case of polymorphism. Organized layers or column are preserved but the stacking of these varies between polytypes. Layers can be translated or re-orientated to describe the relationship between polytypes. Unit cell size and space group can change. Layers in different polytypic structures may exhibit slight structural differences and may not be isomorphic in the strict crystallographic sense. However, the sequence and stacking of layers in a polytype are always subject to well-defined limitations (Chaudhary, 1993; Nespolo, Ferraris & Takeda, 2000; Varn & Canright, 2001; Onoda, Dhaussy & Kanke, 2003).

2.3. The Refinement of Nonroutine Structures

Rae has pioneered the use of several useful features in small molecule refinement, including defining atoms using refinable local coordinates relative to refinable orthonormal axial systems, refinable rigid group parameterizations for thermal motion, and the choice of constraints and restraints (Rae, 1975b; 1975c). Several of Rae's innovations implemented in the RAELS least squares structure refinement package (Rae, 1973; 1974a; 1974b; 1976; 1978) have been used to good advantage in our group over the years to conveniently handle nonroutine refinements. Some aspects such as use of constraints and restraints to control refinement of a structure containing poorly defined groups of disorder overlapped atoms (Haller & Rae, 1984), have subsequently been incorporated into standard routine refinement packages. Other aspects such as the ability to conveniently refine multiply twinned crystals or groups of atoms within larger refinable groups of atoms, essential in the refinement of the multiple twinned-disordered (benzylidene)aniline structures (Haller, Rae, Heerdegen, Hockless & Welberry, 1995) and the four-component metal sepulcherate intergrowth structures (Haller, Rae, Bygott, Hockless, Ralph, Geue & Sargeson, 1999), have been partially, but not fully, incorporated into standard routine refinement packages.

Refinable *TL* (libration) and *TLX* (libration with refinable origin) thermal groups, in addition to often providing more rational models of the atomic displacements, also decrease the total number of refinable variables thereby improving control of the refinement. This capability was utilized in all the refinements noted in the previous paragraph and is useful in relatively routine structures (Tomchick, Gibson, Haller & Dahl, 1987), and is a critical factor in the

successful refinement of extremely data-poor or massively disordered structures (Haller, Ivanca, Nasri, Safo & Scheidt, 1990).

Perhaps the most unusual feature for a standard small molecule refinement package found in RAELS is the ability to conveniently model structure modulations as interacting substructures and evaluating structure factor by combining the structure factors from pseudo symmetry related reflections of a prototype structure. A variety of examples of modulated structure refinements using RAELS exist (Haller & Rae 1993; Rae, Thompson, Withers & Willis, 1990; Rae, Thompson & Withers, 1991; 1992). No other standard small molecule refinement package has all its capabilities.

2.4 References

Allan, D. R.; McGregor, P. A; McLachlan, L. J.; Parsons, S. and Pulham, C. R. (2002). Treatment of `twinning' in isopropylcyclohexane. **Acta Crystallographica** E58: o652-o655.

Baggio, R., Garland, M. T. and Perec, M. (2003). A new polymeric phase of zinc(II) oxydiacetate. **Acta Crystallographica** C59: m30-m32.

Bats, J. W., Ma, K. and Wagner, M. (2002). Isomorphism and phase transition in triferrocenylboroxine and triferrocenylborazine. **Acta Crystallographica** C58: m129-m132.

Baudour, J. L. and Meinnel, J. (1982). Discussion of an order-disorder behaviour Near T_c in the chloranil displacive transition. **Acta Crystallographica** B38: 472-479.

Benno, R. H. and Fritchie Jr., C. J. (1973). Metal-flavin interactions: The crystal structure of bis-(10-methylisoalloxazine)silver nitrite tetrahydrate and similar disordered nitrate-nitrite. **Acta Crystallographica** B29: 2493-2502.

Bernardinelli, G. and Flack, H. D. (1985). Least-squares absolute-structure refinement. Practical experience and ancillary calculation. **Acta Crystallographica** A41: 500-511.

Birkedal, H., Bürgi, H.-B., Komatsu, K. and Schwarzenbach, D. (2003). Polymorphism and stacking disorder in tris(bicyclo[2.1.1]hexeno)benzene. **Journal of Molecular Structure** 647: 233-242.

Boese, R., Gehrke, A., Kapon, M. and Herbstein, F. H. (2000). Determining the crystal structure of twinned 2-methylpyrazine. **Acta Crystallographica** B56: 677-681.

Bolte, M. (1994). Refinement of a twinned structure with *SHELXL93: meso*-2,2'-[1,6-bis(methylamino)-3,4-dithia-l,6-hexanediyl]diphenol. **Acta Crystallographica** C50: 1368-1370.

Bolte, M. and Ketter, M. (1998). The twinned crystal structure of 3,4-dimethyl pyridine hydrobromide at 157 K. **Acta Crystallographica** C54: 963-964.

Bose, D., Rahaman, S. H., Mostafa, G., Walsh, R. D. B., Zaworotko, M. J. and Ghosh, B. K. (2004). Synthesis, structure and properties of $[Zn(dpa)(N_3)_2]$ and $[Zn(dpa)(N_3)(NO_3)]_2$ (dpa=2,2′-dipyridylamine): Composition tailored architectures. **Polyhedron** 23: 545-552.

Braga, D., Cojazzi, G., Emiliani, D., Maini, L., Polito, M., Gobetto, R. and Grepioni, F. (2002). Two concomitant polymorphs and two isomorphous forms with

different chemical compositions, which transform into the same substance upon thermal treatment. **CrystEngComm** 4(50): 277-281.

Chaudhary, S. K. (1993). Impurity- and temperature-dependent structural transforma tions in polytypic crystals of CdI_2, PbI_2 and $CdBr_2$. **Acta Crystallographica** B49: 454-458.

Cooper, R. I., Gould, R. O., Parsons, S. and Watkin; D. J. (2002). The derivation of nonmerohedral twin laws during refinement by analysis of poorly fitting intensity data and the refinement of nonmerohedrally twinned crystal structures in the program *CRYSTALS*. **Journal of Applied Crystallography** 35: 168-174.

Cotton, F. A. and Rice, G. W. (1978). Crystal and molecular structure of tris[tetra-μ-formato-diaquodichromium(ii)] decahydrate: A case of an unusually good false minimum in a structure solution. **Inorganic Chemistry** 17(3): 688-692.

Daniels, P. (1998). Deeasil (SiO_2): Multiple twinning and two-dimensional disorder. **Journal of Applied Crystallography** 31: 559-569.

Degen, A. and Bolte, M. (2001). The twinned crystal structure of 3-indolylacetic acid **Acta Crystallographica** E57: o999-o1000.

Feeder, N. and Jones, W. (1993). Crystal structures and polymorphism in aliphatic *p*-amidobenzoic acids. **Acta Crystallographica** B49: 541-546.

Flack, H. D. (1983). On enantiomorph-polarity estimation. **Acta Crystallographica** A39: 876-881.

Flippen-Anderson, J. L., Deschamps, J. R., George, C., Folk, J. E., Jacobson, A. E. and Rice, K. C. (2002). Twinned 1-{2-[bis(4-fluorophenyl)methoxy]ethyl}-4-(3-phenyl)propyl)piperazinium chloride (GBR12909). **Acta Crystallogra-**

phica E58: o81-o82.

Fütterer, K., Depmeier, W. and Petříček, V. (1995). The low-temperature phase transition sequence of the halide perovskite tetramethylammonium trichloro-germanate(II) and the structure of its incommensurately modulated δ-phase. **Acta Crystallographica** B51: 768-779.

Gainsford, G. J., Chong, S. V., Ingham, B. and Tallon, J. L. (2002). Decaammonium dodecatungstate nonahydrate, $(NH_4)_{10}[H_2W_{12}O_{42}]\cdot 9H2O$: Anionic `isomor-phism'. **Acta Crystallographica** E58: i93-i94.

Giacovazzo, C., Monaco, M. L., Artioli, G., Viterbo, D., Ferraris, G., Gilli, G., Zanotti, G. and Catti, M. (2002). *Fundamentals of Crystallography.* Carlo Giacovazzo, Editor, 2nd edition, **Oxford, New York.**

Grainger, C. T. (1969a). A chart for interpreting the Weissenberg photographs of pseudo-merohedral twins. **Acta Crystallographica** A25: 435-438.

Grainger, C. T. (1969b). Pseudo-merohedral twinning: The treatment of overlapped data. **Acta Crystallographica** A25: 427-434.

Grebille, D., Leligny, H., Ruyter, A., Labbé, Ph. and Raveau, B. (1996). Static disorder in the incommensurate structure of the high T_c superconductor $Bi_2Sr_2CaCu_2O_{8+\delta}$. **Acta Crystallographica** B52: 628-642.

Haller, K. J., Ivanca, M. A., Nasri, H., Safo, M. and Scheidt, W. R. (1990). Refinement of concerted thermal motion in tetraaryl metalloporphyrin derivatives. **Acta Crystallographica** A46: C303.

Haller, K. J. and Rae, A. D. (1984). Controlled refinement of a structure containing poorly defined groups of atoms: (μ_2-carbonyl)-(μ_2-sigma-2-η^2-2,3-diphenyl-1-oxo-penta-2,4-dien-1,4-diyl)-carbonyl-*bis*(η^5-cyclopenta-dienyl)-diiron toluene solvate. **Acta Crystallographica** A40: C427.

Haller, K. J. and Rae A. D. (1993). The modulated crystal structure of a metalloporphyrin π-cation radical. **Acta Crystallographica** A49: S242.

Haller, K. J., Rae, A. D., Bygott, A. M. T., Hockless, D. C. R., Ralph, S. F., Geue, R. J. and Sargeson, A. M. (1999). Four-component intergrowth structures of the metal-ion cage complexes *fac*-(1,5,9,13,20-pentamethyl-3,7,11,15,18,22-hexaazabicyclo[7.7.7]tricosane)M^{II} diperchlorate hydrate, $[M(C_{22}H_{48}N_6)](ClO_4)_2{\cdot}xH_2O$, M = Ni, Zn. **Acta Crystallographica** B55: 380-388.

Haller, K. J., Rae, A. D., Heerdegen, A. P., Hockless, D. C. R. and Welberry, T. R. (1995). The fourfold disordered structures of *p*-chloro-*N*-(*p*-methylbenzylidene) aniline and *p*-methyl-*N*-(*p*-chlorobenzylidene)aniline. **Acta Crystallographica** B5: 187-197.

Hazell, A., Simonsen, O. and Wernberg, O. (1986). Complexes of 2,2'-bipyridine (bpy) and 1,10-phenanthroline (phen) with platinum(II). Structures of $[Pt^{II}(bpy)_{1.3}(phen)_{0.7}](NO_3)_2{\cdot}0.3H_2O$ and $[Pt^{II}(bpy)_2](NO_3)_2{\cdot}H_2O$. **Acta Crystallographica** C42: 1707-1711.

Herbstein, F. H. and Marsh, R. E. (1998). More space-group corrections: from triclinic to centered monoclinic and to rhombohedral; also from $P1$ to $P\bar{1}$ and from *Cc* to *C2/c*. **Acta Crystallographica** B54: 677-686.

Herbstein, F. H. and Samson, S. (1994). X-ray diffraction study of the disorder-to-order transition at ~160 K in the π-molecular compound pyrene···pyromellitic dianhydride. **Acta Crystallographica** B50: 182-191.

Herbst-Irmer, R. and Sheldrick, G. M. (1998). Refinement of twinned structures with *SHELXL97*. **Acta Crystallographica** B54: 443-449.

Herbst-Irmer, R. and Sheldrick, G. M. (2002). Refinement of obverse/reverse twins. **Acta Crystallographica** B58: 477-481.

Ishii, Y. (2000). Anisotropic phasonic diffuse scattering from decagonal quasicrystals. **Materials Science and Engineering A** 294-296: 377-380.

Le Bas, G. and Doucet, J. (1997). Disorder in cyclodextrin clathrates: X-ray diffuse scattering analysis of α-cyclodextrin cyclopentanone hydrate. **Acta Crystallographica** B53: 673-679.

Lutz, M. and Bakker, R. (2003). Redetermination of chloro(triethanol-aminato) zinc(II) at 150 K. **Acta Crystallographica** E59: m74-m76.

Machado, W. G.; Moore, M. and Yacoot, A. (1998). Twinning in natural diamond. II. interpenetrant cubes. **Journal of Applied Crystallography** 31: 777-782.

Mahmoud, M. M. and Wallwork, S. C. (1974). The crystal structures of the 1:1 complexes formed by hexamethylenetetramine with hydroquinone and resorcinol**. Acta Crystallographica** B35: 2370-2374.

Marsh, R. E. and Schomaker, V. (1979). Some incorrect space groups in *Inorganic Chemistry*, vol. 16. **Inorganic Chemistry** 18(8): 2331-2336.

Matsumoto, S. and Mizuguchi, J. (2001). Structures of tetrathiabenzoquinone derivatives and the order-disorder phase transition. **Acta Crystallographica** B57: 82-87.

Meyer, M., Paciorek, W. A., Schenk, K. J., Chapuis, G. and Depmeier, W. (1994). Incommensurately modulated structure of γ-PAMC: New experimental evidence for amplitude and phase fluctuations. **Acta Crystallographica** B50: 333-343.

Murphy, V. J., Rabinovich, D., Hascall, T., Klooster, W. T., Koetzle, T. F. and Parkin, G. (1998). False minima in X-ray structure solutions associated with a "partial polar ambiguity": single x-ray and neutron diffraction studies on the eight-coordinate tungsten hydride complexes, $(PMe_3)_4H_2X_2$ (X = F, Cl, Br) and $W(PMe_3)_4H_2F_2(H_2O)$. **Journal of the American Chemical Society** 120(18): 4372-4387.

Murphy, V. J., Rabinovich, D. and Parkin, G. (1995). False minima and the perils of a polar axis in X-ray structure solutions: Molecular structures of $W(PMe_3)_4H_2X_2$ (X = F, Cl, Br) and $W(PMe_3)_4H_2F_2(H_2O)$. **Journal of the American Chemical Society** 117(38): 9762-9763.

Nespolo, M., Ferraris, G. and Takeda, H. (2000). Twins and allotwins of basic mica polytypes: Theoretical derivation and identification in the reciprocal space. **Acta Crystallographica** A56: 132-148.

Onoda, M.; Dhaussy, A.-C.; Kanke, Y. (2003). Structural characterization of YV_4O_8: simultaneous analysis of coexisting polytypes and simulation of diffuse scattering for a stacking disorder model. **Acta Crystallographica** B59: 429-438.

Rae, A. D. (1973). A new approach to the least-squares refinement of highly covarying parameters in crystal structure determinations. **Acta Crystallographica** A29: 74-77.

Rae, A. D. (1974a). The phase problem and its implications in the least-squares refinement of crystal structures. **Acta Crystallographica** A30: 761-768.

Rae. A. D. (1974b). False minima in the least-squares refinement of noncentrosymmetric crystal structures. **Acta Crystallographica** A30, 853.

Rae, A. D. (1975a). Phase reliability and the refinement of pseudo symmetric crystal structures. **Acta Crystallographica** A31: 575-582.

Rae, A. D. (1975b). Crystal structure refinement using a number of orthonormal axial systems. **Acta Crystallographica** A31: 560-570.

Rae, A. D. (1975c). Rigid-body motion in crystals-the application of constraints on the *TLS* model. **Acta Crystallographica** A31: 570-574.

Rae, A. D. (1976). Rigid-body constraints and the least-squares refinement of crystal structures. **Acta Crystallographica** A32: 895-897.

Rae, A. D. (1978). An optimized conjugate gradient solution for least-square equations. **Acta Crystallographica** A34: 578-582.

Rae, A. D., Thompson, J. G., and Withers, R., (1991). Structure refinement of commensurately modulated bismuth tungstate, Bi_2WO_6. **Acta Crystallographica** B47: 870-881.

Rae, A. D., Thompson, J. G., and Withers, R., (1992). Structure refinement of commensurately modulated bismuth strontium tantalate, $Bi_2SrTa_2O_9$. **Acta Crystallographica** B48: 418-428.

Rae, A. D., Thompson, J. G., Withers, R., and Willis, A. C. (1990). Structure refinement of commensurately modulated bismuth titanate, $Bi_4Ti_3O_{12}$. **Acta Crystallographica** B46: 474-487.

Sadanaga, R. and Takeuchi, Y. (1961). Polysynthetic twinning of micas. **Zeitschrift für Kristallographie** 116: 406-429.

Schaefer, W. P., Marsh, R. E., Rodriguez, G. and Bazan, G. C. (1996). A tribenzylidene-methane-tantalum compound: Some experiences with 'inversion twinning'. **Acta Crystallographica** B52: 465-470.

Steurer, W. and Depmeier, W. (1989). Structure of the incommensurately modulated ε-phase of the layered perovskite $[NH_3(C_3H_7)]_2MnCl_4$ (PAMC) at 130 K. **Acta Crystallographica** B45: 555-562.

Szabó Sr., P., Gonzáles-Arias, A. and Szabó Jr., P. (1980). Substitutional disorder, diffraction and domain size. **Acta Crystallographica** A36: 83-88.

Tolédano, J.-C., Berry, R. S., Brown, P. J., Glazer, A. M., Metselaar, R., Pandey, D., Perez-Mato, J. M., Roth, R. S. and Abrahams, S. C. (2001). Nomenclature of magnetic, incommensurate, composition-changed morphotropic, polytype, transient-structural and quasicrystalline phases undergoing phase transitions. II. Report of an IUCr working group on phase transition nomenclature. **Acta Crystallographica** A57: 614-626.

Tomchick, D. R., Gibson, C. P., Haller, K. J. and Dahl, L. F. (1987). Structural-bonding analysis of several unusual molybdenum clusters: Constrained refinements of disordered and thermally librating ligands. **Acta Crystallographica** A43: C192.

Usman, A., Chantrapromma, S. and Fun, H.-K. (2001). The 143 and 300 K polymorphs of hexamethylenetetraaminium 2,4-di-nitrophenolate monohydrate. **Acta Crystallographica** C57: 1443-1446.

Valkonen, J. (1994). Cadmium selenite-water (4/3) and two polymorphic forms of cadmium selenite. **Acta Crystallographica** C50: 991-994.

van Koningsveld, H. (1983). Twinning by pseudo merohedry in ammonium tetrachlorozincate. A reinvestigation of the crystal structure at room temperature. **Acta Crystallographica** C39: 15-19.

Varn, D. P. and Canright, G. S. (2001). The crystal problem for polytypes. **Acta Crystallographica** A57: 4-19.

Weber, T., Boysen, H., Frey, F. and Neder, R. B. (1997). Modulated structure of the composite crystal urea/*n*-heptadecane. **Acta Crystallographica** B53, 544-552.

Wu, D.-D. and Max, T. C. W. (1996). Polymeric cadmium(II) nitrate adduct of a flexible double betaine: $[Cd_2(L)_2(NO_3)_2(H_2O)_3]_n(NO_3)_{2n}$ [*L* = *meso*-2,5-bis(trimethyl ammonio)adipate]. **Acta Crystallographica** C52: 529-532.

Yacoot, A., Moore, M. and Machado, W. G. (1998). Twinning in natural diamond. I. Contact twins. **Journal of Applied Crystallography** 31: 767-776.

Zuñiga, F. J., Madariaga, G., Paciorek, W. A., Péres-Mato, J. M., Ezpeleta, J. M. and Etxebarria, I. (1989). Modulated structure of thiourea. **Acta Crystallographica** B45, 566-576.

CHAPTER III

POLYTYPISM IN 1,10-PHENANTHROLIN-1-IUM (2-CARBOXYETHYL)(2-CARBOXYLATOETHYL) DICHLOROSTANNATE(IV)

3.1 Abstract

The 1:1 adduct of $[SnCl_2(C_2H_4COOCH_3)_2]$ and 1,10-phenanthroline, $[C_{12}H_8N_2]$, that was set aside for 25 years, when recrystallized from ethanol turned out to be the salt, $[C_{12}H_9N_2]^+\cdot[SnCl_2(C_2H_4COOH)(C_2H_4COO)]^-$. The Sn(IV) in the anion has pseudo octahedral coordination with two *cis* Cl atoms, two C atoms, and two O atoms *trans* to the Cl atoms. The possibility of alternative stacking of layers perpendicular to **c*** offers an explanation for observed twinning and polytypism. An ordered, untwinned, $Z = 2$, crystal structure was determined. Pairs of adjacent anions are linked together by strong intermolecular O−H···O^- hydrogen bonds and the cation contains a strong intramolecular N−H···N hydrogen bond between its two nitrogen atoms. The protonated ring of the cation exhibits increased Lewis acidity and is linked into a network with the anions using a strong N−H···O and weak C−H···O, and C−H···Cl interactions. The remaining rings of the cation form weaker C−H···O and C−H···Cl interactions. The cations stack in columns along **a** with interplanar spacing of 3.24 Å for separations between cations inversion related about 1, 1/2, 1/2 and 3.34 Å for separations between cations inversion related about 1/2, 1/2,1/2.

3.2 Introduction

Supramolecular synthons are important in crystal engineering and molecular networks (Desiraju, 1995; 1997; Langley, Hulliger, Thaimattam & Desiraju, 1998). Crystal structures with donor-acceptor groups (−OH, $-NH_2$, −COOH) create specific strong and weak hydrogen bonding (Kuduva, Craig, Nangia & Desiraju, 1999; Kuduva, Bläser, Boese & Desiraju, 2001; Vishweshwar, Nangia & Lynch, 2002). Both the strong and weak hydrogen bonds are a key aspect of crystalline architecture and help to correctly predict the structure and material properties of an assembly. The networks of supramolecular motifs strongly influence the local structure and ultimately the crystal packing (Liu, Mok & Valiyaveettil, 2001; Ballabh, Trivedi, Dastidar & Suresh, 2002). Previous studies of the organometallic zwitterions, cations, and anions containing coordinated carboxylic acid and carboxylate groups (Braga, Maini & Grepioni, 1998; Braga, Maini, Polito & Grepioni, 1999; Braga, Maini, Grepioni, Elschenbroich, Paganelli & Schiemann, 2001) show very relevant supramolecular aggregates. They show a strong hydrogen bonded interaction when a carboxylic acid and a carboxylate cocrystallize. These important hydrogen bonding interactions suggest the use of such species as synthons for the preparation of supramolecular aggregates.

Sn(IV) and organotin(IV) compounds display a strong biological activity and exhibit antitumor properties. It is hoped to identify compounds containing active antitumor organotin(IV) moieties. Sn(IV) forms a variety of complexes with ligands containing a donor atom (Ng & Das, 1997; Ng, 1998; Lo, Das, Ng & Hook, 1999; Ng & Hook, 1999; Chee, Lo & Ng, 2003a). Organotin complexes with carboxyl groups have been extensively explored with particular interest in polymeric chains and

structure motifs. In some Sn(IV) complexes, the Sn atoms have a distorted bipyramidal geometry (Parvez, Ali, Bhatti, Khokhar, Mazhar & Qureshi, 1999; Parvez, Ali, Mazhar, Bhatti & Khokhar, 1999) and in some they have a distorted octahedral geometry (Hall & Tiekink, 1996).

Ng and coworkers have studied complexes between Sn and 1,10-phenanthroline and related molecules (*e.g.* $[(p\text{-}ClC_6H_4)_3SnCl\cdot H_2O\cdot o\text{-}C_{12}H_8N_2]_2$, Ng & Das, 1996; $[Sn(C_2ClF_2O_2)(C_6H_5)_3\ (H_2O)]_2\cdot C_{12}H_8N_2$, Ng, 1997; $[Sn(C_2F_3O_2)(C_6H_5)_3(H_2O)]\cdot C_{15}H_{11}N_3$, Chee, Lo & Ng, 2003b; $[Sn_2(C_6H_5)_6(C_4H_4O_4)(H_2O)_2]\cdot 2C_{12}H_8N_2$, Chee, Lo & Ng, 2003c). In these structures, the organotin interacts with the phenanthroline indirectly through a coordinated water molecule that forms a short hydrogen bond with one of the 1,10-phenanthroline nitrogen atoms.

We report the supramolecular structure of $[SnCl_2(C_2H_4COOH)(C_2H_4COO)]^-\cdot[C_{12}H_9N_2]^+$. A room temperature data set was collected by Ng (2000) for a $Z = 6$, $P\bar{1}$ structure with $a = 7.225(1)$, $b = 12.576(2)$, $c = 34.334(1)$ Å, $\alpha = 82.14(1)$, $\beta = 86.90(1)$, $\gamma = 74.84(1)°$. His refinement was not successful ($R = 0.32$) though a strong vector in the Patterson function of 2/3, 1/3, 1/3 suggested pseudo translational symmetry. However the ratio of the height of this peak to that of the origin peak is only 0.46, suggesting a simple displacive modulation of an ordered $Z = 2$ parent structure is unlikely. This parent structure would make no contribution to reflections with $-h+k+l \neq 3n$.

When we studied this material we obtained a data set for a perfectly ordered untwinned crystal with a unit cell volume corresponding to $Z = 2$. The most rational explanation of Ng's data set is that it comes from a polytype related to our structure.

Its unit cell is a'' = 7.225(1), b'' = 12.576(2), c'' = 34.394(1), α'' = 82.14(1), β'' = 86.90(1), γ'' = 74.84(1)° suggesting that layers perpendicular to **c*** are common to both structures, since **a**" ≅ −**a**, **b**" ≅ **b**, and $\gamma'' \cong 180-\gamma$.

A suggestion of an appropriate model for Ng′s crystal is made at the end of this chapter.

3.3 X-Ray Crystallography

A colorless single crystal was obtained from a large needle by cleaving to eliminate part of the crystal that was clearly twin related because a reentrant angle defined a twin plane. Reflection intensities were collected on a Bruker-Nonius KappaCCD diffractometer using the COLLECT (Nonius, 1998) software. The diffractrometer was equipped with a fine focus molybdenum X-ray source, (graphite monochromated Mo $K\alpha$ radiation, λ = 0.71073 Å), a 0.3 mm *ifg* capillary collimator, and a series 600 Oxford Cryostream crystal cooler (Oxford Cryosystems, 1997) operating at 200 K. Unit cell determination and data reduction were performed with DENZO-Scalepack (Otwinowski & Minor, 1997). Structure solution used SIR97 (Altomare, Burla, Camalli, Cascarano, Giacovazzo, Guagliardi, Moliterni, Polidori & Spagna, 1999), and refinement used the SHELXTL system (Bruker AXS Inc., 1998). All 18 hydrogen atom positions were located from an electron density difference map. The coordinates and isotropic atomic displacement parameters for the NH and OH hydrogen atoms were refined and the CH hydrogen atoms were included as idealized riding model contributors with $U_{iso} = 1.2U_{eq}$(attached C).

Crystal data and details of the data collection and structure refinement are summarized in Table 3.1. Fractional coordinates and isotropic equivalent atomic

displacement parameters for the refined atoms are given in Table 3.2. Anisotropic atomic displacement parameters for the nonhydrogen atoms are given in Table 3.3. Selected interatomic bond distances and angles are in Tables 3.4 and 3.5. Hydrogen bond parameters are given in Tables 3.6. Calculated hydrogen atom positions and isotropic atomic displacement parameters for the hydrogen atoms are given as supplementary material in Appendix B as Table B.1.

Table 3.1. Experimental details for $[SnCl_2(C_2H_4COOH)(C_2H_4COO)]^-\cdot[C_{12}H_9N_2]^+$.

Crystal data	
Chemical formula	$C_6H_9O_4SnCl_2\cdot C_{12}H_9N_2$
Chemical formula weight	515.93
Cell setting, space group	Triclinic, $P\bar{1}$
***a* (Å)**	**7.1204(1)**
***b* (Å)**	**12.5017(2)**
***c* (Å)**	**12.5780(2)**
***α* (º)**	**114.424(1)**
***β* (º)**	**92.562(1)**
***γ* (º)**	**104.354(1)**
Volume (Å^3)	**973.78(3)**
Z	**2**
D_{calc} (Mg/m^3)	1.760
Radiation type, wavelength (Å)	Mo $K\alpha$, 0.71073
No. of reflections for cell parameters	25,992
θ range (º)	2.91-29.57
Absorption coefficient, μ (mm^{-1})	1.613
Temperature (K)	200(1)
Crystal color, form	Transparent colorless, needles
Crystal size (mm)	0.12 × 0.14 × 0.17

Table 3.1. (Continued).

Data collection	
Diffractometer	Nonius KappaCCD
Data collection method	φ scan plus ω scans with κ offsets
Absorption correction	Multi-scan
T_{min}, T_{max}	0.798, 0.824
No. of measured reflections	28,062
No. of unique independent data	5,019
No. of observed reflections	4,174
Criterion for observed reflections	$I > 2\sigma(I)$
R_{merge} ($P1$, before absorption correction)	0.055
R_{merge} ($P1$, after absorption correction)	0.035
R_{equiv} (P-1 merge (9278 to 5019 data))	0.0244
θ_{max} (º)	28.69
Range of h, k, l	$-9 \rightarrow h \rightarrow 9$ $-16 \rightarrow k \rightarrow 16$ $-16 \rightarrow i \rightarrow 16$
Refinement	
Refinement on	F^2
R[all data], $wR(F^2)$, S	0.0401, 0.0632, 0.966
$R[F^2 > 2\sigma(F^2)]$, $wR(F^2)$, S	0.0288, 0.0594, 1.001
No. of reflections used	5,019
No. of parameters	251
H atom treatment	refined xyzU for NH and OH idealized riding model for CH
$(\Delta/\sigma)_{max}$	0.003
$\Delta\rho$ [max, min, err] (e Å^{-3})	1.31, -0.68, 0.09
Data collection program	COLLECT
Cell and data reduction program	DENZO/Scalepack
Absorption correction program	SORTAV
Structure solution program	SIR97
Structure refinement program	SHELXTL
Structure refinement program	SHELXTL
Graphics program	ORTEP

Computer programs: *COLLECT* (Nonius, 1998); *DENZO-SMN* (Otwinowski & Minor, 1997); *SORTAV* (Blessing, 1997), *SIR97* (Altomare *et al.*, 1999); *SHELXTL* (Bruker AXS Inc., 1998); *ORTEP-III* (Burnett & Jhnson, 1996, Farrugia, 1997).

Table 3.2. Fractional atomic coordinates[a] and isotropic displacement parameters[b] (Å^2) for the nonhydrogen atoms in $[SnCl_2(C_2H_4COOH)(C_2H_4COO)]^-\cdot[C_{12}H_9N_2]^+$.

Atom	*x*	*y*	*z*	U_{iso} or U_{eq}
Sn1	0.40500(2)	0.111904(14)	0.817654(13)	0.02452(6)
Cl11	0.24231(10)	0.04003(6)	0.94939(6)	0.04213(16)
Cl12	0.40291(10)	0.32885(5)	0.92664(5)	0.03442(14)
O11	0.60704(24)	0.17256(16)	0.68119(14)	0.0326(4)
C11	0.7736(3)	0.23390(21)	0.73721(20)	0.0264(5)
O12	0.90751(26)	0.29248(17)	0.69688(16)	0.0330(4)
C12	0.8357(3)	0.24889(23)	0.85953(21)	0.0314(5)
C13	0.7052(3)	0.14767(23)	0.88399(21)	0.0305(5)
O13	0.38182(25)	−0.08906(15)	0.69251(14)	0.0316(4)
C14	0.2685(3)	−0.12828(21)	0.59481(20)	0.0254(5)
O14	0.21802(24)	−0.23959(14)	0.51962(14)	0.0293(4)
C15	0.1926(3)	−0.03730(20)	0.56859(20)	0.0266(5)
C16	0.1690(3)	0.06567(21)	0.68129(20)	0.0263(5)
C31	0.8463(4)	0.76566(25)	0.76727(26)	0.0414(7)
C32	0.8916(4)	0.70094(25)	0.82489(25)	0.0428(7)
C33	0.8819(4)	0.57786(24)	0.75913(22)	0.0353(6)
N34	0.83199(28)	0.51821(18)	0.64223(17)	0.0294(4)
C35	0.7857(3)	0.58269(21)	0.58614(21)	0.0262(5)
C36	0.7889(3)	0.70640(23)	0.64400(24)	0.0333(6)
C37	0.7293(4)	0.76445(24)	0.57683(27)	0.0400(7)
C38	0.6753(4)	0.70452(24)	0.45841(26)	0.0385(6)
C39	0.6767(3)	0.57978(24)	0.39488(24)	0.0317(6)
C40	0.7274(3)	0.51968(22)	0.45920(21)	0.0260(5)
N41	0.71708(29)	0.39916(19)	0.40163(18)	0.0259(4)
C42	0.6642(4)	0.33559(24)	0.28414(21)	0.0329(6)
C43	0.6189(4)	0.39247(26)	0.21674(23)	0.0390(6)
C44	0.6244(4)	0.51338(27)	0.27119(24)	0.0378(6)

[a]Estimated standard deviations of the least significant digits are given in parentheses.

[b]Equivalent isotropic atomic displacement parameters for the atoms refined anisotropically, $U_{eq} = 1/3 \sum_i \sum_j U_{ij}\, a_i^* a_j^*\, \mathbf{a}_i \cdot \mathbf{a}_j$

Table 3.3. Anisotropic atomic displacement parameters[a] in $[SnCl_2(C_2H_4COOH)(C_2H_4COO)]^-\cdot[C_{12}H_9N_2]^+$.

Atom	*U11*	*U22*	*U33*	*U12*	*U13*	*U23*
Sn1	0.02707(9)	0.02620(9)	0.02103(9)	0.00771(7)	0.00218(6)	0.01127(7)
Cl11	0.0500(4)	0.0443(4)	0.0345(3)	0.0064(3)	0.0137(3)	0.0231(3)
Cl12	0.0443(4)	0.0259(3)	0.0296(3)	0.01122(26)	−0.00163(27)	0.00910(26)
O11	0.0277(9)	0.0439(10)	0.0232(9)	0.0010(8)	−0.0010(7)	0.0177(8)
C11	0.0275(12)	0.0285(13)	0.0237(12)	0.0094(10)	0.0045(10)	0.0112(10)
O12	0.0305(10)	0.0394(11)	0.0269(10)	0.0017(8)	0.0009(8)	0.0176(9)
C12	0.0257(12)	0.0414(15)	0.0256(12)	0.0051(11)	0.0006(10)	0.0163(11)
C13	0.0298(13)	0.0406(14)	0.0271(13)	0.0111(11)	0.0022(10)	0.0196(12)
O13	0.0379(10)	0.0278(9)	0.0247(9)	0.0137(8)	−0.0032(7)	0.0060(7)
C14	0.0268(12)	0.0277(12)	0.0232(12)	0.0083(10)	0.0054(9)	0.0123(10)
O14	0.0394(10)	0.0243(9)	0.0226(8)	0.0101(7)	0.0021(7)	0.0087(7)
C15	0.0311(13)	0.0266(12)	0.0219(11)	0.0087(10)	−0.0008(10)	0.0109(10)
C16	0.0261(12)	0.0259(12)	0.0268(12)	0.0077(9)	−0.0012(10)	0.0119(10)
C31	0.0332(14)	0.0330(14)	0.0455(17)	0.0066(11)	0.0061(12)	0.0069(13)
C32	0.0359(15)	0.0448(17)	0.0314(14)	0.0063(13)	−0.0015(12)	0.0051(13)
C33	0.0308(14)	0.0424(15)	0.0297(14)	0.0079(11)	−0.0001(11)	0.0151(12)
N34	0.0254(10)	0.0331(11)	0.0289(11)	0.0067(9)	0.0020(8)	0.0141(9)
C35	0.0206(11)	0.0279(12)	0.0309(13)	0.0053(9)	0.0057(9)	0.0144(11)
C36	0.0239(12)	0.0317(13)	0.0437(15)	0.0065(10)	0.0095(11)	0.0165(12)
C37	0.0330(14)	0.0326(14)	0.0625(15)	0.0106(11)	0.0153(13)	0.0273(14)
C38	0.0289(13)	0.0434(16)	0.0621(19)	0.0140(12)	0.0148(13)	0.0385(15)
C39	0.0204(12)	0.0425(15)	0.0448(15)	0.0084(10)	0.0091(11)	0.0312(13)
C40	0.0184(11)	0.0319(13)	0.0338(13)	0.0062(9)	0.0067(9)	0.0205(11)
N41	0.0264(10)	0.0318(11)	0.0269(11)	0.0092(9)	0.0049(8)	0.0194(9)
C42	0.0327(14)	0.0388(14)	0.0248(12)	0.0054(11)	0.0020(10)	0.0151(11)
C43	0.0361(15)	0.0550(18)	0.0293(13)	0.0067(13)	0.0015(11)	0.0259(13)
C44	0.0299(13)	0.0571(18)	0.0422(16)	0.0120(12)	0.0078(12)	0.0370(15)

[a]Estimated standard deviations of the least significant digits are given in parentheses.

3.4 Results and Discussion

In the structure of $[SnCl_2(C_2H_4COOH)(C_2H_4COO)]^-\cdot[C_{12}H_9N_2]^+$, one proton has transferred from a neutral Sn dicarboxylic acid complex to form a complex monoanion, $[SnCl_2(C_2H_4COOH)(C_2H_4COO)]^-$ with one −COOH and one $-COO^-$ (see Figure 3.1) and the 1,10-phenanthrolin-1-ium(+) monocation, $[C_{12}H_9N_2]^+$, so-called $phenH^+$ (see Figure 3.2). Structures involving ionic building blocks are usually more stable than the corresponding molecular solids, including those formed exploiting strong hydrogen bonds (Lee, Kolthoff & Leussing, 1948; Kuĺba, Makashev & Fedyaev, 1976). The $phenH^+$ cation has two N atoms only 2.74 Å apart and protonation allows a hydrogen bond between these atoms. McBryde (1965) suggested steric factors would usually prevent the transfer of a second proton, but subsequently neutral(phen) (Nishigaki, Yoshioka & Nakatsu, 1978), monoprotonated ($phenH^+$) (Wang, Wang, Liao & Yan, 1999a), and diprotonated ($phenH_2^{2+}$) (Wang, Wang, Liao & Yan, 1999b) have been reported.

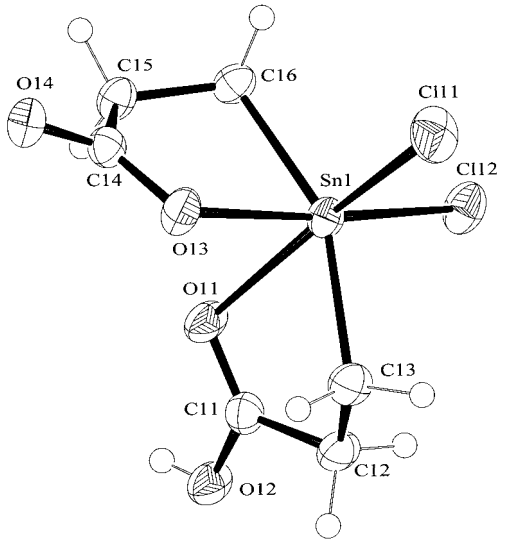

Figure 3.1. *ORTEP* drawing of the $[SnCl_2(C_2H_4COOH)(C_2H_4COO)]^-$ complex anionshowing 50% probability displacement ellipsoids.

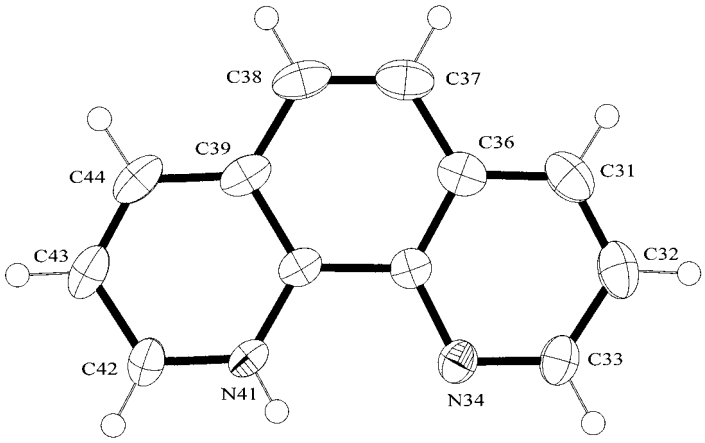

Figure 3.2. *ORTEP* drawing of the $phenH^+$ cation showing 50% probability displacement ellipsoids.

The $[SnCl_2(C_2H_4COOH)(C_2H_4COO)]^-$ anion

This anion has octahedral geometry with the chloride atoms in a *cis* configuration. Each bidentate ligand is coordinated by a C and an O atom with the oxygen atoms *trans* to chloride atoms and the C atoms *trans* to each other. The $Sn{-}C_{carboxylic\ acid}$ distance of 2.127(2) Å is not significantly shorter than the $Sn{-}C_{carboxylate}$ distance of 2.131(2) Å. However, the angle of C−Sn−O (carboxylic acid) of 72.78(7)° is significantly smaller than the C−Sn−O (carboxylate) angle of 77.42(7)°. The oxygen atom of the carboxylic acid group is more weakly bound to the tin atom, *d*[Sn−O11] = 2.519(2) Å, than that of the carboxylate group, *d*[Sn−O13] = 2.306(2) Å. The difference in the tin-oxygen binding is also apparent in the coordination of the chloride anions *trans* to the oxygen atoms. The chloride *trans* to the carboxylic acid is tightly bound, *d*[Sn−Cl11] = 2.404(1) Å, while the chloride *trans* to the carboxylate group has *d*[Sn−Cl12] = 2.486(1) Å. The angles of the

coordination sphere are distorted from ideal octahedral values because of the small bite angle of the chelate rings.

The carbon-oxygen distances, *d*[C11−O11] = 1.232(3) Å and *d*[C11−O12] = 1.307(3) Å, are appropriate for a carboxylic acid functional group with C11−O11 as the double bond and O12 as the OH oxygen. In comparison, *d*[C14−O13] and *d*[C14−O14] are nearly equivalent at 1.272(3) and 1.262(3) Å respectively. This is consistent with the coordination geometry of a monodentate carboxylate group. The sum of the bond angles about C11 and C14 are both 360º showing these carbons to be sp^2 hybridized (see geometric parameters in Table 3.4).

Table 3.4. Selected interatomic bond lengths[a] (Å) and bond angles[a] (°) for $[SnCl_2(C_2H_4COOH)(C_2H_4COO)]^-$.

Coordination sphere			
Sn1−Cl11	2.4045(6)	Cl11−Sn1−Cl12	96.24(2)
Sn1−Cl12	2.4860(6)	Cl11−Sn1− C13	101.30(7)
Sn1−O11	2.5192(18)	Cl11−Sn1−C16	102.65(7)
Sn1−O13	2.3060(17)	Cl12−Sn1−C13	94.67(7)
Sn1−C13	2.127(2)	C1l2−Sn1−C16	94.47(6)
Sn1−C16	2.131(2)	C13−Sn1−C16	153.22(9)
Carboxylic acid $C_2H_4(COOH)$		**Carboxylate $C_2H_4(COO^-)$**	
O11−Sn1−C13	72.78(7)	O13−Sn1− C16	77.42(7)
O11−Sn1−Cl11	172.54(4)	O13−Sn1−Cl11	88.45(5)
O11−Sn1−Cl12	88.87(4)	O13−Sn1−C1l2	171.40(4)
O11−Sn1−C16	82.30(7)	C13−Sn1−O13	91.47(8)
O11−Sn1−O13	87.19(6)		
O11−C11	1.232(3)	O13−C14	1.272(3)
C11−O12	1.307(3)	C14−O14	1.262(3)

Table 3.4. (Continued).

C11−C12	1.502(3)	C14−C15	1.515(3)
C12−C13	1.524(3)	C15−C16	1.521(3)
O12−H12	0.72(3)		
Sn1−O11−C11	107.83(14)	Sn1−O13−C14	112.33(14)
O11−C11−O12	123.2(2)	O13−C14−O14	122.4(2)
O11−C11−C12	121.8(2)	O13−C14−C15	118.4(2)
O12−C11−C12	115.0(2)	O14−C14−C15	119.3(2)
C11−C12−C13	111.7(2)	C14−C15−C16	111.6(2)
C12−C13−Sn1	110.5(2)	C15−C16−Sn1	108.65(14)
C11−O12−H12	107.9(25)		

The 1,10-phenanthrolin-1-ium cation

One of the phen nitrogen atoms is protonated while the other nitrogen is not. The *d*[N41−H41] = 0.79(3) Å value is comparable to literature values of 0.78 Å (Cesario, Dietrich, Edel, Guilhem, Kintzinger, Pascard & Sauvage, 1986), and 0.76 and 0.74 Å (Krishnakumar, Aravamudan, Udupa, Seshasayee & Hamor, 1996). Protonation of N41 causes the C−N−C angle to increase (122.1(2)° in the protonated ring vs 116.5(2)° in the unprotonated ring), in agreement with literature values of, 123.2(3)° for the protonated ring and 116.4(3)° for the unprotonated ring (Bakshi, Cameron & Knop, 1996a) and 121.9(7)° for the protonated ring and 115.2(8)° for the unprotonated ring (Bakshi, Cameron & Knop, 1996b). The bond distances about the N atoms do not differ significantly between the protonated ring and the unprotonated ring (see Table 3.5). This angle increase at the N atom of $phenH^+$ agrees with a previously reported structure (Wang, Wang, Liao & Yan, 1999a). In the case of neutral (Nishigaki, Yoshioka & Nakatsu, 1978) and $phenH_2^{2+}$ (Wang, Wang, Liao &

Yan, 1999b) it was found that the bond angles are similar but the angles in $phenH_2^{2+}$, 122.7°, are greater than for neutral phen, 117.8°. Thus, while it can be said that the NH^+ protonated bond is less repulsive to the N−C bonds than is the N lone pair, the increased effect on the angle in the unprotonated ring of the $phenH^+$ cation is from the strong intramolecular hydrogen bond. It should be noted that a 1:1 disorder of $phenH^+$ would produce an average geometry with equal N environments. The mean values of disorder related distances and angles are in Table 3.5.

Table 3.5. Selected interatomic bond lengths[a] (Å) and bond angles[a] (°) for $[C_{12}H_9N_2]^+$.

Nonprotonated Ring		**Protonated Ring**		**Difference**	**Mean**
C35−N34	1.356(3)	C40−N41	1.356(3)	0σ	1.356(2)
C33−N34	1.326(3)	C42−N41	1.337(3)	+4σ	1.332(2)
C32−C33	1.395(4)	C42−C43	1.384(3)	−3σ	
C31−C32	1.370(4)	C43−C44	1.366(4)	−1σ	
C31−C36	1.401(4)	C44−C39	1.405(4)	+1σ	
C35−C36	1.404(3)	C39−C40	1.400(3)	−1σ	
		N41−H41	0.79(3)		
C33−N34−C35	116.5(2)	C40−N41−C42	122.1(2)	+28σ	119.3(2)
C36−C35−N34	124.1(2)	C39−C40−N41	119.5(2)	−23σ	121.8(2)
N34−C33−C32	123.9(2)	N41−C42−C43	120.2(2)	−12σ	122.1(2)
C31−C36−C35	117.0(2)	C44−C39−C40	118.2(2)	+4σ	
C32−C31−C36	119.3(3)	C43−C44−C39	120.2(2)	+3σ	
C33−C32−C31	119.1(3)	C42−C43−C44	119.6(2)	+1σ	
		C40−N41−H41	122.5(22)		
		C42−N41−H41	115.2(22)		

Table 3.5. (Continued).

Center Ring	
C35−C40	1.442(3)
C37−C38	1.346(4)
C38−C39	1.431(4)
C36−C37	1.431(4)

[a]Estimated standard deviations of the least significant digits are given in parentheses.

Supramolecular structure and hydrogen bonding

The strong anion-anion interactions

The monoanions are held together by strong intermolecular hydrogen bonds (see Figure 3.3 and Table 3.6). The carboxylate oxygen, O14 and the hydrogen atom of O12 of an adjacent monoanion complex has an O14···O12 distance of 2.579(2) Å. This can be compared to the distances of 2.570 Å between monoanions in the structure of $[Cr(\eta^6\text{-}C_6H_6)_2]^+\{[(Fe(\eta^5\text{-}C_5H_4COOH)(\eta^5\text{-}C_5H_4COO)][Fe(\eta^5\text{-}C_5H_4COOH)_2]_{0.5}\}$ (Braga, Maini, Polito & Grepioni, 1998).

The strong anion-cation interactions

The crystal structure is composed of layers of anions, $[SnCl_2(C_2H_4CO_2H)(C_2H_4CO_2)]^-$ and cations, $phenH^+$, held together by strong N−H···O hydrogen bonds, see Figure 3.3. The O14 of the carboxylate ligand participates in a bifurcated hydrogen bonding involving the hydrogen atom on N41 of the adjacent $phenH^+$ cation, with N41···O14 distance 2.688(2) Å.

The intramolecular cation interactions

There is a strong intramolecular hydrogen bond interaction between the N atom in the protonated ring and the N of the unprotonated ring, with the N4···N34 distance 2.737(3) Å. There is part of the bifurcated hydrogen bonding mentioned above. Our values in Table 3.6 may be compared to those of Bakshi, Cameron & Knop (1996b) for the corresponding geometry, *d*[N···N] = 2.722(9) Å, *d*[H···N] = 2.39 Å, N−H···N angle 98º.

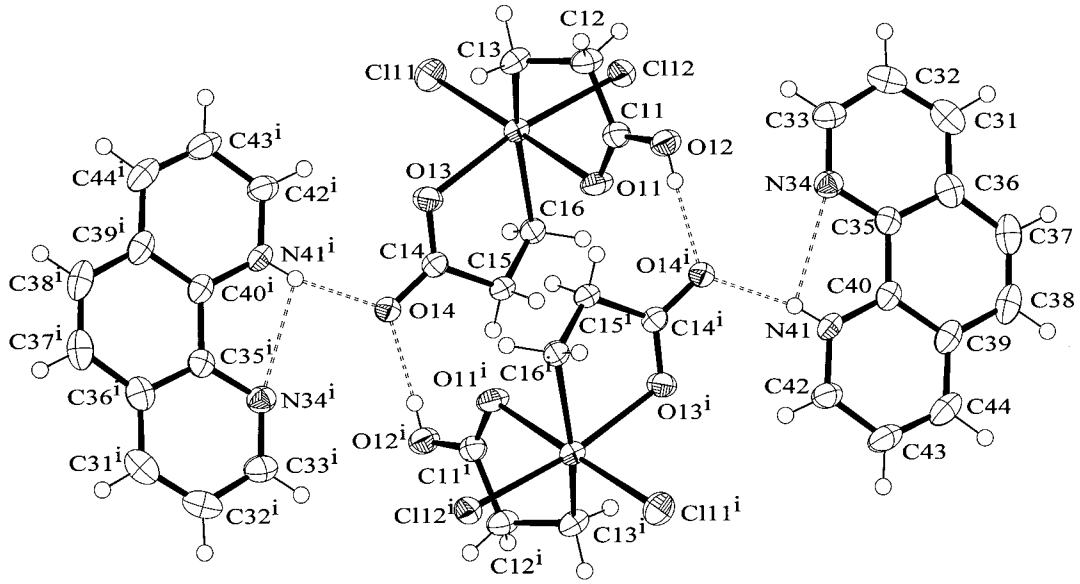

Figure 3.3. *ORTEP* drawing of the $[SnCl_2(C_2H_4COOH)(C_2H_4COO)]^-\cdot phenH^+$ showing the numbering scheme and the strong hydrogen bond interactions (50% probability displacement ellipsoids).

The weak anion-cation interactions

These weaker interactions can play an important role in structure stabilization. The interactions are shown in Figure 3.4. Values are given in Table 3.6. The hydrogen bond involving C42 of the protonated ring is a shorter distance, *d*[C42···O13] = 3.154(3) Å compared to *d*[C33···O12] = 3.377(3) Å involving the other nitrogen containing ring. Distances involving the remaining ring are, *d*[C37···O13] = 3.458(3) Å, *d*[C38···O11] = 3.596(3) Å. The increased Lewis acidity of the protonated ring can be seen in this shorter C···O contact. There are also weak C−H···Cl hydrogen bonds. Average C···Cl distances are similar for the protonated and nonprotonated rings.

The weak cation-cation ($phenH^+\cdots phenH^+$) stacking pairs

The $phenH^+$ stack face-to face and are held together by weak intermolecular interactions. They stack in columns along **a** with adjacent cations related by inversion centers. The inversion at (a) 1/2, 1/2, 1/2 is not equivalent to the inversion at (b) 1, 1/2, 1/2, but centers separated by **a** are equivalent. The center of the C35−C40 bond is shifted 0.94 Å laterally in case (a) and 2.29 Å in case (b). In case (a) the cations are held together by one stronger N−H···π, and two weaker C−H···π interactions and their inversion related interactions (see Table 3.6). In case (b) there is the same number and type of interactions, but the overlap is more optimal (Figure 3.5a and Figure 3.5b). As the (a) and (b) pair alternate along the column the interplanar spacing also alternates with the longer 3.34 Å spacing about 1/2, 1/2, 1/2 and the shorter 3.24 Å spacing about 1, 1/2, 1/2. The shorter spacing indicates stronger interaction for the more optimally overlapped case.

Table 3.6. Hydrogen bonding geometry (Å, º).

D−H···A	D−H	H···A	D···A	D−H···A	Symmetry Code (A)
Strong hydrogen bonds					
O12−H12O···O14	0.72(3)	1.86(3)	2.579(2)	177.3(33)	1−x, −y, 1−z
N41−H41N···O14	0.79(3)	1.91(3)	2.688(2)	166.3(30)	1−x, −y, 1−z
N41−H41N···N34	0.79(3)	2.46(3)	2.737(3)	101.9(24)	x, y, z
C−H···O Weak hydrogen bonds					
C42−H42···O13	0.95	2.40	3.154(3)	136.0	1−x, −y, 1−z
C43−H43···Cl12	0.95	2.74	3.578(3)	147.8	x, y, −1+z
C44−H44···Cl12	0.95	2.86	3.785(3)	165.4	1−x, 1−y, 1−z
C37−H37···O13	0.95	2.86	3.458(3)	122.5	x, 1+y, z
C38−H38···O11	0.95	2.70	3.596(3)	158.4	1−x, 1−y, 1−z
C31−H31···Cl11	0.95	2.95	3.578(3)	125.1	1−x, 1−y, 2−z
C31−H31···Cl11	0.95	3.04	3.619(3)	121.2	1+x, 1+y, z
C32−H32···Cl11	0.95	3.18	3.691(3)	116.4	1−x, 1−y, 2−z
C33−H33···O12	0.95	2.74	3.377(3)	125.3	x, y, z

C−H···π Weak hydrogen bonds

D−H···A	D···A [type (a)]	D···A [type (b)]	Symmetry Code (A)
C33−H33···π		3.277(3)	2−x, 1−y, 1−z
C42−H42···π		3.309(3)	2−x, 1−y, 1−z
N41−H41···π		3.345(8)	2−x, 1−y, 1−z
	3.235(3)		1−x, 1−y, 1−z
C43−H43···π	3.366(3)		1−x, 1−y, 1−z
C44−H44···π	3.399(3)		1−x, 1−y, 1−z

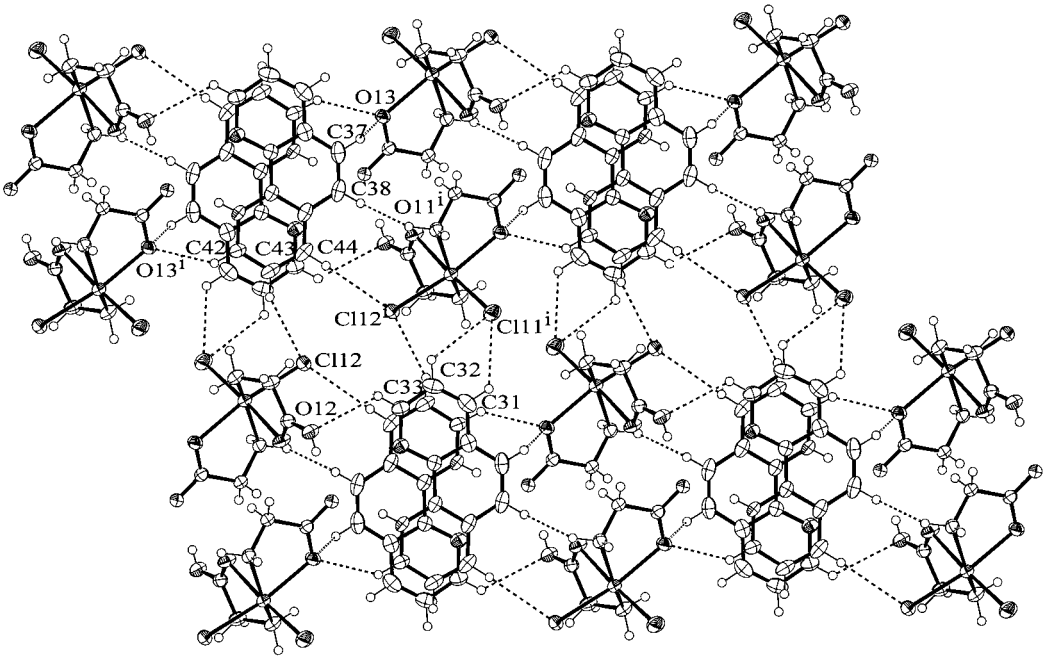

Figure 3.4. *ORTEP* drawing of the weak anion-cation hydrogen bond interactions as dashed lines.

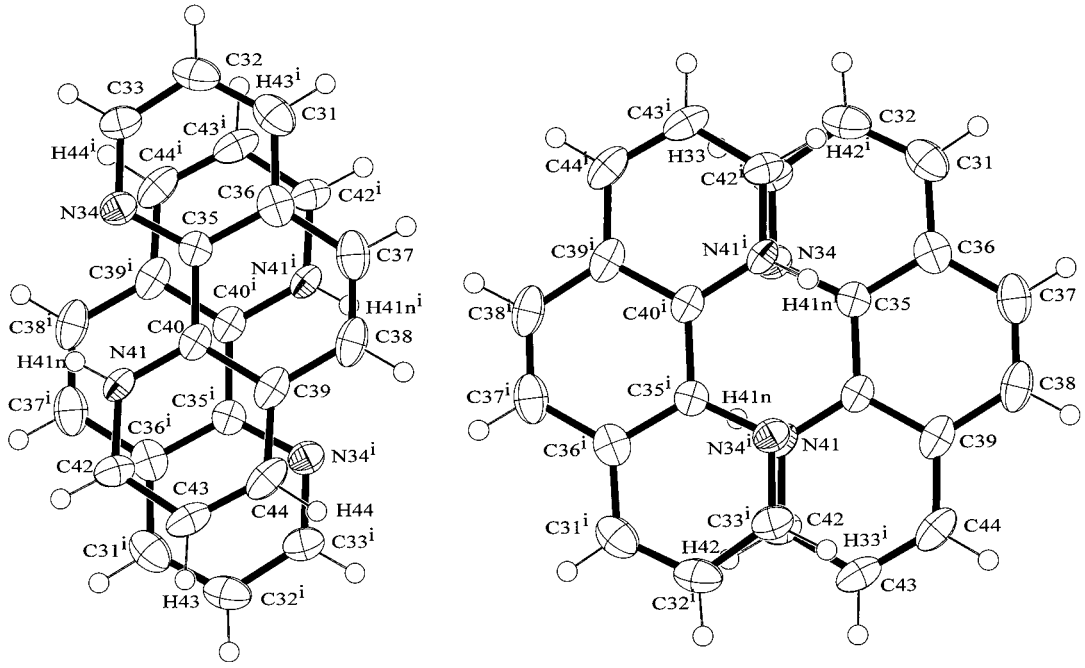

(a) **(b)**

Figure 3.5. Illustration of the of $phenH^+\cdots phenH^+$ stacked pairs. Top views are on the left (a-type about1/2, 1/2, 1/2; b-type about 1, 1/2, 1/2 below).

The possible packing of payers perpendicular to c*

The 200 K unit cell for the $Z = 6$ polytype is related to the 200 K unit cell for the Z = 2 polytype by $\mathbf{a}' = -\mathbf{a}$, $\mathbf{b}' = \mathbf{b}$, $\mathbf{c}' = -\mathbf{a}-\mathbf{b}-\mathbf{3c}$ to give $a' = 7.120$, $b' = 12.502$, $c' = 34.243$ Å, $\alpha' = 81.83$, $\beta' = 86.09$, $\gamma' = 75.65°$. This can be compared with the room temperature cell by Ng (2000) of $a = 7.225(1)$, $b = 12.576(2)$, $c = 34.394(7)$ Å, $\alpha = 82.14(3)$, $\beta = 86.90(3)$, $\gamma = 74.84(3)°$. This $Z = 6$ cell is a change of reduced cell after simply trebling the c axis repeat of the $Z = 2$ cell. Thus $\mathbf{c} = 1/3(-\mathbf{a}'+\mathbf{b}'+\mathbf{c}')$ and this vector corresponds to the largest peak in the Patterson of the $Z = 6$ polytype. However the ratio of the height of this peak to the origin peak is only 0.46. A twinning of the $Z = 2$ structure by a 2-fold screw axis parallel to **c*** creates twin related reflections indexable relative to the reciprocal axes of the reference cell as $-h\mathbf{a}^*-k\mathbf{b}^*+l''\mathbf{c}^*$ where $l'' = l+h2|a^*/c^*|cos\alpha^*+k2|b^*/c^*|cos\beta^* = l+0.5542h+0.9102k$ and this can not be an explanation of the $Z = 6$ cell.

A polytype that would triple the cell volume has the layer sequence ABAABAABA··· where B layers are 2-fold rotated about **c*** versions of A layers with A→A corresponding to the translational repeat **c** and A→B→A corresponding to the translational repeat 2**c**, modulo **a** and **b**. This can be achieved by choosing the location of layer B and only having true inversion centers in the middle of layer B and between adjacent layers A. The relationship between adjacent layers A and B is now a pseudo 2-fold screw parallel to **c***.

In the $Z = 6$ structure corresponding pseudo inversion centers of layers of type A at 1/2**c** and 5/2**c**+m**a**+n**b** are pseudo screw related to a layer of type B with its corresponding center of inversion at 3/2**c**+m/2**a**+n/2**b** where m and n are to be determined and **a**, **b**, **c** refer to the $Z = 2$ structure. As a consequence, the pseudo

screw axis relating the layer at 1/2**c** to that at 3/2**c** passes through the point **c**+*m*/4**a**+*n*/4**b**. Figures 3.6, 3.7 and 3.8 suggested *m* is odd and *n* is even if coincident origins are used for the inversion related adjacent layers of type A and 1/2**c**. Thus a real inversion at 1/2**a**+**b**+3/2**c** is pseudo screw related to the pseudo inversion at 1/2**c**.

The contents of a single layer projected down **c*** is shown in Figure 3.6. The projection of the vector **c** onto the plane of **a** and **b** is given by $-|a^*/c^*|cos\beta^*\mathbf{a}-|b^*/c^*|\cos\alpha^*\mathbf{b} = -0.2771\mathbf{a}-0.4551\mathbf{b}$. Figure 3.7 shows a projection down **a** and identifies an interface between parallel layers at $z = 1$. It suggests an alternative interlayer relationship between adjacent layers as a mechanism for twinning (identification of this interface as the twin plane) or polytypism (a selection between options for the packing of layers, the sequence choice identifying the polytype). A pseudo 2-fold screw operation could relate adjacent layers, the axis passing through the point *x*, 1/2, 0 where *x* is indeterminable from Figure 3.7. Figure 3.8 shows a projection down **b** and suggests the pseudo 2-fold screw axis passes through the point 1/4, *y*, 0, where *y* is indeterminable from Figure 3.8. A consistent description of this pseudo screw axis is that it passes through 1/4, 1/2, 1.

We have created a believable polytype structure from an accurately determined structure. In the process we have found a twin-disorder mechanism. If stacking faults exist, the extra translation by **c** reduces the scale of reflections with $-h'+k'+l' \neq 3n$. If twinning was present in the crystal of the $Z = 6$ modification studied using a conventional serial detector, then real refinement difficulties result. The twin would cause spot splitting of twin related reflections along **c′*** in reciprocal space. To cope with this, a new data set collected using area detector technology is required. The possibility of different polytypes in the one crystal (Rae & Willis, 2003) should

also be considered, requiring careful crystal selection. It should also be noted that interfacially twinned crystals exist and can be identified by the existence of a reentrant angle in the crystal form.

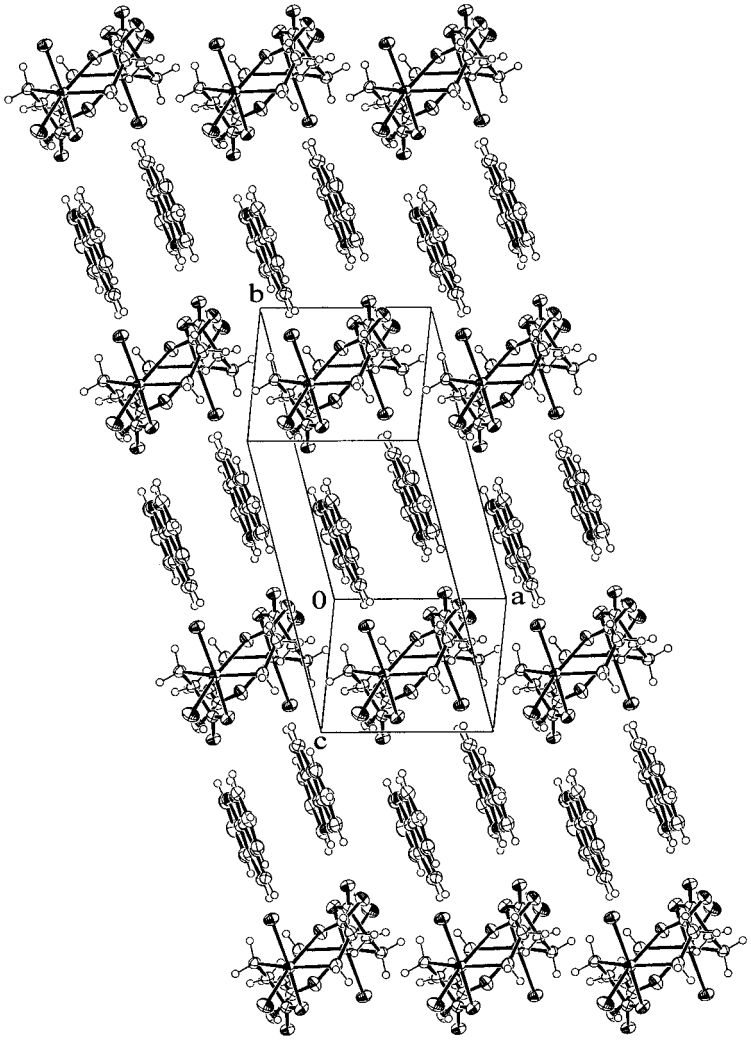

Figure 3.6. The contents of a single layer projected down **c***.

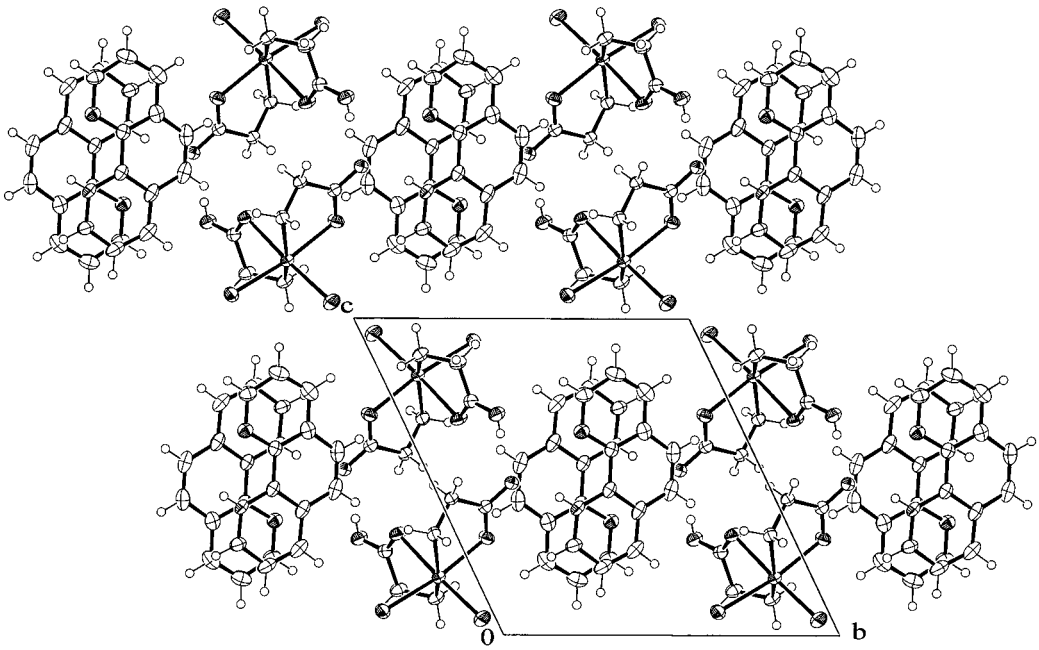

Figure 3.7. Packing diagram projected down **a**.

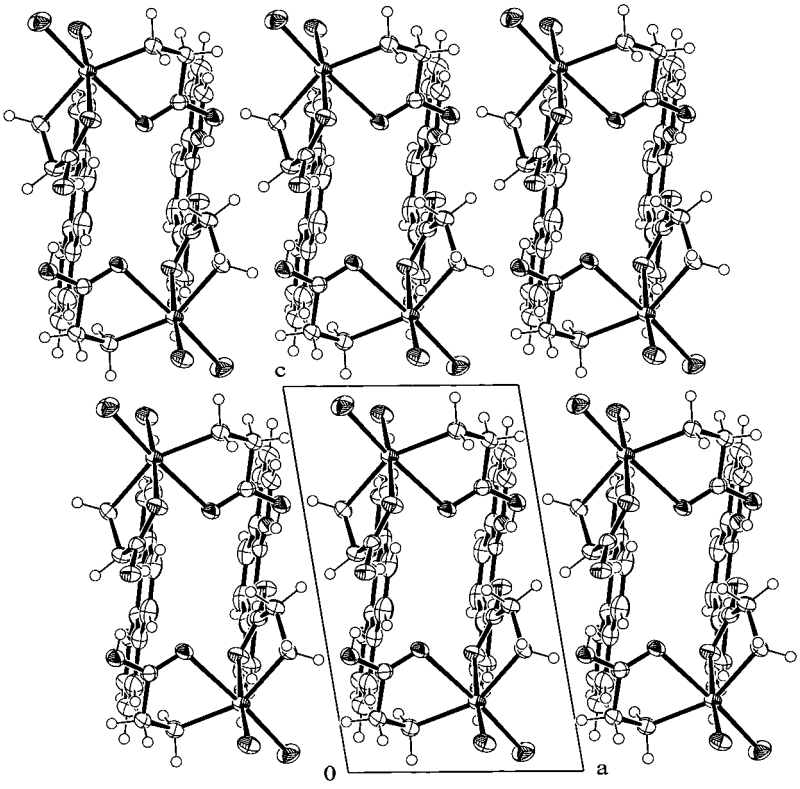

Figure 3.8. Packing diagram projected down **b**.

3.5 References

Altomare, A., Burla, M. C., Camalli, M., Cascarano, G. L., Giacovazzo, C., Guagliardi, A., Moliterni, A. G. G., Polidori, G. and Spagna, R. (1999). SIR97 A new tool for crystal structure determination and refinement. **Journal of Applied Crystallography** 32: 115-119.

Bakshi, P. K., Cameron, T. S. and Knop, O. (1996a). Crystal chemistry of tetraradial species. Part 8. Mix and match: Cation geometry, ion packing, hydrogen bonding, and π-π interactions in *cis*-2,2′-bipyridinium(1+) and 1,10-phenanthrolinium(1+) tetraphenylborates - and what about proton sponges? **Canadian Journal of Chemistry** 74(2): 201-220.

Bakshi, P. K., Cameron, T. S. and Knop, O. (1996b). Polyhalide anions in crystals. Part 1. Triiodides of the Me_4N^+, Me_4P^+, quinuclidinium, 1-azoniapropellane, and 1,4-diazoniabicyclo[2.2.2]octane ($DabcoH_2^{2+}$) cations, and 1,10-phenanthrolinium(1+) tribromide. **Canadian Journal of Chemistry** 74(4): 559-573.

Ballabh, A., Trivedi, D. R., Dastidar, P. and Suresh, E. (2002). Hydrogen bonded supra-molecular network in organic salts: Crystal structures of acid-base salts of dicarboxylic acids and amines. **CrystEngComm** 4(24): 135-142.

Blessing, R. (1997). Outlier treatment in data merging. **Journal of Applied Crystallography** 30: 421-426.

Braga, D., Maini, L. and Grepioni, F. (1998). Crystal engineering of organometallic compounds through cooperative strong and weak hydrogen bonds: A simple route to mixed-metal systems. **Angewandte Chemie International Edition in English** 37(16): 2240-2242

Braga, D., Maini, L., Grepioni, F., Elschenbroich, C., Paganelli, F. and Schiemann, O. (2001). Novel organometallic building blocks for crystal engineering. Synthesis and structural characterization of the dicarboxylic acid $[Cr^{0}(\eta^{6}\text{-}C_{6}H_{5}COOH)_{2}]$, of two polymorphs of its oxidation derivative $[Cr^{I}(\eta^{6}\text{-}C_{6}H_{5}COOH)_{2}]^{+}[PF_{6}]^{-}$, and of the zwitterionic form $[Cr^{I}(\eta^{6}\text{-}C_{6}H_{5}COOH)(\eta^{6}\text{-}C_{6}H_{5}COO)]$. **Organometallics** 20(9): 1875-1881.

Braga, D., Maini, L., Polito, M. and Grepioni, F. (1999). Hydrogen bonds within an ionic environment: The remarkable behavior of the zwitterion $[Co^{III}(\eta^{5}\text{-}C_{5}H_{4}COOH)(\eta^{5}\text{-}C_{5}H_{4}COO)]$. **Organometallics** 18(14): 2577-2579.

Bruker AXS, Inc. (1998). *SHELXTL*, version 5.1, Bruker AXS Inc., Madison, Wisconsin, USA.

Burnett, M. N. and Johnson, C. K. (1996). *ORTEP-III: Oak Ridge Thermal Ellipsoid Plot Program for Crystal Structure Illustrations*, Report ORNL-6895, Oak Ridge National Laboratory, Tennessee, USA.

Chee, C. F., Lo, K. M. and Ng, S. W. (2003a). Aquatriphenyl(trifluoroacetato)tin-2,2′:6′,2″-terpyridine (1/1). **Acta Crystallographica** E59: m174-m175.

Chee, C. F., Lo, K. M. and Ng, S. W. (2003b). μ-Succinato bis(aquatriphenyltin) bis (*o*-phenanthroline). **Acta Crystallographica** E59: m36-m37.

Chee, C. F., Lo, K. M. and Ng, S. W. (2003c). Aquatrichloroacetatotriphenyltin-1,10-phenanthroline (2/2). **Acta Crystallographica** E59: m642-m643.

Cesario, M., Dietrich, C. O., Edel, A., Guilhem, J., Kintzinger, J. P., Pascard, C. and Sauvage, J. P. (1986). Topological enhancement of basicity: Molecular structure and solution study of a monoprotonated catenand. **Journal of the American Chemical Society** 108(20): 6250-6254.

Desiraju, G. R. (1995). Supramolecular synthons in crystal engineering−a new organic synthesis. **Angewandte Chemie International Edition in English** 34(21): 2311-2327.

Desiraju, G. R. (1997). Designer crystals: Intermolecular interactions, network structure structures and supramolecular synthons. **Chemical Communications** (16): 1475-1482.

Farrugia, L. J. (1997). *ORTEP-3* for Windows-a version of *ORTEP-III* with a Graphical User Interface (GUI). **Journal of Applied Crystallography** 30: 565.

Hall, V. J. and Tiekink, E. R. T. (1996). Benzyltrichloro(1,10-phenanthroline-*N,N′*)-tin(IV) benzene solvate (1/1). **Acta Crystallographica** C52: 2141-2143.

Krishnakumar, R., Aravamudan, G., Udupa, M. R. Seshasayee, M. and Hamor, T. A. (1996). Reactions of (diethyldithiocarbamato)halogenotellurium(II); crystal structures of R[Te{S_2CNEt_2}X_2 [R = NEt_4, X = I; R = $H(phen)_2$ (phen = 1,10-phenanthroline), X = I or Br]. **Dalton Transactions** (11): 2253-2259.

Kuduva, S. S., Bläser, D., Boese, R. and Desiraju, G. R. (2001). Crystal engineering of primary cubanecarboxamides. Repetitive formation of an unexpected N−H···O hydrogen-bonded network. **Journal of Organic Chemistry** 66(5): 1621-1626.

Kuduva, S. S., Craig, D. C., Nangia, A. and Desiraju, G. R. (1999). Cubanecarboxylic acids. Crystal engineering considerations and the role of C−H···O hydrogen bonds in determining O−H···O networks. **Journal of the American Chemical Society** 121(9): 1936-1944.

Kuĺba, F. Y., Makashev, Y. A. and Fedyaev, N. I. (1976). Reaction of 1,1-phenanthroline with the hydrogen ion. **Russian Journal of Inorganic Chemistry** 21(8): 1178-1185.

Langley, P. J., Hulliger, J., Thaimattam, R. and Desiraju, G. R. (1998). Supramolecular synthons mediated by weak hydrogen bonding: Forming linear molecular arrays *via* C≡C−H···N≡C and C≡C−H···O_2 N recognition. **New Journal of Chemistry** (12): 1307-1309.

Lee, T. S., Kolthoff, I. M. and Leussing, D. L. (1948). Reaction of ferrous and ferric iron with 1,10-phenanthroline. I. Dissociation constants of ferrous and ferric phenanthroline. **Journal of the American Chemical Society** 70(7): 2348-2352.

Liu, R., Mok, K.-F. and Valiyaveettil, S. (2001). Solid-state self-assembly of a complex from 1,3,5-benzenetricarboxylic acid and 1,3,5-trihydroxybenzene: Influence of strong O−H···O and C−H···O hydrogen bonds. **New Journal of Chemistry** (7): 890-892.

Lo, K. M., Das, V. G. K., Ng, S. W. and Hook, J. M. (1999). *catana*-Poly[triphenyltin-μ-(*N*,*N*-diethylthiocarbamoylthioacetato-*O*:*O*′)], *catana*-Poly[triphenyltin-μ-(*N*-methyl-*N*-phenylthiocarbamoylthioacetato-*O*:*O*′)] and triphenyl (*N*,*N*-tetra-methylenethiocarbamoylthioacetato-*O*)tin. **Acta Crystallographica** C55: 744-748.

McBryde, W. A. E. (1965). An approximate determination of the second-stage protonation constant for 2,2′-bipyridyl, 1,10-phenanthroline, and derivatives. **Canadian Journal of Chemistry** 43: 3472-3476.

Nishigaki, S.; Yoshioka, H. and Nakatsu, K. (1978). The crystal and molecular structure of *o*-phenanthroline. **Acta Crystallographica** B34: 875-879.

Ng, S. W. (1997). Bis[aqua(chlorodifluoroacetato-*O*)triphenyl-tin-l,10-phenanthroline]. **Acta Crystallographica** C53: 1059-1061.

Ng, S. W. (1998). Outer-sphere coordination of a multidentate *N*-heterocycle to tin through water: Monoclinic and triclinic modifications of μ-succinato bis(aqua triphenyltin)-2,4,6-Tris(2-pyridyl)-1,3,5-triazine (1/2). **Acta Crystallographica** C54: 1386-1389.

Ng, S. W. (2000). University of Malaya, Kuala Lumpur, Malaysia, personal communication.

Ng, S. W. and Das, V. G. K. (1996). Outer-sphere coordination of o-phenanthroline in bis [aquachlorotri(*p*-chlorophenyl) tin *o*-phenanthroline]. **Journal of Organometallic Chemistry** 513(1-2): 105-108.

Ng, S. W. and Das, V. G. K. (1997). The first example of a discrete di(carboxylato) triorganostannate: Tetramethylammonium triphenylbis(trifluoroacetato) stannate. **Acta Crystallographica** C53: 212-213.

Ng, S. W. and Hook, J. M. (1999). Diisopropylammonium oxalatotriphenyl-stannate. **Acta Crystallographica** C55: 310-312.

Nonius BV. (1998). *COLLECT: KappaCCD Software*, Nonius BV., Delft, The Netherlands.

Otwinowski, Z. and Minor, W. (1997). *Methods in enzymology,* macromolecular crystallography, part A, edited by C. W. Carter Jr. and R. M. Sweet, vol. 276 pp. 307-326. New York: Academic Press.

Oxford Cryosystems (1997). *600 Series Cryostream Cooler Operation and Instruction Guide*. Oxford Cryosystems, Oxford, UK.

Parvez, M., Ali, S., Bhatti, M. H., Khokhar, M. N., Mazhar, M. and Qureshi, S. I. (1999). Tri-*n*-butyl(*N*-malenoyl-β-alaninato)tin. **Acta Crystallographica** C55: 1427-1429.

Parvez, M., Ali, S., Mazhar, M., Bhatti, M. H. and Khokhar, M. N. (1999). Aqua[4-(4-chlorophenyl)-2-phenylthiazole-5-acetato-*O*]trimethyltin(IV). **Acta Crystallographica** C55: 1280-1282.

Rae, A. D. & Willis, A. C. (2003). 9,10-Phenanthrenequinone, not your average structure. **Zeitschrift für Kristallographie** 218: 221-230

Vishweshwar, P., Nangia, A. and Lynch, V. M. (2002). Recurrence of carboxylic acid-pyridine supramolecular synthon in the crystal structures of some pyrazinecarboxylic acids. **Journal of Organic Chemistry** 67(2): 556-565.

Wang, Y.-Q., Wang, Z.-M., Liao, C.-S. and Yan, C.-H. (1999a). Bis(1,10-phenanthrolin-1-ium) chlorodiiodide(1-) dichloroiodide(1-). **Acta Crystallographica** C55(9): 1503-1506.

Wang, Y.-Q., Wang, Z.-M., Liao, C.-S. and Yan, C.-H. (1999b). 1,10-Phenanthrolinium(2+) dichloroiodide(1-) chloride. **Acta Crystallographica** C55(9): 1506-1508.

CHAPTER IV

PSEUDO SYMMETRY IN $[Mg(H_2O)_6](NO_3)_2 \cdot 2HMT \cdot 4H_2O$; HMT = HEXAMETHYLENETETRAMINE

4.1 Abstract

$[Mg(H_2O)_6](NO_3)_2 \cdot 2HMT \cdot 4H_2O$ crystallized in space group $P2_1/n$, a = 9.429(5) Å, b = 16.137(7) Å, c = 19.275(5) Å, β = 90.523(5)°, V = 2932.7(20) Å^3, Z = 4. Within the asymmetric unit of $P2_1/n$, two HMT molecules, the $[Mg(H_2O)_6]^{2+}$ cation and two of the water molecules are located about an approximate pseudo inversion center. This imposes a pseudo $C\bar{1}$ symmetry for a layer at z = 1/2 and a pseudo $C2/c$ space group symmetry for the substructure containing these entities in all equivalent positions of $P2_1/n$. The rest of the asymmetric unit of $P2_1/n$ contains two nitrate anions and two water molecules (O9 and O10) which lie at an interface between the pseudo $C\bar{1}$ layers described above. This interface approximates $Pb2_1a$ pseudo symmetry should the distortion of β from 90° be ignored. The substructure containing these atoms in all equivalent positions has pseudo *Pbna* symmetry. The true space group $P2_1/n$ is also a subgroup of *Pbna*. Thus, the $P2_1/n$ structure is the result of the interaction of two substructures, one of $C2/c$ symmetry and the other of *Pbna* symmetry. Separate mechanisms for twinning and stacking faults exist. The possibility of polytypism is recognized.

4.2 Introduction

The structures of complexes between organic bases and inorganic salts with a large number of water molecules were first studied by Barbieri (Barbieri & Calzolari 1910; Barbieri & Lanzoni; 1911). Hexamethylenetetramine (HMT) easily forms a large series of complexes with a variety of inorganic salts, $CaBr_2$, $MgCl_2$, $MnCl_2$, $CoCl_2$, $NiC1_2$, $MnBr_2$, $MgBr_2$, $CoBr_2$, $NiBr_2$, NiI_2, CoI_2, MnI_2, MgI_2, $Mg(SCN)_2$, $Mg(NO_3)_2$, $Co(NO_3)_2$, $Mn(NO_3)_2$, $Y(NO_3)_3$, linking with a high number of water molecules (De Santis, Kovacs, Liquori & Mazzarella, 1965). The cubic form of $CaBr_2{\cdot}10H_2O{\cdot}2HMT$ (Addamiano & Giacomello, 1951) grows when crystal growth is kept above 20 °C, the triclinic form grows when the temperature is kept below 20 °C. (Mazzarella, Kovacs, De Santis & Liquori, 1967). Many such complexes have been studied in the class of $MX_2{\cdot}nH_2O{\cdot}2HMT$ (Ganesh, Seshasayee, Aravamudan, Heijdenrijk & Schenk, 1990; Hu, Ye & Ng, 2002; Zhu, You, Qu, Liu, Tan & Ma, 2003; Zhu, Xia, Zeng, Wang & Wang, 2003) in particular isomorphic complexes. They are all triclinic with space group $P\bar{1}$, $Z = 1$.

Hexaaquamagnesium (II) dinitrate bis(hexamethylenetetramine)tetrahydrate, $[Mg(H_2O)_6](NO_3)_2{\cdot}2HMT{\cdot}4H_2O$, studied by IR spectroscopy was reported in a Russian paper (Imanakunov & Lukina, 1979). HMT is coordinated directly to the metal ion and water, to give an octahedral environment at the metal. We report the monoclinic structure of $[Mg(H_2O)_6](NO_3)_2{\cdot}2HMT{\cdot}4H_2O$, with space group $P2_1/n$, $Z = 4$. The molecules are linked together by O−H···N and O−H···O hydrogen bonds.

4.3 Experimental

Preparation of Sample

A colorless aqueous solution (5 mL) containing $Mg(NO_3)_2 \cdot 6H_2O$ (2 mmol, 0.5128 g) was added into a 5 mL aqueous solution of HMT (4 mmol, 0.5608 g). The solution was left to evaporate at room temperature until colorless crystals were formed.

Data Collection, Data Reduction and Structure Solution

Data were collected at 295 K on a Bruker-Nonius KappaCCD diffractometer using the COLLECT (Nonius, 1998) software. The diffractometer was equipped with a graphite monochromator, Mo*Kα* x-radiation source (λ = 0.71073 Å), and a 0.5 mm *ifg* capillary collimator. Data reduction used the EvalCCD package (Duisenberg, Kroon-Batenburg & Schreurs; 2003), and reflections were corrected for absorption using SORTAV (Blessing, 1997). The structure was solved using SIR97 (Altomare, Burla, Camalli, Cascarano, Giacovazzo, Guagliardi, Moliterni, Polidori & Spagna, 1999) and refined with RAELS (Rae, 2000). The ORTEP-III (Burnett & Johnson, 1996; Farrugia, 1997) graphics drawing program was used for illustrations. Crystal data and details of the data collection and structure refinement are summarized in Table 4.1. Statistics for the refinement from RAELS are in Table 4.2. Fractional coordinates and isotropic atomic displacement parameters for the nonhydrogen atoms are given in Table 4.3. Anisotropic atomic displacement parameters for the nonhydrogen atoms are given in Table 4.4. Selected interatomic bond distances and angles are complied in Table 4.5. Hydrogen bond parameters are given in Table 4.6. Derived hydrogen atom positions and isotropic atomic displacement parameters, and

derived anisotropic atomic displacement parameters for the hydrogen atoms are given as supplementary material in Appendix C as Tables C.1, and C.2, respectively. The diffraction patterns for 0*kl*, 1*kl*, and 2*kl* showing alternating weak and strong reflections, characteristic of pseudo symmetry, are given in Figure 4.1.

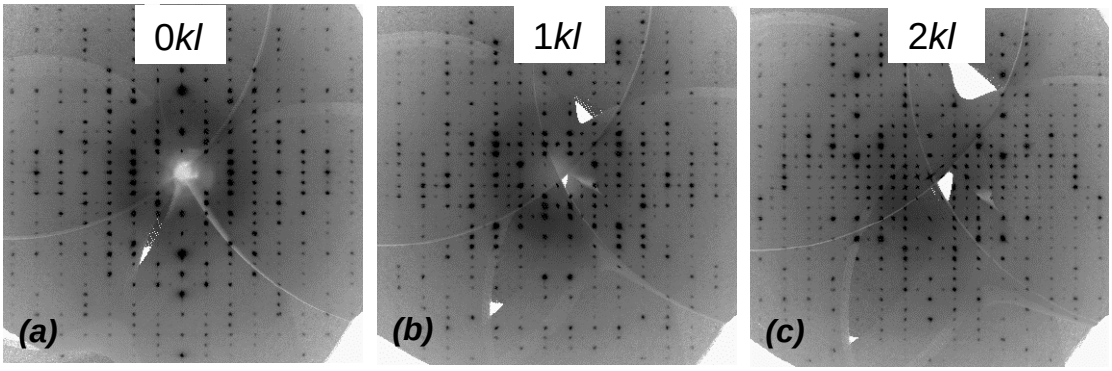

Figure 4.1. Precession photographs at 295 K for $[Mg(H_2O)_6](NO_3)_2{\cdot}2HMT{\cdot}4H_2O$. The diffraction pattern shows that $h+k$ odd reflections are systematic weak: (a) 0*kl*, (b) 1*kl*, (c) 2*kl*.

4.4 Details of the Structure Refinement

In the initial refinement stages restraints and constraints were used. Restraints were imposed on the hydrogen atoms of the HMT, to help with possible refinement problems associated with the pseudo symmetry. Differences between pseudo inversion related distances (C−H and nearest neighbor H···H distances) were restrained to approach zero. These restraints held well and justified their use.

Rigid-body *TLX* models were used to obtain some of the atomic displacement parameters U_{ij} (Rae, 1975a, b). These models involve 15 variables per group and initially 4 groups were used, to separately describe the two HMT molecules and the

two NO_3^- ions. The remaining water O atoms were refined as isolated anisotropic atoms. Hydrogen atoms were given U_{ij} parameters determined by the parameters that described the U_{ij} of the atoms to which they were attached.

Water molecules O9 and O10 and their associated H atoms are less well defined and have O−H distances that are too short when an ordered structure model is refined. Disorder between two possible hydrogen bonding options was assumed and a major and minor component created for each of these water molecules. The label for atoms of the minor component are distinguished by the addition of a prime, ′, to the relevant atom label, *e.g.* O9 and O9′ appear in the atom list. These hydrogen bond connections are implicit in the last eight O–H···O angles on the file

Occupancies are included on this file and are 0.851(11):0.149 for atoms O9/O9′ and their attached H atoms and 0.654(13):0.346 for atoms O10/O10' and their attached H atoms.

All hydrogen atoms were constrained to have the same anisotropic atomic displacement parameters as the atoms to which they are attached. The atoms O9 and O9′ (likewise O10 and O(10′) were constrained to have the same atomic displacement parameters. The only other constraints were to make the waters O9, O9′, O10, O10' and attached H atoms have exactly the same refinable local mm2 symmetry using refinable local coordinates. There are two associated degrees of freedom, corresponding to the O–H bond length and H–O–H bond angle. The angle was initially constrained to be 110°.

Initially these water molecules were also constrained to make the oxygens of each disordered pair of molecules coincide and the H atoms were inserted so that H–O–H atoms were in the same plane as the relevant water O and the two oxygens to

which it is hydrogen bonded making the bisectors of the H–O–H and O···O···O angles coincident. Weak restraints were used to make the O–H···O angles approach 180° (effectively restraining them to approach equality). The rotation of the water molecules was constrained to be about an axis perpendicular to the plane of the water molecule. The position of the disordered water oxygens were allowed to come apart by using restraints on the disordered atom position so that the two hydrogen bonded O–H···O distances of each water approached equality. Equivalents of atoms O4 and O5 hydrogen bond to O10 (and O10′) and O9 (and O9′) respectively. Restraints to make the pairs of distances to a disordered O atom approach equality were also used. In the final refinement cycle (after the previous model had coverged) these restraints were further weakened, the refinement proving stable to this change.

In the final cycles of the refinement all nonhydrogen atoms were refined as independent anisotropic atoms. The hydrogen atom positions could be located on electron density difference maps and all H positional parameters on HMT and the $[Mg(H_2O)_6]^{2+}$ cation were refined. The U_{ij} values of hydrogen atoms were constrained to be the same as the atoms to which they were attached. The value of $R(F)$ was then 0.041 for refinements with $I > 3\sigma(I)$ compared to 0.048 for the restraints-constraints model described earlier. This shows the rigid body thermal atom model was appropriate (reflection refinement statistics in Table 4.2).

Table 4.1. Summary of crystal data, data collection, and structure refinement details.

Crystal data	
Structure Formula	$[Mg(H_2O)_6](NO_3)_2{\cdot}2[(CH_2)_6N_4]{\cdot}4H_2O$
Chemical formula	$C_{12}H_{44}MgN_{10}O_{16}$
Chemical formula weight	608.88
Cell setting, space group	Monoclinic, $P2_1/n$ (No. 14)
a (Å)	9.429(5)
b (Å)	16.137(7)
c (Å)	19.275(5)
α (º)	90
β (º)	90.523(5)
γ (º)	90
Volume (Å^3)	2932.7(20)
Z	4
D_{calc} (Mg/m^3)	1.379
Radiation type, wavelength	Mo$K\alpha$, 0.71073
θ range (º)	4.00-27.50
Absorption coefficient, μ (mm^{-1})	0.143
Temperature (K)	295±2
Crystal color, form	transparent colorless, prism
Crystal size (mm)	0.25×0.20×0.15
Data collection	
Diffractometer	Nonius KappaCCD
Data collection method	φ scan plus ω scans with κ offsets
Absorption collection	Multi-scan
T_{min}, T_{max}	0.966, 0.979
No. of measured reflections	31,908
No. of unique independent data	6453
No. of observed reflections	3297
Criterion for observed reflections	$I > 3\sigma(I)$
R_{int}	0.037
θ_{max} (º)	27.50

Table 4.1. (Continued).

Range of *h, k, l*	$-12 \rightarrow h \rightarrow 11$ $-20 \rightarrow k \rightarrow 20$ $-23 \rightarrow l \rightarrow 24$
Refinement	
Refinement on	*F*
$R[F^2 > 3\ \sigma(F^2)]$, $wR(F^2)$, *S*	0.041, 0.057, 1.45
No. of reflections used	3297
No. of refined parameters	487
H-atom treatment	Refined xyz and calculated U_{ij} based on U_{ij} of attached atom each cycle
Weighting scheme	Based on measured s.u.'s $w = 1/(\sigma^2(F) + 0.0009F^2)$
$(\Delta/\sigma)_{max}$	0.04
$\Delta\rho_{max}$, $\Delta\rho_{min}$ (e Å^{-3})	0.40, –0.34

Computer programs: *COLLECT* (Nonius, 1998); *EVAL14* (Duisenberg, Kroon-Batenburg & Schreurs, 2003); *SIR97* (Altomare *et al*., 1999); *RAELS* (Rae, 2000); *ORTEP-III* (Burnett & Johnson, 1996; Farrugia, 1997).

Table 4.2. Statistics from the RAELS refinement[c].

Class	*h+k* even[a]	*h+k* odd[a]	All *h+k*[a]	Other[b]	Total
Reflections	2016	1281	3297	3156	6453
R(*F*)	0.039	0.048	0.041	0.453	0.106
$R(F^2)$	0.053	0.072	0.056	0.626	0.069
wR	0.058	0.056	0.057	0.460	0.085
Gof	1.54	1.30	1.45	1.54	1.55

a. $I > 3\sigma(I)$.
b. $I < 3\sigma(I)$.
c. Number of independent variables = 487.
Final refinement cycle: maximum shift/error = 0.04.
The weighting scheme for F_{obs} data was $w = 1/(\sigma^2(F_{obs})+(0.03)^2|F_{obs}|^2)$.
The ratio of the mean $|F|$ for the 1281 *h+k* odd reflections to *h+k* even reflections with $I>3\sigma(I)$ was 0.600. For $|F|^2$ the ratio was 0.278.
Final difference map electron density: maximum +0.405 eÅ^{-3}, minimum –0.339 eÅ^{-3}.

Table 4.3. Fractional monoclinic coordinates[a] and equivalent isotropic displacement parameters[b] ($Å^2$) for the nonhydrogen atoms in $[Mg(H_2O)_6](NO_3)_2 \cdot 2HMT \cdot 4H_2O$.

	x	*y*	*z*	U_{eq}
Mg1	0.2666(1)	0.7494(1)	0.4987(1)	0.0290(2)
O1	0.1542(2)	0.8345(1)	0.4421(1)	0.044(1)
O2	0.0873(2)	0.7333(1)	0.5575(1)	0.045(1)
O3	0.3368(2)	0.8451(1)	0.5600(1)	0.042(1)
O4	0.3767(2)	0.6627(1)	0.5553(1)	0.040(1)
O5	0.4451(2)	0.7657(1)	0.4404(1)	0.041(1)
O6	0.1929(2)	0.6546(1)	0.4365(1)	0.043(1)
N11	0.2264(2)	0.0834(2)	0.3151(1)	0.041(1)
N12	0.3788(2)	0.1078(2)	0.4162(1)	0.042(1)
N13	0.1890(2)	0.0063(1)	0.4228(1)	0.036(1)
N14	0.1324(2)	0.1532(1)	0.4175(1)	0.041(1)
C11	0.3707(3)	0.1029(2)	0.3404(2)	0.046(1)
C12	0.1844(3)	0.0036(2)	0.3463(2)	0.039(1)
C13	0.1294(3)	0.1472(2)	0.3412(2)	0.045(1)
C14	0.3335(3)	0.0280(2)	0.4449(2)	0.043(1)
C15	0.2785(3)	0.1713(2)	0.4401(2)	0.045(1)
C16	0.0929(3)	0.0718(2)	0.4459(2)	0.040(1)
N21	0.2445(3)	0.4195(1)	0.6853(1)	0.039(1)
N22	0.0925(2)	0.4011(1)	0.5836(1)	0.038(1)
N23	0.2897(2)	0.4981(1)	0.5801(1)	0.036(1)
N24	0.3354(2)	0.3499(1)	0.5826(1)	0.037(1)
C21	0.1001(3)	0.4035(2)	0.6598(2)	0.041(1)
C22	0.2932(3)	0.4985(2)	0.6561(2)	0.040(1)
C23	0.3377(3)	0.3532(2)	0.6589(2)	0.042(1)
C24	0.1439(3)	0.4806(2)	0.5565(2)	0.038(1)
C25	0.1889(3)	0.3354(2)	0.5589(2)	0.041(1)
C26	0.3812(3)	0.4308(2)	0.5556(2)	0.039(1)
N1	0.6320(3)	0.3547(2)	0.1705(2)	0.051(1)
O11	0.5231(3)	0.3120(2)	0.1735(1)	0.069(1)

Table 4.3. (Continued).

	x	*y*	*z*	U_{eq}
O12	0.6635(3)	0.3910(2)	0.1177(2)	0.092(1)
O13	0.7108(3)	0.3571(3)	0.2212(2)	0.103(1)
N2	–0.1218(3)	0.6188(2)	0.6678(2)	0.055(1)
O21	0.0047(3)	0.6386(2)	0.6735(2)	0.077(1)
O22	–0.1735(4)	0.5996(2)	0.6128(2)	0.102(1)
O23	–0.1978(3)	0.6195(3)	0.7189(2)	0.112(1)
O7	0.6885(3)	0.4379(2)	0.6689(1)	0.058(1)
O8	0.7707(3)	0.0637(2)	0.3324(1)	0.063(1)
O9	–0.0005(4)	0.6227(2)	0.8372(2)	0.070(1)
O10	0.4815(6)	0.3108(4)	0.3245(2)	0.070(1)
O9′	0.0320(16)	0.6380(12)	0.8294(7)	0.070(1)
O10′	0.4520(11)	0.3231(8)	0.3299(5)	0.070(1)

[a]Estimated standard deviations of the least significant digits are given in parentheses.

[b]Equivalent isotropic atomic displacement parameters for the atoms refined anisotropically, $U_{eq} = 1/3 \sum_i \sum_j U_{ij}\, a_i^* a_j^*\, \mathbf{a}_i \cdot \mathbf{a}_j$

Table 4.4. Anisotropic atomic displacement parameters[a] in $[Mg(H_2O)_6](NO_3)_2 \cdot 2HMT \cdot 4H_2O$.

Atom	*U11*	*U22*	*U33*	*U12*	*U13*	*U23*
Mg1	0.0243(4)	0.0271(4)	0.0356(4)	0.0008(3)	0.0012(3)	0.0009(3)
O1	0.044(1)	0.033(1)	0.054(1)	0.001(1)	−0.016(1)	0.006(1)
O2	0.036(1)	0.042(1)	0.058(1)	0.007(1)	0.017(1)	0.010(1)
O3	0.031(1)	0.048(1)	0.048(1)	−0.004(1)	0.004(1)	−0.016(1)
O4	0.042(1)	0.031(1)	0.046(1)	0.000(1)	−0.011(1)	0.007(1)
O5	0.034(1)	0.039(1)	0.049(1)	0.009(1)	0.013(1)	0.010(1)
O6	0.033(1)	0.046(1)	0.050(1)	−0.007(1)	0.002(1)	−0.017(1)
N11	0.043(1)	0.039(1)	0.040(1)	0.000(1)	0.005(1)	0.002(1)
N12	0.031(1)	0.042(1)	0.053(2)	−0.003(1)	0.002(1)	−0.011(1)
N13	0.038(1)	0.032(1)	0.038(1)	−0.002(1)	−0.001(1)	0.000(1)
N14	0.034(1)	0.036(1)	0.053(2)	0.003(1)	0.008(1)	−0.001(1)

Table 4.4. (Continued).

Atom	*U11*	*U22*	*U33*	*U12*	*U13*	*U23*
C11	0.038(2)	0.049(2)	0.051(2)	−0.003(1)	0.011(1)	−0.005(2)
C12	0.045(2)	0.034(2)	0.039(2)	−0.005(1)	−0.001(1)	−0.002(1)
C13	0.045(2)	0.042(2)	0.048(2)	0.006(1)	0.003(1)	0.011(2)
C14	0.037(2)	0.044(2)	0.048(2)	0.007(1)	−0.007(1)	−0.004(2)
C15	0.043(2)	0.036(2)	0.057(2)	−0.005(1)	0.007(1)	−0.014(2)
C16	0.033(2)	0.041(2)	0.046(2)	−0.002(1)	0.007(1)	0.002(1)
N21	0.043(1)	0.036(1)	0.036(1)	−0.002(1)	−0.000(1)	0.001(1)
N22	0.029(1)	0.039(1)	0.045(1)	0.001(1)	0.001(1)	−0.008(1)
N23	0.038(1)	0.029(1)	0.042(1)	−0.001(1)	−0.005(1)	0.004(1)
N24	0.036(1)	0.030(1)	0.046(2)	0.005(1)	0.005(1)	0.003(1)
C21	0.035(2)	0.045(2)	0.043(2)	−0.003(1)	0.007(1)	−0.005(1)
C22	0.046(2)	0.034(2)	0.041(2)	−0.005(1)	−0.008(1)	−0.002(1)
C23	0.044(2)	0.039(2)	0.044(2)	0.006(1)	−0.004(1)	0.008(1)
C24	0.036(1)	0.037(2)	0.041(2)	0.007(1)	−0.008(1)	0.000(1)
C25	0.038(2)	0.034(2)	0.050(2)	0.001(1)	0.003(1)	−0.005(1)
C26	0.034(1)	0.039(2)	0.044(2)	0.001(1)	0.005(1)	0.007(1)
N1	0.052(2)	0.051(2)	0.049(2)	0.006(1)	−0.008(1)	−0.014(1)
O11	0.067(2)	0.067(2)	0.072(2)	−0.012(1)	−0.016(1)	0.007(1)
O12	0.095(2)	0.114(3)	0.068(2)	−0.031(2)	−0.006(2)	0.016(2)
O13	0.081(2)	0.164(3)	0.062(2)	−0.018(2)	−0.024(2)	−0.019(2)
N2	0.070(2)	0.050(2)	0.046(2)	0.000(1)	0.013(1)	0.008(1)
O21	0.062(2)	0.091(2)	0.079(2)	−0.001(1)	0.009(1)	0.020(2)
O22	0.106(3)	0.144(3)	0.056(2)	−0.009(2)	−0.005(2)	−0.007(2)
O23	0.088(2)	0.190(4)	0.059(2)	−0.031(2)	0.025(2)	0.009(2)
O7	0.062(1)	0.067(2)	0.046(1)	−0.009(1)	0.001(1)	−0.015(1)
O8	0.084(2)	0.060(2)	0.044(1)	0.008(1)	0.002(1)	−0.012(1)
O9	0.062(2)	0.084(2)	0.065(2)	−0.030(2)	0.024(2)	−0.026(2)
O10	0.061(3)	0.094(3)	0.054(2)	−0.004(2)	−0.007(2)	0.010(2)
O9′	0.062(2)	0.084(2)	0.065(2)	−0.030(2)	0.024(2)	−0.026(2)
O10′	0.061(3)	0.094(3)	0.054(2)	−0.004(2)	−0.007(2)	0.010(2)

[a]Estimated standard deviations of the least significant digits are given in parentheses.

Table 4.5. Selected interatomic bond lengths[a] (Å) and bond angles[a] (º) for $[Mg(H_2O)_6](NO_3)_2 \cdot 2HMT \cdot 4H_2O$.

Mg1–O1	2.044(2)	N14–C16	1.472(4)
Mg1–O2	2.060(2)	N21–C21	1.466(4)
Mg1–O3	2.050(2)	N21–C22	1.469(4)
Mg1–O4	2.050(2)	N21–C23	1.477(4)
Mg1–O5	2.050(2)	N22–C21	1.471(4)
Mg1–O6	2.062(2)	N22–C24	1.468(4)
N11–C11	1.475(4)	N22–C25	1.478(3)
N11–C12	1.476(4)	N23–C22	1.465(4)
N11–C13	1.470(4)	N23–C24	1.471(3)
N12–C11	1.466(4)	N23–C26	1.468(3)
N12–C14	1.466(4)	N1–O11	1.238(3)
N12–C15	1.472(4)	N1–O12	1.214(4)
N13–C12	1.474(4)	N1–O13	1.222(4)
N13–C14	1.467(4)	N2–O21	1.238(4)
N13–C16	1.464(3)	N2–O22	1.203(4)
N14–C13	1.473(4)	N2–O23	1.223(3)
N14–C15	1.471(4)		
O1–Mg1–O2	87.4(1)	N11–C13–N14	112.4(2)
O1–Mg1–O3	88.0(1)	N12–C14–N13	111.9(2)
O1–Mg1–O5	92.6(1)	N12–C15–N14	111.8(2)
O1–Mg1–O6	91.0(1)	N13–C16–N14	111.8(2)
O2–Mg1–O3	92.3(1)	C21–N21–C22	108.4(2)
O2–Mg1–O4	92.0(1)	C21–N21–C23	108.1(2)
O2–Mg1–O6	87.3(1)	C22–N21–C23	107.9(2)
O3–Mg1–O4	92.8(1)	C21–N22–C24	108.6(2)
O3–Mg1–O5	87.5(1)	C21–N22–C25	108.4(2)
O4–Mg1–O5	88.0(1)	C24–N22–C25	107.8(2)
O4–Mg1–O6	88.2(1)	C22–N23–C24	108.8(2)
O5–Mg1–O6	92.9(1)	C22–N23–C26	108.5(2)
O1–Mg1–O4	179.1(1)	C24–N23–C26	108.0(2)
O2–Mg1–O5	179.9(1)	C23–N24–C25	108.7(2)
O3–Mg1–O6	179.0(1)	C23–N24–C26	108.6(2)

Table 4.5. (Continued).

C11–N11–C12	107.6(2)	C25–N24–C26	108.0(2)
C11–N11–C13	108.2(2)	N21–C21–N22	112.1(2)
C12–N11–C13	107.5(2)	N21–C22–N23	112.0(2)
C11–N12–C14	108.4(2)	N21–C23–N24	111.6(2)
C11–N12–C15	108.8(3)	N22–C24–N23	111.6(2)
C14–N12–C15	107.7(2)	N22–C25–N24	111.5(2)
C12–N13–C14	108.4(2)	N23–C26–N24	111.6(2)
C12–N13–C16	108.2(2)	O11–N1–O12	121.1(3)
C14–N13–C16	108.4(2)	O11–N1–O13	118.6(3)
C13–N14–C15	108.6(2)	O12–N1–O13	120.2(3)
C13–N14–C16	108.1(2)	O21–N2–O22	121.8(3)
C15–N14–C16	107.8(2)	O21–N2–O23	119.8(3)
N11–C11–N12	112.4(2)	O22–N2–O23	118.4(4)
N11–C12–N13	112.1(2)		

[a]Estimated standard deviations of the least significant digits are given in parentheses.

4.5 Results and Discussion

Within the asymmetric unit of $[Mg(H_2O)_6](NO_3)_2 \cdot 2HMT \cdot 4H_2O$, two HMT molecules, the $[Mg(H_2O)_6]^{2+}$ cation and the two water molecules (O7 and O8) are related by an approximate pseudo inversion (1/2−x, $^1/_2$−y, 1−z). This imposes a pseudo $C\bar{1}$ symmetry for a layer at z = 1/2 and a pseudo *C*2/*c* space group symmetry for the substructure containing these entities in all equivalent positions of $P2_1/n$. It is to be noted that the true space group $P2_1/n$ is a subgroup of *C*2/*c*. The nitrate anions and two water molecules (O9 and O10) are at an interface between the pseudo $C\bar{1}$ layers described above and this interface shows $Pb2_1a$ pseudo symmetry if these entities are considered on their own and the distortion of β from 90° is ignored. The substructure containing these atoms in all equivalent positions has pseudo *Pbna*

symmetry. The true space group $P2_1/n$ is also a subgroup of *Pbna*. Thus, we could say that the structure $P2_1/n$ is the result of the interaction between two substructures with each other, one of $C2/c$ symmetry, the other of *Pbna* symmetry, see the projection down **a** of the Figure 4.2.

The pseudo symmetry allows the possibility of stacking faults that would reduce the scale of the $h+k$ odd reflections. If the fraction α of the structure is displaced by *C*-centering, then the value for *F* changes to

$$F' = (1-\alpha)F + \alpha \exp(2\pi i(h+k)/2)F$$

where *F* is the structure factor for a perfectly ordered structure. When $h+k$ is even $F' = F$ but when $h+k$ is odd $F' = (1-2\alpha)F$. Refinement used separate scale constants for $h+k$ even and $h+k$ odd data, and the final ratio of 1:0.968(6) was obtained implying $\alpha = 0.014(3)$, small but possibly significant.

There is also the possibility of twinning, although there is no evidence for this from the crystal chosen for data collection and refinement. Twin related crystals could have a twin interface at $z = \pm 1/4$ using either a *b*-glide or an *a*-glide perpendicular to **c***. Polytypism is possible by turning the twin rule into a symmetry operation. Half of the inversion and pseudo inversion operations at $z = 0$ and 1/2 survive but the 2_1 (and implied *n*-glide) relating adjacent layers are replaced by an *a*-glide perpendicular to **c*** (and the implied 2_1 screw operations). This monoclinic option is also a subgroup of *Pbna*.

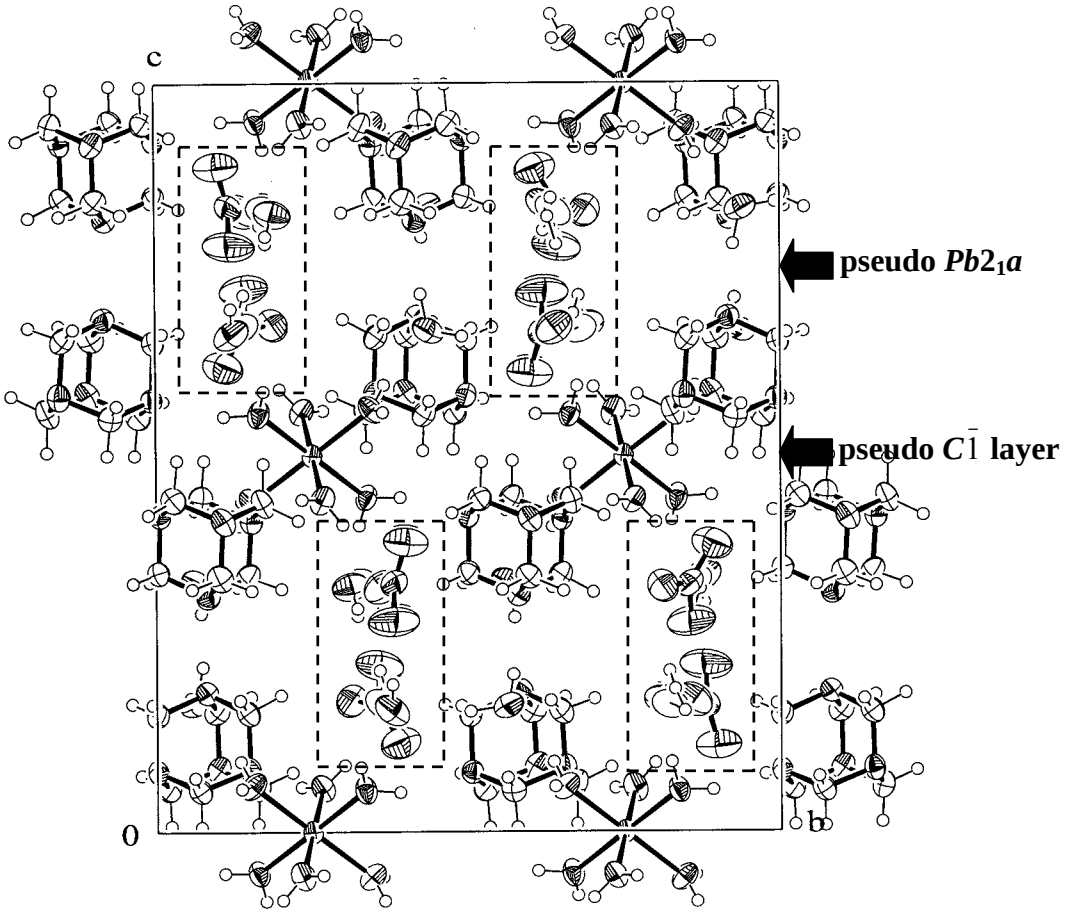

Figure 4.2. A projection of the cell contents down **a**. The $[Mg(H_2O)_6]^{2+}$ and the HMT molecules form pseudo $C\bar{1}$ layers at Z = 0, 1/2. The remaining atoms enclosed by dotted lines form interfacial layers of pseudo $Pb2_1a$ symmetry at $z = \pm 1/4$.

Structure Description

The water molecules of the $[Mg(H_2O)_6]^{2+}$ cation, *i.e.* atoms O1, O2, O3, O4, O5, and O6, each have two protons that can be donated to form hydrogen bonds (Figure 4.3) to neighboring atoms. Each of these hydrate oxygen atoms is linked to a nitrogen atom in a different HMT molecule O1···N13^{i} = 2.817(3) Å, O2···N14^{iii} = 2.810(3) Å, O3···N12^{iv} = 2.820(3) Å, O4···N23 = 2.822(3) Å, O5···N24^{iv} = 2.824(3) Å, O6···N22^{iii} = 2.860(3) Å. Atoms O1 and O2 also form hydrogen bonds to an

oxygen atom of a nitrate anion, O1···O11^{ii} = 2.796(3) Å, O2···O21 = 2.825(3) Å, while O3, O4, O5, and O6 act as hydrogen bond donors to the remaining water molecules, O3···O8^{iv} = 2.746(3) Å, O4···O10^{iv} = 2.698(5) Å, O4···O10′^{iv} = 2.738(9) Å, O5···O9^{v} = 2.735(3) Å, O5···O9′^{v} = 2.774(13) Å, and O6···O7^{iv} = 2.764(3) Å. Each of the four solvate water molecules also uses both protons as hydrogen bond donor atoms (thus, three strong hydrogen bond contacts to each solvate water molecule) forming a unique hydrogen bonding pattern with two solvates, O7 and O8, connecting a hydrate with a nitrate anion and an HMT molecule, and two solvates, O9 and O10, connecting a hydrate with two nitrate anions; O7···N11^{vi} = 2.859(4) Å, O7···O22^{vii} = 3.113(5) Å (Figure 4.4a), O8···N21^{viii} = 2.855(3) Å, O8···O12^{ix} = 3.011(4) Å (Figure 4.4b), O9···O13^{iv} = 2.982(5) Å, O9···O23 = 2.929(4) Å, O9′···O12^{iv} = 3.075(15) Å, O9′···O21 = 3.013(13) Å (Figure 4.4c), O10′···O11 = 3.099(9) Å, O10···O23^{iii} = 3.014(7) Å, O10···O13 = 3.046(6) Å, O10′···O22^{iii} = 3.119(11) Å (Figure 4.4d). Thus, all twenty of the potential strong hydrogen bond donors (OH) are utilized. All the nitrogen atoms of the two HMT molecules are strong hydrogen bond acceptors.

Table 4.6. Hydrogen bonding geometry (Å, º) in $[Mg(H_2O)_6](NO_3)_2 \cdot 2HMT \cdot 4H_2O$.

D–H···*A*	*D*−H	H···*A*	*D*···*A*	*D*–H···*A*
O1−H1A···N13^{i}	0.91(4)	1.94(4)	2.817(3)	163(3)
O1−H1B···O11^{ii}	0.78(4)	2.02(4)	2.796(3)	175(4)
O2−H2A···N14^{iii}	0.84(4)	1.99(4)	2.810(3)	164(4)
O2−H2B···O21	0.82(4)	2.03(4)	2.825(3)	162(3)
O3−H3A···N12^{iv}	0.88(4)	1.95(4)	2.820(3)	167(4)
O3−H3B···O8^{iv}	0.78(4)	1.98(4)	2.746(3)	168(4)
O4−H4A···N23	0.90(3)	1.94(4)	2.822(3)	165(3)
O4−H4B···O10^{iv}	0.87(4)	1.83(4)	2.698(5)	175(4)
O4−H4B···O10'^{iv}	0.87(4)	1.89(4)	2.738(9)	167(4)
O5−H5A···N24^{iv}	0.86(3)	1.98(3)	2.824(3)	168(4)
O5−H5B···O9^{v}	0.82(4)	1.93(4)	2.735(3)	170(3)
O5−H5B···O9'^{iv}	0.82(4)	2.00(4)	2.774(13)	158(3)
O6−H6A···N22^{iii}	0.89(4)	2.00(4)	2.860(3)	163(3)
O6−H6B···O7^{iv}	0.78(4)	1.99(4)	2.764(3)	169(4)
O7−H7A···N11^{vi}	0.97(4)	1.90(4)	2.859(4)	171(3)
O7−H7B···O22^{vii}	0.92(4)	2.24(4)	3.113(5)	159(3)
O8−H8A···N21^{viii}	0.81(4)	2.05(4)	2.855(3)	175(4)
O8−H8B···O12^{ix}	0.98(4)	2.10(4)	3.011(4)	155(3)
O9−H9A···O13^{iv}	0.87	2.12	2.982(5)	177.6
O9−H9B···O23	0.87	2.06	2.929(4)	178.8
O10−H10A···O13	0.87	2.18	3.046(6)	176.9
O10−H10B···O23^{iii}	0.87	2.15	3.014(7)	174.2
O9′−H9′A···O12^{iv}	0.87	2.21	3.075(15)	172.9
O9′−H9′B···O21	0.87	2.16	3.013(13)	167.5
O10′−H10′A···O11	0.87	2.24	3.099(9)	173.8
O10′−H10′B···O22^{iii}	0.87	2.27	3.119(11)	165.7

Symmetry codes:

i:	x,1+y,z	ii:	1/2-x,1/2+y,1/2-z	iii:	-x,1-y,1-z,
iv:	1-x,1-y,1-z	v:	1/2+x,3/2-z,-1/2+z	vi:	1/2+x,1/2-y,1/2+z
vii:	1+x,y, z	viii:	1/2+x,1/2-y,-1/2+z	ix:	3/2-x,-1/2+y,1/2-z

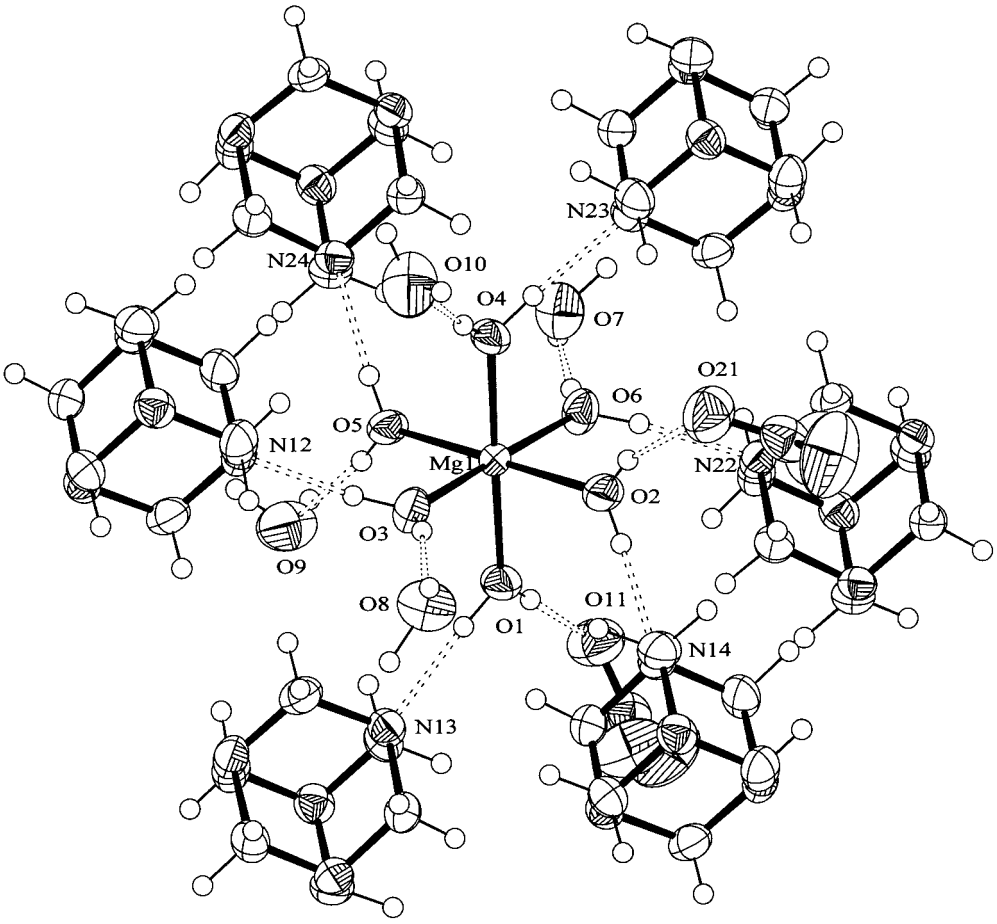

Figure 4.3. Hydrogen bonds pattern in $[Mg(H_2O)_6]^{2+}$ cation, O1, O2, O3, O4, O5 and O6, each have only two protons that can be donated to form hydrogen bonds.

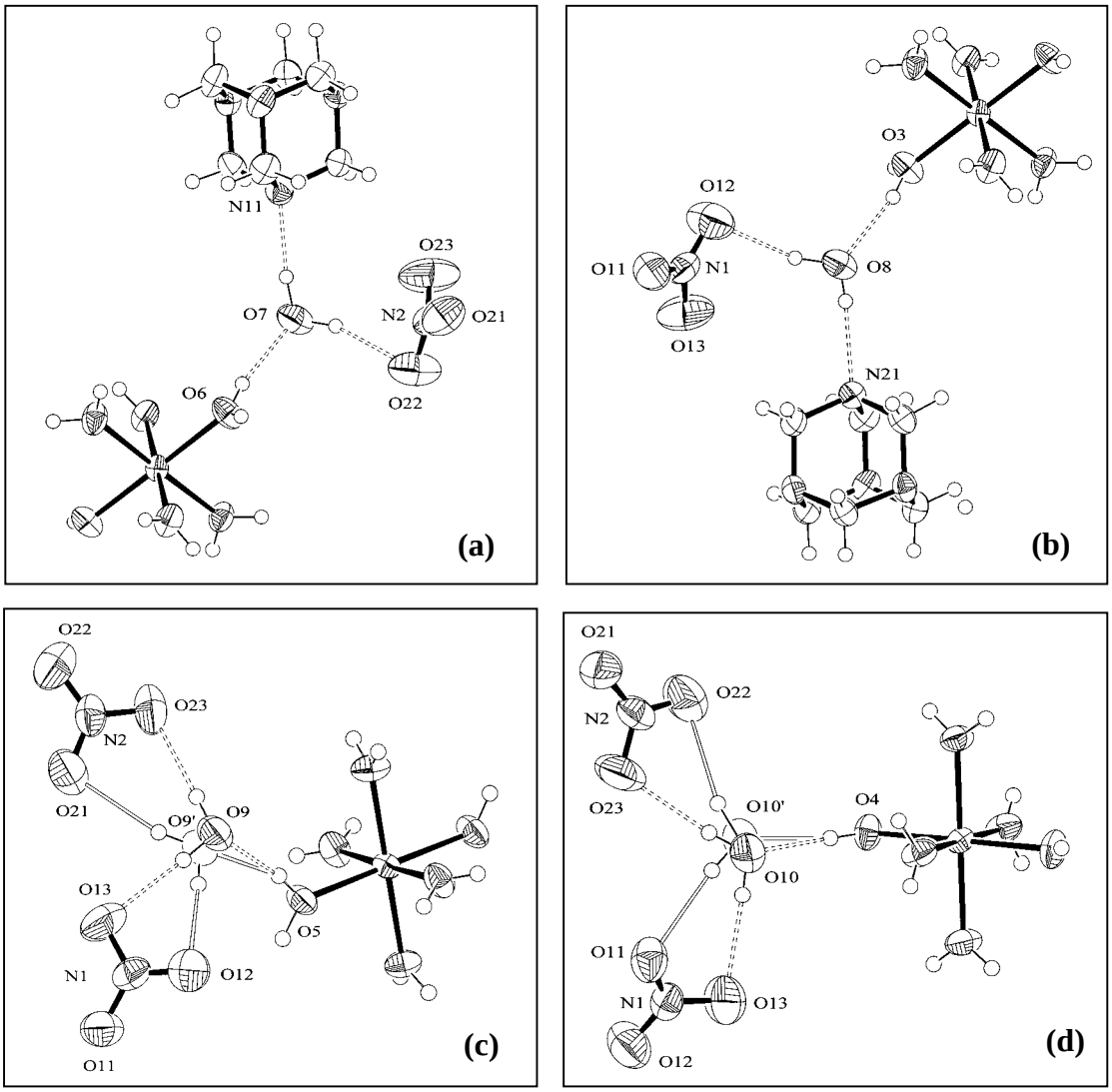

Figure 4.4. Hydrogen bonding interactions of the solvate water molecules. (a) O7, (b) O8, (c) O9, and (d) O10. The two orientations of the disordered water molecules in (c) and (d) are distinguished by dashed hydrogen binds for the major occupancy positions and open hydrogen bonds for the minor occupancy positions.

4.6 References

Addamiano, A. and Giacomello, G. (1951). **Ricerca Scientificca** 21: 2121.

Altomare, A., Burla, M. C., Camalli, M., Cascarano, G. L., Giacovazzo, C., Guagliardi, A., Moliterni, A. G. G., Polidori, G. and Spagna, R. (1999). *SIR97*: A new tool for crystal structure determination and refinement. **Journal of Applied Crystallography** 32: 115-119.

Barbieri, G. A. and Calzolari, F. (1910). **Atti della Accademia Nazionale dei Lincei. Rendiconti Classe di Scienze Fisiche Matematiche Naturali** 19(2): 584.

Barbieri, G. A. and Lanzoni, F. (1911). **Atti della Accademia Nazionale dei Lincei. Rendiconti Classe di Scienze Fisiche Matematiche Naturali** 20(1): 161.

Blessing, R. (1997). Outlier treatment in data merging. **Journal of Applied Crystallography** 30: 421-426.

Burnett, M. N. and Johnson, C. K. (1996). *ORTEP-III: Oak Ridge Thermal Ellipsoid Plot Program for Crystal Structure Illustrations*, Report ORNL-6895, Oak Ridge National Laboratory, Tennessee, USA.

De Santis, P., Kovacs, A. L., Liquori, A. M. and Mazzarella, L. (1965). Structure of the complex $CaBr_2 \cdot 10H_2O \cdot 2(CH_2)_6N_4$. **Journal of the American Chemical Society** 87(21): 4965-4966

Duisenberg, A. J. M., Kroon-Batenburg, L. M. J. and Schreurs, A. M. M. (2003). An intensity evaluation method: *EVAL-14*. **Journal of Applied Crystallography** 36: 220-229.

Farrugia, L. J. (1997). *ORTEP-3* for Windows−a version of *ORTEP-III* with a graphical user interface (GUI). **Journal of Applied Crystallography** 30: 565.

Ganesh V., Seshasayee, M., Aravamudan, G., Heijdenrijk, D. & Schenk, H. (1990). Structure of hexaaquacobalt(II) dinitratebis(hexamethylenetetramine) tetrahydrate. **Acta Crystallographica** C46: 949-951.

Hu, M.-L., Ye, M.-D. and Ng, S. W. (2002). Hexaaquanickel(II) dinitratebis(hexamethylenetetramine) tetrahydrate. **Acta Crystallographica** E58: m486-m487.

Imanakunov, B. I. and Lukina, L. (1979). Coordination of hexamethylenetetramine by inorganic salts. **Zhurnal Neorganicheskoi Khimii** 24(4):916-920.

Mazzarella, L., Kovacs, A. L., De Santis, P. and Liquori, A. M. (1967). Three-Dimensional X-ray analysis of the complex $CaBr_2 \cdot 10H_2O \cdot 2(CH_2)_6N_4$. **Acta Crystallographica** 22: 65-74.

Nonius BV. (1998). *COLLECT*: KappaCCD Software, Nonius BV., Delft, The Netherlands.

Rae, A. D. (2000). *RAELS. A Comprehensive Constrained Least-Squares Refinement Program,* Australian National University, Canberra, Australia.

Rae, A. D. (1975a). Crystal structure refinement using a number of orthonormal axial systems. **Acta Crystallographica** A31: 560-570.

Rae, A. D. (1975b). Rigid-body motion in crystals-The application of constraints on the *TLS* model. **Acta Crystallographica** A31: 570-574.

Zhu, H.-L., Xia, D.-S., Zeng, Q.-F., Wang, Z.-G. & Wang, D.-Q. (2003). Hexaaqua iron(II) dinitrate bis(dihexamethylenetetramine) tetrahydrate. **Acta Crystallographica** E59: m1020-m1021.

Zhu, H.-L., You, Z.-L., Qu, Y., Liu, W.-S., Tan, M.-Y. and Ma, J.-L. (2003). Hexa aquanickel(II) dichloride bis(hexamethylenetetramine) tetrahydrate. **Acta Crystallographica** E59: m924-m925.

CHAPTER V

ISOMORPHISM AND TWINNING IN $[M(H_2O)_6]I_2{\cdot}2(HMT){\cdot}4H_2O$; *M* = Ni, Mn, AND HMT = HEXAMETHYLENETETRAMINE

5.1 Abstract

The two compounds are isomorphic in monoclinic space group $P2_1/n$, $Z = 2$, with $a = 9.2410(6)$ Å, $b = 14.0460(7)$ Å, $c = 10.8733(17)$ Å, and $\beta = 97.310(8)°$ for the $[Ni(H_2O)_6]I_2{\cdot}2HMT{\cdot}4H_2O$, and $a = 9.3639(8)$ Å, $b = 14.1953(12)$ Å, $c = 10.9991(13)$ Å, and $\beta = 97.393(8)°$ for $[Mn(H_2O)_6]I_2{\cdot}2HMT{\cdot}4H_2O$. Both exhibit partial twinning of the crystals. The 0*kl* reflections overlap perfectly, and the splitting of the twin related reflections is a function of the *h* index. The final refinement cycles gave a twin ratio of 0.948(4):0.052 for the Ni complex, and 0.974(3):0.026 for the Mn complex.

5.2 Introduction

The prototypes of the class of complexes $MX_2{\cdot}nH_2O{\cdot}2HMT$, where $M = Ca^{2+}$, Ni^{2+}, Mg^{2+}, Co^{2+}, Ba^{2+}, Zn^{2+}, Mn^{2+}, Cd^{2+}, Sr^{2+}, X = Cl^-, Br^-, I^-, SCN^-, NO_2^-, NO_3^-, ClO_4^-, $S_2O_3^{2-}$, SO_4^{2-}, $S_2O_6^{2-}$, $Cr_2O_7^{2-}$, HMT = hexamethylenetetramine, and usually $n = 10$ were first studied by Barbieri (Barbieri & Calzolari, 1910; Barbieri & Lanzoni,

1911) and subsequently by several other groups (Ganesh, Seshasayee, Aravamudan, Heijdenrijk & Schenk, 1990; Mazzarella, Kovacs, De Santis & Liquor, 1967; Hu, Ye & Ng, 2002; Zhu, You, Qu, Liu, Tan & Ma, 2003; Zhu, Xia, Zeng, Wang & Wang, 2003). The metal ion exists as an $[M(H_2O)_6]^{2+}$ ion, and many of the complexes are isomorphic, crystallizing in space group $P\bar{1}$ with $Z = 1$.

Chapter IV reports the structure of the pseudo symmetric magnesium analog, $[Mg(H_2O)_6](NO_3)_2{\cdot}2(HMT){\cdot}4H_2O$ which crystallizes in the monoclinic space group, $P2_1/n$ with Z = 4. Here we report the structure of isomorphous $[M(H_2O)_6]I_2{\cdot}2HMT{\cdot}4H_2O$ (hexaaquametal(II)diiodide bis(hexamethylenetetramine) tetrahydrate) where *M* = Ni or Mn. Both crystallize in the monoclinic space group $P2_1/n$, but with Z = 2, and both were partially twinned. The splitting of twin related reflections is a function of the *h* index.

5.3 Experimental

Preparation of the Ni(II) and Mn(II) Complexes

A light green solution containing $NiCl_2{\cdot}6H_2O$ (2 mmol, 0.4754 g) and KI (4 mmol, 0.6640 g) in 5 mL water, and a second colorless solution containing hexamethylenetetramine (2 mmol, 0.5608 g) in 5 mL of water, were made by placing crystals in water at 50°C and stirring until dissolved. The warm nickel ion containing solution was added slowly to the HMT solution. The resulting solution was allowed to evaporate at room temperature until light green crystals were formed.

Similarly, a colorless solution containing $MnCl_2{\cdot}6H_2O$ (2 mmol, 0.3958 g) and KI (4 mmol, 0.6640 g) in 5 mL of water at 50°C was added to a warm solution

containing hexamethylenetetramine (2 mmol, 0.5608 g) in 5 mL of water. The resulting solution was allowed to evaporate at room temperature to form colorless crystals.

Data Collection, Data Reduction, and Structure Solution

Data were collected at 295 K on a Bruker-Nonius KappaCCD diffractometer using the COLLECT (Nonius, 1998) software. The diffractrometer was equipped with a graphite monochromator, Mo$K\alpha$ x-radiation source (λ = 0.71073 Å), and an *ifg* capillary collimator.

The diffraction patterns of $[Ni(H_2O)_6]I_2{\cdot}2(HMT){\cdot}4H_2O$ and $[Mn(H_2O)_6]$-$I_2{\cdot}2(HMT){\cdot}4H_2O$ show absences that uniquely define the space group as $P2_1/n$ (No. 14). The Ni and Mn complexes are isomorphic. Simulated precession photographs show a partial twinning of the crystals where 0*kl* reflections overlap perfectly and the splitting of twin related reflections is a function of the *h* index (see Figure 5.1). This can be explained using a 2-fold rotation about the **a** direction to create a twin related cell *i.e.* $\mathbf{a} = \mathbf{a}$, $\mathbf{b} = -\mathbf{b}$, $\mathbf{c} = -\mathbf{c}+f\mathbf{a}$ where $\mathbf{a'}\cdot\mathbf{c} = \mathbf{a}\cdot\mathbf{c}$ implies $f = 2(c/a)cos\beta = -0.29365$ for the Ni complex and −0.29594 for the Mn complex. A reciprocal space vector can be described in the reciprocal space of either cell. Thus $\mathbf{H} = h\mathbf{a}^*+k\mathbf{b}^*+l\mathbf{c}^* = h'\mathbf{a'}^*+k'\mathbf{b'}^*+l'\mathbf{c'}^*$, where $h = \mathbf{a}\cdot\mathbf{H}$, $h' = \mathbf{a'}\cdot\mathbf{H}$ *etc* so that $h' = h$, $k' = -k$, $l' = -l+fh$. The nearest twin related reflection to a reference *hkl* reflection has $h' = h$, $k' = -k$, $l' = -l+N$ where N is the nearest integer to fh. The values of $|N-fh|$ give the separation along $\mathbf{c}^*$ between twin related reflections described in reciprocal space. Reflection data were extracted using the orientation matrix for a single twin component.

Data reduction used the EvalCCD package (Duisenberg, Kroon-Batenburg & Schreurs, 2003), and reflections were corrected for absorption using SORTAV (Blessing, 1997). The structure was solved by direct methods using SIR97 (Altomare, Burla, Camalli, Cascarano, Giacovazzo, Guagliardi, Moliterni, Polidori & Spagna, 1999) and refined with RAELS (Rae, 2000). The ORTEP-III (Burnett & Johnson, 1996; Farrugia, 1997) graphics drawing program was used for illustrations. Crystal data and details of the data collection and structure refinement are summarized in Table 5.1.

Refinement statistics for the Ni and Mn complexes from RAELS are listed in the Tables 5.2 and 5.3, respectively. Fractional coordinates and isotropic atomic displacement parameters for the nonhydrogen atoms are given in Tables 5.4 and 5.5 for the Ni and Mn complexes, respectively. Anisotropic atomic displacement parameters for the nonhydrogen atoms are given in Tables 5.6 and 5.7. Selected interatomic bond distances and angles are complied in Table 5.8, and hydrogen bond parameters are given in Table 5.9. Derived hydrogen atom positions, isotropic atomic displacement parameters, and anisotropic atomic displacement parameters for the hydrogen atoms are given as supplementary material in Appendix D as Table D.1 for Ni and Table D.2 for Mn.

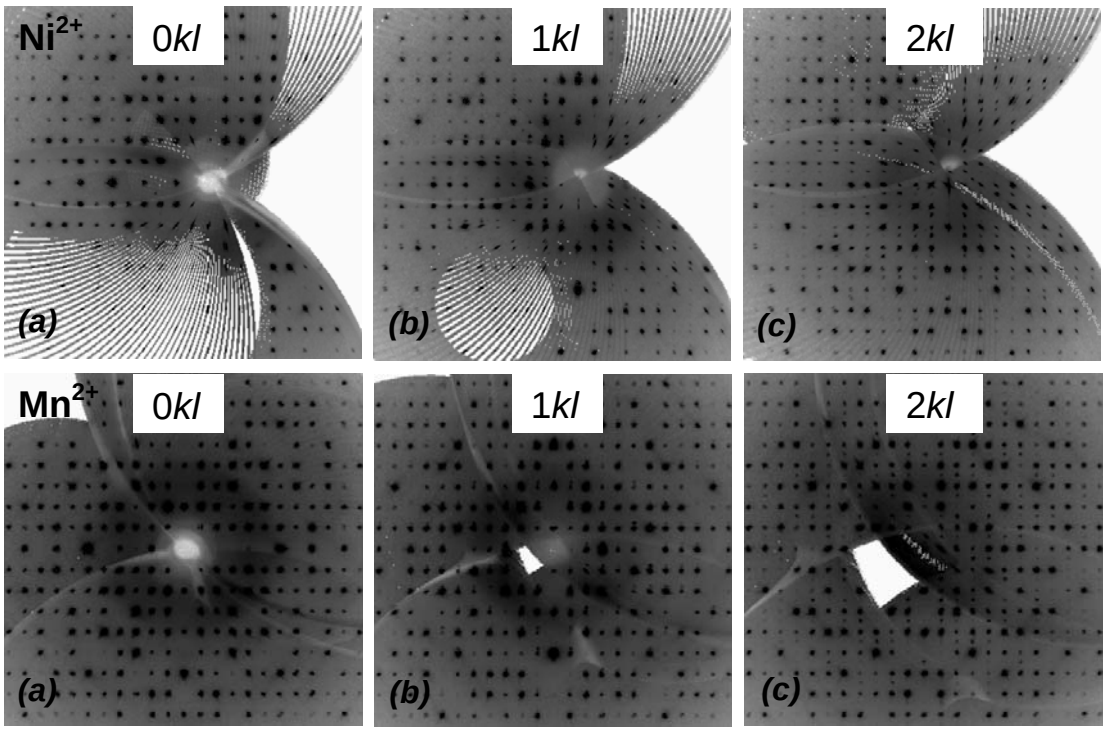

Figure 5.1. Precession photographs at 295 K for $[Ni(H_2O)_6]I_2{\cdot}2HMT{\cdot}4H_2O$ (top) and $[Mn(H_2O)_6]I_2{\cdot}2HMT.4H_2O$ (bottom). Spot splitting resulting from twin related reflections as a function of the *h* index can be seen. The 0*kl* (a) reflections overlap perfectly. The 1*kl* (b) and 2*kl* (c) reflections exhibit spot splitting of twin related reflections as a function of the *h* index.

5.4 Details of the Structure Refinement

The constrained least squares refinement program RAELS (Rae, 2000) was used for refinement. This program allows twin parameters a_i in the model $Y(\mathbf{h_i}) = \sum_i a_i |F(\mathbf{h_i})|^2$ to be modified to become $a_i p_j$ where p_j is a refinable parameter associated with *j*, and *j* is an integer included on the reflection file (p_j = 1.0 if j = 0) (Rae & Edwards, 2001). The reflection file includes *hkl* for each of the two twin components. The program knows to omit the second twin component if it has $h = k = l = 0$. Only

reflections with h = 0, ±3, ±4, ±6, ±7, ±10 were considered to be overlapped, *i.e.* $|N–fh| < 0.25$, and were assigned parameters $p_0 = 1$, p_1, p_2, p_3, p_4, p_5, respectively. The twin ratio at convergence was 0.948(4):0.052 for the Ni complex, and 0.974(3):0.026 for the Mn complex.

Hydrogen atoms were inserted in appropriate geometric positions after each refinement cycle and given the same anisotropic displacement parameter U_{ij} as the atoms to which they were attached. The metal ion was fixed at a center of inversion. There were no other constraints and restraints on positional parameters. The atom displacement parameters for each $M(H_2O)_6$ cation were refined using a 12 parameter *TL* rigid body model centered on the metal atom (Rae, 1975a, 1975b), and the HMT molecules using a 15 parameter *TLX* rigid body model. The program RAELS allows atomic displacement parameters to be described as the sum of various contributions. An additional isolated anisotropic atom parameterization of the *M* atom was allowed but the parameters were small ($\leq 2\sigma$). The I, O4, and O5 atoms were refined as isolated anisotropic atoms. Hydrogen atoms were reincluded after each refinement cycle in sensible calculated positions and given atomic displacement parameters determined by (*TL*, *TLX* or isolated atom) models appropriate to the atoms to which they are attached.

Table 5.1. Summary of crystal data, data collection, and structure refinement details for $[M(H_2O)_6]I_2 \cdot 2\ HMT \cdot 4H_2O$; M = Ni or Mn.

	M = Ni	M = Mn
Crystal data		
Structure Formula	$[Ni(H_2O)_6]I_2 \cdot 2HMT \cdot 4H_2O$	$[Mn(H_2O)_6]I_2 \cdot 2HMT \cdot 4H_2O$
Chemical formula	$C_{12}H_{44}I_2N_8NiO_{10}$	$C_{12}H_{44}I_2N_8MnO_{10}$
Chemical formula weight	773.04	769.26
Cell setting, space group	Monoclinic, $P2_1/n$ (No. 14)	Monoclinic, $P2_1/n$ (No. 14)
a (Å)	9.2410(6)	9.3639(8)
b (Å)	14.0460(7)	14.1953(12)
c (Å)	10.8733(17)	10.9991(13)
α (º)	90	90
β (º)	97.310(8)	97.393(8)
γ (º)	90	90
Volume ($Å^3$)	1399.87	1449.88
Z	2	2
D_{calc} (Mg m^{-3})	1.843	1.769
Radiation type, wavelength	Mo$K\alpha$, 0.71073	Mo$K\alpha$
θ range (º)	5.15-27.53	5.15-27.53
Absorption coefficient, μ (mm^{-1})	2.969	2.649
Temperature (K)	295±2	295±2
Crystal color/form	Light green, prism	Colorless, prism
Crystal size (mm)	0.25×0.20×0.15	0.30×0.20×0.15
Data collection		
Diffractometer	Nonius KappaCCD	Nonius KappaCCD
Data collection method	ϕ scans plus ω scans with κ offsets	ϕ scans plus ω scans with κ offsets
Absorption collection	Multi-scan	Multi-scan
T_{min}, T_{max}	0.500, 0.640	0.535, 0.670

Table 5.1. (Continued).

No. of measured reflections	12627	32048
No. of unique independent data	3152	3250
No. of observed reflections	2467	2668
Criterion for observed reflections	$I > 3\sigma(I)$	$I > 3\sigma(I)$
R_{int}	0.040	0.061
θ_{max} (º)	27.5	27.5
Range of *h, k, l*	$-10 \rightarrow h \rightarrow 11$ $-18 \rightarrow k \rightarrow 15$ $-14 \rightarrow l \rightarrow 14$	$-10 \rightarrow h \rightarrow 11$ $-18 \rightarrow k \rightarrow 15$ $-14 \rightarrow l \rightarrow 14$
Refinement		
Refinement on	*F*	*F*
$R[F^2 > 3\ \sigma(F^2)]$, $wR(F^2)$, *S*	0.045, 0.77, 1.64	0.045, 0.78, 1.73
No. of relections used	2467	2668
No. of refined parameters	106	105
H-atom treatment	Calculated	Calculated
Weighting scheme	Based on measured s.u.'s $w = 1/(\sigma^2(F) + 0.0016F^2)$	Based on measured s.u.'s $w = 1/(\sigma^2(F) + 0.0009F^2)$
$(\Delta/\sigma)_{max}$	0.01	0.01
$\Delta\rho_{max}$, $\Delta\rho_{min}$ (e Å^{-3})	3.65, −2.43	3.52, −2.34

Computer programs: *COLLECT* (Nonius, 1998); *EVAL14* (Duisenberg, Kroon-Batenburg & Schreurs, 2003); *SIR97* (Altomare *et al*., 1999); *RAELS* (Rae, 2000); *ORTEP-III* (Burnett & Johnson, 1996; Farrugia, 1997).

Table 5.2. Reflection refinement statistics for $[Ni(H_2O)_6]I_2 \cdot 2HMT \cdot 4H_2O$.

	No. of reflections	*R(F)*	*R(F²)*	*wR*	*Gof*	*fh*	*|N−fh|*	p_j
$h = 0$[a]	148	0.049	0.083	0.087	1.91	0	0	1
$h = 3$[a]	318	0.039	0.062	0.065	1.39	−0.881	0.119	0.73(6)
$h = 4$[a]	303	0.042	0.056	0.071	1.51	−1.175	0.175	0.41(5)
$h = 6$[a]	237	0.048	0.065	0.076	1.61	−1.762	0.238	0.36(5)
$h = 7$[a]	212	0.052	0.070	0.087	1.83	−2.056	0.056	0.80(7)
$h = 10$[a]	73	0.069	0.111	0.093	1.61	−2.937	0.063	0.90(16)
other h[a]	1176	0.045	0.068	0.078	1.67	−	> 0.25	0
$I<3\sigma(I)$	685	0.468	0.715	0.452	1.41	−	−	−
All reflections	2467	0.045	0.067	0.077	1.64	−	−	−

a. $I>3\sigma(I)$

b. Number of independent variables = 106.
Final refinement cycle: maximum shift/error = 0.01.
The weighting scheme for F_{obs} data, was $w = 1/(\sigma^2(F_o)+(0.04)^2|F_o|^2)$.
The ratio of the mean $|F|$ for the 1281 $h+k$ odd reflections to $h+k$ even reflections with $I>3\sigma(I)$ was 0.600. For $|F|^2$the ratio was 0.278.
Final difference map electron density map: maximum +3.65 eÅ^{-3}, minimum –2.43 eÅ^{-3}.

Table 5.3. Reflection refinement statistics for $[Mn(H_2O)_6]I_2 \cdot 2HMT \cdot 4H_2O$.

	No. of reflections	*R(F)*	*R(F²)*	*wR*	*Gof*	*fh*	*|N−fh|*	p_j
$h = 0$[a]	168	0.051	0.086	0.083	1.88	0	0	1.00
$h = 3$[a]	338	0.041	0.069	0.069	1.54	-0.887	0.113	0.70(8)
$h = 4$[a]	323	0.040	0.054	0.071	1.56	-1.183	0.183	0.50(7)
$h = 6$[a]	263	0.045	0.064	0.080	1.71	-1.775	0.225	0.58(9)
$h = 7$[a]	224	0.049	0.064	0.086	1.85	-2.070	0.070	0.91(11)
$h = 10$[a]	90	0.072	0.109	0.101	1.91	-2.958	0.042	1.00[c]
other h[a]	1262	0.045	0.066	0.080	1.76	−	>0.25	0
$I<3\sigma(I)$	582	0.448	0.752	0.454	1.55	−	−	−
All reflections	2668	0.045	0.067	0.078	1.73	−	−	−

a. $I>3\sigma(I)$

b. Number of independent variables = 105.
Final refinement cycle: maximum shift/error = 0.01.
The weighting scheme for F_{obs} data, was $w = 1/(\sigma^2(F_o)+(0.04)^2|F_o|^2)$.
Final difference map electron density map: maximum + 3.52 eÅ^{-3}, minimum – 2.34 eÅ^{-3}.

c. This value of p_5 for the Mn complex was constrained to be 1.00 after refining to be slightly greater than 1.00. Although the twin ratio was small the values for p_j appear sensible and are in the correct sequence in term of magnitudes.

Table 5.4. Fractional atomic coordinates[a] and equivalent isotropic displacement parameters[b] ($Å^2$) for the nonhydrogen atoms in $[Ni(H_2O)_6]I_2 \cdot 2HMT \cdot 4H_2O$.

	x	*y*	*z*	U_{eq}
Ni1	0.5000	0.5000	0.5000	0.023(1)
I1	0.05762(5)	0.65186(3)	0.18150(4)	0.0527(2)
O1	0.5835(4)	0.4775(3)	0.3382(3)	0.031(1)
O2	0.5268(5)	0.6437(3)	0.4840(4)	0.035(1)
O3	0.7092(4)	0.4905(3)	0.5951(4)	0.034(1)
O4	0.2088(16)	0.5064(9)	-0.0268(13)	0.149(4)
O5	0.4342(12)	0.4309(6)	0.1178(8)	0.132(4)
N1	0.4225(5)	0.8669(4)	0.1362(5)	0.036(1)
N2	0.6863(5)	0.8495(3)	0.1521(4)	0.030(1)
N3	0.5272(5)	0.7279(3)	0.0481(4)	0.034(1)
N4	0.5451(6)	0.7451(3)	0.2713(4)	0.036(1)
C1	0.5626(6)	0.9153(4)	0.1377(5)	0.033(1)
C2	0.4070(6)	0.7986(5)	0.0366(5)	0.038(1)
C3	0.4241(6)	0.8157(5)	0.2557(6)	0.037(1)
C4	0.6667(6)	0.7799(4)	0.0508(5)	0.033(1)
C5	0.6843(6)	0.7971(4)	0.2709(5)	0.034(1)
C6	0.5277(7)	0.6784(4)	0.1658(6)	0.040(2)

[a]Estimated standard deviations of the least significant digits are given in parentheses.

[b]Equivalent isotropic atomic displacement parameters for the atoms refined anisotropically, $U_{eq} = 1/3 \sum_i \sum_j U_{ij} a_i^* a_j^* \mathbf{a}_i \cdot \mathbf{a}_j$

Table 5.5. Fractional atomic coordinates[a] and equivalent isotropic displacement parameters[b] (Å^2) for the nonhydrogen atoms in $[Mn(H_2O)_6]I_2 \cdot 2HMT \cdot 4H_2O$.

	x	*y*	*z*	U_{eq}
Mn1	0.5000	0.5000	0.5000	0.0252(5)
I1	0.05515(4)	0.65442(3)	0.18744(4)	0.0560(2)
O1	0.5841(4)	0.4726(3)	0.3297(3)	0.037(1)
O2	0.5301(5)	0.6500(2)	0.4839(3)	0.040(1)
O3	0.7186(4)	0.4896(3)	0.5997(3)	0.040(1)
O4	0.2006(13)	0.5042(9)	-0.0144(11)	0.161(4)
O5	0.4437(11)	0.4352(5)	0.1029(6)	0.123(3)
N1	0.4246(5)	0.8677(3)	0.1349(4)	0.039(1)
N2	0.6843(4)	0.8492(3)	0.1548(4)	0.034(1)
N3	0.5284(5)	0.7282(3)	0.0521(4)	0.038(1)
N4	0.5429(5)	0.7486(3)	0.2730(4)	0.040(1)
C1	0.5633(6)	0.9152(3)	0.1380(4)	0.037(1)
C2	0.4108(5)	0.7976(4)	0.0375(5)	0.042(1)
C3	0.4245(6)	0.8182(4)	0.2525(5)	0.042(1)
C4	0.6663(5)	0.7789(4)	0.0553(4)	0.038(1)
C5	0.6805(5)	0.7995(4)	0.2720(4)	0.038(1)
C6	0.5255(7)	0.6811(4)	0.1706(5)	0.045(1)

[a]Estimated standard deviations of the least significant digits are given in parentheses.

[b]Equivalent isotropic atomic displacement parameters for the atoms refined anisotropically, $U_{eq} = 1/3 \sum_i \sum_j U_{ij} a_i^* a_j^* \mathbf{a}_i \cdot \mathbf{a}_j$

Table 5.6. Anisotropic atomic displacement parameters[a] in $[Ni(H_2O)_6]$ I_2 ·2HMT·$4H_2O$.

Atom	*U11*	*U22*	*U33*	*U12*	*U13*	*U23*
Ni1	0.024(1)	0.022(1)	0.022(1)	0.001(1)	0.002(1)	0.000(1)
I1	0.0465(3)	0.0523(3)	0.0562(3)	-0.0045(2)	-0.0058(2)	0.0233(2)
O1	0.037(2)	0.032(2)	0.026(1)	0.007(1)	0.004(1)	0.004(1)
O2	0.051(2)	0.018(2)	0.035(2)	-0.005(1)	0.000(1)	0.001(1)
O3	0.027(1)	0.040(2)	0.033(1)	0.001(1)	-0.005(1)	-0.002(2)
O4	0.136(9)	0.133(9)	0.169(10)	0.018(7)	-0.016(8)	-0.026(7)
O5	0.192(10)	0.085(5)	0.095(5)	0.059(6)	-0.074(6)	-0.058(5)
N1	0.029(1)	0.037(2)	0.039(2)	0.005(1)	-0.001(1)	0.002(1)
N2	0.028(1)	0.031(1)	0.032(1)	-0.002(1)	0.002(1)	0.003(1)
N3	0.035(2)	0.032(2)	0.034(1)	-0.004(1)	0.002(1)	-0.001(1)
N4	0.043(2)	0.033(2)	0.033(1)	-0.004(1)	0.004(1)	0.009(1)
C1	0.037(2)	0.026(1)	0.036(1)	0.002(1)	0.002(1)	0.006(1)
C2	0.031(1)	0.045(2)	0.036(1)	0.000(1)	-0.004(1)	0.001(1)
C3	0.033(1)	0.043(2)	0.038(2)	-0.004(1)	0.009(1)	0.000(1)
C4	0.032(1)	0.035(1)	0.033(1)	-0.001(1)	0.005(1)	0.001(1)
C5	0.033(1)	0.036(2)	0.031(1)	0.002(1)	-0.003(1)	0.006(1)
C6	0.048(2)	0.027(2)	0.043(2)	-0.005(1)	0.006(1)	0.005(1)

[a]Estimated standard deviations of the least significant digits are given in parentheses.

Table 5.7. Anisotropic atomic displacement parameters[a] in $[Mn(H_2O)_6]I_2 \cdot 2HMT \cdot 4H_2O$.

Atom	*U11*	*U22*	*U33*	*U12*	*U13*	*U23*
Mn1	0.0257(4)	0.0237(4)	0.0260(4)	0.0004(3)	0.0020(3)	0.0001(3)
I1	0.0500(3)	0.0553(3)	0.0596(3)	-0.0004(1)	-0.0039(2)	0.0244(2)
O1	0.045(2)	0.038(1)	0.030(1)	0.008(1)	0.009(1)	0.002(1)
O2	0.061(2)	0.022(1)	0.035(2)	-0.007(1)	-0.002(1)	0.002(1)
O3	0.030(1)	0.048(2)	0.040(1)	0.000(1)	-0.004(1)	0.002(1)
O4	0.140(9)	0.176(11)	0.159(9)	0.023(7)	-0.013(7)	-0.043(8)
O5	0.174(8)	0.086(4)	0.088(4)	0.051(5)	-0.063(5)	-0.046(3)
N1	0.031(1)	0.041(1)	0.044(1)	0.008(1)	0.000(1)	0.003(1)
N2	0.029(1)	0.036(1)	0.037(1)	-0.003(1)	0.002(1)	0.002(1)
N3	0.042(2)	0.034(1)	0.038(1)	-0.003(1)	0.001(1)	-0.003(1)
N4	0.047(2)	0.037(1)	0.036(1)	-0.003(1)	0.005(1)	0.010(1)
C1	0.042(1)	0.028(1)	0.040(1)	0.002(1)	0.002(1)	0.005(1)
C2	0.033(1)	0.049(2)	0.040(1)	-0.001(1)	-0.007(1)	0.001(1)
C3	0.036(1)	0.049(2)	0.043(1)	-0.002(1)	0.012(1)	0.000(1)
C4	0.035(1)	0.040(1)	0.038(1)	0.002(1)	0.008(1)	0.000(1)
C5	0.036(1)	0.042(2)	0.035(1)	0.003(1)	-0.005(1)	0.005(1)
C6	0.056(2)	0.029(1)	0.049(2)	-0.005(1)	0.005(1)	0.005(1)

[a]Estimated standard deviations of the least significant digits are given in parentheses.

Table 5.8. Selected interatomic bond lengths[a] (Å) and bond angles[a] (º) for $[M(H_2O)_6]I_2 \cdot 2HMT \cdot 4H_2O$; *M* = Ni or Mn.

	$Ni(H_2O)_6]I_2 \cdot 2HMT \cdot 4H_2O$	$Mn(H_2O)_6]I_2 \cdot 2HMT \cdot 4H_2O$
*M*1−O1	2.033(3)	2.158(3)
*M*1−O2	2.043(3)	2.158(3)
*M*1−O3	2.078(4)	2.199(3)
N1−C1	1.461(8)	1.459(7)
N1−C2	1.441(8)	1.457(7)
N1−C3	1.484(8)	1.472(7)
N2−C1	1.463(7)	1.463(6)
N2−C4	1.466(7)	1.475(6)
N2−C5	1.489(7)	1.473(6)
N3−C2	1.483(7)	1.471(7)
N3−C4	1.479(7)	1.475(6)
N3−C6	1.455(7)	1.468(6)
N4−C3	1.489(8)	1.481(7)
N4−C5	1.480(7)	1.479(7)
N4−C6	1.475(8)	1.472(7)
O1−*M*1−O2	90.9(2)	92.3(1)
O1−*M*1−O3	89.4(2)	90.0(1)
O2−*M*1−O3	89.5(2)	89.1(1)
C1−N1−C2	108.7(5)	109.1(4)
C1−N1−C3	107.8(4)	107.5(4)
C2−N1−C3	108.7(5)	108.0(4)
C1−N2−C4	108.0(4)	109.1(4)
C1−N2−C5	108.7(4)	108.1(4)
C4−N2−C5	108.0(4)	108.2(4)

Table 5.8. (Continued).

	$Ni(H_2O)_6]I_2{\cdot}2HMT{\cdot}4H_2O$	$Mn(H_2O)_6]I_2{\cdot}2HMT{\cdot}4H_2O$
C2−N3−C4	108.2(4)	108.4(4)
C2−N3−C6	108.2(5)	107.6(4)
C4−N3−C6	108.3(4)	108.5(4)
C3−N4−C5	108.2(4)	108.0(4)
C3−N4−C6	109.2(5)	108.1(4)
C5−N4−C6	108.7(5)	108.9(4)
N1−C1−N2	112.7(4)	112.3(4)
N1−C2−N3	112.4(4)	112.5(4)
N1−C3−N4	110.3(4)	111.6(4)
N2−C4−N3	111.6(4)	111.4(4)
N2−C5−N4	110.7(4)	111.1(4)
N3−C6−N4	111.7(5)	111.7(4)

[a]Estimated standard deviations of the least significant digits are given in parentheses.

5.5 Results and Discussion

Each structure contains a $[M(H_2O)_6]^{2+}$ dication located on an inversion center. Each of the six independent hydrate hydrogen atoms is involved in a strong hydrogen bond. Every nitrogen atom of the HMT is also involved in strong hydrogen bonding, N1, N2, and N4 to water molecules of the $[M(H_2O)_6]^{2+}$ dication in different equivalent positions, and N3 to the water solvate, O5. The I^- ion is involved in four hydrogen bonds, two involving different equivalent positions of the water solvate O4.

Since the Ni and Mn compounds are isomorphic we shall infer that the first of any pair of values applies to the Ni compound, the second to the Mn compound. A unique hydrogen bonding scheme exists. The hydrate oxygen atoms, O1, O2, and O3,

each donate both available protons to form hydrogen bonds, namely O1···N2^{i} = 2.778(6) Å, 2.776(5) Å, O1···O5 = 2.690(7) Å, 2.718(6) Å, O2···N4 = 2.740(6) Å, 2.726(5) Å, O2···I1^{ii} = 3.576(4) Å, 3.553(3) Å, O3···N1^{ii} = 2.805(6) Å, 2.789(5) Å, O3···I1^{iii}= 3.634(4) Å, 3.588(3) Å. Therefore, the hydrogen atoms on O1, O2, and O3 are indisputably located. The solvate oxygen atoms, O4 and O5, each have two donor and one acceptor strong hydrogen bond contacts. The O1···O5 contact has already been noted. The donor contacts O5···N3^{v} = 2.918(8) Å, 2.910(7) Å and O5···O4 = 2.665(15) Å, 2.656(13) Å locate the hydrogen atoms attached to O5. The O5···O4 contact has now been used, leaving the contacts O4···I1 = 3.473(13) Å, 3.480(11) Å, and O4···I1^{iv} = 3.575(13) Å, 3.640(11) Å to locate the hydrogen atoms attached to O4 (see Figure 5.2). The O···N and O···O distances in the Ni compound, O···O [2.665(15)-2.690(7) Å], O···N [2.740(6)-2.918(8) Å], and O···I [3.473(13)-3.634(4) Å], are nearly the same as in the Mn compound, O···O [2.656(13)-2.718(6) Å], O···N [2.726(5)-2.789(5) Å], and O···I [3.480(11)-3.640(11) Å], but slightly different than in the chloro analog, $[Ni(H_2O)_6]Cl_2 \cdot 2HMT \cdot 4H_2O$ (Hu, Ye & Ng, 2002), O···O [2.714(3)-2.739(3) Å], O···N [2.799(3)-2.823(3) Å], and O···Cl [3.168(3)-3.253(3) Å].

Table 5.9. Hydrogen bonding geometry (Å, °).

$[Ni(H_2O)_6]I_2 \cdot 2(HMT) \cdot 4H_2O$				
D–H···*A*	*D*–H	H···*A*	*D*···*A*	*D*–H···*A*
O1–H1A···N2^{i}	1.00	1.78(1)	2.78(2)	173.2(4)
O1–H1B···O5	1.00	1.70(1)	2.69(2)	172.7(4)
O2–H2A···N4	1.00	1.75(1)	2.74(2)	168.3(3)
O2–H2B···I1^{ii}	1.00	2.59(1)	3.58(1)	169.7(2)
O3–H3A···N1^{ii}	1.00	1.84(1)	2.81(2)	162.4(3)
O3–H3B···I1^{iii}	1.00	2.66(1)	3.63(1)	164.3(2)
O4–H4A···I1	1.00	2.47(1)	3.47(1)	178.7(8)
O4–H4B···I1^{iv}	1.00	2.58(1)	3.58(1)	178.8(8)
O5–H5A···N3^{v}	1.00	1.93(1)	2.92(2)	169.0(4)
O5–H5B···O4	1.00	1.68(1)	2.67(1)	168.5(5)
$[Mn(H_2O)_6]I_2 \cdot 2(HMT) \cdot 4H_2O$				
D–H···*A*	*D*–H	H···*A*	*D*···*A*	*D*–H···*A*
O1–H1A···N2^{i}	1.00	1.78(1)	2.78(2)	174.5(2)
O1–H1B···O5	1.00	1.72(2)	2.72(2)	174.4(3)
O2–H2A···N4	1.00	1.73(1)	2.73(2)	170.5(2)
O2–H2B···I1^{ii}	1.00	2.56(1)	3.56(1)	171.6(2)
O3–H3A···N1^{ii}	1.00	1.81(1)	2.79(2)	164.2(2)
O3–H3B···I1^{iii}	1.00	2.61(1)	3.59(1)	165.9(2)
O4–H4A···I1	1.00	2.48(1)	3.48(1)	175.9(7)
O4–H4B···I1^{iv}	1.00	2.64(1)	3.64(1)	176.0(7)
O5–H5A···N3^{v}	1.00	1.92(1)	2.91(2)	171.5(4)
O5–H5B···O4	1.00	1.66(1)	2.66(1)	171.1(5)

Symmetry codes: i: 1/2−x,−1/2+y,1/2−z ii: 1/2+x,3/2−y,1/2+z iii: 1−x,1−y,1−z
iv: −x, 1−y, −z v: 1−x,1−y, −z

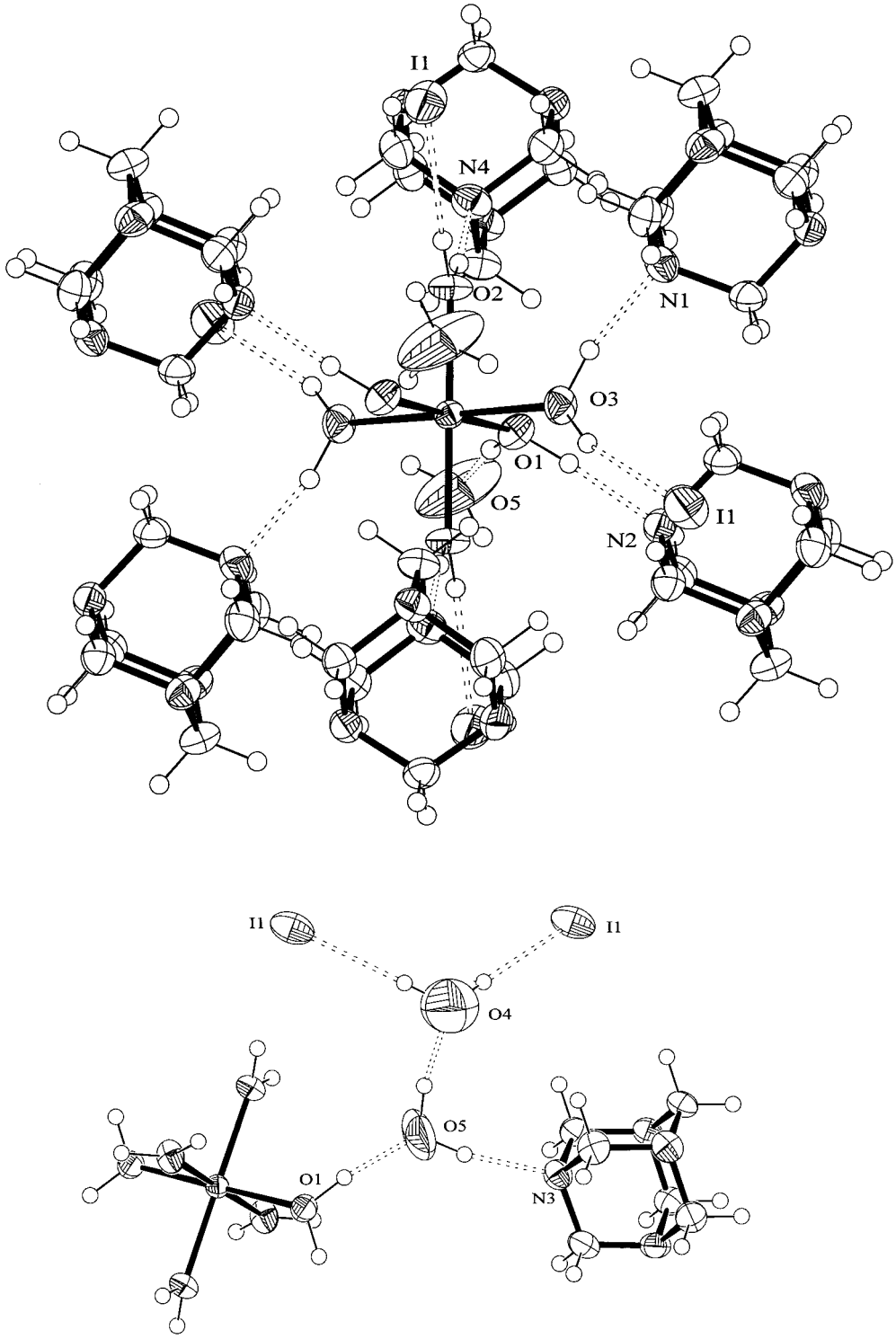

Figure 5.2. Hydrogen bond pattern in $[M(H_2O)_6]I_2 \cdot 2(HMT) \cdot 4H_2O$, M = Ni, Mn. O1, O2, and O3 in the $[M(H_2O)_6]^{2+}$ cation, and solvate O4 and O5 each form two donor and one acceptor hydrogen bonds.

The twin plane

A twinning mechanism is required to explain the spot splitting. This involves the identification of a twin plane that can be the interface between twin related components. The twin rule in reciprocal space is clear and the independent components of the intensity pattern can be described either by a two fold rotation axis about **a** or a mirror plane perpendicular to **c***. In real space the twin plane can either be a mirror or a glide plane perpendicular to **c*** or contain a 2 or a 2_1 operation parallel to **a**.

Inspection of the structure shows that the most likely twin plane coincides with an *n*-glide of the $P2_1/n$ structure, *e.g.* at y = 3/4. HMT molecules related by the *n*-glide 1/2+x, 3/2–y, 1/2+z could equally well be related by the pseudo 2_1 screw axis 1/2+x, 3/2–y, 0.804–z (see the projection of the structure down **a** in Figures 5.3 and 5.4.).

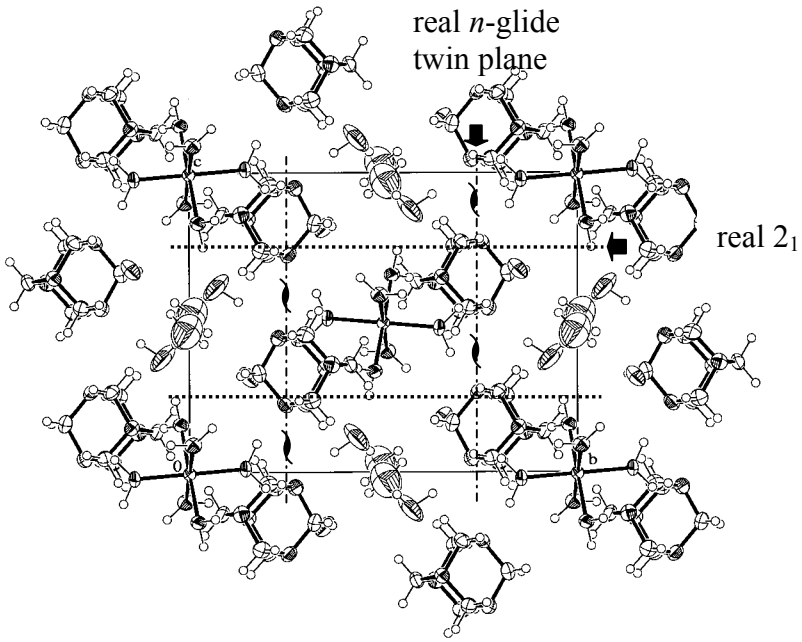

Figure 5.3. A projection down **a** show the twin plane containing a pseudo 2_1 screw axis parallel to **a**. Note that the screw axis goes through y = 3/4, *z* = 0.402.

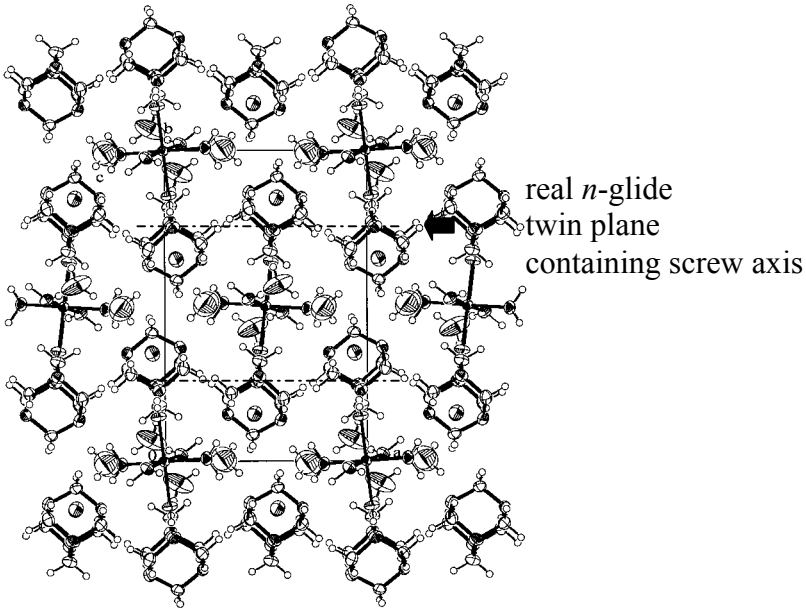

Figure 5.4. A projection down **a** show the twin plane at y = ±1/4 containing a pseudo 2_1 screw axis parallel to **a**.

5.6 References

Altomare, A., Burla, M. C., Camalli, M., Cascarano, G. L., Giacovazzo, C., Guagliardi, A., Moliterni, A. G. G., Polidori, G. and Spagna, R. (1999). *SIR97*: A new tool for crystal structure determination and refinement. **Journal of Applied Crystallography** 32: 115-119.

Barbieri, G. A. and Calzolari, F. (1910). **Atti della Accademia Nazionale dei Lincei. Rendiconti Classe di Scienze Fisiche Matematiche Naturali** 19(2): 584.

Barbieri, G. A. and Lanzoni, F. (1911). **Atti della Accademia Nazionale dei Lincei. Rendiconti Classe di Scienze Fisiche Matematiche Naturali** 20(1): 161.

Blessing, R. (1997). Outlier treatment in data merging. **Journal of Applied Crystallography** 30: 421-426.

Burnett, M. N. and Johnson, C. K. (1996). *ORTEP-III***.** Report ORNL-6895, Oak Ridge National Laboratory, Tennessee, USA.

De Santis, P., Kovacs, A. L., Liquori, A. M. and Mazzarella, L. (1965). Structure of the complex $CaBr_2 \cdot 10H_2O \cdot 2(CH_2)_6N_4$. **Journal of the American Chemical Society** 87(21): 4965-4966

Duisenberg, A. J. M., Kroon-Batenburg, L. M. J. and Schreurs, A. M. M. (2003). An intensity evaluation method: *EVAL-14*. **Journal of Applied Crystallography** 36: 220-229.

Farrugia, L. J. (1997). *ORTEP-3* for Windows−a version of *ORTEP-III* with a graphical user interface (GUI). **Journal of Applied Crystallography** 30: 565.

Ganesh V., Seshasayee, M., Aravamudan, G., Heijdenrijk, D. & Schenk, H. (1990). Structure of hexaaquacobalt(II) dinitratebis(hexamethylenetetramine) tetrahydrate. **Acta Crystallographica** C46: 949-951.

Hu, M.-L., Ye, M.-D. and Ng, S. W. (2002). Hexaaquanickel(II) dinitratebis(hexa-methylenetetramine) tetrahydrate. **Acta Crystallographica** E58: m486-m487.

Imanakunov, B. I. and Lukina, L. (1979). Coordination of hexamethylenetetramine by inorganic salts. **Zhurnal Neorganicheskoi Khiii** 24(4):916-920.

Mazzarella, L., Kovacs, A. L., De Santis, P. and Liquori, A. M. (1967). Three-Dimensional X-ray analysis of the complex $CaBr_2 \cdot 10H_2O \cdot 2(CH_2)_6N_4$. **Acta Crystallographica** 22: 65-74.

Nonius BV. (1998). *COLLECT*: KappaCCD Software, Nonius BV., Delft, The Netherlands.

Rae, A. D. (2000). *RAELS. A Comprehensive Constrained Least-Squares Refinement Program,* Australian National University, Canberra, Australia.

Rae, A. D. (1975a). Crystal structure refinement using a number of orthonormal axial systems. **Acta Crystallographica** A31: 560-570.

Rae, A. D. (1975b). Rigid-body motion in crystals-The application of constraints on the *TLS* model. **Acta Crystallographica** A31: 570-574.

Rae, A. D. and Edward, A. J. (2001). Refinement of partially overlapped CCD reflection data from twinned crystal. Proceedings, 20th European Crystallography conference at Cracow, Poland, p147.

Zhu, H.-L., Xia, D.-S., Zeng, Q.-F., Wang, Z.-G. & Wang, D.-Q. (2003). Hexaaqua iron(II) dinitrate bis(dihexamethylenetetramine) tetrahydrate. **Acta Crystallographica** E59: m1020-m1021.

Zhu, H.-L., You, Z.-L., Qu, Y., Liu, W.-S., Tan, M.-Y. and Ma, J.-L. (2003). Hexa aquanickel(II) dichloride bis(hexamethylenetetramine) tetrahydrate. **Acta Crystallographica** E59: m924-m925.

CHAPTER VI

REDETERMINATION OF TRIETHYLPHOSPHINE SULFIDE: A COMMENSURATELY MODULATED STRUCTURE

6.1 Abstract

The published structure of $PS(C_2H_5)_3$ is described as having a 1:1 disorder in space group $P6_3mc$ with Z = 2 with $P31c$ describing a proposed ordered structure rather than $P6_3$. Synthetic precession photographs obtained from data collection on a Nonius CCD diffractometer clearly indicate a doubling of the *a* and *b* axes. The parent $P6_3mc$ structure can also be described as a *C*-centred orthorhombic cell of $Ccm2_1$ symmetry with $\mathbf{a}_p' = 2\mathbf{a}_p+\mathbf{b}_p$, $\mathbf{b}_p' = \mathbf{b}_p$, $\mathbf{c}_p' = \mathbf{c}_p$ with four molecules per cell. The dominant modulation creating the extra reflections is a combination of displacements parallel to c. This mode lowers this orthorhombic symmetry to $Pnm2_1$ with three fold twinning or disorder restoring hexagonal diffraction symmetry. Further modulations of the parent structure seem necessary, with partial ordering in a mode of $Pna2_1$ symmetry a reasonable option. This suggests a probable six fold twinning since local symmetry of an average structure would then be lowered to *Pn*. Absences in the diffraction pattern suggest that the *n*-glide is a dominant feature within a layer and adjacent layers are related by anti translational symmetry destroying the *C*-centering. The distinction between twinning and disorder about a 3-fold axis is difficult to make.

6.2 Introduction

The structural studies of phosphorus compounds are important to the metal-ligand interactions and charges transfer, notably P−O linkages in the phosphine oxide compounds and P−S linkages in phosphine sulfide compounds (Cotton & Soderberg, 1963; Dobado, Martinez-Garcia, Molina & Sundberg, 1998). Trimethylphosphine oxide, $PO(CH_3)_3$, and trimethylphosphine sulfide, $PS(CH_3)_3$, were also studied by vibration spectroscopy (Wilkins, Hargen, Hedberg, Shen & Hedberg, 1975). Etter & Baures (1988) used triphenylphosphine oxide as a crystallization aid with compounds that do not pack well by themselves. Addition of triphenylphosphine oxide to the mother liquor allowed energetically preferred multicomponent crystals to form.

Tricyclohexylphosphine sulfide, $SP(C_6H_{11})_3$, contains a distortion about the phosphorus atoms at 295 K when refined using space group $Pn2_1a$ (Kerr, Boorman, Misener & van Roode, 1977). A less problematic structure at 163 K was obtained when refinement used space group *Pnma* (Reibenspies, Draper, Struck & Darensbourg, 1996). The second model is disordered by the mirror plane.

The crystal structure of triethylphosphine sulfide requires consideration of disorder, twinning and structure modulation. The structure of triethylphosphine sulfide, $PS(C_2H_5)_3$ has previously been determined by X-ray crystallography (Van Meerssche, 1954, Van Meerssche & Léonard, 1959a) and compared to $PSe(C_2H_5)_3$ (Van Meerssche & Léonard, 1959b). The hexagonal unit cell for $PS(C_2H_5)_3$ had a = 8.980(10) Å, b = 8.980(10) Å, c = 6.320(10) Å, γ = 120°, Z = 2, at 295 K determined by Weissenberg photographs (Cu$K\alpha$), space group $P6_3mc$ or possibly $P31c$ with twinning. The molecules in the crystal were not refined with certainty. A 1:1 disorder in space groups $P6_3mc$ was considered more likely than an ordered arrangement in

*P*31*c* with twinning (Figure 6.1). There are two molecules in the cell that sit on *c*-glide related sites 1/3, 2/3, *z* and 2/3, 1/3, *z*+1/2. The removal of the inherent disorder implied by the mirror planes of $P6_3mc$ reduces the symmetry to *P*31*c*. The inter-atomic distances could not be determined well because the disorder overlaps CH_3 groups. Large atomic displacement parameters along the *z* direction (U_{33} for P was 0.1178 $Å^2$) were observed and an *R* factor of 0.126 was obtained.

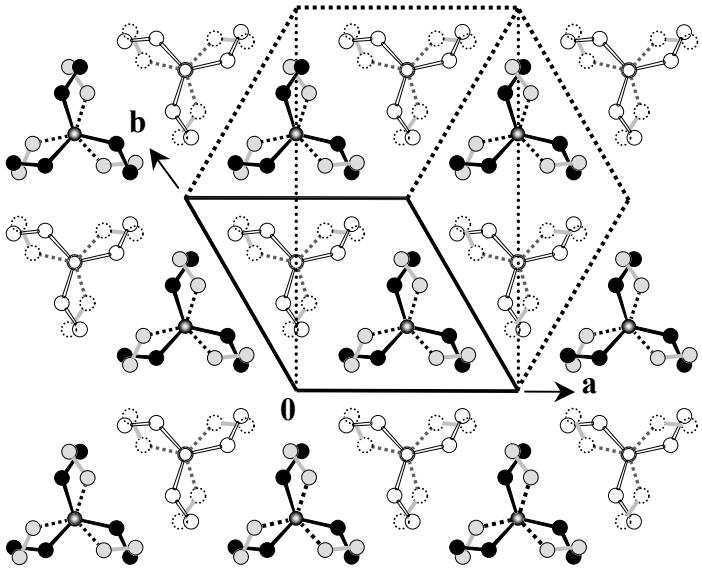

Figure 6.1. The 1:1 disorder of $PS(C_2H_5)_3$ in the hexagonal space group $P6_3mc$.

All distances and angles in the molecule differ from Cambridge Structure Database, CSD, average values; *d*[P=S] = 1.864(30) Å (CSD 1.954(5) Å, difference 0.09 Å), *d*[P−C] = 1.865(40) Å (CSD 1.806(9) Å, difference 0.059 Å), *d*[C−C] = 1.38(7) Å (CSD 1.513(14) Å, difference 0.133 Å), and ∠S−P−C = 112º, ∠C−P−C = 107º, ∠P−C−C = 114º. The authors mentioned that the C−C single bond distances

that were not well determined as they lie near the mirror planes created by the 1:1 disorder.

We have redetermined the crystal structure of triethylphosphine sulfide at lower temperature (200 K) using data collected on a KappaCCD diffractometer. The synthetic precession photograph of the *hk*1 reflections shows extra (weak) reflections between the strong reflections of the hexagonal cell that appear to double the *a* and *b* axes to create a fourfold increase in unit cell volume (see Figure 6.2).

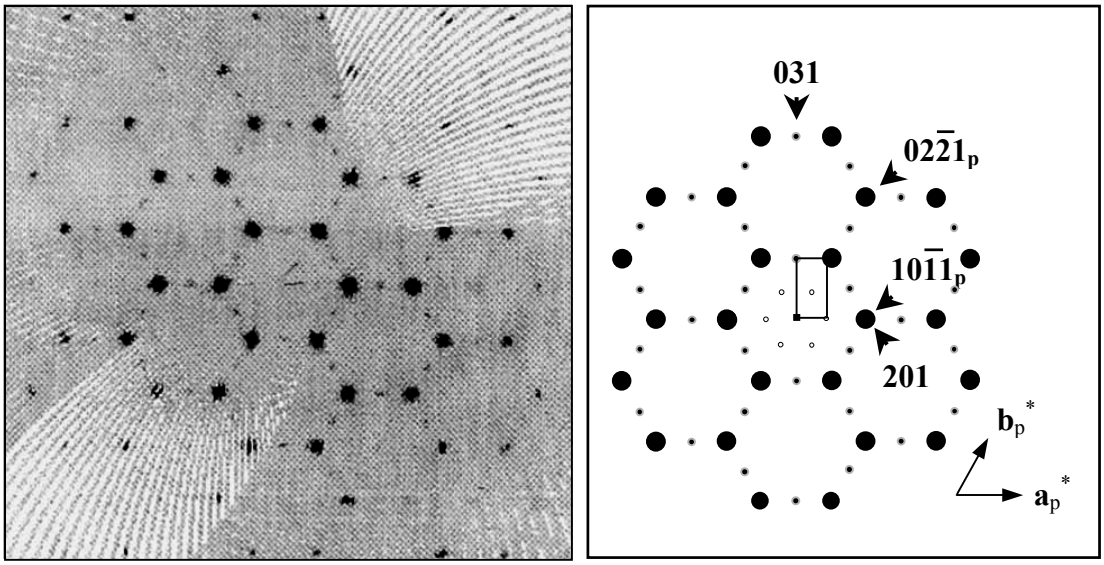

Figure 6.2. A synthetic precession photographs of the *hk*1 reflections. The *a* and *b* axes need to be doubled.

6.3 X-Ray Crystallography

Data collection at 200 K used a Nonius KappaCCD diffractometer equipped with a graphite monochromated Mo*Kα* x-radiation source (λ = 0.71073) and an *ifg* capillary collimator operated with the COLLECT program package (Nonius BV, 1998). Temperature was controlled using an Oxford Cryosystems 600 system (Oxford Cryostream, 1997). Data reduction used Denzo-Scalepack (Otwinowski & Minor, 1997). Crystal data and details of the data collection and structure refinement are summarized in Table 6.1.

Fractional coordinates and isotropic atomic displacement parameters for the refined atoms of our final model are given in Table 6.2. Anisotropic atomic displacement parameters for the nonhydrogen atoms are given in Table 6.3. Selected interatomic bond distances and angles are given in Table 6.4. Derived atom positions and isotropic atomic displacement parameters for the hydrogen atoms are given as supplementary material in Appendix E as Tables E.1 and E.2, respectively.

Merging the reflections

Step 1: Merge assuming $P\bar{1}$ diffraction symmetry.

3099 sets of multiply observed reflections. R_{merge} = 0.0453

Step 2: merge resulting reflections assuming $P\bar{3}$ diffraction symmetry.

1823 sets of multiply observed reflections. R_{merge} = 0.0456

Step 3: merge resulting reflections assuming $P\bar{3}\,1m$ diffraction symmetry.

941 sets of multiply observed reflections. R_{merge} = 0.0294

Step 4: merge resulting reflections assuming *P6/mmm* diffraction symmetry.

437 sets of multiply observed reflections. R_{merge} = 0.0316

The extra reflections appeared to maintain the diffraction symmetry of the parent structure and exactly equal twinning was imposed by merging the reflections. The data set of $P\bar{3}\,1m$ diffraction symmetry was used and a twin rule relating *hkl* to $-h-kl$ was used to approximate *P6/mmm* diffraction symmetry.

Hexagonal diffraction and weak reflections

The hexagonal diffraction symmetry appears to be maintained by the extra reflections of the parent structure and an exactly equal twinning model. The parent hexagonal structure ($P6_3mc$) can be re-described using any one of three 3-fold rotation related orthorhombic *C*-centered subgroups of $Ccm2_1$ symmetry, for example using the cell $\mathbf{a}_o = 2\mathbf{a}_p+\mathbf{b}_p$, $\mathbf{b}_o = \mathbf{b}_p$, $\mathbf{c}_o = \mathbf{c}_p$. This shows the possibility of combining component structures defined relative to these 3-fold related cells, using either disorder or twinning (Figure 6.3).

Possible explanations of the extra reflections in the diffraction pattern

(1). There is an ordered structure in $P6_3$ with cell $\mathbf{a} = 2\mathbf{a}_p$, $\mathbf{b} = 2\mathbf{b}_p$, $\mathbf{c} = \mathbf{c}_p$. This structure has two 2 related molecules of one chirality on the three fold axes at 1/3, 2/3, z and 2/3, 1/3, 1/2+z and six molecules of the other chirality in general positions 1/3, 1/6, z *etc.* This structure can be rejected as it does not retain the *c*-glide absence condition for the parent reflections since it produces a 3/4:1/4 disorder for molecules related by the mirror plane of $P6_3mc$ if the crystal is described modulo the parent cell $\mathbf{a}_p$, $\mathbf{b}_p$, $\mathbf{c}_p$.

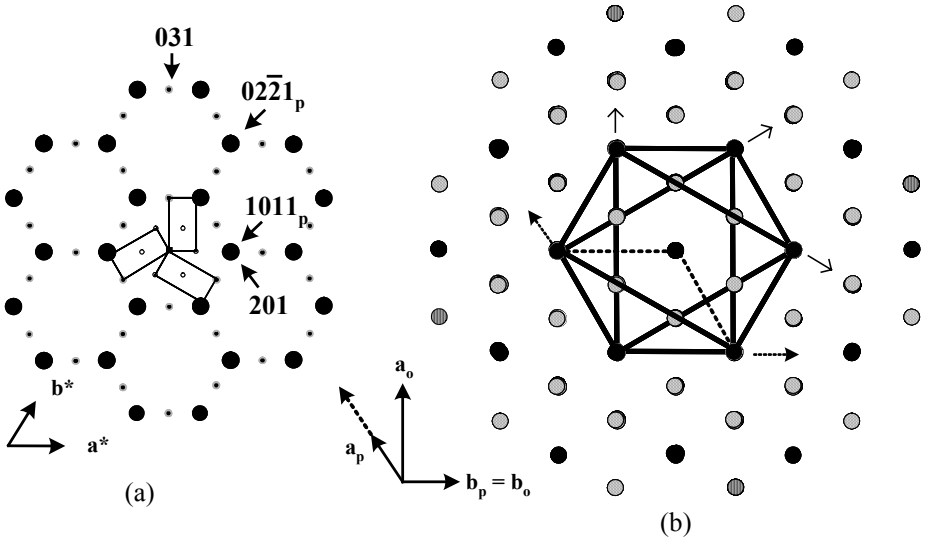

Figure 6.3. Schematic illustration showing possible orientations of orthorhombic cell component to create an apparently hexagonal system. (a) reciprocal lattices, (b) real lattice.

(2). The parent $P6_3mc$ structure may be re-described using the symmetry elements of the orthorhombic subgroup $Ccm2_1$ in one of three equivalent orientations. The extra reflections correspond to violating the absence condition for *C*-centering. Twinning or disordering the resultant primitive structure using a 3-fold rotation axis of the parent structure restores hexagonal symmetry to the diffraction pattern.

The mirror operation ceases to be a symmetry element upon ordering and this allows potentially ordered structures in space groups $Pna2_1$ or $Pca2_1$ but not $Pnm2_1$ or $Pcm2_1$. These space groups are all of those that have the maximum symmetry assuming a subgroup of $Ccm2_1$ and a primitive lattice. The $Pnm2_1$ and $Pcm2_1$ symmetry options could be obtained by displacing molecules related by the *C*-centering in opposite directions along **c**.

Modulation of an idealized 1:1 disordered *P*6$_3$*mc* parent structure modulo 2$\mathbf{a}_p$, 2$\mathbf{b}_p$, $\mathbf{c}_p$

There are eight molecules of symmetry 3 in the cell 2$\mathbf{a}_p$, 2$\mathbf{b}_p$, $\mathbf{c}_p$. Partial ordering of a disorder with no displacement can be described in terms of eight components. Two associated with each choice of a modulation vector **q**.

i.e.	$\mathbf{q_0} = 0$	$P31c$ and $P6_3$ in the parent cell $\mathbf{a}_p$, $\mathbf{b}_p$, $\mathbf{c}_p$
	$\mathbf{q_1} = \mathbf{a}_p^*/2$	$Pna2_1$ and $Pca2_1$ in cell $2\mathbf{a}_p+\mathbf{b}_p$, $\mathbf{b}_p$, $\mathbf{c}_p$
	$\mathbf{q_2} = (-\mathbf{a}_p^*+\mathbf{b}_p^*)/2$	$Pna2_1$ and $Pca2_1$ in cell $-\mathbf{a}_p+\mathbf{b}_p$, $-\mathbf{a}_p+\mathbf{b}_p$, $\mathbf{c}_p$
	$\mathbf{q_3} = -\mathbf{b}_p^*/2$	$Pna2_1$ and $Pca2_1$ in cell $-\mathbf{a}_p-2\mathbf{b}_p$, $\mathbf{a}_p$, $\mathbf{c}_p$

Molecular *z*-displacements can also be described by eight components.

i.e.	$\mathbf{q}_0 = 0$	$P6_3mc$ and $P3m1$ in the parent cell $\mathbf{a}_p$, $\mathbf{b}_p$, $\mathbf{c}_p$
	$\mathbf{q}_1 = \mathbf{a}_p^*/2$	$Pnm2_1$ and $Pcm2_1$ in cell $2\mathbf{a}_p+\mathbf{b}_p$, $\mathbf{b}_p$, $\mathbf{c_p}$
	$\mathbf{q}_2 = (-\mathbf{a}_p^*+\mathbf{b}_p^*)/2$	$Pnm2_1$ and $Pcm2_1$ in cell $-\mathbf{a}_p+\mathbf{b}_p$, $-\mathbf{a}_p+\mathbf{b}_p$, $\mathbf{c}_p$
	$\mathbf{q}_3 = -\mathbf{b}_p^*/2$	$Pnm2_1$ and $Pcm2_1$ in cell $-\mathbf{a}_p-\mathbf{2b}_p$, $\mathbf{a}_p$, $\mathbf{c}_p$

Modulation of the *Cmc*2$_1$ subgroup of the parent *P*6$_3$*mc* structure

$Ccm2_1$ has eight symmetry elements with respect to axes $\mathbf{a}'$, $\mathbf{b}'$, $\mathbf{c}'$

x, y, z; –x, –y, 1/2+z; –x, y, 1/2+z; x, –y, z

1/2+x, 1/2+y, z; 1/2−x, 1/2−y, 1/2+z; 1/2−x, 1/2+y, 1/2+z; 1/2+x, 1/2−y, z

$Pnm2_1$, $Pcm2_1$, $Pna2_1$ and $Pca2_1$ are subgroups of $Ccm2_1$ that are consistent with individual irreducible representations associated with the modulation vector $\mathbf{q} = \mathbf{a}'^*$. The Fourier transform of the class of reflections $\mathbf{g}+\mathbf{q}'$ is anti-symmetric with

respect to *C*-centering and can be described as a sum of symmetrized modes with the symmetries given above if the anti-symmetry is ignored. The scattering density associated with a symmetrized mode has the same scattering density at 4 of the 8 equivalent positions of $Ccm2_1$ and minus this scattering density at the other four.

Inspection of synthetic precession photographs shows the *n*-glide absence condition holds whereas both the *c*-glide and *a*-glide absence conditions do not. *i.e.* $0k'l'$, $k'+l' = 2n+1$, but not $0k'l'$, $l' = 2n+1$ nor $h'0l'$, $h' = 2n+1$ when reflections are indexed relative to the orthorhombic cell. This suggests that the true space group associated with the Fourier transform of reflections **g**+**q** (**g** is a parent reflection and has *h* even, *k* even and **q** is specifically $\mathbf{q}_1$, $\mathbf{q}_2$ or $\mathbf{q}_3$) is *Pn* allowing the coexistence of an occupancy mode that has essentially $Pna2_1$ symmetry (ordering the disorder) and a displacive mode of essentially $Pnm2_1$ symmetry (dominantly a *z* displacement). The refinement can be initiated by creating modulations of the parent structure that are linear combinations of such modes.

The occupancy modulation

An occupancy modulation wave for $\mathbf{q}_1 = 1/2\mathbf{a}_p^*$ then forms a component of *Pn* symmetry in the cell $2\mathbf{a}_p+\mathbf{b}_p$, $\mathbf{b}_p$, $\mathbf{c}_p$. An equal number of **R** and **L** at height *z* is maintained in such a modulation. Different numbers of **R** and **L** at a height *z* can only be obtained if $\mathbf{q}_0 = 0$ modes are used. This would lower the symmetry of the Fourier transform of the parent reflections so as to destroy the *c*-glide absences in these reflections. In Figure 6.4 molecules at the same height are denoted by + (or - for the other option). The choice between two mirror related molecules is shown as either **R** or **L**. Three 3-fold rotation related orderings are shown and the average modulo the parent shell of any one component has space group $P6_3mc$. However an equal

combination of the three components creates an average which both produces extra reflections and has 3-fold symmetry.

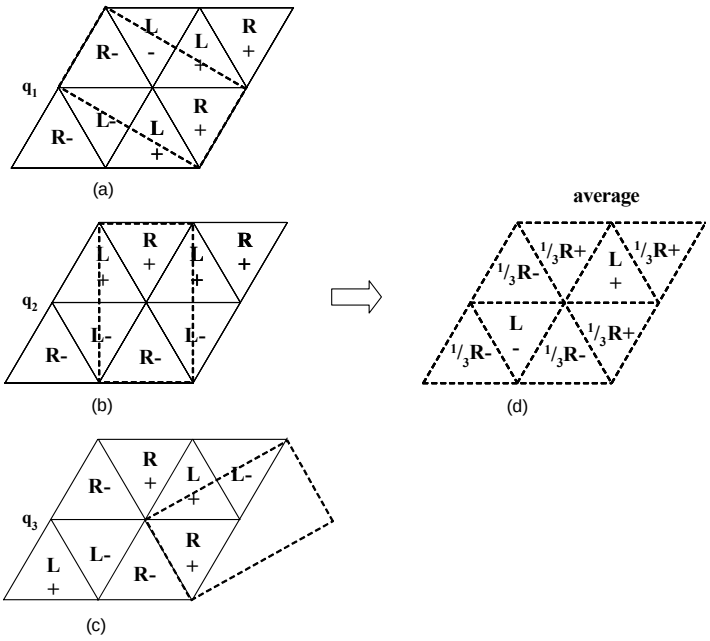

Figure 6.4. The model of occupation modulation modes of symmetry $Pna2_1$.

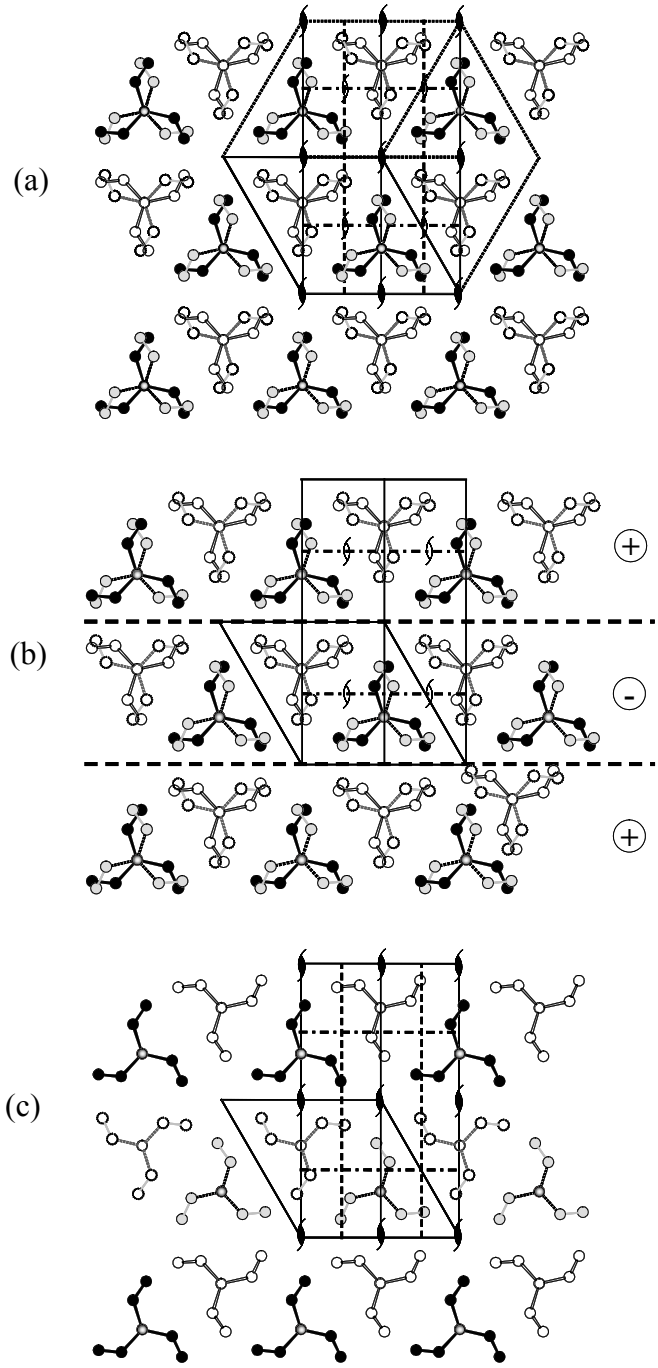

Figure 6.5. The structure of $PS(C_2H_5)_3$ (a) $Ccm2_1$ symmetry, (b) $Pnm2_1$ symmetry showing ±z displacements in layers perpendicular to **a***, (c) $Pna2_1$ with partial ordering of ethyl group.

Creating reflection files

Using the orthorhombic cell $\mathbf{a}_p'$, $\mathbf{b}_p'$, $\mathbf{c}_p'$, the 6-fold twin related reflections are obtained by using the transformation $h+k/2$, $k/2$, l; on each set of indices applicable to the hexagonal cell. When h and k are both even integer values for h', k', l' are obtained for all 6 derived indices. When h and k are both odd integer, only $\pm(-k, h+k, l)$ produce integral h', k', l' and we are looking at only two of the 6 twin components. Likewise, when h is odd and k is even, only the $\pm(h, k, l)$ reflections are observed and when h is even and k is odd, only the $\pm(h+k, -h, l)$ reflections are observed.

A reflection file containing such a set of indices was produced. For example if $h, k, l; = -2, 6, -7$ the 6 fold twin related reflections for orthorhombic cell are 1, 3, −7; −4, 2 −7; −5, −1, −7; −1, −3, −7; 4, −2, −7; 5, 1, −7. It was later decided not to use this file but to use a file indexed relative to the hexagonal cell.

If a 3-fold symmetry operator is used to disorder the structure in *P*3 (see Figure 6.4) with $a = 2a_p$, $b = 2b_p$, $c = 2c_p$, then we use 2 twin related reflections described relative to the hexagonal cell, *i.e.* h, k, l and $-h, -k, l$.

Are domains of *Pn* structure in different orientations coherent or incoherent?

Is the structure best described as a twin or a disorder?

For perfectly twinned reflection data there is the implication that for any reflection **h**, the observed intensity is

$$I(\mathbf{h}) = 1/\mathrm{N} \sum_{m=1,N} |F(\mathbf{R}_m\mathbf{h})|^2 = \sum_{n=1,N} |F_n(\mathbf{h})|^2$$

where $|F(\mathbf{R}_n\mathbf{h})|^2$ is the intensity for an untwinned crystal for the twin-rule related reflection $\mathbf{R}_m\mathbf{h}$ and $F_n(\mathbf{h})$ is the Fourier transform of the *n*th symmetrized component of the scattering density chosen so that

$$F_n(\mathbf{h}) = 1/N \sum_{m=1,N} \chi_{mn} F(\mathbf{R}_m\mathbf{h})$$

provided the χ_{mn} are elements of a unitary matrix.

The number of independent components $F_n(\mathbf{h})$ for any **h** is the number of non equivalent, not systematically zero, values of $|F(\mathbf{R}_n\mathbf{h})|^2$. Thus for the extra reflections with *h* and *k* not both even there are just two symmetrized components which can be chosen to have $Pna2_1$ and $Pnm2_1$ symmetry respectively. These components are anti-symmetric with respect to *C*-centering. For the *h* even, *k* even reflections there is the possibility of 6 symmetrized components formed from the three orientations of the orthorhombic space groups $Ccm2_1$ and *Cc*, the latter being anti-symmetric with respect to the mirror operation. These can be combined to form a component of the parent $P6_3mc$ symmetry and one of *P*31*c* symmetry, the latter being anti-symmetric with respect to the mirror operations, leaving 4 other components.

It was decided to make the contributions from these other components exactly zero to prevent the introduction of uncontrollable noise in the refinement. By refining a structure in space group *P*3 where the 3-fold rotation exactly disorders an ordered *Pn* structure we create the same additional reflections that a twinning model does, see Figure 6.4. A comparison between twinning and disorder is now considered.

Consider the three substructure components of *Pn* symmetry. In the disorder model, each component has an occupancy of 1/3 so that $F(\mathbf{h}) = 1/3 \sum_{m=1,3} F(\mathbf{R}_m\mathbf{h})$ where $F(\mathbf{R}_m\mathbf{h})$ is the structure factor for a single component with occupancy 1 and $I(\mathbf{h}) = 1/9 \sum_{m=1,3} F(\mathbf{R}_m\mathbf{h})|^2$.

For the twin model $I(\mathbf{h}) = 1/3 \sum_{m=1,3} |F(\mathbf{R}_m\mathbf{h})|^2$ is on a different scale.

When *h* and *k* are both even, all three $|F(\mathbf{R}_m\mathbf{h})|^2$ are about equal so that

$I(\mathbf{h}) = 1/3 \sum_{m=1,3} |F(\mathbf{R}_m\mathbf{h})|^2$ for both the disorder and twin model.

When h and k are not both even, only one of the three $F(\mathbf{R}_m\mathbf{h})$ is not zero. If the non zero one is chosen, then $I(\mathbf{h}) = 1/9\ |F(\mathbf{R}_m\mathbf{h})|^2$ for the disorder model but $I(\mathbf{h}) = 1/3\ |F(\mathbf{R}_m\mathbf{h})|^2$ for the twin model. The disorder model becomes the twin model if the scale of $F(\mathbf{h})$ for these reflections is increased by $\sqrt{3}$. If this scale is an independent variable its value in the range 1 to $\sqrt{3}$ gives the mix of the two models.

There is a problem here in that the dominant cause of the extra reflections is a z displacement of the 1/2 the molecules in the cell by an amount opposite in sign to the z displacement of the other half of the molecules and to a first order approximation the amplitude of these reflections is proportional to the displacement. Thus a change in scale is compensated by a change in displacement. The Fourier transform of the parent (h even, k even) reflections produces scattering density that is the same at positions separated by $\mathbf{a}_p = 1/2\mathbf{a}$ or $\mathbf{b}_p = 1/2\mathbf{b}$. Changes to the scale of displacements can be largely compensated by changing the U_{33} component of atom displacement parameters. However the feature is refinable though the discrimination between models is not good.

A further problem is the correlation of anisotropic displacement parameters and the origin of the *Pn* structure which is fixed by the location of the disordering 3-fold axis. The parent reflections are much better measured and errors are detectable in these reflections.

Attempts at refinement

The program RAELS was used. It uses orthonormal crystal coordinates *X*, *Y*, *Z* (obtained from fractional coordinates *x*, *y*, *z* (Rae, 1975a) defined relative to orthonormal crystal axes **A**, **B**, **C** defined parallel to the directions of **a, c* x a, c***. For the hexagonal system **C** is the same direction as **c** and **B** is the same direction as **b***. We chose the asymmetric unit for *P*3 as one of the three *Pn* components. The hexagonal cell contains 8 molecules and thus contains two unit cells of the *Pn* component. We make the translational repeat equal $\mathbf{a}_p = 1/2\mathbf{a}$ and locate the *n* glides as implied by the parent symmetry at $y = 1/4$ and 3/4. The 8 molecules were located using the multi axial transformation possibilities allowed in RAELS (Haller, Rae, Heerdegen, Hockless, & Welberry, 1995) using two independent molecules plus associated equivalent positions, defined by fixed translations or reflections perpendicular to **B** followed by a translation.

We can maintain some of the $Pnm2_1$ component by disordering using the 2_1 screw axis $1/2-x$, $1/2-y$, $1/2+z$ as the disordering operation. In RAELS it is possible to do structure factor algebra and mix twinning and disorder. By having the structure factor for an ordered structure for both *h*,*k*,*l* and −*h*,−*k*,*l* the disorder creates the structure factors

$$F'(hkl) = (1-a)\,F(hkl)+a\,(-1)^{h+k+l}F(-h-kl)$$

and $F'(-h-kl) = (1-a)\,F(-h-kl)+a\,(-1)^{h+k+l}F(hkl)$ which are then combined to form a twin with intensity $I(hkl) = (1-b)\,|F(hkl)|^2+b\,|F(-h-kl)|^2$. Parameters *a* and *b* are both refinable. The twinning parameter and the disorder parameter are correlated.

We initiated this refinement by simply displacing one reference molecule by +0.1 Å in the **c** direction and the other reference molecule by −0.1 Å. Without the

displacements, there are $CH_2\cdots CH_3$ contacts between adjacent molecules of about 3.83 Å and $CH_3\cdots CH_3$ contacts between adjacent molecules of about 3.91 Å With the displacements half the contacts between now non equivalent molecules get shorter and the other half get longer, the $CH_2\cdots CH_3$ contacts being most effected. The choice of sign is simply a choice between origins which has no effect on structure factor amplitudes.

Refinement used rigid body *TL* parameterization centered on the P atom and constrained by the parent site symmetry of 3 symmetry (4 parameters) and this was constrained to be the same for all molecules.

The first refinement only allowed shifts to parameter combinations that were anti-symmetric with respect to the translation 1/2**b**. The removal of the disorder has two options which are related by a mirror plane of the parent structure. The molecule without the CH_3 entities and remaining H were constrained to be equal and have 3-fold rotation symmetry. The remaining C atoms were restrained so that all C−C bonds approached equality and all P−C−C angles approached equality. This refinement was repeated in a hierarchical fashion by noting the magnitudes for rotation and translation displacements and then only varying the bigger contributors in an initial refinement. Refinement allowed a variation in the disorder and the scale of the weak extra reflections. As mentioned earlier the scale and the displacement parameters are correlated.

The refinement was only partially satisfactory, but refinement with *Pc* symmetry for the asymmetric unit is much worse implying the z displacements as defined by an asymmetric unit of *Pn* symmetry is appropriate. Any attempt at refining

parameter combinations omitted by this limited model could not be meaningfully controlled and no improvement in refinement statistics could be obtained.

The *z* displacement pattern of the molecules is undoubtedly correct. The disordering pattern is also correct. If it were wrong the disorder would refine to 1:1 to minimize the contribution of an inappropriate aspect of the model. The problem is that the structure is being described as some global average structure when this is probably not so. Also, mutual interaction between domains that contribute to *h* even, *k* odd and *h* odd, *k* even reflections respectively can induce a contribution to the *h* odd, *k* odd reflections, and this has not been allowed.

Table 6.1. Summary of crystal data, data collection, and structure refinement details.

Crystal data	
Structure Formula	$PS(CH_3)_3$
Chemical formula	C_3H_9PS
Chemical formula weight	150.22
Cell setting, space group	hexagonal, *Pn*
a (Å)	17.902(2)
b (Å)	17.902(2)
c (Å)	6.2979(8)
α (º)	90
β (º)	90
γ (º)	120
Volume ($Å^3$)	1748.(4)
Z	6
D_{calc} (Mg/m^3)	0.856
Radiation type, wavelength	Mo*Kα*, 0.71073

Table 6.1. (Continued).

θ range (º)	2.91-25.03
Temperature (K)	295±2
Data collection	
Diffractometer	Nonius KappaCCD
Data collection method	φ scan plus ω scans with κ offsets
Absorption collection	Multi-scan
No. of measured reflections	38046
No. of unique independent data	1124
No. of observed reflections	605
Criterion for observed reflections	$I > 3\sigma(I)$
R_{int}	0.066
θ_{max} (º)	25.04
Range of *h, k, l*	$-21 \rightarrow h \rightarrow 21$ $-21 \rightarrow k \rightarrow 21$ $-7 \rightarrow l \rightarrow 7$
Refinement	
Refinement on	*F*
$R[F^2 > 3\ \sigma(F^2)]$, $wR(F^2)$, *S*	0.139, 0.206, 5.90
No. of reflections used	605
No. of refined parameters	32
Weighting scheme	Based on measured s.u.'s $w = 1/(\sigma^2(F) + 0.0004F^2)$
Data collection program	COLLECT
Cell and data reduction program	DENZO/Scalepack

Computer programs: *COLLECT* (Nonius, 1998); *DENZO-SMN* (Otwinowski & Minor, 1997); *RAELS* (Rae, 2000)

Table 6.2. Statistics from the RAELS refinement.

	Reflections	*R(F)*	*R(F^2)*	*wR*	*Gof*
I>3σ(*I*) *h* even *k* even	278	0.085	0.0150	0.107	3.95
I>3σ(*I*) *h*, *k* not both even	325	0.300	0.502	0.337	7.15
I < 3 σ(*I*)	521	0.559	1.081	0.787	2.72
All *I* > 3 σ(*I*)	603	0.134	0.168	0.204	5.90

a. Ratio of scales for K F_{calc} K(others)/K(*h* even, *k* even) = 1.208(25).
b.Disorder about 2_1 screw 1/2−x, 1/2−y, 1/2+z 0.803(14):0.197
c. Twin ratio: 0.500(3):0.500
d. The average intensity for the reflections in sets 1 to 3 is in the ratio 1000 : 46 : 9

Table 6.3. Fractional atomic coordinates[a] and equivalent isotropic displacement parameters[b] (Å^2) for the nonhydrogen atoms in $PS(C_2H_5)_3$.

	x	*y*	*z*	U_{eq}
P1	0.3385(4)	0.6688(4)	–0.0212(6)	0.033(1)
S1	0.3452(5)	0.6692(6)	0.2947(9)	0.041(1)
C11	0.4182(9)	0.7698(9)	–0.1390(24)	0.042(1)
C12	0.4274(29)	0.8515(11)	–0.0479(27)	0.055(3)
C13	0.2352(9)	0.6497(9)	–0.1178(23)	0.042(1)
C14	0.1553(10)	0.5769(21)	–0.0204(30)	0.055(2)
C15	0.3551(9)	0.5866(9)	–0.1422(23)	0.042(2)
C16	0.4371(16)	0.5887(25)	–0.0798(31)	0.055(4)
P2	0.8385(3)	0.6688(4)	–0.0212(6)	0.033(1)
S2	0.8452(5)	0.6692(9)	0.2947(9)	0.041(1)
C21	0.9182(9)	0.7698(9)	–0.1390(24)	0.042(1)
C22	0.9274(29)	0.8515(11)	–0.0479(27)	0.055(3)
C23	0.7352(9)	0.6497(9)	–0.1178(23)	0.042(1)
C24	0.6553(10)	0.5769(21)	–0.0204(30)	0.055(2)
C25	0.8551(9)	0.5866(9)	–0.1422(23)	0.042(2)
C26	0.9371(16)	0.5887(25)	–0.0798(31)	0.055(4)

Table 6.3. (Continued).

	x	y	z	U_{eq}
P3	0.3282(4)	0.1645(4)	0.0212(6)	0.033(1)
S3	0.3209(5)	0.1595(6)	0.3370(9)	0.041(1)
C31	0.3495(9)	0.2673(9)	–0.0847(24)	0.042(2)
C32	0.4293(17)	0.3436(12)	0.0019(28)	0.055(3)
C33	0.4129(9)	0.1474(9)	–0.0815(24)	0.042(1)
C34	0.4039(23)	0.0628(14)	–0.0145(31)	0.054(4)
C35	0.2298(9)	0.0842(9)	–0.1058(21)	0.042(1)
C36	0.1462(12)	0.0755(29)	–0.0312(28)	0.055(2)
P4	0.8282(4)	0.1645(4)	0.0212(6)	0.033(1)
S4	0.8209(5)	0.1595(6)	0.3370(9)	0.041(1)
C41	0.8495(9)	0.2673(9)	–0.0847(24)	0.042(2)
C42	0.9293(17)	0.3436(12)	0.0019(28)	0.055(3)
C43	0.9129(9)	0.1474(9)	–0.0815(24)	0.042(1)
C44	0.9039(23)	0.0628(14)	–0.0145(31)	0.054(4)
C45	0.7298(9)	0.0842(9)	–0.1058(21)	0.042(1)
C46	0.6462(12)	0.0755(29)	–0.0312(28)	0.055(2)
P5	0.1697(4)	0.8312(4)	0.4788(6)	0.033(1)
S5	0.1759(5)	0.8308(6)	0.7947(9)	0.041(1)
C51	0.1484(9)	0.7302(9)	0.3610(24)	0.042(1)
C52	0.0759(22)	0.6485(11)	0.4521(27)	0.055(3)
C53	0.0855(9)	0.8503(9)	0.3822(23)	0.042(1)
C54	0.0784(27)	0.9231(21)	0.4796(30)	0.055(2)
C55	0.2685(9)	0.9134(9)	0.3578(23)	0.042(2)
C56	0.3484(13)	0.9113(25)	0.4202(31)	0.055(4)
P6	0.6697(4)	0.8312(4)	0.4788(6)	0.033(1)
S6	0.6759(5)	0.8308(6)	0.7947(9)	0.041(1)
C61	0.6484(9)	0.7302(9)	0.3610(24)	0.042(1)
C62	0.5759(22)	0.6485(11)	0.4521(27)	0.055(3)
C63	0.5855(9)	0.8503(9)	0.3822(23)	0.042(1)
C64	0.5784(27)	0.9231(21)	0.4796(30)	0.055(2)

Table 6.3. (Continued).

	x	y	z	U_{eq}
C65	0.7685(9)	0.9134(9)	0.3578(23)	0.042(2)
C66	0.8484(13)	0.9113(25)	0.4202(31)	0.055(4)
P7	0.1637(4)	0.3355(4)	0.5212(6)	0.033(1)
S7	0.1615(5)	0.3405(6)	0.8370(9)	0.041(1)
C71	0.0822(9)	0.2327(9)	0.4153(24)	0.042(2)
C72	0.0857(26)	0.1564(12)	0.5019(28)	0.055(3)
C73	0.2655(9)	0.3526(9)	0.4185(24)	0.042(1)
C74	0.3411(12)	0.4372(14)	0.4855(31)	0.054(4)
C75	0.1457(9)	0.4158(9)	0.3942(21)	0.042(1)
C76	0.0707(21)	0.4245(29)	0.4688(28)	0.055(2)
P8	0.6637(4)	0.3355(4)	0.5212(6)	0.033(1)
S8	0.6615(5)	0.3405(6)	0.8370(9)	0.041(1)
C81	0.5822(9)	0.2327(9)	0.4153(24)	0.042(2)
C82	0.5857(26)	0.1564(12)	0.5019(28)	0.055(3)
C83	0.7655(9)	0.3526(9)	0.4185(24)	0.042(1)
C84	0.8411(12)	0.4372(14)	0.4855(31)	0.054(4)
C85	0.6457(9)	0.4158(9)	0.3942(21)	0.042(1)
C86	0.5707(21)	0.4245(29)	0.4688(28)	0.055(2)

[a]Estimated standard deviations of the least significant digits are given in parentheses.

[b]Equivalent isotropic atomic displacement parameters for the atoms refined anisotropically, $U_{eq} = 1/3 \sum_i \sum_j U_{ij} a_i^* a_j^* \mathbf{a}_i \cdot \mathbf{a}_j$

Table 6.4. Anisotropic atomic displacement parameters[a] in $PS(C_2H_5)_3$.

Atom	*U11*	*U22*	*U33*	*U12*	*U13*	*U23*
P1	0.037(1)	0.037(1)	0.026(2)	0.019(1)	0.000	0.000
S1	0.049(2)	0.049(2)	0.026(2)	0.024(1)	–0.001(1)	0.000(1)
C11	0.045(1)	0.040(1)	0.034(2)	0.016(1)	0.003(1)	0.001(1)
C12	0.070(6)	0.037(1)	0.049(4)	0.019(1)	0.001(1)	–0.002(5)
C13	0.040(1)	0.053(3)	0.034(2)	0.024(1)	–0.003(1)	–0.001(1)
C14	0.037(1)	0.069(6)	0.049(4)	0.018(1)	0.000(1)	0.001(1)
C15	0.053(3)	0.044(1)	0.034(2)	0.028(2)	0.001(1)	–0.001(1)
C16	0.066(5)	0.070(6)	0.048(4)	0.049(6)	0.002(1)	–0.001(1)
P2	0.037(1)	0.037(1)	0.026(2)	0.019(1)	0.000	0.000
S2	0.049(2)	0.049(2)	0.026(2)	0.024(1)	–0.001(1)	0.000(1)
C21	0.045(1)	0.040(1)	0.034(2)	0.016(1)	0.003(1)	0.003(1)
C22	0.070(6)	0.037(1)	0.049(4)	0.019(1)	0.001(1)	0.001(1)
C23	0.040(1)	0.053(3)	0.034(2)	0.024(1)	–0.003(1)	–0.001(1)
C24	0.037(1)	0.069(6)	0.049(4)	0.018(1)	0.000(1)	0.000(1)
C25	0.053(3)	0.044(1)	0.034(2)	0.028(2)	0.001(1)	–0.001(1)
C26	0.066(5)	0.070(6)	0.048(4)	0.049(6)	0.002(1)	–0.001(1)
P3	0.037(1)	0.037(1)	0.026(2)	0.019(1)	0.000	0.000
S3	0.049(2)	0.049(2)	0.026(2)	0.024(1)	0.001(1)	0.000(1)
C31	0.053(3)	0.040(1)	0.034(2)	0.024(1)	0.001(1)	0.001(1)
C32	0.065(5)	0.037(1)	0.048(4)	0.016(1)	0.001(1)	0.001(1)
C33	0.044(1)	0.053(1)	0.034(2)	0.029(2)	0.002(1)	0.000(1)
C34	0.070(6)	0.064(5)	0.048(4)	0.049(6)	0.001(1)	–0.001(1)
C35	0.041(1)	0.045(1)	0.034(2)	0.016(1)	–0.004(1)	–0.003(1)
C36	0.037(1)	0.069(6)	0.049(4)	0.019(1)	–0.003(3)	–0.001(1)
P4	0.037(1)	0.037(1)	0.026(2)	0.019(1)	0.000	0.000
S4	0.049(2)	0.049(2)	0.026(2)	0.024(1)	0.001(1)	0.000(1)
C41	0.053(3)	0.040(1)	0.034(2)	0.024(1)	0.001(1)	0.001(1)
C42	0.065(5)	0.037(1)	0.048(4)	0.016(1)	0.001(1)	0.001(1)
C43	0.044(1)	0.053(1)	0.034(2)	0.029(2)	0.002(1)	0.000(1)
C44	0.070(6)	0.064(5)	0.048(4)	0.049(6)	0.001(1)	–0.001(1)
C45	0.041(1)	0.045(1)	0.034(2)	0.016(1)	–0.004(1)	–0.003(1)
C46	0.037(1)	0.069(6)	0.049(4)	0.019(1)	–0.003(3)	–0.001(1)

Table 6.4. (Continued).

Atom	*U11*	*U22*	*U33*	*U12*	*U13*	*U23*
P5	0.037(1)	0.037(1)	0.026(2)	0.019(1)	0.000	0.000
S5	0.049(2)	0.049(2)	0.026(2)	0.024(1)	–0.001(1)	0.000(1)
C51	0.053(3)	0.040(1)	0.034(2)	0.024(1)	–0.001(1)	–0.003(1)
C52	0.068(6)	0.037(1)	0.049(4)	0.018(1)	–0.001(1)	–0.001(1)
C53	0.045(1)	0.053(1)	0.034(2)	0.029(2)	–0.002(1)	0.000(1)
C54	0.069(6)	0.069(6)	0.049(4)	0.051(6)	0.000(1)	0.001(1)
C55	0.041(1)	0.044(1)	0.034(2)	0.016(1)	0.003(1)	0.003(1)
C56	0.038(1)	0.070(6)	0.048(4)	0.021(1)	0.003(1)	0.001(1)
P6	0.037(1)	0.037(1)	0.026(2)	0.019(1)	0.000	0.000
S6	0.049(2)	0.049(2)	0.026(2)	0.024(1)	–0.001(1)	0.000(1)
C61	0.053(3)	0.040(1)	0.034(2)	0.024(1)	–0.001(1)	–0.003(1)
C62	0.068(6)	0.037(1)	0.049(4)	0.018(1)	–0.001(1)	–0.001(1)
C63	0.045(1)	0.053(1)	0.034(2)	0.029(2)	–0.002(1)	0.000(1)
C64	0.069(6)	0.069(6)	0.049(4)	0.051(6)	0.000(1)	0.001(1)
C65	0.041(1)	0.044(1)	0.034(2)	0.016(1)	0.003(1)	0.003(1)
C66	0.038(1)	0.070(6)	0.048(4)	0.021(1)	0.003(1)	0.001(1)
P7	0.037(1)	0.037(1)	0.026(2)	0.019(1)	0.000	0.000
S7	0.049(2)	0.049(2)	0.026(2)	0.024(1)	–0.001(1)	0.000(1)
C71	0.045(1)	0.040(1)	0.034(2)	0.016(1)	–0.002(1)	–0.003(1)
C72	0.070(6)	0.037(1)	0.048(4)	0.021(1)	0.000(0)	–0.001(1)
C73	0.040(1)	0.053(3)	0.034(2)	0.024(1)	0.003(1)	0.000(1)
C74	0.038(1)	0.064(5)	0.048(4)	0.016(1)	0.002(1)	0.001(1)
C75	0.052(3)	0.045(1)	0.034(2)	0.028(2)	–0.001(1)	0.003(1)
C76	0.068(6)	0.069(6)	0.049(4)	0.050(6)	–0.001(1)	0.001(1)
P8	0.037(1)	0.037(1)	0.026(2)	0.019(1)	0.000	0.000
S8	0.049(2)	0.049(2)	0.026(2)	0.024(1)	–0.001(1)	0.000(1)
C81	0.045(1)	0.040(1)	0.034(2)	0.016(1)	–0.002(1)	–0.003(1)
C82	0.070(6)	0.037(1)	0.048(4)	0.021(1)	0.000(0)	–0.001(1)
C83	0.040(1)	0.053(3)	0.034(2)	0.024(1)	0.003(1)	0.000(1)
C84	0.038(1)	0.064(5)	0.048(4)	0.016(1)	0.002(1)	0.001(1)
C85	0.052(3)	0.045(1)	0.034(2)	0.028(2)	–0.001(1)	0.003(1)
C86	0.068(6)	0.069(6)	0.049(4)	0.050(6)	–0.001(1)	0.001(1)

[a]Estimated standard deviations of the least significant digits are given in parentheses.

Table 6.5. Selected interatomic bond lengths[a] (Å) and bond angles[a] (°) for $PS(CH_3)_3$.

P1−S1	1.992(4) . .	C12−C56	3.985(36) . 1_554
P1−C11	1.810(11) . .	C12−C56	3.654(33) . .
P1−C13	1.810(11) . .	C12−C64	3.786(46) . 1_554
P1−C15	1.810(11) . .	C13−C51	3.978(18) . .
C11−C12	1.502(14) . .	C14−C51	3.695(43) . .
C13−C14	1.502(14) . .	C14−C52	3.786(46) . .
C15−C16	1.502(14) . .	C14−C75	3.830(26) . .
C11−C16	3.444(34) . .	C14−C76	3.994(51) . 1_554
C13−C12	3.558(36) . .	C15−C74	3.469(19) . 1_554
C15−C14	3.577(34) . .	C16−C62	3.654(33) . 1_554
P3−S3	1.992(4) . .	C16−C62	3.985(35) . .
P3−C31	1.810(11) . .	C16−C74	3.625(23) . 1_554
P3−C33	1.810(11) . .	C16−C74	4.281(45) . .
P3−C35	1.810(11) . .	C32−C73	3.998(38) . .
C31−C32	1.501(14) . .	C32−C86	4.014(30) . 1_554
C33−C34	1.501(14) . .	C33−C82	3.998(38) . 1_554
C35−C36	1.501(14) . .	C34−C12	4.014(28) . 1_545
C31−C36	3.557(36) . .	C34−C55	3.469(19) . 1_545
C33−C32	3.415(33) . .	C34−C56	4.281(45) . 1_544
C35−C34	3.373(31) . .	C34−C56	3.625(23) . 1_545
C11−C63	3.978(18) . 1_554	C35−C54	3.830(26) . 1_544
C1−C64	3.695(43) . 1_554	C36−C54	3.994(52) . 1_545
C12−C34	4.014(28) . 1_565	C36−C72	4.014(30) . .
S1−P1−C11	112.9(4) . . .	S3−P3−C31	112.9(4) . . .
S1−P1−C13	112.9(4) . . .	S3−P3−C33	112.9(4) . . .
S1−P1−C15	112.9(4) . . .	S3−P3−C35	112.9(4) . . .
C11−P1−C13	105.8(4) . . .	C31−P3−C33	105.8(4) . . .
C11−P1−C15	105.8(4) . . .	C31−P3−C35	105.8(4) . . .
C13−P1−C15	105.8(4) . . .	C33−P3−C35	105.8(4) . . .
P1−C11−C12	117.7(12) . . .	P3−C31−C32	114.3(12) . . .
P1−C13−C14	117.9(12) . . .	P3−C33−C34	113.2(11) . . .
P1−C15−C16	115.1(11) . . .	P3−C35−C36	117.9(12) . . .

Symmetry positions: 1. x,y,z; 2. −y,x−y,z; 3. −x+y,−x,z

6.4 Comparison to the Previous Determination

Our bond distances and angles for the coordination geometry in $PS(C_2H_5)_3$ are more reliable than those previously determined.

The P=S distances [1.992(4) Å] it is significantly longer than the 1.864(3) Å of the previous determination and close to the average value from the CSD [1.992(4) Å]. Specific values in the literature are 1.959(2) Å for $PS(CH_3)_3$ and 1.970 Å for $SP(C_6H_{11})_3$). The P−C distances [1.810(11) Å] are similar to the average value from the CSD [1.806(9) Å] and close to the values (1.798(2) Å for $PS(CH_3)_3$, 1.840-1.844 Å for $SP(C_6H_{11})_3$), but significantly different to the value [1.865(4) Å] of the previous determination. Our C−C single distance [1.502(14) Å] compares to the CSD value of [1.513(14) Å] and the C−C distances for $PS(C_6H_{11})_3$ [1.505-1.532 Å]. This distance is far longer than the 1.38(7) Å of the previous structure determination. The U_{eq} for P was lowered to 0.036 $Å^2$, both by reducing temperature and modeling a disorder.

6.5 References

Cotton, F. A. and Soderberg, R. H. (1963). The crystal and molecular structure of bis-(trimethylphosphine oxide)-cobalt(II) dinitrate. **Journal of the American Chemical Society** 85(16): 2402-2406.

Dobado, J. A., Martinez-Garcia, H., Molina, J. M. and Sundberg, M. R. (1998). Chemical bonding in hypervalent molecules revised. Application of the atoms in molecules theory to Y_3X and Y_3XZ (Y = H or CH_3; X = N, P or As; Z = O or S) compounds. **Journal of the American Chemical Society** 120(33): 8461-8471.

Etter, M. C. and Baures, P. W. (1988). Triphenylphosphine oxide as a crystallographic aid. **Journal of the American Chemical Society** 110(2): 639-640.

Haller, K. J., Rae, A. D., Heerdegen, A. P., Hockless, D. C. R. and Welberry, T. R. (1995). The fourfold disordered structures of *p*-chloro-*N*-(*p*-methylbenzylidene) aniline and *p*-methyl-*N*-(*p*-chlorobenzylidene)aniline. **Acta Crystallographica** B5: 187-197.

Kerr, K. A., Boorman, P. M., Misener, B. S. and van Roode, J. G. H. (1977). Crystal structure studies of Group V chalcogenide compounds. I. The structure of tricyclohexylphosphine sulphide. **Canadian Journal of Chemistry** 55: 3081-3085.

Nonius BV. (1998). *COLLECT: KappaCCD software*, Nonius BV., Delft, The Netherlands.

Otwinowski, Z. and Minor, W. (1997). Methods in enzymology. 276: 307-326.

Oxford Cryosystems (1997). *Oxford Cryostream Cooler, 600 series.* Oxford Cryosystem, Oxford, UK.

Rae, A. D. (2000). *RAELS. A comprehensive constrainted least squares program,* Australian National University, Canberra, Australia.

Rae, A. D. (1975a). Crystal structure refinement using a number of orthonormal axial systems. **Acta Crystallographica** A31: 560-570.

Rae, A. D. (1975b). Rigid-body motion in crystals-The application of constraints on the *TLS* model. **Acta Crystallographica** A31: 570-574.

Reibenspies, J. H., Draper, J. D., Struck, G. and Darensbourg, D. J. (1996). Crystal

structure studies of tricyclohexylphosphine sulphide, $(C_6H_{11})_3PS$. **Zeitschrift für Kristallographie** 211: 400.

Sheldrick, G. M. (1997). *SHELXL97*. University of Göttingen, Germany.

van Meersche, M. (1954). X-ray determination of the structure of triethylphosphine sulphide. **Bull. Acad. Belg. Cl. sci.** 40: 846-854.

van Meersche, M. and Léonard, A. (1959a). Affinement de la structure de $SP(C_2H_5)_3$. **Bulletin des Societes Chimiques Belges** 68: 683-698.

van Meersche, M. and Léonard, A. (1959b). Structure de $SP(C_2H_5)_3$ and $SeP(C_2H_5)_3$. **Acta Crystallographica** 12: 1053-1054.

Wilkins, C. J., Hagen, K., Hedberg, L., Shen, Q. and Hedberg, K. (1975). An electron diffraction investigation of the molecular structure of gaseous trimethylphosphine oxide, trimethylphosphine sulfide, trimethylarsine oxide, and trimethylarsine sulfide. **Journal of the American Chemical Society** 97(22): 6352-6358.

CHAPTER VII

THE COMMENSURATELY MODULATED STRUCTURE OF COCRYSTALLIZED COPPER(4,4′-BIPYRIDYL)SULFATE COORDINATION POLYMER WITH TEREPHTHALIC ACID

7.1 Abstract

Solvothermal reaction of copper sulfate pentahydrate, terephthalic acid and 4,4′-bipyridine produced the product $[Cu(bipy)]_2SO_4 \cdot (TPA)$, a = 19.597(4) Å, b = 34.771(3) Å, c = 16.274(3) Å, β = 107.52(3)°, *C2/c*, Z = 16, that is describable as a commensurate modulation of an idealized *C2/c*, Z = 4 parent structure with $a_p = a/2$, $b_p = b/2$, $c_p = c$. In the parent structure, polymeric chains of [−Cu^I−bypi−Cu^I−bypi−] are propagated by an *n*-glide, 1/2+x, 1/2−y, −1/2+z, and are cross linked (Cu−O−S−O−Cu) by the sulfate groups which lie on 2-fold axes. The terephthalic acids lie on centers of inversion and are hydrogen bonded to the non-Cu bonded oxygen atoms of the sulfate groups. The parent *n*-glide cannot remain a symmetry element of the modulated structure. A (3+1) dimensional approach, modulation vector $(\mathbf{a}_p^* + \mathbf{b}_p^*)/2$, suggests the possibility of a twinned triclinic crystal but observations of weak reflections with h even, k even, $h+k = 4n+2$, preclude this option. A (3+2) dimensional approach with modulation vectors $\mathbf{a}_p^*/2$, $\mathbf{b}_p^*/2$ allows for space group *C*2/*c* with options for the selection of the quarter of the parent structure symmetry elements to be retained. In the correct model, the terephthalic acids no longer sit on

inversion centers. Residual disorder about a 2-fold axis remains, but an ordered structure in a lower symmetry space group was shown to be inappropriate.

7.2 Introduction

Coordination polymers form a variety of useful 1D, 2D and 3D porous solid materials, *e.g.* infinite framework (Kawata, Kitagawa, Machida, Nakamoto, Kondo, Katada, Kikuchi & Ikemoto, 1995; Li, Davis, Groy, Kelley & Yaghi, 1998), ion exchange (Hoskin & Robson, 1990; Yaghi, Li & Groy, 1997), zeolites (Venkataraman, Gardner, Lee & Moore, 1995), and catalysts (Fujita, Kwon, Washizu & Ogura, 1994; Sawaki, Dewa & Aoyama, 1998).

Supramolecular coordination polymers of the inorganic-organic hybrid frameworks have interesting structural topologies and sometimes unexpected properties. The inorganic-organic hybrid frameworks using the mixed ligands pyridyl (N-donor) and carboxylate (O-donor) play an important part in the construction of novel coordination polymers (Okubo, Kondo, Kitagawa, 1997; Patrick, Stevens, Storr, Thompson, 2003; Konar, Manna, Zangrando, Chaudhuri, 2004; Zhang, Xu, Lin & You, 2004). The 4,4′-bipyridine (bipy) is used in the construction of a variety of architectures, and is an excellent bridging ligand with metal ions to form linear (Dong, Smith, Layland & Loye, 2000), zigzag (Li, Xu, You, Dong & Guo, 1993), ladder (Tao, Yin, Huang & Zheng, 2002), grid (Du, Chen, Bu & Ribas, 2002), T-shape (Gudbjartson, Biradha, Poirier & Zaworotko, 1999) and brick wall (Fujita, Kwon, Washizu & Ogura, 1994) networks. The flexible bipy ligand can adopt different conformations leading to new and unpredictable structure motifs. In some networks the geometric constraints imposed by the metal ion coordination sphere

leads to disorder of the ligand ($Cu(4,4'\text{-bipy})_{1.5}\cdot NO_3(H_2O)$, Yaghi & Li, 1995; $[Ag(bipy)NO_3]$, Yaghi & Li, 1996). 1,4-dicarboxylic acid or terephthalic acid (TPA) is a bidentate bridging ligand and provides rigid frameworks due to the potential bidentate of carboxylate groups (Baeg & Lee, 2003).

Anions such as NO_3^-, SO_4^{2-}, ClO_4^- can be involved in the mechanism of polymer formation and have the ability to act in a polydentate manner, often linking cations together. They are capable of binding metal centers in bidentate or bridging modes (Boldog, Rusanov, Chernega, Sieler & Domasevitch, 2001). The energy of anion coordination in supramolecular structures can vary over a wide range and its influence is difficult to predict (Yaghi, Li, Groy, 1997; Soldatov, Enright, Ripmeester, Lipkowski & Ukraintseva, 2001) since weak bridging interaction can distort a polymeric structure (Tang, Gao, Bu, Liao, Yana, Jiang & Wang, 2000; Xu, Wang, Peng & Huang, 2003).

Hydrothermal and solvothermal synthesis of $CuNO_3$, bipy and TPA to form a complex of $[Cu_4(terephthalate)_3(bipy)_2]_n$ (Lo, Chui, Shek, Lin, Zhang, Wen & Willams, 2000) involved the production of a new architectures for the formation of coordination polymers. It is challenging to control and predict the final products, of such syntheses, especially for mixed-valence copper, Cu(I)-Cu(II). The hydrothermal reaction of $Cu(NO_3)_2\cdot 2.5H_2O$, bipy and terephthalic acid forms a 2D Cu(II) coordination polymer $\{[Cu(terephthalate)(bipy)]\cdot(TPA)\}_n$ (Baeg & Lee, 2003).

We report herein the solvothermal reaction of the $CuSO_4\cdot 5H_2O$, bipy and TPA to form the dimer of $[Cu(bipy)]_2(SO_4)\cdot(TPA)$. The compound was interesting in that the observed data ($I > 3\ \sigma(I)$) fell into three distinct groups; 2327 data with h = even, k = even, $h+k$ = 4n, 37 data with h = even, k = even, $h+k$ = 4n+2, and 2659 data h =

odd, k = odd, $h+k$ = 2n. We describe the parent polymeric chains as a commensurate displacive modulation of an idealized Z = 4 parent structure with $a_p = a/2$, $b_p = b/2$, $c_p = c$. The structure refined well.

7.3 X-Ray Crystallography

The solvothermal reaction of $CuSO_4 \cdot 5H_2O$, terephthalic acid, ($C_8H_6O_4$), and 4,4′-bipyridine ($C_{10}H_8N_2$) produced rhombic slabs of a yellow product $[Cu(C_{10}H_8N_2)]_4(SO_4)_2 \cdot 2(C_8H_6O_4)$.

Data were collected at 295 K on a SMART CCD diffractometer equipped with a molybdenum X-ray source. A normal focus X-ray tube, graphite monochromator ($\lambda_{MoK\alpha}$ = 0.71073 Å). Structure solution used SIR97 (Altomare, Burla, Camalli, Cascarano, Giacovazzo, Guagliardi, Moliterni, Polidori & Spagna, 1999), and refinement used the program RAELS (Rae, 2000) that allows the use of refinable local coordinates relative to refinable orthonormal axial systems and the use of refinable *TLS* rigid body thermal motion parameters (Rae, 1975a; b).

Crystal data and details of the data collection and structure refinement are summarized in Table 7.1, and statistics for the refinements from RAELS are in Table 7.2. Fractional coordinates and isotropic atomic displacement parameters for the refined atoms are given in Table 7.3. Anisotropic atomic displacement parameters for the non hydrogen atoms are given in Table 7.4. Selected inter-atomic bond distances and angles with comparison to the literature compounds are in Table 7.5, and hydrogen bond parameters are given in Table 7.6. Derived hydrogen atom positions and isotropic atomic displacement parameters, derived anisotropic atomic

displacement parameters for the hydrogen atoms are given as supplementary material in Appendix F as Tables F.1, and F.2 respectively.

Table 7.1. Summary of crystal data, data collection, and structure refinement details.

Crystal data	
Structure Formula	**[**$Cu(C_{10}H_8N_2)]_2\ SO_4\ [(C_8H_6O_4)]$
Chemical formula	$C_6H_9O_4SnCl_2 \cdot C_{12}H_9N_2$
Chemical formula weight	701.6
Cell setting, space group	monoclinic; *C*2/*c*
a (Å)	19.597(4)
b (Å)	34.771(3)
c (Å)	16.274(3)
α (º)	90
β (º)	107.52(3)
γ (º)	90
Volume ($Å^3$)	10,574.8
Z	16
D_{calc} (Mg/m^3)	1.763
Radiation type, wavelength	Mo$K\alpha$, 0.71073
θ range (º)	3-27.45
Absorption coefficient, μ (mm^{-1})	1.75
Temperature (K)	295(2)
Crystal color, form	yellow
Crystal size (mm)	rhombic slabs
Data collection	
Diffractometer	Bruker SMART CCD
Data collection method	φ scan plus ω scans with χ offsets
Absorption correction	Multi-scan
No. of measured reflections	86,910
No. of unique independent data	15,167
No. of observed reflections	11,944
Criterion for observed reflections	$I > 3\sigma(I)$

Table 7.1. (Continued).

R_{equiv} (*C2/m* merge (9278 to 5019 data))	0.0526
θ_{max} (º)	27.45
Range of *h, k, l*	$-10 \rightarrow h \rightarrow 11$ $-18 \rightarrow k \rightarrow 15$ $-14 \rightarrow l \rightarrow 14$
Refinement	
Refinement on	*F*
R[all data], $wR(F^2)$, *S*	0.03
$R[F^2 > 2\sigma(F^2)]$, $wR(F^2)$, *S*	0.179, 0.107, 2.28
No. of reflections used	11,944
No. of parameters	289
H atom treatment	Refined xyz and calculated U_{ij} based on U_{ij} of attached atom each cycle
Weighting scheme	Based on measured s.u.'s $w = 1/(\sigma^2(F) + 0.0001F^2)$
Data collection program	SMART
Absorption correction program	SADABS
Structure solution program	SIR97
Structure refinement program	RAELS
Graphics program	ORTEP

Computer programs: *COLLECT* (Nonius, 1998); *SIR97* (Altomare *et al*., 1999); *RAELS* (Rae, 2000); *ORTEP-III* (Burnett & Johnson, 1996; Farrugia, 1997); SMART (Bruker AXS, 1997); SADABS (Sheldrick, 1997)

7.4 Structure Determination and Refinement

The parent structure

There exists an idealized $Z = 4$ parent structure with space group $C2/c$ and $a_p = a/2$, $b_p = b/2$, $c_p = c$. This structure is easily determined by standard methods if the reflections are re-indexed for the parent structure and the extra reflections removed. The coordinates for this structure are obtained from our final model (Table 7.2) by saying $x_p = 2x$, $y_p = 2y$, $z_p = z$. The structure can be understood as a

commensurate displacive modulation of this parent. In the parent, polymeric [−Cu^{I}−bipy−Cu^{I}−bipy−] chains are propagated by an *n*-glide, 1/2+*x*, 1/2−*y*, −1/2+*z*, and are cross linked (Cu−O−S−O−Cu) by equivalents of the sulfate which lies on a 2-fold axis. The TPA is on a center of inversion and its equivalents and hydrogen bonds to the free oxygen atoms of the bridging sulfate ions. The Cu atom and the bipy are at general positions; the apparent local 2-fold through the Cu atom and the apparent inversion center in the bipy are not symmetry elements of this parent *C*2/*c* structure.

Choosing the asymmetric unit for the modulated structure

The asymmetric unit, $[Cu(bipy)]_2(SO_4)\cdot TPA$, contains four Cu atoms, four bipy ligands, two, [1+2(1/2)], sulfate ligands, and two TPA molecules. The *n*-glide cannot be a symmetry element of the final structure. The polymer chain then has 4 units propagated by the pseudo glide plane 1/4+x, 1/4−y, −1/2+x, identifying their contribution to an asymmetric unit. In the final structure the 2_1 screw axes of the parent structure are necessarily destroyed and half the 2-fold axes become 2_1 screw axes. This causes half the sulfates to be in general positions and the other half to be on 2-fold axes. In the asymmetric unit there are two non equivalent 2-fold symmetry sites and one general position. The sites in Table 7.2 have been chosen so as to connect the sulfates to the asymmetric unit of the polymer chain. Only half the *c*-glide operations and none of the *n*-glide operations remain when the parent structure is modulated. By choosing the *c*-glides at $y = 0$, we select between alternative origins $1/2\mathbf{b}_p$ apart in the parent structure. Fixing the origin to comply with the standard setting of *C*2/*c* decides whether the TPA lie on 4 non equivalent inversion centers at 1/4, 1/4, 0; 1/4, 3/4, 0; 0, 0, 0; 0, 1/2, 1/2 and their equivalents or on two general positions and their equivalents. The latter option was shown to be the correct choice.

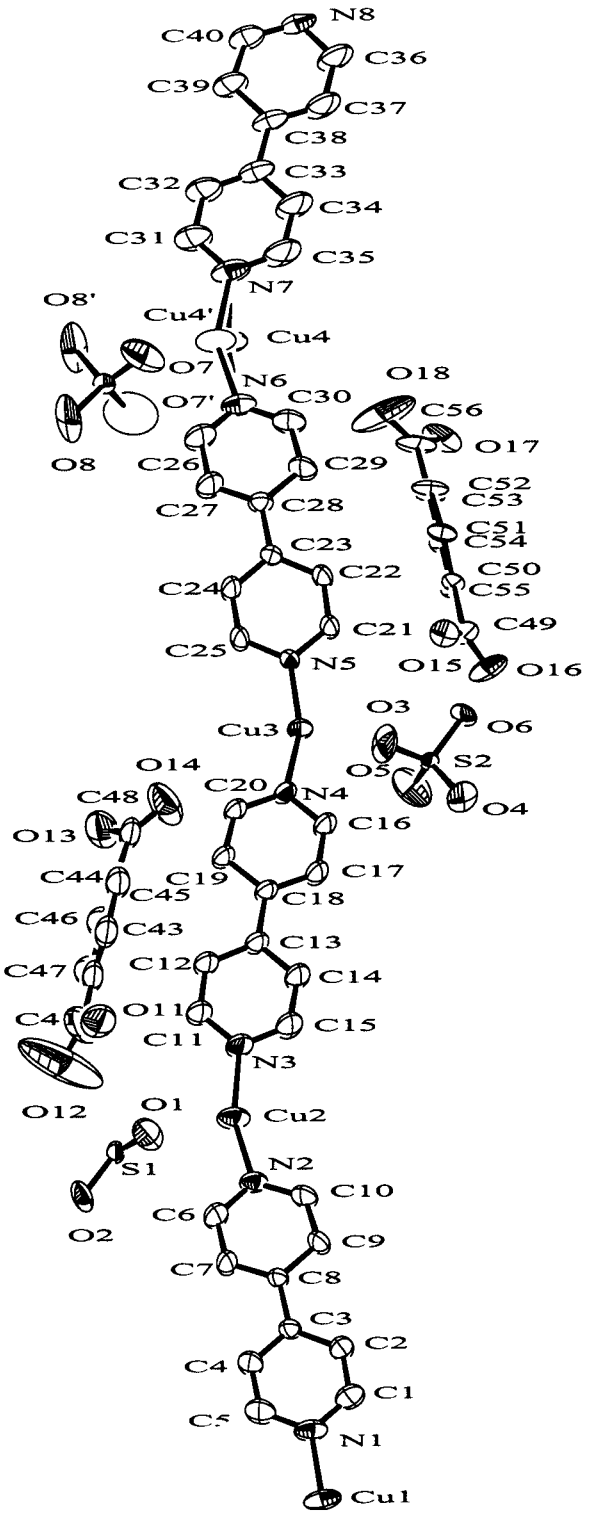

Figure 7.1. (a) View of 1D chain formed by $\{[Cu(bipy)]_2(SO_4)\cdot TPA\}_n$.

Initiating refinement of the extra reflections

To initiate refinement of the extra reflections one selects between origin options and creates an initiating displacement to phase reflections with *k* odd. These reflections calculate as zero using the parent structure symmetry. The sign of the displacement simply constitutes a choice between equivalent origins. Anisotropic displacement parameters suggested that pseudo translation related Cu should move in opposite directions parallel to **b**. Moving Cu1 and Cu3 in this way led eventually to successful refinement when the correct choice of model (choice of retained symmetry elements) was made.

The application of restraints and constraints helps refinement by eliminating noise created by allowing unreasonable geometry and atom displacement parameters. The final model has a 1:1 disorder confined to the S3 sulfate and the bond-connected Cu4. Refinement was constrained by making differences in bond valences (Brese & O'Keeffe, 1991) of the Cu^{I} atoms approach zero and making differences in Cu−N bond lengths about the same Cu approach zero using restraints. The sulfates were initially constrained to have a common geometry with the 2-fold symmetry implied by the parent structure but this constraint was later removed. The use of refinable local coordinates defined relative to refinable local orthonormal axial systems (Haller, Rae, Heerdegen, Hockless & Welberry, 1995) allowed equal planar object constraints to be used on pseudo glide related rings of the bipyridine and TPA groups. Multiple axis systems allowed the carboxylic acid groups centered on the attaching C of a ring to also be used after distinguishing the C=O from the C−O−H using hydrogen bonding arguments.

Rigid body models (Rae, 1975a, 1975b) were used to describe the anisotropic displacement parameters of some groups of atoms. The associated H atoms were included in these models. Each bipy was described by a *TLX* model as was each TPA and sulfate. The first sulfate was ordered about a 2-fold axis and its parameters were constrained by the site symmetry. The carboxylic acid groups were allowed an extra single libration centered on the relevant ring C atom. The orientation of this libration was also refined.

As a final stage of refinement, an attempt was made to order the disorder using space groups $C\bar{1}$ and *Cc*. These options involve doubling the asymmetric unit and constraints were used to impose *C*2/*c* symmetry on parts of the structure. A twinning parameter was included. These models were successfully controlled but were not successful in improving refinement. The disordered *C*2/*c* model is preferred.

The polymeric chain

The asymmetric unit contains two formula units of $[Cu(bipy)]_2(SO_4)\cdot TPA$ and was chosen to show that the structure consists of pseudo glide propagated chains $[-Cu^{I}-bipy-Cu^{I}-bipy-Cu^{I}-bipy-Cu^{I}-bipy-]_n$ of alternating copper atoms and bipy ligands. Sulfates at y = 1/4 lie on a 2-fold axis and link $[Cu^{I}-O-S-O-Cu^{I}]$ adjacent chains at y = 1/8. Adjacent chains at y = 1/8 are also bridged by SO_4^{2-} groups at y = 0 that are pseudo *n*-glide related and lie on pseudo 2-fold axes. The sulfate groups alternate across the chains as the chains progress through the crystal. The Cu(I) atoms are thus three coordinate with N−Cu−N angles of about [152.4(2)-163.0(2) °] and Cu−Cu distances of about 3.18 Å. The cocrystallized TPA molecules hydrogen bond to the uncoordinated oxygen atoms of the sulfate groups and sit on pseudo *n*-glide

related pseudo inversion centers. They form a bridge between layers of polymeric chains separated by 1/4 in *y*. The asymmetric unit is shown in Figure 7.1. It is to be noted that the sulfate centered on S3 is disordered about a true 2-fold axis and the Cu (Cu4) to which it is coordinated is also 1:1 disordered. This corrected otherwise unreasonable bond lengths and angles.

Table 7.2. Statistic for the refinements from RAELS.

Class	Reflections	$R(F)$	$R(F^2)$	wR	*Gof*
h even, *k* even, *h*+*k* = 4n[a]	2179	0.067	0.099	0.088	3.48
h even, *k* even, *h*+*k* = 4n+2[a]	18	0.265	0.531	0.256	2.42
h odd, *k* odd, *h*+*k* = 2n[a]	2586	0.100	0.156	0.100	2.72

a. $I > 3\sigma(I)$.
b. Number of independent variables = 289.
c. The weighting scheme for F_{obs} data was $w = 1/(\sigma^2(F_{obs})+(0.01)^2|F_{obs}|^2)$.

Table 7.3. Fractional monoclinic coordinates[a] and equivalent isotropic displacement parameters[b] (Å^2) for the refined atoms in $\{[Cu(bipy)]_2SO_4 \cdot TPA\}_n$.

	x	*y*	*z*	U_{eq}
Cu1	0.82103(5)	0.16286(3)	−0.67199(5)	0.057(0)
Cu2	0.57187(4)	0.09909(3)	−0.17270(5)	0.054(0)
Cu3	0.31976(4)	0.14722(2)	0.33035(5)	0.0395(2)
Cu4	0.0681(1)	0.0959(1)	0.8311(1)	0.068(0)
Cu4′	0.0708(1)	0.0875(1)	0.8337(1)	0.068(0)
S1	0.5000(0)	0.0139(1)	−0.2500(0)	0.039(2)
S2	0.2529(1)	0.2401(1)	0.2555(1)	0.025(1)
S3	0.0032(3)	0.0067(1)	0.7444(4)	0.039(4)
O1	0.5597(2)	0.0371(1)	−0.2012(3)	0.065(1)
O2	0.5241(3)	−0.0103(1)	−0.3086(3)	0.068(2)

Table 7.3. (Continued).

	x	*y*	*z*	U_{eq}
O3	0.2918(3)	0.2077(1)	0.2970(3)	0.076(1)
O4	0.2963(3)	0.2637(1)	0.2166(3)	0.077(2)
O5	0.1887(3)	0.2274(1)	0.1924(3)	0.086(3)
O6	0.2349(2)	0.2649(1)	0.3205(2)	0.046(2)
O7	0.0435(6)	0.0347(2)	0.8018(7)	0.092(4)
O8	0.0424(6)	−0.0190(3)	0.7059(9)	0.125(7)
O7′	−0.0524(6)	0.0258(2)	0.6786(7)	0.139(7)
O8′	−0.0426(6)	−0.0148(3)	0.7836(9)	0.155(9)
O11	0.3988(2)	0.0015(2)	−0.0871(4)	0.083(2)
O12	0.3108(4)	−0.0256(3)	−0.1831(4)	0.276(7)
O13	0.1134(3)	0.0042(2)	0.1028(4)	0.091(3)
O14	0.1844(3)	0.0500(2)	0.1670(4)	0.112(3)
O15	0.1580(2)	0.2511(2)	0.4179(3)	0.045(1)
O16	0.0699(3)	0.2827(2)	0.3322(3)	0.064(1)
O17	−0.1377(2)	0.2497(1)	0.6082(3)	0.071(2)
O18	−0.0587(3)	0.2075(2)	0.6739(3)	0.152(5)
N1	0.7852(2)	0.1545(1)	−0.5776(2)	0.049(2)
N2	0.6196(2)	0.1135(1)	−0.2532(2)	0.040(1)
N3	0.5394(2)	0.1033(1)	−0.0746(2)	0.050(2)
N4	0.3703(2)	0.1363(1)	0.2506(2)	0.035(1)
N5	0.2839(2)	0.1398(1)	0.4244(2)	0.029(1)
N6	0.1217(2)	0.1038(1)	0.7540(2)	0.051(2)
N7	0.0342(2)	0.0985(1)	0.9277(2)	0.066(2)
N8	−0.1278(3)	0.1474(1)	1.2520(3)	0.050(2)
C1	0.7657(2)	0.1826(1)	−0.5330(2)	0.058(2)
C2	0.7376(2)	0.1766(1)	−0.4675(2)	0.052(1)
C3	0.7267(1)	0.1397(1)	−0.4412(2)	0.032(1)
C4	0.7467(2)	0.1113(1)	−0.4869(2)	0.058(2)
C5	0.7746(2)	0.1184(1)	−0.5519(2)	0.068(2)
C6	0.6421(3)	0.0864(1)	−0.2965(3)	0.058(2)

Table 7.3. (Continued).

	x	*y*	*z*	U_{eq}
C7	0.6778(3)	0.0943(1)	−0.3560(3)	0.053(2)
C8	0.6925(1)	0.1312(1)	−0.3743(2)	0.030(1)
C9	0.6689(3)	0.1605(1)	−0.3286(3)	0.051(1)
C10	0.6339(3)	0.1500(1)	−0.2707(3)	0.054(1)
C11	0.5207(2)	0.0745(1)	−0.0312(2)	0.052(2)
C12	0.4907(2)	0.0794(1)	0.0329(2)	0.049(2)
C13	0.4766(1)	0.1159(1)	0.0590(2)	0.039(1)
C14	0.4958(2)	0.1450(1)	0.0145(2)	0.059(2)
C15	0.5257(2)	0.1390(1)	−0.0492(2)	0.065(2)
C16	0.3901(3)	0.1648(1)	0.2082(3)	0.051(1)
C17	0.4251(3)	0.1589(1)	0.1471(3)	0.052(1)
C18	0.4417(1)	0.1227(1)	0.1261(2)	0.036(1)
C19	0.4209(3)	0.0920(1)	0.1708(3)	0.044(2)
C20	0.3864(3)	0.1006(1)	0.2304(3)	0.043(2)
C21	0.2640(2)	0.1684(1)	0.4671(2)	0.046(1)
C22	0.2372(2)	0.1634(1)	0.5340(2)	0.049(1)
C23	0.2283(1)	0.1268(1)	0.5640(2)	0.031(1)
C24	0.2487(2)	0.0978(1)	0.5202(2)	0.053(2)
C25	0.2752(2)	0.1040(1)	0.4537(2)	0.049(3)
C26	0.1454(3)	0.0760(1)	0.7136(3)	0.069(3)
C27	0.1812(3)	0.0828(1)	0.6538(3)	0.062(2)
C28	0.1947(1)	0.1194(1)	0.6320(2)	0.036(1)
C29	0.1698(3))	0.1495(1)	0.6744(3)	0.060(2)
C30	0.1347(3)	0.1399(1)	0.7329(3)	0.065(2)
C31	0.0092(2)	0.0717(1)	0.9704(3)	0.071(3)
C32	−0.0205(2)	0.0795(1)	1.0338(3)	0.067(2)
C33	−0.0273(1)	0.1171(1)	1.0597(2)	0.053(2)
C34	−0.0018(2)	0.1441(1)	1.0159(3)	0.086(2)
C35	0.0275(3)	0.1352(1)	0.9530(3)	0.093(2)
C36	−0.1046(5)	0.1736(1)	1.2074(4)	0.080(1)

Table 7.3. (Continued).

	x	*y*	*z*	U_{eq}
C32	−0.0205(2)	0.0795(1)	1.0338(3)	0.067(2)
C33	−0.0273(1)	0.1171(1)	1.0597(2)	0.053(2)
C34	−0.0018(2)	0.1441(1)	1.0159(3)	0.086(2)
C35	0.0275(3)	0.1352(1)	0.9530(3)	0.093(2)
C36	−0.1046(5)	0.1736(1)	1.2074(4)	0.080(1)
C37	−0.0717(4)	0.1645(1)	1.1458(4)	0.081(1)
C38	−0.0608(1)	0.1272(1)	1.1266(2)	0.050(2)
C39	−0.0852(3)	0.0988(1)	1.1736(3)	0.061(2)
C40	−0.1173(3)	0.1105(1)	1.2335(3)	0.059(2)
C41	0.3341(2)	−0.0100(1)	−0.1164(3)	0.099(3)
C42	0.2865(1)	−0.0025(1)	−0.0597(2)	0.063(2)
C43	0.3280(2)	0.0072(1)	0.0232(2)	0.064(1)
C44	0.2947(2)	0.0156(1)	0.0864(2)	0.065(2)
C45	0.2204(2)	0.0142(1)	0.0655(2)	0.061(2)
C46	0.1789(2)	0.0044(1)	−0.0174(2)	0.075(2)
C47	0.2122(2)	−0.0040(1)	−0.0805(2)	0.078(2)
C48	0.1701(2)	0.0245(1)	0.1172(2)	0.064(2)
C49	0.0948(2)	0.2650(1)	0.3958(2)	0.042(1)
C50	0.0512(1)	0.2576(1)	0.4571(2)	0.026(1)
C51	0.0820(2)	0.2496(1)	0.5443(2)	0.035(1)
C52	0.0381(2)	0.2410(1)	0.5959(2)	0.047(1)
C53	−0.0359(1)	0.2405(1)	0.5596(1)	0.038(1)
C54	−0.0667(1)	0.2485(1)	0.4724(2)	0.027(1)
C55	−0.0229(2)	0.2571(1)	0.4208(2)	0.027(1)
C56	−0.0794(2)	0.2310(1)	0.6201(2)	0.062(2)

[a]Estimated standard deviations of the least significant digits are given in parentheses.
[b]Equivalent isotropic atomic displacement parameters for the atoms refined anisotropically, $U_{eq} = 1/3 \sum_i \sum_j U_{ij}\, a_i^* a_j^*\, \mathbf{a}_i \cdot \mathbf{a}_j$

Table 7.4. Anisotropic atomic displacement parameters[a] in $[Cu(bipy)]_2SO_4 \cdot TPA$.

Atom	*U11*	*U22*	*U33*	*U12*	*U13*	*U23*
Cu1	0.053(1)	0.091(1)	0.041(1)	0.000(0)	0.034(0)	0.013(0)
Cu2	0.060(1)	0.073(1)	0.043(1)	−0.004(0)	0.036(0)	0.000(0)
Cu3	0.0506(5)	0.0413(4)	0.0390(4)	−0.0009(3)	0.0322(3)	0.0008(3)
Cu4	0.066(1)	0.106(1)	0.046(1)	−0.005(1)	0.037(1)	0.003(1)
Cu4′	0.066(1)	0.106(1)	0.046(1)	−0.005(1)	0.037(1)	0.003(1)
S1	0.066(1)	0.106(1)	0.046(1)	−0.005(1)	0.037(1)	0.003(1)
S2	0.032(2)	0.023(1)	0.029(2)	0.004(1)	0.023(1)	0.003(1)
S3	0.060(6)	0.032(2)	0.049(8)	−0.001(3)	0.052(7)	−0.002(2)
O1	0.071(2)	0.060(3)	0.074(4)	−0.013(1)	0.036(3)	−0.018(2)
O2	0.109(3)	0.031(2)	0.099(4)	−0.015(2)	0.086(3)	−0.022(2)
O3	0.089(3)	0.041(1)	0.102(3)	0.037(2)	0.037(2)	0.024(1)
O4	0.112(3)	0.060(3)	0.103(3)	−0.013(2)	0.097(3)	0.006(2)
O5	0.062(3)	0.101(3)	0.082(3)	−0.009(2)	0.000(1)	−0.042(2)
O6	0.062(2)	0.043(2)	0.050(2)	0.002(1)	0.044(2)	−0.010(1)
O7	0.082(4)	0.125(5)	0.066(10)	−0.020(5)	0.018(6)	−0.043(5)
O8	0.186(11)	0.042(2)	0.235(15)	−0.006(4)	0.197(12)	−0.024(5)
O7′	0.102(11)	0.199(9)	0.083(7)	0.030(5)	−0.021(9)	−0.006(6)
O8′	0.258(16)	0.045(2)	0.281(17)	−0.032(8)	0.260(14)	−0.023(8)
O11	0.101(3)	0.079(4)	0.091(3)	0.016(2)	0.064(3)	0.012(3)
O12	0.204(8)	0.464(18)	0.237(8)	−0.185(10)	0.181(7)	−0.246(11)
O13	0.111(3)	0.070(4)	0.122(5)	−0.011(3)	0.082(3)	−0.017(3)
O14	0.141(5)	0.079(3)	0.160(5)	−0.026(3)	0.112(4)	−0.050(3)
O15	0.034(1)	0.055(2)	0.063(2)	0.008(1)	0.039(2)	0.002(2)
O16	0.051(2)	0.094(2)	0.063(2)	0.013(2)	0.043(2)	0.039(2)
O17	0.061(2)	0.100(3)	0.079(2)	−0.018(2)	0.063(2)	−0.034(2)
O18	0.108(4)	0.265(6)	0.122(4)	0.044(4)	0.094(4)	0.110(5)
N1	0.047(3)	0.073(3)	0.037(2)	−0.010(1)	0.025(2)	0.001(1)
N2	0.042(2)	0.052(3)	0.034(2)	−0.009(1)	0.021(2)	−0.001(1)
N3	0.065(3)	0.049(3)	0.050(2)	0.005(1)	0.040(3)	0.008(1)
N4	0.042(3)	0.033(2)	0.037(2)	0.005(1)	0.022(2)	0.010(1)
N5	0.037(2)	0.024(2)	0.030(2)	0.002(1)	0.017(2)	−0.002(1)

Table 7.4. (Continued).

Atom	*U11*	*U22*	*U33*	*U12*	*U13*	*U23*
N6	0.044(3)	0.081(4)	0.035(2)	−0.003(1)	0.022(2)	0.006(1)
N7	0.062(4)	0.099(4)	0.049(3)	0.013(2)	0.037(3)	0.020(1)
N8	0.038(3)	0.082(3)	0.037(2)	0.012(2)	0.020(2)	0.023(1)
C1	0.079(3)	0.055(3)	0.057(2)	−0.017(2)	0.045(2)	0.003(1)
C2	0.081(3)	0.037(2)	0.056(2)	−0.016(2)	0.047(2)	−0.005(1)
C3	0.038(2)	0.033(2)	0.031(2)	−0.006(1)	0.018(2)	−0.004(1)
C4	0.092(3)	0.041(2)	0.065(2)	0.003(2)	0.060(2)	−0.003(2)
C5	0.100(4)	0.062(3)	0.069(3)	0.000(2)	0.066(3)	−0.006(2)
C6	0.091(3)	0.038(2)	0.065(2)	−0.010(2)	0.055(2)	0.002(2)
C7	0.089(3)	0.028(2)	0.064(2)	−0.003(2)	0.056(2)	0.000(2)
C8	0.037(2)	0.028(2)	0.030(2)	−0.006(1)	0.018(2)	−0.005(1)
C9	0.085(3)	0.032(2)	0.056(2)	−0.012(2)	0.051(2)	−0.013(1)
C10	0.081(3)	0.045(2)	0.054(2)	−0.008(2)	0.050(2)	−0.011(1)
C11	0.074(4)	0.044(3)	0.056(3)	0.007(1)	0.046(3)	0.008(1)
C12	0.069(3)	0.039(2)	0.053(2)	0.008(1)	0.043(3)	0.009(1)
C13	0.048(2)	0.038(2)	0.041(2)	0.004(1)	0.027(2)	0.009(1)
C14	0.094(3)	0.040(2)	0.068(2)	0.003(2)	0.062(3)	0.009(1)
C15	0.104(4)	0.046(3)	0.073(3)	0.003(2)	0.069(3)	0.010(1)
C16	0.081(3)	0.033(2)	0.059(2)	0.008(2)	0.051(2)	0.012(1)
C17	0.084(3)	0.033(2)	0.061(2)	0.005(2)	0.053(2)	0.011(1)
C18	0.043(2)	0.034(2)	0.038(2)	0.004(1)	0.024(2)	0.009(1)
C19	0.064(3)	0.033(2)	0.049(2)	0.006(1)	0.039(2)	0.011(1)
C20	0.061(2)	0.033(2)	0.048(2)	0.004(1)	0.037(2)	0.010(1)
C21	0.078(3)	0.023(2)	0.055(2)	0.002(2)	0.048(2)	−0.002(1)
C22	0.084(2)	0.026(2)	0.057(2)	−0.001(2)	0.052(2)	−0.006(1)
C23	0.037(2)	0.030(2)	0.030(2)	0.002(1)	0.017(2)	−0.001(1)
C24	0.091(3)	0.025(3)	0.065(2)	0.008(1)	0.058(2)	0.005(1)
C25	0.093(3)	0.023(3)	0.064(2)	0.005(1)	0.060(2)	−0.001(1)
C26	0.098(5)	0.065(3)	0.069(3)	−0.004(1)	0.061(4)	0.012(2)
C27	0.095(4)	0.047(3)	0.068(3)	0.003(1)	0.060(3)	0.011(2)
C28	0.039(2)	0.041(3)	0.031(2)	0.001(1)	0.018(2)	0.001(1)

Table 7.4. (Continued).

Atom	*U11*	*U22*	*U33*	*U12*	*U13*	*U23*
C29	0.092(3)	0.052(3)	0.060(2)	−0.003(2)	0.058(2)	−0.008(1)
C30	0.086(3)	0.072(4)	0.058(2)	0.001(2)	0.054(3)	−0.004(1)
C31	0.074(5)	0.095(3)	0.063(3)	−0.001(2)	0.049(4)	0.007(2)
C32	0.069(4)	0.088(3)	0.060(3)	−0.002(2)	0.046(3)	0.009(2)
C30	0.086(3)	0.072(4)	0.058(2)	0.001(2)	0.054(3)	−0.004(1)
C31	0.074(5)	0.095(3)	0.063(3)	−0.001(2)	0.049(4)	0.007(2)
C32	0.069(4)	0.088(3)	0.060(3)	−0.002(2)	0.046(3)	0.009(2)
C33	0.043(3)	0.085(3)	0.040(2)	0.011(2)	0.023(2)	0.022(1)
C34	0.123(4)	0.087(3)	0.083(3)	0.018(2)	0.082(3)	0.029(2)
C35	0.133(5)	0.094(3)	0.088(3)	0.020(2)	0.090(4)	0.030(2)
C36	0.113(4)	0.081(3)	0.076(2)	0.025(2)	0.073(3)	0.033(2)
C37	0.115(3)	0.081(3)	0.077(2)	0.022(2)	0.075(3)	0.032(2)
C38	0.038(3)	0.081(3)	0.037(2)	0.011(2)	0.020(2)	0.022(1)
C39	0.062(3)	0.080(3)	0.057(2)	−0.001(2)	0.042(2)	0.013(2)
C40	0.056(3)	0.081(3)	0.053(2)	−0.002(2)	0.037(2)	0.013(2)
C41	0.125(4)	0.086(5)	0.119(4)	−0.023(3)	0.089(3)	−0.033(3)
C42	0.098(3)	0.027(3)	0.084(3)	0.008(2)	0.058(2)	0.007(2)
C43	0.095(3)	0.033(2)	0.084(3)	0.008(2)	0.057(3)	0.008(2)
C44	0.095(3)	0.037(2)	0.084(3)	0.007(2)	0.057(3)	0.005(2)
C45	0.096(3)	0.023(2)	0.084(3)	0.008(2)	0.057(2)	0.009(2)
C46	0.095(3)	0.061(3)	0.087(3)	0.003(2)	0.057(3)	−0.001(2)
C47	0.098(3)	0.069(4)	0.087(3)	0.001(3)	0.058(3)	−0.006(2)
C48	0.099(3)	0.028(2)	0.086(3)	0.012(2)	0.060(2)	0.012(2)
C49	0.034(1)	0.057(2)	0.048(2)	0.010(1)	0.034(1)	0.012(1)
C50	0.023(1)	0.034(2)	0.029(1)	0.006(1)	0.020(1)	−0.002(1)
C51	0.025(1)	0.057(2)	0.026(1)	0.002(1)	0.014(1)	−0.007(1)
C52	0.037(1)	0.090(2)	0.020(1)	−0.004(1)	0.017(1)	−0.006(1)
C53	0.034(1)	0.064(2)	0.026(1)	−0.002(1)	0.025(1)	−0.009(1)
C54	0.024(1)	0.035(2)	0.031(1)	0.005(1)	0.021(1)	−0.004(1)
C55	0.023(1)	0.037(2)	0.028(1)	0.008(1)	0.018(1)	0.005(1)
C56	0.057(2)	0.109(2)	0.037(1)	−0.012(2)	0.041(1)	−0.012(2)

[a]Estimated standard deviations of the least significant digits are given in parentheses.

Table 7.5. Selected interatomic bond lengths[a] (Å) and bond angles[a] (º) for $[Cu(bipy)]_2SO_4$.TPA.

Cu1–O5	2.267(5)	O13–C48	1.277(3)
Cu1–N1	1.893(2)	O14–C48	1.176(4)
Cu1–N8	1.890(2)	O15–C49	1.277(3)
Cu1–O1	2.202(4)	O16–C49	1.176(4)
Cu2–N2	1.892(2)	O17–C56	1.277(3)
Cu2–N3	1.893(2)	O18–C56	1.176(4)
Cu3–O3	2.199(4)	N1–C1	1.339(3)
Cu3–N4	1.892(2)	N1–C5	1.360(4)
Cu3–N5	1.884(2)	N2–C6	1.329(4)
Cu4–O7	2.200(6)	N2–C10	1.347(4)
Cu4–N6	1.883(2)	N3–C11	1.339(3)
Cu4–N7	1.884(2)	N3–C15	1.360(4)
Cu4′–O7′	2.176(6)	N4–C16	1.329(4)
Cu4′–N6	1.944(3)	N4–C20	1.347(4)
Cu4′–N7	1.912(3)	N5–C21	1.339(3)
S1–O1	1.447(4)	N5–C25	1.360(4)
S1–O2	1.453(4)	N6–C26	1.329(4)
S2–O3	1.415(4)	N6–C30	1.347(4)
S2–O4	1.456(4)	N7–C31	1.339(3)
S2–O5	1.435(5)	N7–C35	1.360(4)
S2–O6	1.486(3)	N8–C36	1.329(4)
S3–O7	1.416(6)	N8–C40	1.347(4)
S3–O8	1.439(7)	C1–C2	1.355(4)
S3–O7′	1.439(7)	C2–C3	1.391(4)
S3–O8′	1.453(7)	C3–C4	1.361(3)
O11–C41	1.277(3)	C3–C8	1.471(4)
O12–C41	1.176(4)	C4–C5	1.352(4)
C6–C7	1.382(4)	C37–C38	1.367(4)
C7–C8	1.367(4)	C38–C39	1.419(3)
C8–C9	1.419(3)	C39–C40	1.372(4)
C9–C10	1.372(4)	C41–C42	1.520(4)

Table 7.5. (Continued).

C11–C12	1.355(4)	C42–C43	1.392(3)
C12–C13	1.391(4)	C42–C47	1.392(3)
C13–C14	1.361(3)	C43–C44	1.403(4)
C13–C18	1.472(4)	C44–C45	1.392(3)
C14–C15	1.352(4)	C45–C46	1.392(3)
C16–C17	1.382(4)	C45–C48	1.520(4)
C17–C18	1.367(4)	C46–C47	1.403(4)
C18–C19	1.419(3)	C49–C50	1.520(4)
C19–C20	1.372(4)	C50–C51	1.392(3)
C21–C22	1.355(4)	C50–C55	1.392(3)
C22–C23	1.391(4)	C51–C52	1.403(4)
O17–C56	1.361(3)	C52–C53	1.392(3)
C23–C28	1.470(4)	C53–C54	1.392(3)
C24–C25	1.352(4)	C53–C56	1.520(4)
C26–C27	1.382(4)	C54–C55	1.403(4)
C27–C28	1.367(4)	O2–O11	2.624(5)
C28–C29	1.419(3)	O4–O17	2.526(5)
C29–C30	1.372(4)	O6–O15	2.538(4)
C31–C32	1.355(4)	O8–O13	2.534(12)
C32–C33	1.391(4)	O8′–O13	2.650(11)
C33–C34	1.361(3)	O12–O14	3.027(10)
C33–C38	1.473(4)	O16–O16	3.202(11)
C34–C35	1.352(4)		
C36–C37	1.382(4)		
O5–Cu1–N1	103.6(2)	O8–S3–O8′	110.7(5)
O5–Cu1–N8	102.9(2)	O7′–S3–O8′	97.8(9)
O1–Cu2–N2	99.1(2)	Cu2–O1–S1	132.9(3)
O1–Cu2–N3	102.2(2)	Cu3–O3–S2	159.9(4)
O3–Cu3–N4	99.5(2)	Cu1–O5–S2	115.4(3)
O3–Cu3–N5	101.9(2)	Cu4–O7–S3	148.3(7)
O7–Cu4–N6	97.3(4)	Cu4′–O7′–S3	126.3(6)

Table 7.5. (Continued).

O7–Cu4–N7	96.8(3)	S1–O2–O11	134.2(3)
O7′–Cu4′–N6	109.2(4)	S2–O4–O17	133.5(3)
O7′–Cu4′–N7	100.3(4)	S2–O6–O15	130.4(2)
N1–Cu1–N8	152.4(2)	S3–O8–O13	129.3(7)
N2–Cu2–N3	157.6(2)	S3–O8′–O13	139.2(7)
N4–Cu3–N5	158.4(2)	O2–O11–C41	114.1(3)
N6–Cu4–N7	163.0(2)	O8–O13–C48	112.8(4)
O1–S1–O1	112.1(4)	O6–O15–C49	117.4(3)
O1–S1–O1	108.3(3)	O4–O17–C56	115.1(3)
O1–S1–O1	109.4(3)	O14–O12–C41	150.3(3)
O2–S1–O2	109.2(4)	O12–O14–C48	108.2(3)
O3–S2–O4	110.9(3)	O18–O18–C56	131.2(2)
O3–S2–O5	109.0(3)	C1–N1–C5	114.3(2)
O3–S2–O6	109.3(3)	C6–N2–C10	115.6(2)
O4–S2–O5	111.3(3)	C11–N3–C15	114.3(2)
O4–S2–O6	106.2(3)	C18–N4–C20	115.6(2)
O5–S2–O6	110.1(3)	C21–N5–C25	114.3(2)
O7–S3–O8	116.7(8)	C26–N6–C30	115.6(2)
O7–S3–O7′	108.6(6)	C31–N7–C35	114.3(2)
O7–S3–O8′	111.1(7)	Cu1–N1–C1	124.4(2)
O8–S3–O7′	110.3(8)	Cu1–N1–C5	121.3(2)
Cu2–N2–C6	119.4(3)	N2–O10–C9	125.1(3)
Cu2–N2–C10	125.0(2)	N3–C11–C12	124.4(3)
Cu2–N3–C11	127.0(2)	C11–C12–C13	121.4(3)
Cu2–N3–C15	118.4(2)	C12–C13–C14	113.9(3)
Cu3–N4–C16	120.2(2)	C12–C13–C18	123.5(2)
Cu3–N4–C20	124.1(2)	C14–C13–C18	122.6(2)
Cu3–N5–C21	123.9(2)	C13–C14–C15	123.0(3)
Cu3–N5–C25	121.8(2)	N3–C15–C14	123.1(3)
Cu4–N6–C26	124.8(3)	N4–C16–C17	123.4(3)

Table 7.5. (Continued).

Cu4–N6–C30	119.5(3)	C16–C17–C18	121.5(3)
Cu4–N7–C31	132.5(2)	C13–C18–C17	122.1(2)
Cu4–N7–C35	112.9(2)	C13–C18–C19	121.9(2)
Cu1–N8–C36	119.9(3)	C17–C18–C19	115.9(3)
Cu1–N8–C40	124.3(3)	C18–C19–C20	118.6(3)
C36–N8–C40	115.6(2)	N4–C20–C19	125.1(3)
N1–C1–C2	124.4(3)	N5–C21–C22	124.4(3)
C1–C2–C3	121.4(3)	C21–C22–C23	121.4(3)
C2–C3–C4	113.9(3)	C22–C23–C24	113.9(3)
C2–C3–C8	124.0(2)	C22–C23–C28	123.8(2)
C4–C3–C8	122.0(2)	C24–C23–C28	122.1(2)
C3–C4–C5	123.0(3)	C23–C24–C25	123.0(3)
N1–C5–C4	123.1(3)	N5–C25–C24	123.1(3)
N2–C6–C7	123.4(3)	N6–C26–C27	123.4(3)
C6–C7–C8	121.5(3)	C26–C27–C28	121.5(3)
C3–C8–C7	121.5(2)	C23–C28–C27	121.6(2)
C3–C8–C9	122.5(2)	C23–C28–C29	122.3(2))
C7–C8–C9	115.9(3)	C27–C28–C29	115.9(3)
C8–C9–C10	118.6(3)	C28–C29–C30	118.6(3)
N6–C30–C29	125.1(3)	C44–C45–C48	131.4(2)
N7–C31–C32	124.4(3)	C46–C45–C48	107.9(2)
C31–C32–C33	121.4(3)	C45–C46–C47	119.7(1)
C32–C33–C34	113.9(3)	C42–C47–C46	119.7(1)
C32–C33–C38	123.6(2)	O13–C48–O14	123.8(3)
C34–C33–C38	122.5(2)	O13–C48–C45	116.2(2)
C33–C34–C35	123.0(3)	O14–C48–C45	120.0(2)
N7–C35–C34	123.1(3)	O15–C49–O16	123.8(3)
N8–C36–C37	123.4(3)	O15–C49–C50	116.2(2)
C36–C37–C38	121.5(3)	O16–C49–C50	120.0(2)
C33–C38–C37	122.0(2)	C49–C50–C51	123.1(2)
C33–C38–C39	122.1(2)	C49–C50–C55	116.3(2)

Table 7.5. (Continued).

C37–C38–C39	115.9(3)	C51–C50–C55	120.5(3)
C38–C39–C40	118.6(3)	C50–C51–C52	119.7(1)
N8–C40–C39	125.1(3)	C51–C52–C53	119.7(1)
O11–C41–O12	123.8(3)	C52–C53–C54	120.5(3)
O11–C41–C42	116.2(2)	C52–C53–C56	116.3(2)
O12–C41–C42	120.0(2)	C54–C53–C56	123.2(2)
C41–C42–C43	110.1(2)	C53–C54–C55	119.7(1)
C41–C42–C47	129.4(2)	C50–C55–C54	119.7(1)
C43–C42–C47	120.5(3)	O17–C56–O18	123.8(3)
C42–C43–C44	119.7(1)	O17–C56–C53	116.2(2)
C43–C44–C45	119.7(1)	O18–C56–C53	120.0(2)
C44–C45–C46	120.5(3)		

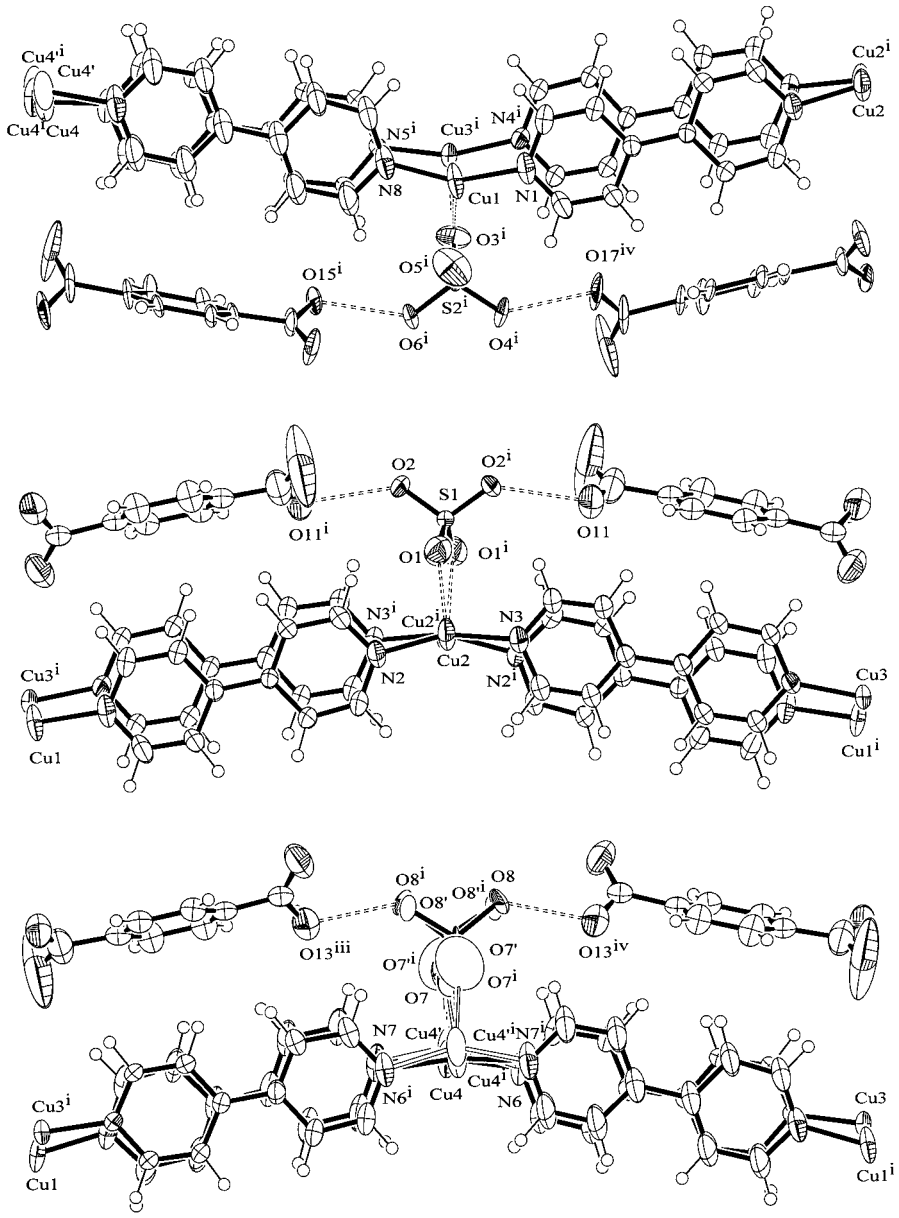

Figure 7.2. View of SO_4^{2-} groups, two O atoms bridged to double stranded polymeric chains and two free O atoms linked to TPA molecules. Cu1−O5^{i} = 2.267(5) Å; (c) Cu2−O1 = 2.202(4), O2−O11^{i} = O2^{i}−O11 = 2.624(5) Å; (d) Cu3−O3 = 2.199(4), O4−O17^{iv} = 2.526(5) Å, O6−O15 = 2.538(4) Å; (e) Cu4−O7 = 2.200(6), Cu4′−O7′ = 2.176(6), O8−O13^{v} = 2.534(12), O8′−O13^{iii} = 2.650(11) Å.

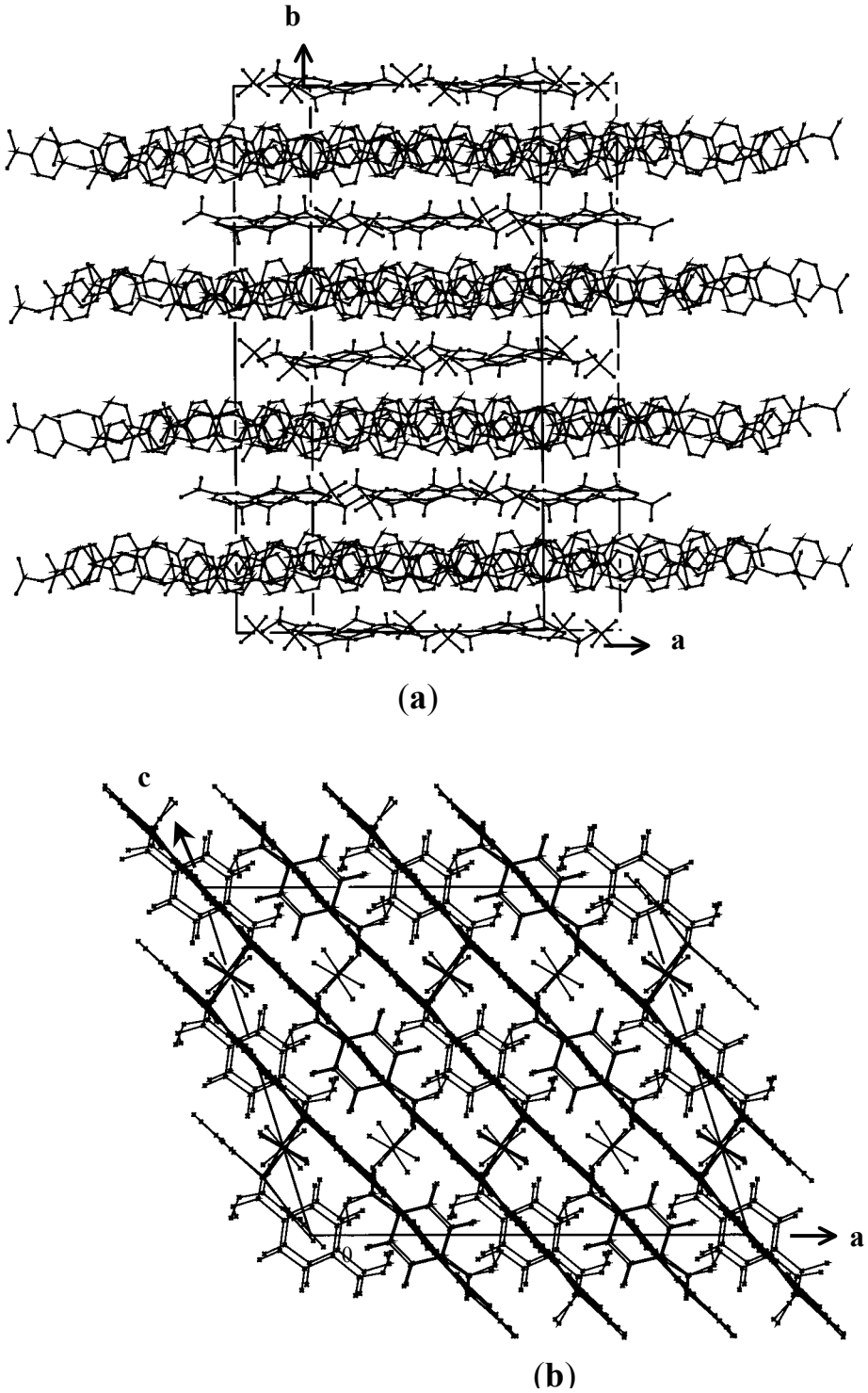

Figure 7.3. (a) packing diagram along [001], (b) packing diagram along [010].

Understanding the structure modulation options

There are 32 symmetry elements for the parent *C*2/*c* structure modulo 2$\mathbf{a}_p$, 2$\mathbf{b}_p$, $\mathbf{c}_p$. In this expanded cell these symmetry elements are

(0,0,0+; 1/2,1/2,0+) x, y, z −x, −y, −z −x, y, 1/2−z x, −y, 1/2+z

plus add (1/2,0,0) to each of the first eight

plus add (1/4, 1/4,0) to each of the first eight

plus add (3/4,1/4,0) to each of the first eight

In the parent structure the scattering density is identical at all 32 of these equivalent positions. In the final structure the scattering density is the same at sets of eight equivalent positions related by the true symmetry elements of *C2/c*.

The pseudo symmetry elements

x, y, z −1/4+x, 1/4−y, 1/2+z −1/2+x, y, 1+z −3/4+x, 1/4−y, 1/2+z

of the polymer chain are related by an *n*-glide in the parent structure but describe non equivalent components of the asymmetric unit in the modulated structure.

The first step is to create an intermediate model in which we create a scattering density component that is anti-symmetric with respect to the translation 1/2$\mathbf{a}_p$+1/2$\mathbf{b}_p$ and makes a contribution to only a quarter of the observed reflections. These are the reflections with $\mathbf{h} = \mathbf{g}+\mathbf{q}$ where $\mathbf{g}$ is a parent reflection corresponding to *h* even, *k* even, *h*+*k* = 4*n* and $\mathbf{q} = \mathbf{a}^*+\mathbf{b}^*$. These reflections are not the same as those with $\mathbf{h} = \mathbf{g}-\mathbf{a}^*+\mathbf{b}^*$ that are related by a 2-fold rotation about $\mathbf{b}$. There is thus the possibility of two identical triclinic structures that are twin related. However this twinning would not create the weakly observed reflections with *h* even, *k* even, *h*+*k* =

4n+2. Therefore the correct structure contains some coherent combination of two triclinic modulations that interact with each other to create these reflections.

Two triclinic structures are possible, one with the TPA on inversion centers, the other with the TPA between inversion centers. We are thus looking at structure modulations that correspond to basis functions of two different doubly degenerate irreducible representations. A feature of such a concept is that any linear combination of basis functions of a degenerate irreducible representation is also a basis function. Thus two different *C*2/*c* structures can be formed from the coherent addition of two rotation related triclinic modulations, namely $\rho_1(\mathbf{r}) = \rho_A(\mathbf{r}) + \rho_B(\mathbf{r})$ and $\rho_2(\mathbf{r}) = \rho_A(\mathbf{r}) - \rho_B(\mathbf{r})$. The reverse relationship is obvious, *i.e.* $\rho_A(\mathbf{r}) = 1/2[\rho_1(\mathbf{r}) + \rho_2(\mathbf{r})]$ and $\rho_B(\mathbf{r}) = 1/2[\rho_1(\mathbf{r}) - \rho_2(\mathbf{r})]$. Two *C*2/*c* structures differ in that one is changed to the other by the translation $1/2\mathbf{a}_p + 1/2\mathbf{b}_p = 1/4\mathbf{a} + 1/4\mathbf{b}$. This translation interchanges the locations of the 2 fold axes and the 2_1 screw axes.

(3+n)-Dimensional descriptions of the modulated structure

A (3+1) dimensional approach corresponds to creating the twin related triclinic symmetry options. The observation of h = even, k = even, $h + k$ = 4n + 2 reflections requires the coexistence of two modulation vectors in the same crystal domain. This could be described as a (3+2) dimensional approach.

However this becomes academic if the parent structure is changed from *C*2/*c* to *P*2/*c* by destroying the unsustainable 2_1 and *n* operations of the *C*2/*c* parent structure. The structure options then correspond to deciding how two identical *P*2/*c* substructures separated by the pseudo translation $1/2\mathbf{a}_p + 1/2\mathbf{b}_p$ interact to form the final structure. A *P*2/*c* substructure can be modulated to *C*2/*c* to create the extra

reflections. There are two choices for the location of the two fold axes and two choices for the location of the c glides of the possible final structures. The intensities of half these reflections can be destroyed if the other substructure is related by an exact translation, either $1/2\mathbf{a}_p+1/2\mathbf{b}_p = 1/4\mathbf{a}+1/4\mathbf{b}$ or $1/4\mathbf{a}-1/4\mathbf{b}$. In this instance, only inversion centers of the translationally related structures coincide in space. The *c*-glides (or 2-fold rotations) of one substructure lie midway between the *c*-glides (or 2-fold rotations) of the other.

If the symmetry elements of the two modulated substructures coincide then the *C*2/*c* symmetry is maintained and the translationally related substructures can not be equivalent. There are no rules as to how the parent structure should be initially separated into two identical substructures but this does not matter when the final symmetry is *C*2/*c*. The *C*2/*c* structures are doubly degenerate, since an identical structure translated by $1/4\mathbf{a}+1/4\mathbf{b}$ can be created from the parent structure, however these structures have their true symmetry elements (other than the inversions) in different positions.

A stacking fault that translates the structure by $1/4\mathbf{a}+1/4\mathbf{b}$ or $1/4\mathbf{a}-1/4\mathbf{b}$ or $1/2\mathbf{a}$ would lower the scale for the intensity of the satellite reflections. The observed disorder in the final $Z = 16$ structure suggests that the repeat unit of the polymer chain could well be doubled again, the extra reflections being lost by stacking faults.

7.5 References

Altomare, A., Burla, M. C., Camalli, M., Cascarano, G. L., Giacovazzo, C., Guagliardi, A., Moliterni, A. G. G., Polidori, G. and Spagna, R. (1999). *SIR97* A New Tool for Crystal Structure Determination and Refinement. **Journal of Applied Crystallography** 32: 115-119.

Baeg, J. Y. and Lee, S. W. (2003). A porous, two-dimensional copper coordination-polymer containing guest molecules: Hydrothermal synthesis, structure, and thermal property of [Cu(BDC)(bipy)](BDCH$_2$) (BDC = 1,4-benzenedicarboxylate; bipy = 4,4′-bipyridine). **Inorganic Chemistry Communications** 6(3): 313-316.

Boldog, I., Rusanov, E. B., Chernega, A. N., Sieler, J. and Domasevitch, K. V. (2001). One- and two-dimensional coordination polymers of 3,3′,5,5′-tetramethyl-4,4′-bipyrazolyl, a new perspective crystal engineering module. **Polyhedron** 20(9-10): 887-897.

Brese, N. E. and O'Keeffe, M. (1991). Bond valence parameters for solids. **Acta Crystallographica** B47: 192-197.

Dong, Y.-B., Smith, M. D., Layland, R. C. and Loye, H.-C. z. (2000). Novel hydrogen-bonded two- and three-dimensional networks generated from the reaction of metal nitrate hydrates (M = Cd, Co) with the bidentate linear ligand 4,4′-bipyridine. **Dalton Transactions** (5): 775-780.

Du, M., Chen, S.-T., Bu, X.-H. and Ribas, J. (2002). Crystal structure and properties of a Cu^{II} coordination polymer with 2-D grid-like host architecture for the

inclusion of organic guest molecule. **Inorganic Chemistry Communications** 5(11): 1003-1006.

Fujita, M., Kwon, Y. J., Washizu, S. and Ogura, K. (1994). Preparation, clathration ability, and catalysis of two-dimension square network material composed of cadmium(II) and 4,4′-Bipyridine. **Journal of the American Chemical Society** 116(3): 1151-1152.

Gudbjartson, H., Biradha, K., Poirier, K. M. and Zaworotko, M. J. (1999). Novel nanoporous coordination polymer sustained by self-assembly of T-shaped moieties. **Journal of the American Chemical Society** 121(11): 2599-2600.

Haller, K. J., Rae, A. D., Heerdegen, A. P., Hockless, D. C. R. and Welberry, T. R. (1995). The fourford disordered structures of *p*-chloro-*N*-(*p*-methylbenzylidene) aniline and *p*-methyl-*N*-(*p*-chlorobenzylidene)aniline. **Acta Crystallographica** B5: 187-197.

Hoskin, B. F.; Robson, R. (1990). Design and construction of a new class of scaffolding-like materials comprising infinite polymeric frameworks of 3D-linked molecular rods. A reappraisal of the $Zn(CN)_2$ and $Cd(CN)_2$ structures and the synthesis and structure of the diamond-related frameworks $[N(CH_3)_4][Cu^{I}Zn^{II}(CN)_4]$ and Cu^{I}[4,4′,4″,4‴-tetracyanotetraphenylmethane] $BF_4.xC_6H_5NO_2$. **Journal of the American Chemical Society** 112(4): 1546-1554.

Kawata, S., Kitagawa, S., Machida, H., Nakamoto, T., Kondo, M., Katada, M., Kikuchi, K. and Ikemoto, I. (1995). Oxamide oxime-based copper(II) coordination polymers. Two- and three-dimensional structures controlled by dicarboxylates. **Inorganica Chimica Acta** 229(1-2): 211-219.

Konar, S., Manna, S. C., Zangrando, E. and Chaudhuri, N. R. (2004). Crystal structure and magnetic behavior of a copper(II)-(pyrazine 2,3-dicarboxylate) coordination polymer: 3D architecture stabilized by H-bonding. **Inorganica Chimica Acta** 357(5): 1593-1597.

Li, H., Davis, C. E., Groy, T. L., Kelley, D. G. and Yaghi, O. M. (1998). Coordinatively unsaturated metal centers in the extended porous framework of $Zn_3(BDC)_3 \cdot 6CH_3OH$ (BDC = 1,4-Benzenedicarboxylate). **Journal of the American Chemical Society** 120(9): 2186-2187.

Li, M., Xu, Z., You, X., Dong, Z. and Guo, G. (1993). Crystal structure and mass spectra of copper(I) complex with a chain arrangement: $[\mu$-4,4′-bipy-Cu(TTA)$]_n$. **Polyhedron** 12(8): 921-924.

Lo, S. M.-F., Chui, S. S.-Y., Shek, L.-Y., Lin, Z., Zhang, X. X., Wen, G.-h. and Williams, I. D. (2000). Solvothermal synthesis of a stable coordination polymer with copper-I-copper-II dimer units: $[Cu_4\{1,4\text{-}C_6H_4(COO)_2\}_3(4,4'\text{-bipy})_2]_n$. **Journal of the American Chemical Society** 122(26): 6293-6294.

Okubo, T., Kondo, M. and Kitagawa, S. (1997). Synthesis, structure, and magnetic properties of one-dimensional copper(II) coordination polymer, $\{[Cu(\text{pyrazine-2,3-dicarboxylate})(H_2O)_2]\cdot 2H_2O\}_n$. **Synthetic Metals** 85(1-3): 1661-1662.

Patrick, B. O., Stevens, C. L., Storr, A. and Thompson, R. C. (2003). Structural and magnetic properties of three copper(II) pyridine-2,3-dicarboxylate coordination polymers incorporating the same chain motif. **Polyhedron** 22(22): 3025-3035.

Plater, M. J., Foreman, M. R. St J., Howie, R. A., Skakle, J. M. S. and Slawin, A. M. Z. (2001). Hydrothermal synthesis of polymeric metal carboxylates from benzene-1,2,4,5-tetracarboxylic acid and benzene-1,2,4-tricarboxylic acid. **Inorganica Chimica Acta** 315(1): 126-132.

Rae, A. D. (2000). *RAELS. A Comprehensive Constrained Least Squares Refinement Program*, Australian National University, Canberra, Australia.

Rae, A. D. (1975a). Crystal structure refinement using a number of orthonormal axial systems. **Acta Crystallographica** A31: 560-574.

Rae, A. D. (1975b). Rigid-body motion in crystals-The application of constraints on the *TLS* model. **Acta Crystallographica** A31: 570-574.

Tang, J., Gao, E., Bu, W., Liao, D., Yana, S., Jiang, Z. and Wang, G. (2000). Synthesis and crystal structure of oxalato-bridged dicopper(II) complex with hydrogen bonds $[Cu_2(\mu\text{-}C_2O_4)(bpy)_2(H_2O)_2(NO_3)_2]$. **Journal of Molecular Structure** 525(1-3): 271-275.

Sawaki, T., Dewa, T. and Aoyama, Y. (1998). Immobilization of soluble metal complexes with a hydrogen-bonded organic network as a supporter. A simple route to microporous solid Lewis acid catalysts. **Journal of the American Chemical Society** 120(33): 8539-8540.

Soldatov, D. V. Enright, G. D., Ripmeester, J. A., Lipkowski, J., Ukraintseva, E. A. (2001). Flexibility of soft supramolecular materials: Polymorphous transition in the $[Cu(pyridine)_4(NO_3)_2]$*2(pyridine) inclusion compound. **Journal of Supramolecular Chemistry** 1(4-6): 245-251.

Tao, J., Yin, X., Huang, R. and Zheng, L. (2002). Hydrothermal synthesis of a novel microporous framework sustained by polycatenated $[Cu^{I}_2(ip)(4,4'$-

bipyridine)]$_n$ (ip = isophthalate) ladders. **Inorganic Chemistry Communications** 5(11): 1000-1002.

Venkataraman, D., Gardner, G. B., Lee, S. and Moore, J. S. (1995). Zeolite-like behavior of a coordination network. **Journal of the American Chemical Society** 117(46): 11600-11601.

Xu, L., Wang, E., Peng, J. and Huang, R. (2003). A novel coordination polymer with double chains structure: Hydrothermal syntheses, structures and magnetic properties of [Cu(phen)(H_2O)$_2SO_4$]$_n$ (phen = 1,10-phenanthroline). **Inorganic Chemistry Communications** 6(6): 740-743.

Yaghi, O. M. and Li, H. (1995). Hydrothermal Synthesis of a Metal-Organic Framework Containing Large Rectangular Channels. **Journal of the American Chemical Society** 117(41): 10401-10402.

Yaghi, O. M. and Li, H. (1996). T-Shaped molecular building units in the porous structure of Ag(4,4′-bpy)NO_3. **Journal of the American Chemical Society** 118(1): 295-296.

Yaghi, O. M., Li, H. and Groy, T. L. (1997). A Molecular railroad with large pores: synthesis and structure of Ni(4,4′-bpy)$_{2.5}$(H_2O)$_2$(ClO_4)$_2$ 1.5(4,4′-bpy) 2H_2O. **Inorganic Chemistry** 36(20): 4292-4293.

Zhang, K.-L., Xu, Y., Lin, J.-G. and You, X.-Z. (2004). {[Cu(mal)(bipy)]·2H_2O}$_n$: A new one-dimensional ladder-like copper(II) complex based on the mixed N- and O-donor ligands with intrachain ferromagnetic interactions. **Journal of Molecular Structure** 703(1-3): 63-67.

CHAPTER VIII

THE ORDER-DISORDER PHASE TRANSITION OF POLYMERIC Ag(Bipy)NO_3

8.1 Abstract

The room temperature *Fddd* form of Ag(bipy)NO_3, contains a disordered nitrate ion. A reexamination of the diffraction pattern using synthetic plots of undistorted reciprocal space showed previously unreported planes of diffuse scattering indexable as $3k\pm l = 4n$ for the 296 K cell; a = 12.8424(2), b = 9.9429(1), c = 34.4621(4) Å. It was found that the space group was *Fddd* at 160 K and above but a loss of systematic absences indicated *F*12/*d*1 (*i.e. C*2/*c*) at 150 K and below. The phase change is associated with an ordering of the nitrate ion. The 100 K structure, *C*2/*c*, a = 12.7506(14), b = 9.8596(11), c = 18.3794(21) Å, β = 109.980(7)° was determined. Refinement gave a 0.754(1):0.246 twin with no disorder and $R(F)$ = 0.021 for 2293 (out of 2486) reflections with $I > 3\sigma(I)$. If the *C*2/*c* structure is described as *F*12/*d*1 the appropriate cell has $a' = a$, $b' = b$, c' = 34.5469(21) Å, β' = 89.684(7)°. Chains are cross-linked by Ag−Ag contacts of 2.958(1) Å and Ag···O contacts of 2.749(2) and 2.747(2) Å. The chains zig-zag and this allows the Ag atoms to avoid closer contact with the NO_3^- ions. Along a chain adjacent Ag atoms, (3**b**±**c**)/4 apart, are displaced 0.221(1) Å in opposite directions perpendicular to the chain. The 200 K structure, *Fddd*, a = 12.8226(4), b = 9.9373(3), c = 34.4498(10) Å

was refined as a 1:1 disorder of all atoms after disordering the 100 K structure to create a starting model. Constrained refinement gave $R(F) = 0.028$ for 1004 (out of 1270) reflections with $I > 3\sigma(I)$. The Ag displacements were reduced to ±0.123(3) Å. The disordered nitrate ion had three significant Ag···O contact distances and a different local environment compared to the ordered structure. The diffuse scattering indicated that mistakes in NO_3^- positions cause a localized straightening of the adjacent chains that moves substantial amounts of these chains along their lengths.

8.2 Introduction

Ag(bipy)NO_3, bipy = 4,4′-bipyridine = $C_{10}H_8N_2$, is known to exist in two very different crystallographic forms. One is orthorhombic, *Pnma*, $Z = 4$ with a = 10.5315(16), b = 11.5313(17), c = 9.0821(13) Å at 293 K (Bi, Sun, Cao & Hong, 2003). Columns of polymeric $[-Ag(bipy)-]_n$ parallel to **b** are linked by NO_3^- ions to form layers of $P2_1ma$ symmetry perpendicular to **c***. The NO_3^- ions have four different Ag···O contacts, two to a silver atom on one column [2.794(6) and 2.835(6) Å] and two to a silver atom on an adjacent column [2.787(5) and 2.747(6) Å]. There are no Ag−Ag contacts. Adjacent layers are inversion related by the remaining symmetry elements of *Pnma* (see Figure 8.1).

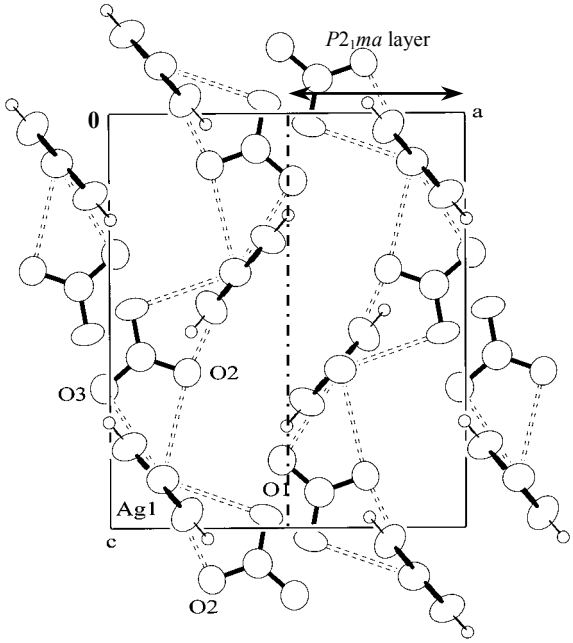

Figure 8.1. Packing diagrams for the *Pnma* of [Ag(bipy)NO_3]. Projection down **b**. Ag and NO_3^- are on the mirror planes at 1/4 and 3/4, bipy's are above and below the mirrors at y = ±1/4.

The other known form is orthorhombic, *Fddd*, *Z* = 16 with *a* = 9.9122(10), *b* = 12.9515(15), *c* = 34.482(4) Å at 290 K collected on an Enraf-Nonius CAD4 diffractometer (Robinson & Zaworotko, 1995) and *a* = 9.914(2), *b* = 34.488(7), *c* = 12.963(3) Å at 293 K collected on a four-circle Nicolet diffractometer (Yaghi & Li, 1996). The nitrate anions are disordered about a 2-fold axis.

We have found that the *Fddd* structure at 296 K exhibits diffuse scattering in planes through the strongest reflections, and have redetermined the *Fddd* structure at 200 K. The *Fddd* structure orders at low temperature (< 150 K) to form a monoclinic structure of *C*2/*c* symmetry which we have determined at 100 K. The conventional low temperature monoclinic cell has the shortest axis as the unique axis. We therefore

have chosen the *Fddd* cell to make **a** and **b** common to both the high and low temperature forms with **b** the monoclinic unique axis.

8.3 Experimental

Preparation of sample

Colorless crystals were obtained by slow evaporation at room temperature from a solution of equivalent amounts of $AgNO_3$ (3 mmol, 0.5096 g) and 4,4′-bipyridine (3 mmol, 0.4686 g) in methanol.

Data collection and reduction

Data were collected on a Bruker-Nonius KappaCCD diffractometer using the COLLECT (Nonius, 1998) software. The diffractrometer was equipped with a graphite monochromated fine focus Mo$K\alpha$ x-radiation source (λ = 0.71073 Å), a 0.5 mm *ifg* capillary collimator, and an Oxford Cryosystem 600 (Oxford Cryosystem, 1997) low temperature device. Data sets were obtained for cooling and heating sequences using a 20° hr^{-1} rate between the data sets at temperatures 200, 180, 160, 150, 140, 120, 100 K and 120, 140, 150, 160, 180 K. The *F*-centered unit cell was found for each temperature from phi/chi scan data and used to create synthetic precession photographs (undistorted plots of reciprocal space). The data reduction used the EvalCCD package (Duisenberg, Kroon-Batenburg & Schreurs, 2003). Absorption corrections were carried out using SORTAV (Blessing, 1997) to produce a merged set of reflections for *F*-centered orthorhombic symmetry.

The 100 K crystal had twin components related by a rotation around c*. The reflection intensities were obtained using the *C*-centered cell, a = 12.7506(14), b =

9.8596(11), c = 18.3794(21) Å, β = 109.980(7)º and setting the requirements for spot size and spot resolution so that no twin-overlapped reflections were resolved. The 3:1 twin ratio implied that twin-overlapped reflections related by the twin operation had the difference in their integrated intensities reduced by a factor of 1/2 compared to an untwinned crystal. The average of their intensities is unaffected by twinning.

The 200 K structure had *Fddd*, a = 12.8226(4), b = 9.9373(3), c = 34.4498(10) Å. The cell was also determined at 296 K, a = 12.8424(2), b = 9.9429(1), c = 34.4621(4) Å for comparison with the previously determined cells.

Crystal data and experimental details of the data collection and structure refinement are summarized in Table 8.1. Refinement statistics from RAELS for the 100 K and 200 K structures are listed in Tables 8.2 and 8.3, respectively. Fractional coordinates and isotropic atomic displacement parameters for the refined atoms are given in Table 8.4. Anisotropic atomic displacement parameters for the nonhydrogen atoms for 100K and 200 K are given in Tables 8.5 and 8.6, respectively. Selected interatomic bond distances and angles are compiled in Table 8.7. A comparison of the cells for the monoclinic and orthorhombic structures is in Table 8.8. Intermolecular interactions are given in Table 8.9. Derived hydrogen atom positions and isotropic atomic displacement parameters and derived anisotropic atomic displacement parameters for the hydrogen atoms are given as supplementary material in Appendix G as Tables G.1 and G.2 for 100 K and 200 K, respectively.

Pictures of undistorted reciprocal space

The indexing of all reflections in this section is with respect to an *F*-centered cell related to the room temperature cell. The diffraction patterns for 0*kl*, 1*kl*, and 2*kl* show diffuse scattering was present at room temperature, 200 K, 180 K, 160 K, and 150 K but essentially disappeared at lower temperatures. The pictures for room temperature are shown in Figure 8.2.

At 160 K and above (for both increasing and decreasing temperature) the diamond glide absence conditions of *Fddd* hold (see Figure 8.3). At 150 K and below, the diffraction patterns show that the *h*0*l* absence condition, $h+l \neq 4n$, still holds but the *hk*0, $h+k \neq 4n$ and 0*kl*, $k+l \neq 4n$ absence conditions no longer hold, suggesting a monoclinic *F*12/*d*1 structure. *F*12/*d*1 is a nonstandard setting of *C*2/*c*. Spot splitting on the *h*0*l*, *h*1*l*, and *h*2*l* layers shows that the crystals have become twinned and the twin rule involves a 2-fold rotation about **c*** or a mirror perpendicular to **c***. Spots are split as a function of *h* along the **c*** direction, equal to $-0.01493h\mathbf{c}^*$ at 100 K.

Extracting reflection intensities required the identification of a reduced cell at each temperature. This cell can be in any one of four 222 related orientations for *Fddd* and either of two .2. related orientations for *F*.2/*d*. (*C*2/*c*). Allowing this to be uncontrolled creates the situation seen in Figure 8.3 where the 150 K data set has been described using a reduced cell which is related to that used at 160 K by a 180° rotation about **c***. A full set of synthetic precession photographs is in Figure G.1 and accounts of reflection data processing using EvalCCD and SORTAV are in Appendix G1.

A 2-fold rotation about **c*** creates a twin related cell where $\mathbf{a}' = -\mathbf{a}$, $\mathbf{b}' = -\mathbf{b}$, $\mathbf{c}' = \mathbf{c}+f\mathbf{a}$ where $f = -2(c/a)\cos\beta$ since $\mathbf{a}'\cdot\mathbf{c}' = \mathbf{a}\cdot\mathbf{c}$. A general reciprocal space vector can

be described with respect to either cell. Thus, $\mathbf{H} = h\mathbf{a}^*+k\mathbf{b}^*+l\mathbf{c}^* = h'\mathbf{a}'^*+k'\mathbf{b}'^*+l'\mathbf{c}'^*$, where $h = \mathrm{a}\cdot\mathbf{H}$, $h' = \mathbf{a}'\cdot\mathbf{H}$ *etc*. so that $h' = -h$, $k' = -k$, $l' = fh+l$. To find the nearest reflection of the twin related component we simply change l' to the nearest integer of $fh+l$. The value for l' can depend on the reference cell chosen to describe **a**, **b**, **c**.

We can describe the monoclinic structure using a number of different cells. However, there is a standard setting that describes the structure in space group *C*2/*c* where $\mathbf{a} = \mathbf{a}_o$, $\mathbf{b} = \mathbf{b}_o$, $\mathbf{c} = 1/2(\mathbf{c}_o-\mathbf{a}_o)$ and the monoclinic distortion of the orthorhombic cell $\mathbf{a}_o$, $\mathbf{b}_o$, $\mathbf{c}_o$ has $\beta_o < 90°$. Note that for this choice of cell **c** is smaller than **c′** for the pseudo symmetry related cell $\mathbf{a}' = -\mathbf{a}_o$, $\mathbf{b}' = -\mathbf{b}_o$, $\mathbf{c}' = 1/2(\mathbf{c}_o+\mathbf{a}_o)$. For either monoclinic cell the twin related reflections are h, k, l and $-h$, $-k$, $h+l$ for all observed h and the spot splitting is $[(fh+l) - (h+l)]\mathbf{c}^* = (fh-h)\mathbf{c}^*$.

The diffuse scattering is predominantly in those planes perpendicular to the directions $3\mathbf{b}_o\pm\mathbf{c}_o$ described by $(3\mathbf{b}_o\pm\mathbf{c}_o)\cdot\mathbf{H} = 4n$ and includes Bragg reflections with $3k_o\pm l_o = 4n$. The diffuse scattering decreases as the angle between **H** and $3\mathbf{b}_o\pm\mathbf{c}_o$ increases. The diffuse scattering intensity increases as n increases indicating coherent displacement motions along the $3\mathbf{b}_o\pm\mathbf{c}_o$ directions. The $[-\mathrm{Ag(bipy)}-]_n$ chains propagate along these directions in the orthorhombic cell.

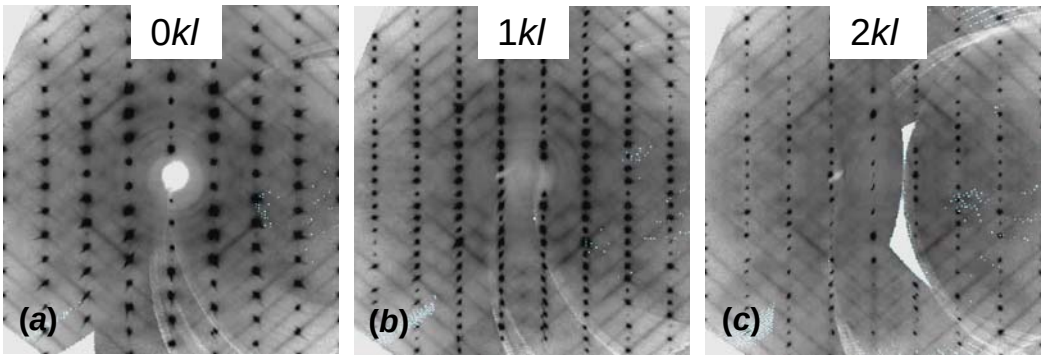

Figure 8.2. Synthetic precession photographs at 295 K. For (a) 0*kl*, (b) 1*kl*, (c) 2*kl*, showing diffuse scattering described by the planes $3k_o \pm l_o = 4n$.

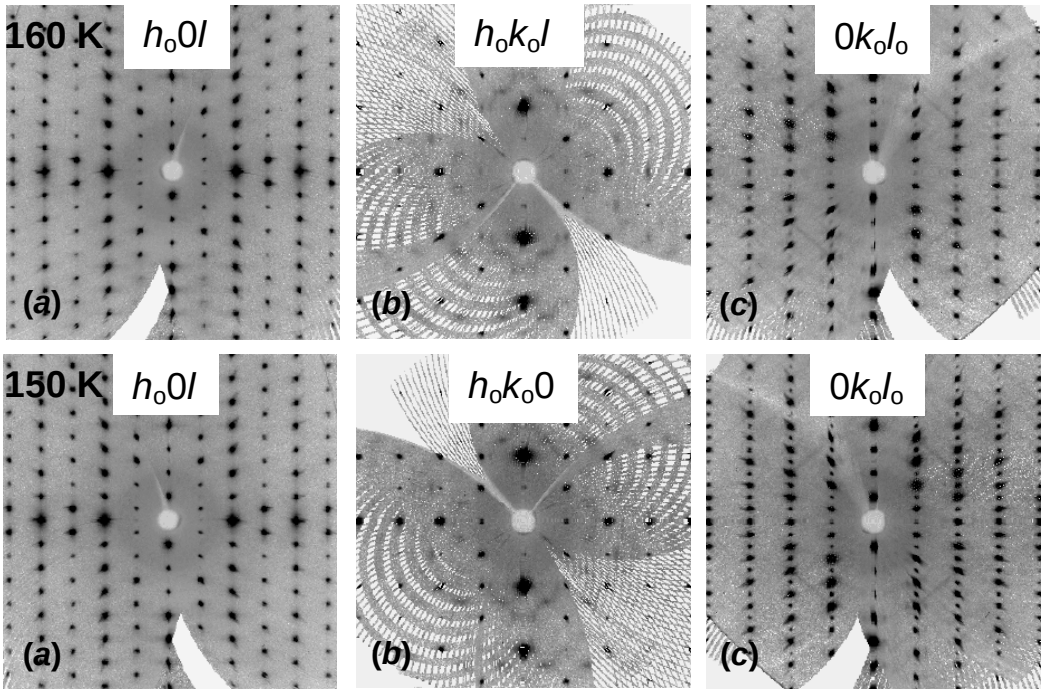

Figure 8.3. Diffraction patterns at 160 K and 150 K. The (a) h_o0l_o, $h_o+l_o \neq 4n$, (b) h_ok_o0, $h_o+k_o \neq 4n$, and (c) $0k_ol_o$, $k_o+l_o \neq 4n$ absence conditions hold at 160 K, but the last two are violated at 150 K. The reduced cell responsible for indexing at 160 K is not the same as that for indexing at 150 K, see text.

Table 8.1. Summary of crystal data, data collection, and structure refinement details for $[Ag(bipy)NO_3]_n$.

	100K	200K
Crystal data		
Chemical formula	$C_{10}H_8AgN_2.NO_3$	$C_{10}H_8AgN_2.NO_3$
Chemical formula weight	326.06	326.06
Cell setting, space group	Monoclinic, *C*2/*c*	Orthorhombic, *Fddd*
a (Å)	12.7506(14)	12.8226(4)
b (Å)	9.8596(11)	9.9373(3)
c (Å)	18.379(2)	34.4498(10)
α (º)	90	90
β (º)	109.980(7)	90
γ (º)	90	90
V (Å ^{3})	2171.5(4)	4389.7(2)
Z	8	16
D_x (Mg m^{-3})	1.995	1.974
Radiation type, wavelength (Å)	Mo*Kα*, 0.71073	Mo*Kα*, 0.71073
θ range (º)	3.1–27.5	3.1–27.5
Absorption coefficient, μ (mm^{-1})	1.86	1.84
Temperature (K)	100±1	200±1
Crystal color, form	Transparent colorless block	Transparent colorless block
Crystal size (mm)	0.34×0.32×0.30	0.34×0.32×0.30
Data collection		
Diffractometer	Nonius KappaCCD	Nonius KappaCCD
Data collection method	φ scan plus ω scans with κ offsets	φ scan plus ω scans with κ offsets

Table 8.1. (Continued).

Absorption correction	Multi-scan (based on symmetry-related measurements)	Multi-scan (based on symmetry-related measurements)
T_{min}, T_{max}	0.530, 0.570	0.530, 0.570
No. of measured, independent, and observed reflections	28278, 2486, 2350	14031, 1270, 1004
Criterion for observed reflections	$I > 3\sigma(I)$	$I > 3\sigma(I)$
R_{int}	0.039	0.048
θ_{max} (Å)	27.5	27.5
Range of *h, k, l*	$-16 \rightarrow h \rightarrow 16$ $-11 \rightarrow k \rightarrow 12$ $-23 \rightarrow l \rightarrow 23$	$-16 \rightarrow h \rightarrow 16$ $-11 \rightarrow k \rightarrow 12$ $-44 \rightarrow l \rightarrow 43$
Refinement		
Refinement on	*F*	*F*
$R[F^2 > 3\sigma(F^2)]$, $wR(F^2)$, *S*	0.021, 0.032, 1.29	0.028, 0.047, 1.32
No. of relections	2350 reflections	1004 reflections
No. of parameters	84	63
H-atom treatment	Calc idealized each cycle	Calc idealized each cycle
Weighting scheme	Based on measured s.u.'s $w = 1/(\sigma^2(F) + 0.0004F^2)$	Based on measured s.u.'s $w = 1/(\sigma^2(F) + 0.0009F^2)$
$(\Delta/\sigma)_{max}$	0.1	0.1
$\Delta\rho_{max}$, $\Delta\rho_{min}$ (e Å^{-3})	0.65, –0.43	0.50, –0.43

Computer programs: *COLLECT* (Nonius, 1998); *DIRAX* (Duisenberg, 1992); *EVAL14* (Duisenberg, Kroon-Batenburg & Schreurs, 2003); *SIR97* (Altomare *et al*., 1999); *RAELS* (Rae, 2000); *ORTEP-III* (Burnett & Johnson, 1996;.Farrugia, 1997).

8.4 Results and Discussion

Ordering and twinning the *C*2/*c* structure at 100 K

The *C*2/*c* structure is a redescription of an *F*12/*d*1 structure, the symmetry of which is a subgroup of *Fddd* symmetry. This allows a distortion of the β_o angle of the *F*-centered cell away from 90°. The standard *C*-centered cell selects the smallest value for the *c* axial length implying a transformation.

(i) $\mathbf{a} = \mathbf{a}_o$, $\mathbf{b} = \mathbf{b}_o$, $\mathbf{c} = 1/2(\mathbf{c}_o - \mathbf{a}_o)$ should $\beta_o < 90°$

or (ii) $\mathbf{a}' = -\mathbf{a}_o$, $\mathbf{b}' = -\mathbf{b}_o$, $\mathbf{c}' = 1/2(\mathbf{c}_o + \mathbf{a}_o)$ should $\beta_o > 90°$

Coordinate transformations assuming no origin shift or change of reference equivalent position are (i) $x = x_o + z_o$, $y = y_o$, $z = 2z_o$

or (ii) $x' = -x_o + z_o$, $y' = -y_o$, $z' = 2z_o$

The standard setting (origin choice 2, an inversion center at the origin) of *Fddd* has the symmetry operation x+1/4, −y, z+1/4.

For the axis transformations (i) and no change of origin, this symmetry element becomes x+1/2, −y, z+1/2 which is not a symmetry element for the standard setting of *C*2/*c*. In *C*2/*c* there is a center of inversion at 1/4, 1/4, 0 as well as at the origin. The transformation (i) $x = x_o + z_o + 1/4$, $y = y_o + 1/4$, $z = 2z_o$ locates asymmetry units of *Fddd* in the correct positions for the standard setting of *C*2/*c* which now includes the *n*-glide x+1/2, −y+1/2, z+1/2.

For the axial transformation (ii) and no change of origin the symmetry element x+1/4, −y, z+1/4 becomes x, −y, z+1/2 which is the standard *c*-glide operation. The origin can be shifted by 1/2**b** with no change in structure factor amplitudes or

symmetry elements. Thus (ii) $x' = -x_o+z_o$, $y' = -y_o+1/2$, $z' = 2z_o$ locates asymmetric units of *Fddd* in the correct position for the standard setting of *Fddd*.

The relationship between (i) and (ii) is (iii) $x' = -x+z+{}^1/_4$, $y' = -y+{}^3/_4$, $z' = z$ and corresponds to a 2-fold rotation about **c***. If we use the fractional coordinate transformation (iii) and leave the cell unchanged, we interchange the structure factor amplitudes for the two twin components of the *C*2/*c* structure.

Our first successful solution used transformation (i) and produced a twin ratio of 0.246(1):0.754 which is inconsistent with the major twin component being the first orientation matrix file produced. The transformation (iii) on this answer produced a refinement with a twin ratio 0.754(1):0.246.

As noted by Rae & Willis (2003), a pseudo symmetry operation that acts exactly on fractional coordinates and atomic displacement parameters simply swaps the twin ratio without changing agreement factors. However, if constraints and restraints are used it is possible to show that the distortion of the unit cell creates a preference for one structure over the other. We restrained differences in distances between pseudo-equivalent bond lengths to obtain a preference for the structure producing the correct twin ratio. Using the same weighting scheme for least squares refinement, namely $w = 1/(\sigma^2(F_{obs})+(0.02)^2|F_{obs}|^2)$, we obtained a goodness of fit of 1.289 compared to 1.392 and *R(F)* = 0.0207 compared to 0.0223 for the observed data, $I > 3\sigma(I)$.

The second decision that must be made in the refinement of the *C*2/*c* structure is that having chosen the unit cell and the symmetry operations one must distinguish between the two possible orientations of the NO_3^- ions. One leads to satisfactory refinement. The other could not produce a value of *R(F)* less than 0.30.

Details of the refinement models

The structures were refined using RAELS (Rae, 2000). The 200 K structure was initially refined in *Fddd* with only the NO_3^- ions disordered. This locates the Ag atom on a 2-fold axis parallel to **c** at 0.00993(3), 0.125, 0.125 with a 222 site at 1/8, 1/8, 1/8 halfway between two Ag atoms, 2.951(1) Å apart. This 2-fold axis, which ceases to be a symmetry operation of the 100 K structure, relates bipy molecules that are centrosymmetric with their inversion centers at 0, −1/4, 1/4 and 0, 1/2, 0. These inversion centers are also inversion centers for the 100 K structure. The chain so described propagates in the 3**b**−**c** direction and, for *Fddd*, the asymmetric unit contains one half of one Ag site and half of one bipy molecule. The nitrate was restrained to approximate local *mm2* symmetry with the N2−O2 bond being the direction of the local 2-fold axis of the ion. The atomic displacement parameters of the half bipy and Ag were refined using a 12 parameter *TL* model (Rae, 1975a, b) with the center of action on the inversion center in the middle of the bipy. The program RAELS allows atomic displacement parameters to be described as the sum of various contributions. An additional parameterization of the Ag atom as an isolated anisotropic atom constrained by its site symmetry was therefore included. The NO_3^- ion was refined using a *TLX* model with only two principal libration axes nonzero.

A notable feature is that the atomic displacement parameters of the Ag were essentially determined by the *TL* model and that the dominant Ag displacement was perpendicular to the direction of propagation of the chain, coming from a libration about an axis approximately in the **a** direction. This suggests a zig-zag displacement of the chain about inversion centers in the middle of the bipy molecules. This was verified by the study of the 100 K structure. Hydrogen atoms were reincluded in

geometrically determined positions after each refinement cycle and given atomic displacement parameters determined by the *TL* parameters of the bipy molecules.

The 100 K structure was then refined. Alternative solutions were discussed earlier and we shall only describe the modeling of the correct structure as comparative refinement details were also given earlier. Restraints on differences in pseudo-equivalent bond lengths involving the bipy ligand created a contrast between solutions related by the transformation $x' = -x+z+1/4$, $y' = -y+3/4$, $z' = z$ (see earlier). Restraints on torsional angles to control the planarity of the ring were also used. Isolated atoms were used for positional parameters. The Ag atom was refined as an isolated atom with anisotropic atomic displacement parameters. Each of the two half bipy molecules attached to the Ag was refined using its own independent *TL* model centered on the relevant inversion center in the middle of the bipy. The *TLX* model for the nitrate ion was the same parameterization as before. Initial refinement cycles constrained the two *TL* models for to be related by the pseudo 2-fold axis passing approximately through the Ag in the **c*** direction

The transformation $\mathbf{a} = \mathbf{a}_o$, $\mathbf{b} = \mathbf{b}_o$, $\mathbf{c} = 1/2(\mathbf{c}_o-\mathbf{a}_o)$ implies that reflections indexed as h_o, k_o, l_o for the reciprocal lattice cell $\mathbf{a}_o$, $\mathbf{b}_o$, $\mathbf{c}_o$ of the *F*-centered lattice become reindexed as $h, k, l = h_o, k_o, 1/2(l_o-h_o)$ for the *C*-centered cell **a**, **b**, **c**. Thus the diamond glide absence condition $h_o = 0$, $k_o+l_o = 4n+2$ becomes $h = 0$, $k+2l = 4n+2$ and the diamond glide absence condition $l_o = 0$, $h_o+k_o = 4n+2$ becomes $h+2l = 0$, $h+k = 4n+2$. The observed intensities of these reflections would be reduced should disorder of the NO_3^- occur. Reflections with $I > 3\sigma(I)$ having these characteristics were given indices 2 and 3 respectively so that they could be monitored separately from the remaining reflections with $I > 3\sigma(I)$. It was found that all reflections were on scale and

refined well implying that twinning, but not disorder, occurred in the crystal studied at 100 K. Final agreement factors for the 100 K structure are given in Table 8.2. The indices for the second twin component were obtained from the first twin component as $-h$, $-k$, $h+l$ and the twin ratio refined to 0.754(1):0.246.

The refinement of the 200 K structure was then reconsidered using a disordering of the total structure rather than just the NO_3 group. The refinement was initiated using fractional coordinates of the 100 K structure. The appropriate coordinate transformation, see earlier, is $x_o = -x+1/2z$, $y_o = -y+1/2$, $z_o = 1/2z$. The modeling was not the same as for the 100 K structure. The two bipy half molecules were constrained to be planar and equal using refinable local orthonormal coordinates relative to refinable local orthonormal axes centered on the crystal inversion centers coincident with the center of the relevant bipy molecule (Rae, 1975a). The *TL* parameterization of the two half occupancy bipy ligands was constrained to be symmetry related. Final agreement factors for the 200 K structure are given in Table 8.3.

Table 8.2. Agreement factors for the 100 K structure.

	Reflections	*R(F)*	$R(F^2)$	*wR*	*Gof*
$I>3\sigma(I)$ and Index 1[a]	2293	0.021	0.031	0.030	1.30
$I>3\sigma(I)$ and Index 2[a]	43	0.019	0.033	0.028	1.26
$I>3\sigma(I)$ and Index 3[a]	14	0.016	0.020	0.024	1.04
All $I>3\sigma(I)$	2350	0.021	0.032	0.030	1.29
$I<3\sigma(I)$	136	0.383	0.691	0.366	1.37
All data	2486	0.024	0.032	0.032	1.32

a. Index 1, $I>3\sigma(I)$ and not of index 2 and 3; Index 2, $I>3\sigma(I)$ and $h = 0$, $k+2l = 4n+2$; Index 3, $I>3\sigma(I)$ and $k+2l = 0$, $h+k = 4n+2$

Number of independent variables = 84

Final refinement cycle: maximum shift/error = 0.1

Final difference map electron density: maximum +0.650 eÅ^{-3}, minimum −0.429 eÅ^{-3}

Table 8.3. Agreement factors for the 200 K structure.

		Reflections	*R(F)*	$R(F^2)$	*wR*	*Gof*
$I>3\sigma(I)$	Model 1[a, b]	1004	0.028	0.053	0.047	1.37
	Model 2 [a, b]	1004	0.028	0.053	0.047	1.32
$I<3\sigma(I)$	Model 1	266	0.391	0.528	0.467	1.81
	Model 2	266	0.363	0.522	0.449	1.76
All data	Model 1	1270	0.048	0.057	0.069	1.73
	Model 2	1270	0.044	0.055	0.066	1.66

a. The first line is for model 1 in which only the NO_3^- were disordered over two sites.

The second line is for model 2 in which all atoms were disordered over two sites.

b, Number of independent variables = 62 (model 1) and 63 (model 2)

Final refinement cycle: maximum shift/error = 0.1 (model 1 and 2)

Final difference map electron density: maximum +0.787 e Å^{-3}, minimum −1.232 e Å^{-3}, (model 1) and maximum +0.502 e Å^{-3}, minimum −0.429 e Å^{-3} (model 2).

Table 8.4. Fractional atomic coordinates and equivalent isotropic displacement parameters ($Å^2$) for the nonhydrogen atoms in $[Ag(bipy)NO_3]_n$ at 100 K and 200 K.

	x	*y*	*z*	U_{eq}
100 K (*C*2/*c*)				
Ag	0.12065(2)	0.35147(2)	0.26167(1)	0.0202(1)
N1	0.1587(2)	0.4975(2)	0.3539(1)	0.018(1)
C2	0.1977(2)	0.4640(2)	0.4289(1)	0.018(1)
C3	0.2329(2)	0.5589(2)	0.4883(1)	0.017(1)
C4	0.2288(2)	0.6968(2)	0.4695(1)	0.015(1)
C5	0.1873(2)	0.7318(2)	0.3910(1)	0.018(1)
C6	0.1528(2)	0.6300(2)	0.3355(2)	0.019(1)
N1′	0.0639(2)	0.2157(2)	0.1645(1)	0.018(1)
C2′	0.0284(2)	0.2660(2)	0.0928(1)	0.017(1)
C3′	0.0006(2)	0.1862(2)	0.0264(1)	0.017(1)
C4′	0.0113(2)	0.0452(2)	0.0347(1)	0.015(1)
C5′	0.0479(2)	−0.0083(2)	0.1096(1)	0.019(1)
C6′	0.0728(2)	0.0795(2)	0.1726(2)	0.021(1)
N2	0.3192(2)	0.1018(2)	0.3518(2)	0.021(1)
O1	0.2754(2)	−0.0081(2)	0.3237(1)	0.027(1)
O2	0.4199(2)	0.1222(3)	0.3597(2)	0.039(1)
O3	0.2652(2)	0.1888(3)	0.3724(2)	0.043(2)
200 K (*Fddd*)				
Ag	0.0103(1)	0.1344(2)	0.1273(1)	0.040(1)
N1	0.0199(6)	−0.0067(4)	0.1747(1)	0.029(1)
C2	0.0188(7)	0.0301(4)	0.2121(1)	0.031(1)
C3	0.0112(6)	−0.0605(3)	0.2425(1)	0.031(1)
C4	0.0042(1)	−0.1992(2)	0.2341(1)	0.026(1)
C5	0.0054(5)	−0.2362(4)	0.1953(1)	0.032(1)
C6	0.0133(6)	−0.1381(4)	0.1666(1)	0.034(1)
N1′	0.0211(6)	0.2762(4)	0.0802(1)	0.030(1)
C2′	0.0165(7)	0.2300(4)	0.0437(1)	0.030(1)
C3′	0.0082(6)	0.3126(3)	0.0115(1)	0.030(1)

Table 8.4. (Continued).

	x	*y*	*z*	U_{eq}
C4′	0.0044(1)	0.4533(2)	0.0169(1)	0.026(1)
C5′	0.0093(5)	0.5002(4)	0.0548(1)	0.033(1)
C6′	0.0175(6)	0.4096(4)	0.0854(1)	0.036(1)
N2	−0.1375(5)	0.3890(6)	0.1748(1)	0.034(3)
O1	−0.1001(5)	0.4942(6)	0.1637(2)	0.053(2)
O2	−0.2322(5)	0.3778(6)	0.1793(2)	0.060(4)
O3	−0.0813(8)	0.2905(9)	0.1820(2)	0.102(5)

[a]Estimated standard deviations of the least significant digits are given in parentheses.

[b]Equivalent isotropic atomic displacement parameters for the atoms refined anisotropically, $U_{eq} = 1/3 \sum_i \sum_j U_{ij}\, a_i^* a_j^*\, \mathbf{a}_i \cdot \mathbf{a}_j$

Table 8.5. Anisotropic atomic displacement parameters[a] in $[Ag(bipy)NO_3]_n$ at 100 K.

Atom	U_{11}	U_{22}	U_{33}	U_{12}	U_{13}	U_{23}
Ag	0.0177(1)	0.0235(1)	0.0185(1)	−0.0029(1)	0.0048(1)	−0.0138(1)
N1	0.016(1)	0.020(1)	0.018(1)	−0.002(1)	0.007(1)	−0.004(1)
C2	0.019(1)	0.017(1)	0.019(1)	−0.003(1)	0.008(1)	−0.002(1)
C3	0.020(1)	0.016(1)	0.016(1)	−0.002(1)	0.008(1)	0.000(1)
C4	0.016(1)	0.0164(4)	0.014(1)	−0.002(1)	0.007(1)	0.000(1)
C5	0.022(1)	0.0182(3)	0.014(1)	−0.001(1)	0.006(1)	0.000(1)
C6	0.022(1)	0.0208(5)	0.015(1)	−0.001(1)	0.006(1)	−0.002(1)
N1′	0.014(1)	0.020(1)	0.019(1)	−0.001(1)	0.004(0)	0.011(1)
C2′	0.013(1)	0.017(1)	0.021(1)	−0.001(1)	0.004(1)	−0.010(1)
C3′	0.014(1)	0.016(1)	0.019(1)	−0.000(1)	0.004(1)	−0.009(1)
C4	0.012(1)	0.016(1)	0.017(1)	−0.001(1)	0.004(1)	−0.008(1)
C5′	0.020(1)	0.017(1)	0.017(1)	0.000(1)	0.004(1)	−0.008(1)
C6′	0.023(1)	0.020(1)	0.017(1)	−0.001(1)	0.005(1)	−0.009(1)
N2	0.027(2)	0.015(1)	0.021(1)	0.004(1)	0.008(1)	0.002(1)
O1	0.039(3)	0.022(1)	0.022(1)	−0.006(1)	0.011(1)	0.000(1)
O2	0.033(2)	0.053(2)	0.033(1)	−0.014(1)	0.013(1)	−0.009(1)
O3	0.055(2)	0.037(2)	0.033(2)	0.024(1)	0.013(1)	−0.004(1)

[a]Estimated standard deviations of the least significant digits are given in parentheses.

Table 8.6. Anisotropic atomic displacement parameters[a] in $[Ag(bipy)NO_3]_n$ at 200 K.

Atom	U_{11}	U_{22}	U_{33}	U_{12}	U_{13}	U_{23}
Ag	0.043(1)	0.042(1)	0.036(1)	0.007(1)	0.006(1)	0.024(1)
N1	0.035(1)	0.030(1)	0.022(1)	−0.002(1)	−0.002(1)	0.008(1)
C2	0.041(1)	0.030(1)	0.022(1)	−0.004(1)	−0.005(1	0.008(1)
C3	0.041(1)	0.030(1)	0.021(1)	−0.004(1)	−0.005(1)	0.007(1)
C4	0.028(1)	0.030(1)	0.021(1)	−0.003(1)	−0.004(1)	0.007(1)
C5	0.045(1)	0.030(1)	0.021(1)	−0.002(1)	−0.003(1)	0.007(1)
C6	0.050(1)	0.030(1)	0.021(1)	0.000(1)	−0.002(1)	0.008(1)
N1′	0.030(1)	0.025(1)	0.034(1)	0.001(1)	0.003(1)	0.009(1)
C2′	0.030(1)	0.025(1)	0.034(1)	0.004(1)	0.005(1)	0.009(1)
C3′	0.031(1)	0.024(1)	0.034(1)	0.004(1)	0.006(1)	0.008(1)
C4′	0.021(1)	0.024(1)	0.034(1)	0.003(1)	0.005(1)	0.008(1)
C5′	0.040(1)	0.024(1)	0.034(1)	0.002(1)	00.004(1)	0.009(1)
C6′	0.048(2)	0.025(1)	0.034(1)	0.000(1)	0.002(1)	0.009(1)
N2	0.050(6)	0.030(3)	0.023(2)	0.012(2)	−0.002(2)	0.002(2)
O1	0.073(6)	0.048(3)	0.038(3)	−0.013(2)	0.002(2)	0.002(2)
O2	0.052(5)	0.071(3)	0.059(4)	−0.006(2)	−0.005(3)	0.015(2)
O3	0.117(8)	0.088(4)	0.103(6)	0.073(5)	0.035(5)	0.048(5)

[a]Estimated standard deviations of the least significant digits are given in parentheses.

Table 8.7. Selected interatomic bond lengths[a] (Å) and bond angles[a] (º) for $[Ag(bipy)(NO_3)]_n$.

100 K			
Ag−Ag	2.958(0) . 2_555	N1′−C6′	1.351(3)
Ag−N1	2.150(1)	C2′−C3′	1.391(3)
Ag−N1'	2.150(1)	C3′−C4′	1.400(3)
Ag−O1	2.749(2) . 6_555	C4′−C4′	1.501(4) . 3_555
Ag−O3	2.747(2)	C4′−C5′	1.397(3)
N1−C2	1.337(3)	C5′−C6′	1.393(3)
N1−C6	1.345(3)	N2−O1	1.246(3)
C2−C3	1.391(3)	N2−O2	1.258(4)
C3−C4	1.400(3)	N2−O3	1.238(3)
C4−C4	1.496(4) . 7_566	C2−O3	3.130(3)
C4−C5	1.399(3)	C6−O2	3.151(3) . 5_455
C5−C6	1.391(3)	C6′−O1	3.199(3)
N1′−C2′	1.334(3)		
Ag−Ag−N1	93.3(1) 2_555 . .	N1−C6−C5	122.7(2) . . .
Ag−Ag−N1′	80.9(1) 2_555 . .	Ag−N1′−C2′	119.6(1) . . .
Ag−Ag−O1	126.7(0) 2_555 . 6_555	Ag−N1′−C6′	122.4(1) . . .
Ag−Ag−O3	120.6(1) 2_555 . .	C2′−N1′−C6′	117.8(2) . . .
N1−Ag−N1′	173.4(1) . . .	N1′−C2′−C3′	123.6(2) . . .
N1−Ag−O1	95.2(1) . . 6_555	C2′−C3′−C4′	118.7(2) . . .
N1−Ag−O3	83.9(1) . . .	C3'−C4′−C4′	121.0(2) . . 3_555
N1′−Ag−O1	86.0(1) . . 6_555	C3′−C4′−C5′	118.0(2) . . .
N1′−Ag−O3	101.7(1) . . .	C4′−C4′−C5′	121.0(2) 3_555 . .
O1−Ag−O3	112.6(1) 6_555 . .	C4′−C5′−C6′	119.2(2) . . .
Ag−N1−C2	123.5(2) . . .	N1′−C6′−C5′	122.7(2) . . .
Ag−N1−C6	118.3(2) . . .	O1−N2−O2	118.8(2) . . .
C2−N1−C6	117.9(2) . . .	O1−N2−O3	120.8(3) . . .
N1−C2−C3	123.4(2) . . .	O2−N2−O3	120.4(3) . . .
C2−C3−C4	118.9(2) . . .	Ag−O1−N2	116.1(2) 6_545 . .
C3−C4−C4	121.5(2) . . 7_566	C6′−O1−N2	103.9(2) . . .

Table 8.7. (Continued).

C3−C4−C5	117.7(2) . . .	C6′−O1−O2	117.2(1) . . .
C4−C4−C5	120.8(2) 7_566 . .	Ag−O3−N2	118.8(2) . . .
C4−C−C6	119.4(2) . . .		
Symmetry positions: 1. x,y,z; 2. −x,y,1/2−z; 3. −x,−y,−z; 4. x,−y,1/2+z; 5. 1/2+x,1/2+y,z; 6. 1/2−x,1/2+y,1/2−z; 7. 1/2−x,1/2−y,−z; 8. 1/2+x,1/2−y,1/2+z			
200 K			
Ag−Ag	2.946(1) . 3_555	N2−O1	1.212(8) . .
Ag−N1	2.154(3) . .	N2−O2	1.229(9) . .
Ag−N1'	2.155(3) . .	N2−O3	1.240(9) . .
Ag−O1	2.855(6) . 27_445	Ag−Ag	0.246(5) . 2_555
Ag−O3	2.708(7) . .	Ag−Ag	2.948(1) . 4_555
Ag−O1	2.691(6) . 28_455	Ag−N1	2.168(4) . 2_555
Ag−O2	2.987(6) . 28_455	Ag−N1'	2.170(4) . 2_555
Ag−O3	2.928(7) . 2_555	C2−O3	3.070(8) . .
N1−C2	1.340(4) . .	C6′−O1	3.202(8) . .
N1−C6	1.338(5) . .	C2′−O3	3.082(8) . 2_555
C2−C3	1.384(4) . .	C5′−O1	3.098(7) . 2_565
C3−C4	1.410(4) . .	N2−N2	0.425(11) . 28_455
C4−C4	1.492(6) . 13_545	O1−O2	1.696(8) . 28_455
C4−C5	1.388(4) . .	O1−O3	1.135(11) . 28_455
C5−C6	1.392(5) .	O2−O3	1.153(10) . 28_455
N1′−C2′	1.340(4) . .	N1−N1′	0.257(6) . 2_555
N1′−C6′	1.338(5) . .	C2−C2′	0.224(5) . 2_555
C2′−C3′	1.384(4) . .	C3−C3′	0.144(5) . 2_555
C3′−C4′	1.410(4) . .	C4−C4′	0.054(1) . 2_555
C4′−C4′	1.492(6) . 5_565	C5−C5′	0.148(6) . 2_555
C4′−C5′	1.388(4) . .	C6−C6′	0.231(6) . 2_555
C5′−C6′	1.392(5) . .		

Table 8.7. (Continued).

Ag−Ag−N1	89.1(2) 3_555 . .	C2′−N1′−C6′	117.7(3) . . .
Ag−Ag−N1′	84.0(2) 3_555 . .	N1′−C2′−C3′	123.5(3) . . .
Ag−Ag−O1	133.7(1) 3_555 . 27_445	C2′−C3′−C4′	119.1(3) . . .
Ag−Ag−O3	118.1(3) 3_555 . .	C3′−C4′−C4′	121.1(2) . . 5_565
N1−Ag−N1′	173.0(1) . . .	C3′−C4′−C5′	117.1(3) . . .
N1−Ag−O1	95.6(2) . . 27_445	C4'−C4'−C5'	121.8(2) 5_565 . .
N1−Ag−O3	82.6(2) . . .	C4′−C5′− C6″	119.9(3) . . .
N1−Ag−O3	99.5(2) . . 2_555	N1′−C6′−C5′	122.8(3) . . .
N1′−Ag−O1	89.6(2) . . 27_445	O1−N2−O2	120.5(6) . . .
N1′−Ag−O3	100.2(2) . . .	O1−N2−O3	120.9(8) . . .
O1−Ag−O3	108.2(3) 27_445 . .	O2−N2−O3	118.6(7) . . .
Ag−N1−C2	123.4(2) . . .	Ag−O1−N2	107.1(5) 27_455 . .
Ag−N1−C6	118.3(3) . . .	Ag−O3−N2	124.5(4) . . .
C2−N1−C6	117.7(3) . . .	N1−Ag−O1	89.0(2) . . 28_455
N1−C2−C3	123.5(3) . . .	N1−Ag−O2	93.9(2) . . 28_455
C2−C3−C4	119.1(3) . . .	N1′−Ag−O1	96.1(2) . . 28_455
C3−C4−C4	121.1(2) . . 13_545	N1′−Ag−O2	86.7(2) . . 28_455
C3−C4−C5	117.1(3) . . .	N1′−Ag−O3	83.6(2) . . 2_555
C4−C4−C5	121.8(2) 13_545 . .	O1−Ag−O1	84.3(2) 27_445 . 28_455
C4−C5−C6	119.9(3) . . .	O1−Ag−O2	126.6(2) 27_445 . 28_455
N1−C6−C5	122.8(3) . . .	O1−Ag−O3	22.6(2) 27_445 . 2_555
Ag−N1′−C2'	118.7(3) . . .	O1−Ag−O3	24.3(2) 28_455 . .
Ag−N1′−C6'	123.0(3) . . .	O3−Ag−O3	130.7(5) . . 2_555

Symmetry positions: 1. x,y,z; 2. x,1/4−y,1/4−z; 3. 1/4−x,y, 1/4−z; 4. 1/4−x,1/4−y,z; 5. −x,−y,−z; 6. −x,1/4+y,1/4+z; 7 .1/4+x,−y,1/4+z; 8. 1/4+x,1/4+y,−z; 9. x,1/2+y,1/2+z; 10. x,3/4−y,3/4−z; 11. 1/4−x,1/2+y,3/4−z; 12. 1/4−x,3/4−y,1/2+z; 13. −x,1/2−y,1/2−z; 14. −x,3/4+y,3/4+z; 15. 1/4+x,1/2−y,3/4+z; 16. 1/4+x,3/4+y,1/2−z; 17. 1/2+x,y,1/2+z; 18. 1/2+x,1/4−y,3/4−z; 19. 3/4−x,y,3/4−-z; 20. 3/4−x,1/4−y,1/2+z; 21. 1/2−x, −y,1/2−z; 22 1/2-x,1/4+y,3/4+z; 23. 3/4+x,-y,3/4+z; 24. 3/4+x,1/4+y,1/2−z; 25. 1/2+x,1/2+y,z; 26. 1/2+x,3/4−y,1/4−z; 27.3/4−x,1/2+y,1/4−z; 28. 3/4−x,3/4−y,z; 29. 1/2−x,1/2−y, −z; 30. 1/2−x,3/4+y,1/4+z; 31. 3/4+x,1/2−y,1/4+z; 32. 3/4+x,3/4+y, −z

Discussion and comparison of the structures

To compare the monoclinic and orthorhombic structures it is useful to use axes associated with the pseudo orthorhombic cell for the monoclinic cell, *i.e.* $\mathbf{a}_o = \mathbf{a}$, $\mathbf{b}_o = \mathbf{b}$, $\mathbf{c}_o = 2\mathbf{c}+\mathbf{a}$ cell parameters are given in Table 8.8. The chains run perpendicular to $\mathbf{a}_o^*$. The chain through the origin propagates in the $3\mathbf{b}_o+\mathbf{c}_o = \mathbf{a}+3\mathbf{b}+2\mathbf{c}$ direction (see Figure. 8.4). The adjacent chain connected through the NO_3^- ion is related by the 2-fold axis 1/2–x, 1/2+y, 1/2–z and thus propagates in the $-\mathbf{a}+3\mathbf{b}-2\mathbf{c} = 3\mathbf{b}_o-\mathbf{c}_o$ direction. However, the angle between these two directions is further away from 90° in the 100 K structure (98.860°) compared to the 200 K structure (98.256°). The chain repeat $1/2|3\mathbf{b}_o\pm\mathbf{c}_o|$ is shorter at 100 K than at 200 K even though the value of $\mathbf{c}_o$ is longer. This is associated with the idea that the chain is straighter at 200 K than at 100 K.

Table 8.8. Cell parameter comparison for monoclinic and orthorhombic structures. Using the pseudo orthorhombic cell $\mathbf{a}_o = \mathbf{a}$, $\mathbf{b}_o = \mathbf{b}$, $\mathbf{c}_o = 2\mathbf{c}+\mathbf{a}$ for the monoclinic cell.

Temperature	100 K	200 K
a_o (Å)	12.7506(14)	12.8226(4)
b_o (Å)	9.8596(11)	9.9373(3)
c_o (Å)	34.5469(21)	34.4498(10)
β_o (°)	89.684(7)	90
Volume (Å^3)	4343.0(8)	4389.7(2)
$1/2\|3\mathbf{b}_o\pm\mathbf{c}_o\|$	22.7398(1)	22.7790(7)

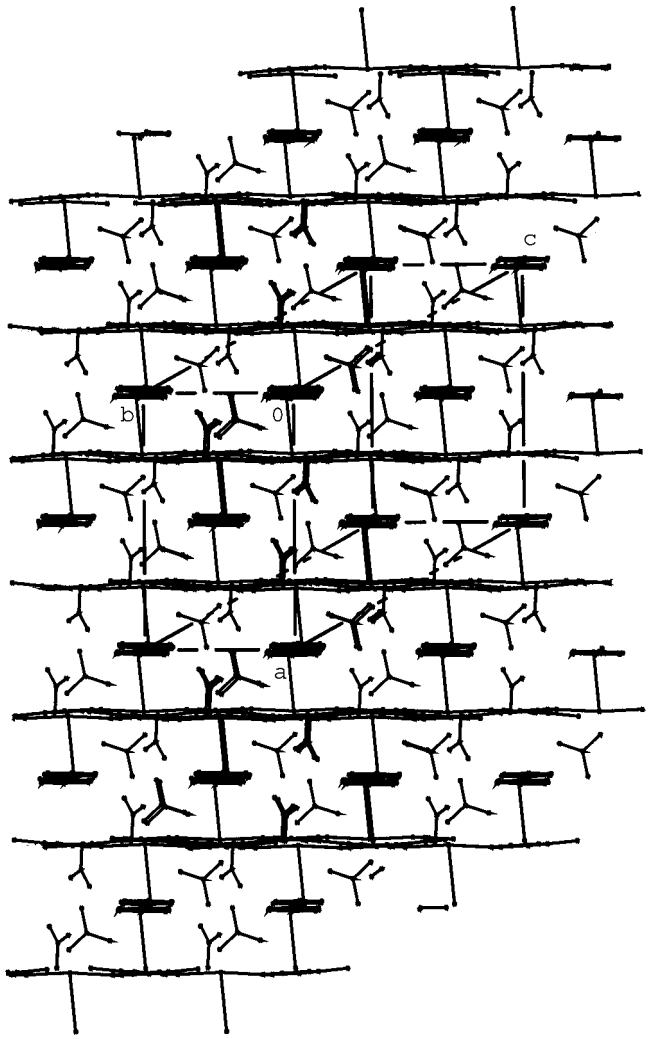

Figure 8.4. Projection of the structure down the chain through the origin that propagates in the $3\mathbf{b}_o+\mathbf{c}_o = \mathbf{a}+3\mathbf{b}+2\mathbf{c}$ direction.

The silver atom in the ordered *C2/c* structure at 100 K is coordinated to two different NO_3^- ions with Ag···O1 ($^1/_2-x$, $^1/_2+y$, $^1/_2-z$) = 2.749(2) Å and Ag···O3 = 2.747(2) Å, essentially equal distances. The NO_3^- ion has N2−O2 = 1.258(4) Å, longer than N2−O1 = 1.246(3) Å and N2−O3 = 1.238(3) Å. The projection down **b** (see Figure 8.5) shows that adjacent Ag atoms (both along a chain and between chains) are shifted in opposite directions along $\mathbf{c}_o$ and are associated with an ordering

of the NO_3^- ions and an induced distortion of the unit cell. These displacements are ±[1/2(0.01167)(34.547)] = ±0.202(1) Å. A refinement using the transformed coordinates that reverse the twin ratio (see earlier) made the Ag···O1 distance longer [2.764(2) Å] and Ag···O3 shorter [2.740(3) Å]. This suggests the cell distortion is associated with having these distances equal. There is also a displacement of the Ag parallel to **b** of 0.093(2) Å away from the 2-fold axis parallel to **a** of *Fddd* making the net displacement 0.222(1) Å essentially perpendicular to the chain direction.

Figure 8.6 shows a projection down **a** of the cell contents of the 100 K structure with all the CH groups omitted for ease of viewing. The plane of each bipy is approximately perpendicular to **a**, see Figure 8.5. Lines in the directions $3\mathbf{b}_o \pm \mathbf{a}_o$ joining centers of inversion on the middle of bipy molecules are drawn. This shows the ±0.202 Å displacements of the Ag atoms along $\mathbf{c}_o$ and that they cause a zig-zag displacement of the polymer chains. The NO_3^- ions connect chains that run in the two different directions. The Ag−NO_3−Ag−NO_3 connections are propagated by the screw axes 1/2−x, 1/2+y, 1/2−z. A column of NO_3^- ions can be described as those NO_3^- ions nearest this screw axis. A reorientation of one NO_3^- ion in this column could well induce reorientation of an adjacent NO_3^- ion in this column with associated movements of Ag atoms. However this does not create the dominant feature of the diffuse scattering.

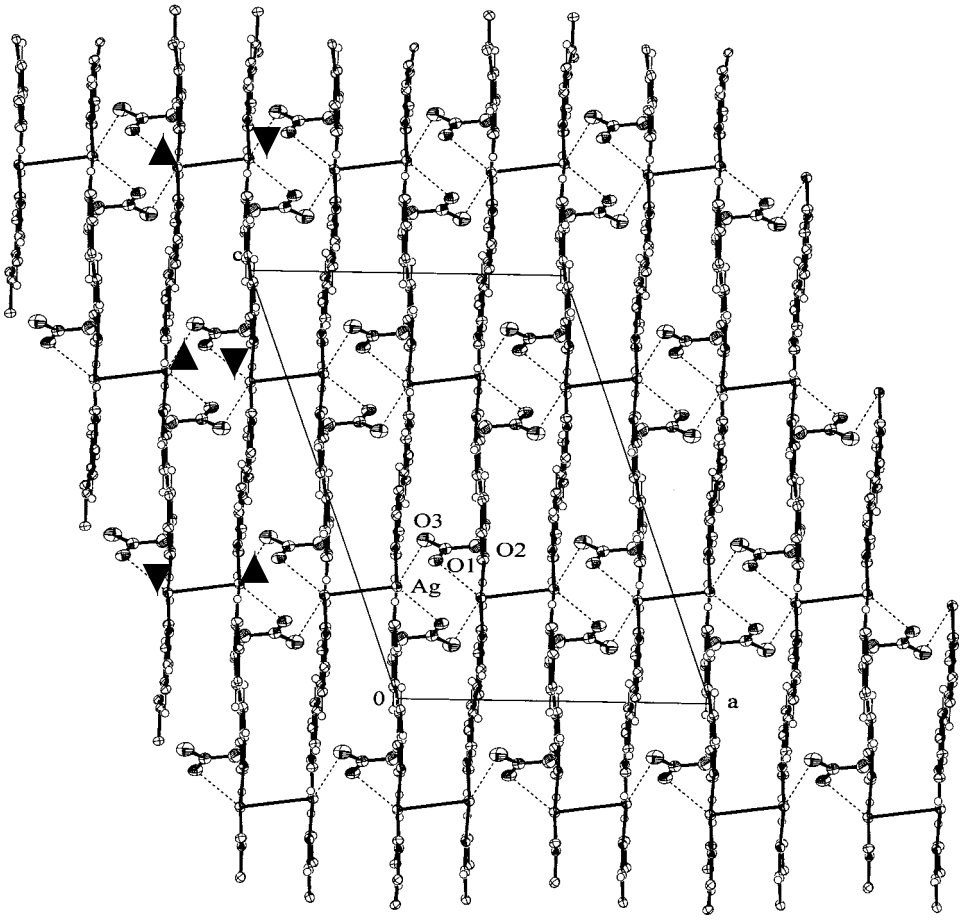

Figure 8.5. A projection down **b** showing an ordering of the NO_3^- ions has moved adjacent Ag atoms in opposite directions parallel to $\mathbf{c}_o$ and causes a distortion of the unit cell.

The fully disordered model of the 200 K structure has the Ag displacement reduced to ±0.079(2) Å parallel to $\mathbf{c}_o$ and 0.123(3) Å overall. For these reduced displacements amplitudes of the structure we get Ag···O3 = 2.708(7) Å and Ag···O1 (−1/4−x, −1/2+y, 1/4−z) = 2.855(6) Å. However, now there are also three Ag···O distances associated with the alternative NO_3^- orientation, namely Ag···O1 (−1/4−x, 3/4−y, z) = 2.691(6) Å, Ag···O2 (−1/4−x, 3/4−y, z) = 2.987(6) Å, and Ag···O3 (x, 1/4−y, 1/4−z) = 2.928(7) Å.

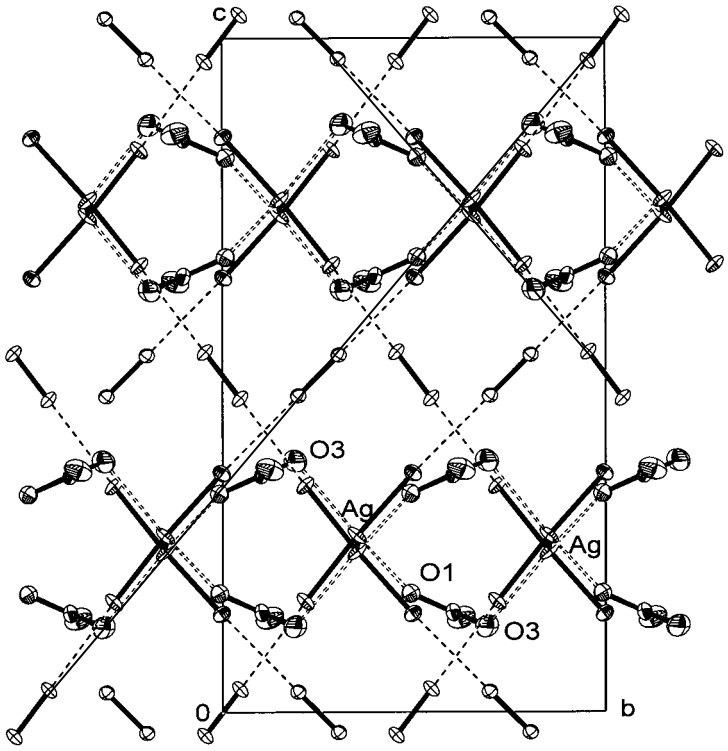

Figure 8.6. A projection down **a** of the cell contents of the 100 K structure. For easier viewing atoms C2, C3, C5, C6 and C2′, C3′, C5′, C6′ and the associated hydrogen atoms are omitted. The solid lines are between inversion centers in the directions $3\mathbf{b}_o \pm \mathbf{c}_o$. The **...** lines denote Ag···O bonds. The --- lines show the zig-zag of the polymer chains.

The NO_3^- ion can rotate by approximately 60° rather than 180° to take up the alternative position defined by the rotation −1/4−x, 3/4−y, z. The major libration of the NO_3^- ion has a principal value of 0.031(1) radians^2 at 100 K but 0.084(5) radians^2 at 200 K. This libration axis is approximately perpendicular to the plane of the NO_3^- ion. The corresponding root mean square angle displacements are ±10.1(2)° and

±16.6(5)° respectively. When the approximately 60° rotation occurs to make the NO_3^- go to its second position, O3 going to the alternative O1 position, with little Ag···O change of distance, O2 going to the alternative O3 position with a decrease in Ag···O distance, and O1 going to the alternative O2 position with an increase in Ag···O of distance. This change in position must induce a change in the Ag positions in the chains and this change decreases the distance to the alternative O3 position and increases the distance to the alternative O2 position. The structure at 200 K has the Ag described by a bimodal distribution of positions but the displacement amplitude is reduced because the NO_3^- ions are in various orientations, not necessarily correlated on either side of a Ag atom site.

The infinite zig-zag chains of the coordination polymer, $[Ag(bipy)]_n$, are formed from T-shaped Ag(I) metal atom motifs, each coordinated to N atoms of the *trans*-bipyridine ligands, namely Ag−N and Ag−N′, and cross-linked to the adjacent chains through Ag−Ag bonds. This forms 3 interpenetrating networks (Yaghi & Li, 1996) with origins separated by the cell repeat **b**. At 100 K the nitrate ions interconnect these networks using a 2_1 screw parallel to **b** to relate nitrate ions attached to the same Ag and to create $Ag{-}NO_3{-}Ag{-}NO_3$ columns parallel to **b**. It seems reasonable to assume that cooperative movement of nitrate ions along the 2_1 screw axes is the ordering mechanism accompanied by local displacement of Ag atoms and displacement of adjacent polymer chains along their length.

Weaker interactions in the 100 K structure

At 100 K the O2 is not involved in coordination to a Ag atom. Instead it is linked by three weak noncovalent interactions to the C atoms of the bipyridine on the polymer chains. Two of these interactions are weak C−H···O hydrogen bonds, the

other a noncovalent C(δ^+)···O(δ^-) dipole-dipole interaction (see Table 8.9). There are also weak interactions involving O1 and O3.

Table. 8.9. Geometries of C−H···O hydrogen bonds (Å, º) and noncovalent dipole-dipole interactions.

C−H···O to bipy edges				
D−H···*A*	*D*−H	H···*A*	*D*···*A*	*D*−H···*A*
C3−HC3···O1^{i}	1.00	2.64	3.529(3)	148.1
C5−HC5···O1^{ii}	1.00	2.37	3.212(3)	141.0
C6′−HC6′···O1	1.00	2.41	3.198(3)	135.6
C6−HC6···O2^{iii}	1.00	2.45	3.386(3)	154.9
C3′−HC3′···O2^{iv}	1.00	2.46	3.444(3)	168.1
C2−HC2···O3	1.00	2.47	3.129(3)	123.2
Dipole-dipole interactions to bipy (α-C)				
D−H···*A*			*D*···*A*	
C6(δ^+)···O2(δ^-)^{v}			3.150(3)	
C2′(δ^+)···O1(δ^-)^{iii}			3.309(3)	

i −x+1/2, −y+1/2, 1−z ii x, y+1, z iii −x+1/2, y+1/2,−z+1/2
iv x−1/2, −y+1/2, z−1/2 v x−1/2, y+1/2, z

Interpretation of the diffuse scattering

For stationary atoms the structure factor is $F(\mathbf{H}) = \sum_n f_n^o(\mathbf{H})\exp(2\pi i\mathbf{r}_n\cdot\mathbf{H})$ where $\mathbf{r}_n$ is the position of the nth atom at the time of the diffraction event and $f_n^o(\mathbf{H})$ is the atom scattering factor for the nth stationary atom. Thus, the intensity is $|F(\mathbf{H})|^2 = \sum_{m,n} f_n^o(\mathbf{H})f_m^o(\mathbf{H})^*\exp(2\pi i(\mathbf{r}_n-\mathbf{r}_m)\cdot\mathbf{H})$. However, for a real structure $F(\mathbf{H}) = \sum_{n,n1,n2,n3} f_n^o(\mathbf{H})\exp(2\pi i(\mathbf{r}_n+n_1\mathbf{a}+n_2\mathbf{b}+n_3\mathbf{c}+\Delta\mathbf{r}_{nn1n2n3})\cdot\mathbf{H})$ in a crystal, where $\mathbf{r}_n$ is the average position of an atom modulo the unit cell **a**, **b**, **c** and $\Delta\mathbf{r}_{nn1n2n3}$ is the displacement from the expected position for the nth atom in the cell at the crystal

lattice position $n_1\mathbf{a}+n_2\mathbf{b}+n_3\mathbf{c}$ and n_1 = 1 to N_1, n_2 = 1 to N_2, n_3 = 1 to N_3 defining $N_1N_2N_3$ unit cells. When averaged over all **H** with a particular magnitude the expectation value of $|F(\mathbf{H})|^2$ is $\sum_n |f_n^o(\mathbf{H})|^2$. If displacements are correlated in planes, the intensity lost in the Bragg reflections is relocated in reciprocal lattice lines perpendicular to these planes. If displacements are correlated in columns the intensity lost in the Bragg reflections is relocated in planes perpendicular to these columns. If displacements are uncorrelated, the lost intensity of the Bragg reflections is relocated everywhere.

The case we need to consider is when all atoms in a substructure (a polymer chain) have a common displacement $\Delta\mathbf{r}_{n1n2}\mathbf{c}$ (along the polymer chain) but these displacements are uncorrelated between substructures (parallel polymer chains). We have chosen **c** as the polymer chain direction and $\Delta\mathbf{r}_{nn1n2n3} = \Delta\mathbf{r}_{n1n2}$ for all n, n_3 where the quantity $\Delta\mathbf{r}_{n1n2}$ is dependent on the numbers n_1 and n_2 that define a particular chain.

We shall now look at the value of $F(\mathbf{H})$ per unit cell volume. We can say that $F(\mathbf{H}) = F_1(\mathbf{H})\, F_2(\mathbf{H})\, F_3(\mathbf{H})$ where $F_1(\mathbf{H}) = \sum_n f_n^o(\mathbf{H})\exp(2\pi i\mathbf{r}_n\cdot\mathbf{H})$,

$F_2(\mathbf{H}) = \sum_{n3} \exp(2\pi i\, n_3\mathbf{c}\cdot\mathbf{H})/N_3$, and $F_3(\mathbf{H}) = \sum_{n1,n2} \exp(2\pi i(n_1\mathbf{a}+n_2\mathbf{b}+\Delta\mathbf{r}_{n1n2}\mathbf{c}\cdot\mathbf{H})/N_1N_2$

$F_1(\mathbf{H})$ is the structure factor for stationary atoms in their average positions in a unit cell. Since only the atoms in one unit cell are included, $F_1(\mathbf{H})$ is a continuous function of **H**. F_2 (**H**) is equal to 1 whenever $\mathbf{c}\cdot\mathbf{H}$ equals an integer *i.e.* $\mathbf{H} = h\mathbf{a}^*+k\mathbf{b}^*+l\mathbf{c}^*$ where only l has to be an integer since $\mathbf{c}\cdot\mathbf{a}^* = \mathbf{c}\cdot\mathbf{b}^* = 0$ and $\mathbf{c}\cdot\mathbf{c}^* = 1$. The bigger N_3 is, the sharper the planes of intensity in reciprocal space defined by $\mathbf{c}\cdot\mathbf{H} = l$.

For $F_3(\mathbf{H})$ we consider two cases. The first is the Bragg reflection case where h, k, l are integers. Then $F_3(\mathbf{H}) = \langle \exp(2\pi i\Delta\mathbf{r}_{n1n2}l)\rangle = \langle \exp(2\pi^2 Ul^2)\rangle$ where $\langle\ \rangle$

means an average value and U is the mean square value of $\Delta\mathbf{r}_{n1n2}$ averaged over all chains. The intensity lost at the Bragg reflections in a plane $\mathbf{c}\cdot\mathbf{H} = l$ is redistributed between reflections in this plane. The diffuse intensity in each plane increases as l increases and is 0 if $l = 0$. It also decreases as $|h\mathbf{a}^*+k\mathbf{b}^*|$ increases.

In our crystal the chains are in directions $3\mathbf{b}_o\pm\mathbf{c}_o$ and the chain repeat is the centering operator $1/2(3\mathbf{b}_o\pm\mathbf{c}_o)$, implying planes of diffuse scattering should be defined by $1/2(3\mathbf{b}_o\pm\mathbf{c}_o)\cdot\mathbf{H} = n$, an integer. However, (see earlier) the diffuse scattering is only dominant for the layers $(3\mathbf{b}_o\pm\mathbf{c}_o)\cdot\mathbf{H} = 4n$, *i.e.* every second layer. This is easily explained by looking at the factor $F_1(\mathbf{H})$, the structure factor of a single chain repeat. This repeat along $3\mathbf{b}_o\pm\mathbf{c}_o$ has Ag atoms related by an inversion in the middle of a bipy and are separated by $1/4(3\mathbf{b}_o\pm\mathbf{c}_o)$ along the length of the chain. Their position can therefore be described as being at $\pm(3/8\mathbf{b}_o+1/8\mathbf{c}_o+\delta\mathbf{r})$. The dominant term in $F_1(\mathbf{H})$ is thus $f_{Ag}^o \cos(2\pi(3/8h+1/8l+\mathbf{H}\cdot\delta\mathbf{r}))$ which has large magnitude when $3k+l = 4n$ but is small when $3k+l = 4n+2$. The effect of the $\mathbf{H}\cdot\delta\mathbf{r}$ term is small since $\delta\mathbf{r}$ has a magnitude in the order of 0.2 Å and can be ignored at the level of first order approximation corresponding to our simplified description of the diffuse scatting.

It should be noted that the Ag atom displacements perpendicular to the polymer chain can be described in two parts. Each Ag has a choice between two sites at $\mathbf{r}_n+n_1\mathbf{a}+n_2\mathbf{b}+n_3\mathbf{c}\pm\delta\mathbf{r}_n$ or $\mathbf{r}_n\pm\delta\mathbf{r}_n$ relative to the origin of the cell at $n_1\mathbf{a}+n_2\mathbf{b}+n_3\mathbf{c}$. The zig-zag nature of the polymer chain implies the dominant diffuse planes see a 0.50:0.50 population of the two sites in each cell. Further detail of local order in the 200 K structure is thus not easily obtained from the limited form of the diffuse scattering despite the fact that the Ag atomic displacement parameters were largest for

displacements perpendicular to the polymer chain. The diffuse scattering supports a correlated displacement of appreciable lengths of polymer chain along its length.

8.5 References

Altomare, A., Burla, M. C., Camalli, M., Cascarano, G. L., Giacovazzo, C. Guagliardi, A. Moliterni, A. G. G., Polidori, G. and Spagna, R. (1999). *SIR*97: A new tool for crystal structure determination and refinement. **Journal of Applied Crystallography** 32: 115-119.

Bi, H., Sun, D., Cao, R. and Hong, M. (2003). Chain structure of $\{[Ag(bipy)]NO_3\}_n$. **Acta Crystallographica** E58, m324-m325.

Blessing, R. H. (1995). An empirical correction for absorption anisotropy. **Acta Crystallographica** A51: 33-38.

Burnett, M. N. and Johnson, C. K. (1996). *ORTEP-III***.** Report ORNL-6895, Oak Ridge National Laboratory, Tennessee, USA.

Duisenberg, A. J. M. (1992). Indexing in single-crystal diffractometry with an obstinate list of reflections. **Journal of Applied Crystallography** 25: 92-96.

Duisenberg, A. J. M., Kroon-Batenburg, L. M. J. and Schreurs, A. M. M. (2003). An intensity evaluation method: *EVAL-14*. **Journal of Applied Crystallography** 36: 220-229.

Farrugia, L. J. (1997). *ORTEP-3* for Windows - a version of *ORTEP-III* with a graphical user interface (GUI). **Journal of Applied Crystallography** 30: 565.

Nonius BV. (1998). *COLLECT*: *KappaCCD Software,* Nonius BV., Delft, The Netherlands.

Oxford Cryosystems (1997). *600 Series Cryostream Cooler Operation and Instruction Guide,* Oxford Cryosystems, Oxford, UK.

Rae, A. D. (1975a). Crystal structure refinement using a number of orthonormal axial systems. **Acta Crystallographica** A31: 560-570.

Rae, A. D. (1975b). Rigid-body motion in crystals-the application of constraints on the *TLS* model. **Acta Crystallographica** A31: 570-574.

Rae, A. D. (2000). *RAELS. A Comprehensive Constrainted Least Squares Refinement Program.* The Australian National University, Australia.

Rae, A. D. & Willis, A. C. (2003). 9,10-Phenanthrenequinone, not your average structure. **Zeitschrift für Kristallographie** 218: 221-230.

Robinson, F. and Zaworotko, M. J. (1995). Triple interpenetration in [Ag(4,4′-bipyridine)][NO_3], a cationic polymer with a three-dimensional motif generated by self-assembly of "T-shaped" building blocks. **Chemical Communications** 2413-2414.

Yaghi, O. M. and Li, H. (1996). T-shaped molecular building units in the porous structure of Ag(4,4′-bpy)·NO_3. **Acta Crystallographica** 118(1): 295-296.

CHAPTER IX

CONCLUSIONS

9.1 Conclusions

In a sense, the dominant theme of this thesis has been the study of the effect of intermolecular forces on crystal structure. Cocrystallization can lead to important interactions which cause some crystals to best be described as a coexistence of substructures where the dominant building principals define individual substructures. The organization of the substructures to create a real crystal is not always ideal and alternative packings of substructures allows the creation of disorder, stacking faults, twinning, and polytype possibilities. These phenomena can create problems for crystal structure determination and refinement. It has been shown that a careful consideration of how a crystal packs allows good geometrical information to be obtained from a problem structure, and as a result considerable information is obtained about the interfaces between substructures. This has real implications for crystal structure prediction and understanding phase changes and polytypes.

It is the strengths of intermolecular interactions that create the building principals here identified with substructures, and that define the potential interactions between the substructures. Principals are often defined quite simply by covalently bound or coordinately bound groups of atoms, while the interactions between the substructures are defined by the noncovalent interactions. The most important

noncovalent interactions, along with an indication of their approximate energy ranges (Steed & Atwood, 2000), are listed following:

- Ion-Ion interaction (100-300 kJ mol^{-1})
- Ion-Dipole interaction (50-200 kJ mol^{-1})
- Hydrogen bonding (4-120 kJ mol^{-1})
- Dipole-Dipole interaction (5-50 kJ mol^{-1})
- Cation-π interaction (5-80 kJ mol^{-1})
- π-π stacking interaction (0-50 kJ mol^{-1})
- van der Waals interaction (<5 kJ mol^{-1})

Strong hydrogen bonds may be sufficient to determine solid state structure. Weak hydrogen bonds play a role in structure stabilization and can be significant when large numbers act in concert. For example, individual weak electrostatic interactions between aromatic rings (denoted π-π stacking in the list above, but also denoted as C−H···π elsewhere) may be as little as 1 or 2 kJ mol^{-1}, but in highly concerted systems such as the multiple phenyl embraces (Dance & Scudder, 1995) they can become several tens of kJ mol^{-1} and become the dominant determiners of the supramolecular structure.

Underlying the dominant theme of this thesis is the subtheme that when the interaction of substructures leads to phenomena (*vide supra*) that cause difficulty in refinement of the structure using conventional programs, success can be obtained from the method of analysis of substructure packing and interactions in conjunction with the use of structure factor algebra pioneered by Rae (2005) and implemented in the RAELS refinement program. The structure factor algebra combines sums and differences of structure factors and squared structure factors for substructure

components, which are used together with constraints and restraints, and with appropriate selection of reflections on index conditions, as detailed in the preceding chapters, to initiate and control the refinement process. A summary of the types of interacting substructures studied in this thesis are given in the following paragraphs.

Substructures that are essentially the same; in Chapter IV pseudo symmetry of $[Mg(H_2O)_6](NO_3)_2{\cdot}2HMT{\cdot}4H_2O$. Within the asymmetric unit of $[Mg(H_2O)_6](NO_3)_2{\cdot}2HMT{\cdot}4H_2O$, two HMT molecules, the $[Mg(H_2O)_6]^{2+}$ cation and the two water molecules are approximately pseudo inversion center. This imposes a pseudo $C\bar{1}$ symmetry for a layer at z = 1/2 and a pseudo $C2/c$ space group symmetry for the substructure containing these entities in all equivalent positions of $P2_1/n$. The rest of the asymmetric unit of $P2_1/n$ contains two nitrate anions and two water molecules, which lie at an interface between the pseudo $C\bar{1}$ layers described above. This interface approximates $Pb2_1a$ pseudo symmetry should the distortion of β from 90° be ignored. The substructure containing these atoms in all equivalent positions has pseudo *Pbna* symmetry. The true space group $P2_1/n$ is also a subgroup of *Pbna*. Thus, the $P2_1/n$ structure is the result of the interaction of two substructures, one of $C2/c$ symmetry and the other of *Pbna* symmetry. Separate mechanisms for twinning and stacking faults exist. The possibility of polytypism was recognized.

Interleaving substructures of two types; coordination polymers in Chapter VII of $[Cu(bipy)]_2SO_4{\cdot}TPA$ and in Chapter VIII of $Ag(bipy)NO_3$. The polymeric chains of $[-Cu^{I}-bipy-Cu^{I}-bipy-]$ are propagated by an *n*-glide, and are cross linked (Cu−O−S−O−Cu) by the sulfate groups which lie on 2-fold axes. The terephthalic acids lie on centers of inversion and are hydrogen bonded to sulfates. In the polymeric $Ag(bipy)NO_3$, the infinite zig-zag chains of the coordination polymer, $[Ag(bipy)]_n$,

are formed from T-shaped Ag(I) metal atom motifs, each coordinated to N atoms of the *trans*-bipyridine ligands, namely Ag−N and Ag−N′, and cross-linked to the adjacent chains through Ag−Ag bonds. This forms 3 interpenetrating networks with origins separated by the cell repeat **b**. At 100 K the nitrate ions interconnect these networks using a 2_1 screw parallel to **b** to relate nitrate ions attached to the same Ag and to create Ag−NO_3−Ag−NO_3 columns parallel to **b**. It seems reasonable to assume that cooperative movement of nitrate ions along the 2_1 screw axes is the ordering mechanism accompanied by local displacement of Ag atoms and displacement of adjacent polymer chains along their length. The silver atom in the ordered *C2/c* structure at 100 K is coordinated to two different NO_3^- ions with Ag···O1 Å and Ag···O3, essentially equal distances. The NO_3^- ions connect chains that run in the two different directions. The Ag−NO_3−Ag−NO_3 connections are propagated by the screw axes. A column of NO_3^- ions can be described as those NO_3^- ions nearest this screw axis. A reorientation of one NO_3^- ion in this column could well induce reorientation of an adjacent NO_3^- ion in this column with associated movements of Ag atoms.

Interaction between substructures: in Chapter VI $[Mg(H_2O)_6](NO_3)_2{\cdot}2HMT{\cdot}4H_2O$ shows strong hydrogen bonds between $[Mg(H_2O)_6]^{2+}$, HMT, NO_3^-, and H_2O; the isomorphic complexes of $[M(H_2O)_6]I_2{\cdot}2HMT{\cdot}4H_2O$], where M = Ni and Mn in Chapter V have strong and weak hydrogen bonds between $[M(H_2O)_6]^{2+}$, HMT, I^-, and H_2O; in Chapter VI, $PS(C_2H_5)_3$ has weak interactions between the ethyl groups in the unit cell; in Chapter VII, $\{[Cu(bipy)]_2SO_4{\cdot}TPA\}_n$ has coordination bonds within the $[Cu(bipy)]_n$ polymer chains and between Ag^+ and SO_4^{2-}, and strong hydrogen bond interactions between the $[Cu(bipy)]_n$ polymer chains and TPA; and in Chapter VIII $[Ag(bipy)NO_3]_n$ has

coordination bonds within $[Ag(bipy)]^+$ and between [Ag(bipy)] and NO_3^- and weak hydrogen bonds between $[Ag(bipy)]^+$ and NO_3^-.

Polytypic behavior, twinning, and stacking faults are possible in several structures. In Chapter III $[SnCl_2(C_2H_4COOH)(C_2H_4COO)]^-\cdot[C_{12}H_9N_2]^+$. The possibility of alternative stacking of layers perpendicular to **c*** offers an explanation for observed twinning and polytypism. In Chapter IV $[Mg(H_2O_6)](NO_3)_2\cdot 2HMT\cdot 4H_2O$, separate mechanisms for twinning and stacking faults exist. The possibility of polytypism was recognized. In Chapter V $[M(H_2O)_6]I_2\cdot 2HMT\cdot 4H_2O]$, where *M* = Ni and Mn twinning including partial and perfect overlap the of diffraction intensities exists. The possibility that the parent $P6_3mc$ structure of $PS(C_2H_5)_3$ in Chapter VI can also be described as a *C*-centered orthorhombic cell of $Ccm2_1$ symmetry with four molecules per cell was noted. This mode lowers the orthorhombic symmetry to $Pnm2_1$ with three fold twinning or disordering restores the hexagonal diffraction symmetry. Further modulations of the parent structure seems necessary, with partial ordering in a mode $Pna2_1$ symmetry a reasonable option. This suggests a probable six fold twinning since local symmetry of an average structure would then be lowered to *Pn*. The parent structure of $\{[Cu(bipy)]_2SO_4\cdot TPA\}_n$ in Chapter VII is involved in commensurate displacive modulation of an idealized Z = 2 parent structure. A (3+1) dimensional approach, modulation vector $(\mathbf{a}_p^*+\mathbf{b}_p^*)/2$, suggests the possibility of a twinned triclinic crystal but observations of weak reflections with *h* even, *k* even, $h+k = 4n+2$, preclude this option. In Chapter VIII a new low temperature phase (>150 K) of $[Ag(bipy)NO_3]_n$ with an ordered structure (monoclinic, $C2/c$) is reported. The phase transition to the ordered structure results in twinning.

9.2 References

Dance, I. and Scudder, M. (1995). The sextuple phenyl embrace, a ubiquitous concerted supramolecular motif. **Chemical Communication** (10): 1039-1040.

Rae, A. D. (2005). The Pseudo Symmetry of Interfaces and Their Role in Defining Twin Disorder Parameters for the Refinement of Problem Crystal Structures. Proceedings of the 9th Annual National Symposium on Computational Science and Engineering, 23-25 March 2005, Bangkok, Thailand, pp 4-8.

Steed, J. W. and Atwood, J. L. (2000). **Supramolecular Chemistry.** Wiley, Chichester, England.

APPENDICES

APPENDIX A

SUPPLEMENTARY MATERIALS FOR EXPERIMENTAL DETAILS

A.1 Materials and Methods

Chemicals

The starting materials, approximately 98% pure, were purchased from Fluka, Carlo Erba reagenti, Acros, and were used without further purification. Solvents were use without purification. All crystallization was performed by preparation at room temperature with controlled.

Methods: Single crystal growth

Single crystals suitable for X-ray diffraction were prepared at room temperature (295 K) by chemical method. The formation of cocrystals can be from proton donors and acceptors require molecules matched geometrically and stoichiometrically.

(i) Donor-acceptor facile acid-base reactions

(ii) good solubility of the molecules in solvents

(iii) precipitation of the complexes from the solutions

There are two easy techniques for crystal growth may attempts to formed single-crystal for X-ray diffraction. For compounds which are not sensitive to ambient conditions in the laboratory, solvent evaporation is an excellent method and anti-solvent diffusion is suitable for the case it is desirable to grow the crystals as slowly as possible, and quality is far more important than quantity.

(A) Solvent Evaporation:

This is the most common methodology for crystal growth, and involves simply evaporating solvent from the solution of the compound until saturation is reached and crystals form. Evaporation is the one of the easiest methods for crystallizing small molecule compounds. The choice of solvent is very important because it can greatly influence the mechanism of crystal growth and because the solvent may be incorporated into the crystalline lattice. An extension on this technique involves the use of two solvents, one in which the material to be crystallized is soluble and a second in which it is insoluble.

Place a small amount of the sample in a vial, dissolve in a minimum amount of soluble solvent (methanol, ethanol, water, dichloromethane, chloroform, *etc*) cover the opening with lab–film. Standing for slow evaporation by leave the sample in a place that is free from vibrations and not in direct sunlight or next to a source of heat. For growth crystals at low temperature can be keep in refrigerator. Do not keep picking it up. As the solvent slowly evaporates, crystals should form. Washed, Filter and Dried crystal at room temperature.

(B) Anti-solvent Diffusion:

The diffusion methods are often tried when evaporation methods do not immediately succeed. This is probably the most successful method to grow a crystal. Two vials are needed where one can fit inside the other. In the inner vial the compound to be crystallized is dissolved in a small quantity of a moderately non-volatile solvent, such as methanol, ethanol, water, dichloromethane, chloroform, acetonitrile, and even methylene chloride. In the outer vial, a volatile solvent in which the compound is insoluble such as pentane, diethyl ether or hexane.

Place a small amount of the sample in a small vial (inner vial) and dissolve in a minimum amount of solvent, then placing this inner vial inside a larger vial (outer

vial) that contains a small portion of a solvent in which the sample is insoluble. The vertical surfaces of the inner vial should not touch the outer vial to keep the outer solution from rising by capillary action and filling the inner vial. The outer vial is then sealed. During crystallization, vapor from the solvent of the outer vial slowly diffuses into the solution in the inner vial causing the material to precipitate. Leave the sample in a place that is free from vibrations and not in direct sunlight or next to a source of heat. For growth crystals at low temperature can be keep in refrigerator. Standing until the crystals should form. Do not keep picking it up. The volatile anti-solvent will slowly evaporate and diffuse into the solution, lowering the solubility of the sample. If no crystals form, even when all the anti-solvent has diffused into the solvent, try another pair of solvents.

A.2 X-Ray Crystallography

The suitable single crystals were obtained by optical microscope. Crystals were mounted onto a thin glass capillary with glued to the end. The data collection performed by using the Nonius-KappaCCD area detector. The diffractometer operator equipped with graphite monochromated Mo$K\alpha$ radiation (λ = 0.71073 Å) and X-ray type operated at tube power levels of 40 kV and 20 mA. The low temperature was controlled by using an Oxford Cryosystem 600 apparatus. The data collection was controlled by COLLECT program.

APPENDIX B

SUPPLEMENTARY MATERIALS FOR

$[SnCl_2(CH_2COOH)(CH_2COO)]^-\cdot[C_{12}H_9N_2]^+$

Table B.1. Derived fractional coordinates[a] and isotropic atomic displacement parameters[b] (Å^2) for the hydrogen atoms in $[SnCl_2(CH_2COOH)(CH_2COO)]^-\cdot[C_{12}H_9N_2]^+$.

	x	*y*	*z*	U_{eq}
H12O	0.8682(45)	0.2760(28)	0.6354(27)	0.050(7)
H12A	0.8295(3)	0.3281(2)	0.9173(2)	0.038
H12B	0.9708(3)	0.2472(2)	0.8680(2)	0.038
H13A	0.7215(3)	0.1726(2)	0.9687(2)	0.037
H13B	0.7441(3)	0.0733(2)	0.8467(2)	0.037
H15A	0.0665(3)	-0.0798(2)	0.5165(2)	0.032
H15B	0.2833(3)	-0.0025(2)	0.5281(2)	0.032
H16A	0.0445(3)	0.0392(2)	0.7046(2)	0.032
H16B	0.1710(3)	0.1369(2)	0.6679(2)	0.032
H31	0.8537(4)	0.8481(2)	0.8094(3)	0.050
H32	0.9283(4)	0.7386(3)	0.9067(2)	0.052
H33	0.9123(4)	0.5351(2)	0.7996(2)	0.043
H37	0.7280(4)	0.8456(2)	0.6160(3)	0.048
H38	0.6365(4)	0.7447(2)	0.4174(3)	0.046
H41N	0.7339(42)	0.3611(27)	0.4356(26)	0.050(7)
H42	0.6577(4)	0.2529(2)	0.2476(2)	0.040
H43	0.5849(4)	0.3487(3)	0.1349(2)	0.047
H44	0.5938(4)	0.5519(3)	0.2264(2)	0.046

[a]Estimated standard deviations of the least significant digits are given in parentheses.

[b]Equivalent isotropic atomic displacement parameters for the atoms refined anisotropically, $U_{eq} = 1/3 \sum_i \sum_j U_{ij}\, a_i^* a_j^*\, \mathbf{a}_i \cdot \mathbf{a}_j$

```
##############################################################################
###    CIF submission form for molecular structure report (Acta Cryst. B)  ###
###                                        Version: 2.0.2  (6 July 1998)  ###
##############################################################################
data_kh02d
# SUBMISSION DETAILS
_publ_contact_author_name            'Dr. Kenneth J. Haller'
_publ_contact_author_address
; School of Chemistry
  Institute of Science
  Suranaree University of Technology
  Nahkon Ratchasima 30000
  Thailand
;
_publ_contact_author_email           'haller@ccs.sut.ac.th'
_publ_contact_author_fax             '66(44)224-185'
_publ_contact_author_phone           '66(44)224-303'

_publ_contact_letter
; ?
;
_publ_requested_journal              'Acta Crystallographica Section B'
_publ_requested_category             ?

_publ_section_title
;
Structural Study of Sn(IV) Phenanthroline Complex
;
_publ_section_title_footnote
; ?
;

loop_
 _publ_author_name
 _publ_author_footnote
 _publ_author_address
'Somphon, Weenawan'
; # footnote
;
; School of Chemistry
  Institute of Science
  Suranaree University of Technology
  Nahkon Ratchasima 30000
  Thailand
;
'Haller, Kenneth J.'
; # footnote
;
; School of Chemistry
  Institute of Science
  Suranaree University of Technology
  Nahkon Ratchasima 30000
  Thailand
;
'Ng, Seik Weng'
; # footnote
;
; Institute of Postgraduate Studies
  University of Malaya
  Kuala Lampur 50603
  Malaysia
;
'Rae, A. David'
; # footnote
;
; Research School of Chemistry
  The Australian National University
  Canberra ACT 0200
  Australia
;
#==============================================================================
_chemical_name_systematic
;
 ?
;
_chemical_name_common                ?
_chemical_formula_moiety             'C12 H9 N2 1+, C6 H9 Cl2 O4 Sn1 1-'
_chemical_formula_structural
; (Sn Cl2 ((C H2)2 C O2) ((C H2)2 C O2 H)) (C12 H9 N2)'
;
_chemical_formula_analytical         ?
_chemical_formula_sum                'C18 H18 Cl2 N2 O4 Sn1'
_chemical_formula_weight             515.94
_chemical_melting_point              ?
_chemical_compound_source            ?

loop_
 _atom_type_symbol
 _atom_type_description
 _atom_type_scat_dispersion_real
 _atom_type_scat_dispersion_imag
 _atom_type_scat_source
 'C'  'C'   0.0033   0.0016
 'International Tables Vol C Tables 4.2.6.8 and 6.1.1.4'
 'H'  'H'   0.0000   0.0000
```

```
 'International Tables Vol C Tables 4.2.6.8 and 6.1.1.4'
 'Sn'  'Sn'  -0.6537   1.4246
 'International Tables Vol C Tables 4.2.6.8 and 6.1.1.4'
 'Cl'  'Cl'   0.1484   0.1585
 'International Tables Vol C Tables 4.2.6.8 and 6.1.1.4'
 'O'  'O'   0.0106   0.0060
 'International Tables Vol C Tables 4.2.6.8 and 6.1.1.4'
 'N'  'N'   0.0061   0.0033
 'International Tables Vol C Tables 4.2.6.8 and 6.1.1.4'

_space_group_crystal_system      'triclinic'
_space_group_IT_number           2
_space_group_name_H-M_alt        'P -1'
_space_group_name_Hall           '-P 1'

loop_
 _space_gropu_symop_id
 _space_group_symop_operation_xyz
  1 'x, y, z'
  2 '-x, -y, -z'

_cell_length_a                  7.1204(1)
_cell_length_b                 12.5017(2)
_cell_length_c                 12.5780(2)
_cell_angle_alpha              114.4242(11)
_cell_angle_beta                92.5620(11)
_cell_angle_gamma              104.3542(12)
_cell_volume                   973.78(3)
_cell_formula_units_Z          2
_cell_measurement_temperature    200(1)
_cell_measurement_reflns_used    25992
_cell_measurement_theta_min      2.910
_cell_measurement_theta_max      29.575

_exptl_crystal_description       'needle'
_exptl_crystal_colour_primary    'transparent colorless'
_exptl_crystal_size_min           0.12
_exptl_crystal_size_mid           0.14
_exptl_crystal_size_max           0.17
_exptl_crystal_density_meas       ?
_exptl_crystal_density_diffrn     1.760
_exptl_crystal_density_method     'not measured'
_exptl_crystal_F_000              512
_exptl_absorpt_coefficient_mu     1.613
_exptl_absorpt_correction_type    'multi-scan'
_exptl_absorpt_correction_T_min   0.798
_exptl_absorpt_correction_T_max   0.824
_exptl_absorpt_process_details    'SORTAV, (Blessing, 1995)'

_exptl_special_details
;
The data crsytal was cut from a larger needle shaped crystal by
cleaving along an obvious twin plane (reentrant angles), followed
by cutting approximately perpendicular to the twin plane. The
crystal was hard to cut, and fragmented giving a somewhat irregular
shaped data crystal.
;

_diffrn_ambient_temperature          200(1)
_diffrn_radiation_wavelength         0.71073
_diffrn_radiation_type               'Mo K\a'
_diffrn_radiation_collimation        'ifg 0.3 mm capillary collimator'
_diffrn_source                       'fine-focus sealed X-ray tube'
_diffrn_source_target                Mo
_diffrn_source_current               25
_diffrn_source_voltage               40
_diffrn_radiation_monochromator      'horizonatlly mounted graphite crystal'
_diffrn_detector                     '95 mm CCD camera'
_diffrn_detector_area_resol_mean     9
_diffrn_measurement_specimen_support 'hollow glass fiber'
_diffrn_measurement_device           '\k four-circle goniostat'
_diffrn_measurement_device_type      'Nonius KappaCCD'
_diffrn_measurement_method           '\f scan plus \w scans with \k offsets'

_diffrn_reflns_number               28062
_diffrn_reflns_av_R_equivalents     0.035
_diffrn_reflns_av_unetI/netI        0.055
_diffrn_reflns_limit_h_min           -9
_diffrn_reflns_limit_h_max            9
_diffrn_reflns_limit_k_min          -16
_diffrn_reflns_limit_k_max           16
_diffrn_reflns_limit_l_min          -16
_diffrn_reflns_limit_l_max           16
_diffrn_reflns_theta_min             3.00
_diffrn_reflns_theta_max             28.69
_diffrn_reflns_theta_full            28.69
_diffrn_reflns_resolution_max        0.74
_diffrn_measured_fraction_theta_max  0.999
_diffrn_measured_fraction_theta_full 0.999

# diffrn_reflns above is data collection; reflns below is reported

# _reflns_number of reflns in the full sphere data set = 9278
_reflns_Friedel_coverage      1.0
_reflns_limit_h_min            -9
_reflns_limit_h_max             9
```

```
_reflns_limit_k_min           -16
_reflns_limit_k_max            16
_reflns_limit_l_min           -16
_reflns_limit_l_max            16
_reflns_d_resolution_high     0.74
_reflns_av_R_equivalents      0.0244
_reflns_av_unetI/netI         0.0582

_reflns_number_total          5019
_reflns_number_gt             4174
_reflns_threshold_expression  'I>2\s(I)'

_computing_data_collection      'Collect (Nonius BV, 1997-2000)'
_computing_cell_refinement      'Denzo/Scalepack (Otwinowski & Minor, 1997)'
_computing_data_reduction       'Denzo/Scalepack (Otwinowski & Minor, 1997)'
_computing_structure_solution   'SIR97 (Altomare, et al., 1999)'
_computing_structure_refinement 'SHELXTL (Bruker AXS Inc. 1998)'
_computing_molecular_graphics   'ORTEP (Burnett & Johnson 1996; Farrugia 1997)'
_computing_publication_material ?

_refine_special_details
;
 Refinement on F^2^ for ALL reflections.  Weighted R-factors wR and all
 goodness of fit values S are based on F^2^, conventional R-factors R are
 based on F, with F set to zero for negative F^2^. The observed criterion
 of F^2^ > 2sigma(F^2^) is used only for calculating _R_factor_obs etc.
 and is not relevant to the choice of reflections for refinement.
 R-factors based on F^2^ are statistically about twice as large as those
 based on F, and R-factors based on ALL data will be even larger.
 xyz and U were refined for the OH and NH hydrogen atoms. The CH~2~ and
 CH hydrogen atoms were included in the refinement as riding atom
 contributions with idealized geometry, and CH distances set at the
 temperature adjusted values of 0.99 Angstroms for the CH^2^ hydrogens
 and 0.95 Angstroms for the CH distances as defined within SHELXTL.
;

_atom_sites_solution_primary      direct
_atom_sites_solution_hydrogens    difmap
_refine_ls_structure_factor_coef  Fsqd
_refine_ls_matrix_type            full
_refine_ls_weighting_scheme       calc
_refine_ls_weighting_details
         'calc w=1/[\s^2^(Fo^2^)+(0.000P)^2^] where P=(Fo^2^+2Fc^2^)/3'
_refine_ls_hydrogen_treatment     mixed
_refine_ls_extinction_method      none
_refine_ls_extinction_coef        ?
_refine_ls_number_reflns          5019
_refine_ls_number_parameters      251
_refine_ls_number_restraints      0
_refine_ls_R_factor_all           0.0401
_refine_ls_R_factor_gt            0.0288
_refine_ls_wR_factor_all          0.0632
_refine_ls_wR_factor_ref          0.0594
_refine_ls_goodness_of_fit_all    0.966
_refine_ls_goodness_of_fit_ref    1.001
_refine_ls_restrained_S_all       0.966
_refine_ls_restrained_S_obs       1.001
_refine_ls_shift/su_max           0.003
_refine_ls_shift/su_mean          0.000
_refine_ls_d_res_high             0.74

_refine_diff_density_max    1.31
_refine_diff_density_min   -0.68
_refine_diff_density_rms    0.09

loop_
 _atom_site_label
 _atom_site_type_symbol
 _atom_site_fract_x
 _atom_site_fract_y
 _atom_site_fract_z
 _atom_site_U_iso_or_equiv
 _atom_site_adp_type
 _atom_site_occupancy
 _atom_site_calc_flag
 _atom_site_refinement_flags
 _atom_site_disorder_group
Sn1  Sn 0.40500(2)   0.111904(14) 0.817654(13) 0.02452(6)  Uani 1 d . .
Cl11 Cl 0.24231(10)  0.04003(6)   0.94939(6)   0.04213(16) Uani 1 d . .
Cl12 Cl 0.40291(10)  0.32885(5)   0.92664(5)   0.03442(14) Uani 1 d . .
O11  O  0.60704(24)  0.17256(16)  0.68119(14)  0.0326(4)   Uani 1 d . .
C11  C  0.7736(3)    0.23390(21)  0.73721(20)  0.0264(5)   Uani 1 d . .
O12  O  0.90751(26)  0.29248(17)  0.69688(16)  0.0330(4)   Uani 1 d . .
H12O H  0.8696(45)   0.2762(28)   0.6364(27)   0.049(7)    Uiso 1 d . .
C12  C  0.8357(3)    0.24889(23)  0.85953(21)  0.0314(5)   Uani 1 d . .
H12A H  0.8293       0.3297       0.9186       0.038    Uiso 1 calc R .
H12B H  0.9737       0.2473       0.8683       0.038    Uiso 1 calc R .
C13  C  0.7052(3)    0.14767(23)  0.88399(21)  0.0305(5)   Uani 1 d . .
H13A H  0.7220       0.1730       0.9704       0.037    Uiso 1 calc R .
H13B H  0.7451       0.0718       0.8458       0.037    Uiso 1 calc R .
O13  O  0.38182(25) -0.08906(15)  0.69251(14)  0.0316(4)   Uani 1 d . .
C14  C  0.2685(3)   -0.12828(21)  0.59481(20)  0.0254(5)   Uani 1 d . .
O14  O  0.21802(24) -0.23959(14)  0.51962(14)  0.0293(4)   Uani 1 d . .
C15  C  0.1926(3)   -0.03730(20)  0.56859(20)  0.0266(5)   Uani 1 d . .
H15A H  0.0640      -0.0807       0.5153       0.032    Uiso 1 calc R .
H15B H  0.2853      -0.0018       0.5272       0.032    Uiso 1 calc R .
C16  C  0.1690(3)    0.06567(21)  0.68129(20)  0.0263(5)   Uani 1 d . .
```

```
H16A H  0.0418       0.0387       0.7050       0.032    Uiso 1 calc R .
H16B H  0.1709       0.1384       0.6676       0.032    Uiso 1 calc R .
C31  C  0.8463(4)    0.76566(25)  0.76727(26)  0.0414(7)   Uani 1 d . .
H31  H  0.8537       0.8498       0.8105       0.050    Uiso 1 calc R .
C32  C  0.8916(4)    0.70094(25)  0.82489(25)  0.0428(7)   Uani 1 d . .
H32  H  0.9292       0.7394       0.9085       0.051    Uiso 1 calc R .
C33  C  0.8819(4)    0.57786(24)  0.75913(22)  0.0353(6)   Uani 1 d . .
H33  H  0.9128       0.5342       0.8005       0.042    Uiso 1 calc R .
N34  N  0.83199(28)  0.51821(18)  0.64223(17)  0.0294(4)   Uani 1 d . .
C35  C  0.7857(3)    0.58269(21)  0.58614(21)  0.0262(5)   Uani 1 d . .
C36  C  0.7889(3)    0.70640(23)  0.64400(24)  0.0333(6)   Uani 1 d . .
C37  C  0.7293(4)    0.76445(24)  0.57683(27)  0.0400(7)   Uani 1 d . .
H37  H  0.7278       0.8474       0.6168       0.048    Uiso 1 calc R .
C38  C  0.6753(4)    0.70452(24)  0.45841(26)  0.0385(6)   Uani 1 d . .
H38  H  0.6358       0.7455       0.4164       0.046    Uiso 1 calc R .
C39  C  0.6767(3)    0.57978(24)  0.39488(24)  0.0317(6)   Uani 1 d . .
C40  C  0.7274(3)    0.51968(22)  0.45920(21)  0.0260(5)   Uani 1 d . .
N41  N  0.71708(29)  0.39916(19)  0.40163(18)  0.0259(4)   Uani 1 d . .
H41N H  0.7345(42)   0.3603(26)   0.4354(26)   0.049(7)    Uiso 1 d . .
C42  C  0.6642(4)    0.33559(24)  0.28414(21)  0.0329(6)   Uani 1 d . .
H42  H  0.6577       0.2511       0.2468       0.039    Uiso 1 calc R .
C43  C  0.6189(4)    0.39247(26)  0.21674(23)  0.0390(6)   Uani 1 d . .
H43  H  0.5840       0.3477       0.1331       0.047    Uiso 1 calc R .
C44  C  0.6244(4)    0.51338(27)  0.27119(24)  0.0378(6)   Uani 1 d . .
H44  H  0.5929       0.5527       0.2253       0.045    Uiso 1 calc R .

loop_
 _atom_site_aniso_label
 _atom_site_aniso_U_11
 _atom_site_aniso_U_22
 _atom_site_aniso_U_33
 _atom_site_aniso_U_23
 _atom_site_aniso_U_13
 _atom_site_aniso_U_12
Sn1  0.02707(9) 0.02620(9) 0.02103(9) 0.01127(7)   0.00218(6)  0.00771(7)
Cl11 0.0500(4)  0.0443(4)  0.0345(3)  0.0231(3)    0.0137(3)   0.0064(3)
Cl12 0.0443(4)  0.0259(3)  0.0296(3)  0.00910(26) -0.00163(27) 0.01122(26)
O11  0.0277(9)  0.0439(10) 0.0232(9)  0.0177(8)   -0.0010(7)   0.0010(8)
C11  0.0275(12) 0.0285(13) 0.0237(12) 0.0112(10)   0.0045(10)  0.0094(10)
O12  0.0305(10) 0.0394(11) 0.0269(10) 0.0176(9)    0.0009(8)   0.0017(8)
C12  0.0257(12) 0.0414(15) 0.0256(12) 0.0163(11)   0.0006(10)  0.0051(11)
C13  0.0289(13) 0.0406(14) 0.0271(13) 0.0196(12)   0.0022(10)  0.0111(11)
O13  0.0379(10) 0.0278(9)  0.0247(9)  0.0060(7)   -0.0032(7)   0.0137(8)
C14  0.0268(12) 0.0277(12) 0.0232(12) 0.0123(10)   0.0054(9)   0.0083(10)
O14  0.0394(10) 0.0243(9)  0.0226(8)  0.0087(7)    0.0021(7)   0.0101(7)
C15  0.0311(13) 0.0266(12) 0.0219(11) 0.0109(10)  -0.0008(10)  0.0087(10)
C16  0.0261(12) 0.0259(12) 0.0268(12) 0.0119(10)  -0.0012(10)  0.0077(9)
C31  0.0332(14) 0.0330(14) 0.0455(17) 0.0069(13)   0.0061(12)  0.0066(11)
C32  0.0359(15) 0.0448(17) 0.0314(14) 0.0051(13)  -0.0015(12)  0.0063(13)
C33  0.0308(14) 0.0424(15) 0.0297(14) 0.0151(12)  -0.0001(11)  0.0079(11)
N34  0.0254(10) 0.0331(11) 0.0289(11) 0.0141(9)    0.0020(8)   0.0067(9)
C35  0.0206(11) 0.0279(12) 0.0309(13) 0.0144(11)   0.0057(9)   0.0053(9)
C36  0.0239(12) 0.0317(13) 0.0437(15) 0.0165(12)   0.0095(11)  0.0065(10)
C37  0.0330(14) 0.0326(14) 0.0625(19) 0.0273(14)   0.0153(13)  0.0106(11)
C38  0.0289(13) 0.0434(16) 0.0621(19) 0.0385(15)   0.0148(13)  0.0140(12)
C39  0.0204(12) 0.0425(15) 0.0448(15) 0.0312(13)   0.0091(11)  0.0084(10)
C40  0.0184(11) 0.0319(13) 0.0338(13) 0.0205(11)   0.0067(9)   0.0062(9)
N41  0.0264(10) 0.0318(11) 0.0269(11) 0.0194(9)    0.0049(8)   0.0092(9)
C42  0.0327(14) 0.0388(14) 0.0248(12) 0.0151(11)   0.0020(10)  0.0054(11)
C43  0.0361(15) 0.0550(18) 0.0293(13) 0.0259(13)   0.0015(11)  0.0067(13)
C44  0.0299(13) 0.0571(18) 0.0422(16) 0.0370(15)   0.0078(12)  0.0120(12)

loop_
 _geom_bond_atom_site_label_1
 _geom_bond_atom_site_label_2
 _geom_bond_distance
 _geom_bond_site_symmetry_2
 _geom_bond_publ_flag
Sn1 C13  2.127(2)   . y
Sn1 C16  2.131(2)   . y
Sn1 O13  2.3060(17) . y
Sn1 Cl11 2.4045(6)  . y
Sn1 Cl12 2.4864(6)  . y
Sn1 O11  2.5192(18) . y
O11 C11  1.232(3)   . y
C11 O12  1.307(3)   . y
C11 C12  1.502(3)   . y
O12 H12O 0.72(3)    . y
C12 C13  1.524(3)   . y
O13 C14  1.272(3)   . y
C14 O14  1.262(3)   . y
C14 C15  1.515(3)   . y
C15 C16  1.521(3)   . y
C31 C32  1.370(4)   . y
C31 C36  1.401(4)   . y
C32 C33  1.395(4)   . y
C33 N34  1.326(3)   . y
N34 C35  1.356(3)   . y
C35 C36  1.404(3)   . y
C35 C40  1.442(3)   . y
C36 C37  1.431(4)   . y
C37 C38  1.346(4)   . y
C38 C39  1.431(4)   . y
C39 C40  1.400(3)   . y
C39 C44  1.405(4)   . y
C40 N41  1.356(3)   . y
N41 C42  1.337(3)   . y
```

```
N41 H41N 0.79(3)    . y
C42 C43  1.384(3)   . y
C43 C44  1.366(4)   . y

loop_
 _geom_angle_atom_site_label_1
 _geom_angle_atom_site_label_2
 _geom_angle_atom_site_label_3
 _geom_angle
 _geom_angle_site_symmetry_1
 _geom_angle_site_symmetry_3
 _geom_angle_publ_flag
C13  Sn1 C16  153.22(9)  . . y
C13  Sn1 O13   91.47(8)  . . y
C16  Sn1 O13   77.42(7)  . . y
C13  Sn1 Cl11 101.30(7)  . . y
C16  Sn1 Cl11 102.65(7)  . . y
O13  Sn1 Cl11  88.45(5)  . . y
C13  Sn1 Cl12  94.67(7)  . . y
C16  Sn1 Cl12  94.47(6)  . . y
O13  Sn1 Cl12  171.40(4) . . y
Cl11 Sn1 Cl12  96.24(2)  . . y
C13  Sn1 O11   72.78(7)  . . y
C16  Sn1 O11   82.30(7)  . . y
O13  Sn1 O11   87.19(6)  . . y
Cl11 Sn1 O11  172.54(4)  . . y
Cl12 Sn1 O11   88.87(4)  . . y
C11  O11 Sn1  107.83(14) . . y
O11  C11 O12  123.2(2)   . . y
O11  C11 C12  121.8(2)   . . y
O12  C11 C12  115.0(2)   . . y
C11  O12 H12O 107.9(25)  . . y
C11  C12 C13  111.7(2)   . . y
C12  C13 Sn1  110.5(2)   . . y
C14  O13 Sn1  112.33(14) . . y
O14  C14 O13  122.4(2)   . . y
O14  C14 C15  119.3(2)   . . y
O13  C14 C15  118.4(2)   . . y
C14  C15 C16  111.6(2)   . . y
C15  C16 Sn1  108.65(14) . . y
C32  C31 C36  119.3(3)   . . y
C31  C32 C33  119.1(3)   . . y
N34  C33 C32  123.9(2)   . . y
C33  N34 C35  116.5(2)   . . y
N34  C35 C36  124.1(2)   . . y
N34  C35 C40  117.8(2)   . . y
C36  C35 C40  118.1(2)   . . y
C31  C36 C35  117.0(2)   . . y
C31  C36 C37  123.4(2)   . . y
C35  C36 C37  119.6(2)   . . y
C38  C37 C36  121.6(3)   . . y
C37  C38 C39  120.8(2)   . . y
C40  C39 C44  118.2(2)   . . y
C40  C39 C38  118.5(2)   . . y
C44  C39 C38  123.2(2)   . . y
N41  C40 C39  119.5(2)   . . y
N41  C40 C35  119.2(2)   . . y
C39  C40 C35  121.3(2)   . . y
C42  N41 C40  122.1(2)   . . y
C42  N41 H41N 115.2(22)  . . y
C40  N41 H41N 122.5(22)  . . y
N41  C42 C43  120.2(2)   . . y
C44  C43 C42  119.6(2)   . . y
C43  C44 C39  120.2(2)   . . y

 _geom_special_details
;
 All esds (except the esd in the dihedral angle between two l.s. planes)
 are estimated using the full covariance matrix.  The cell esds are taken
 into account individually in the estimation of esds in distances, angles
 and torsion angles; correlations between esds in cell parameters are only
 used when they are defined by crystal symmetry.  An approximate (isotropic)
 treatment of cell esds is used for estimating esds involving l.s. planes.

TABLE of Least Squares Planes (x,y,z in crystal coordinates) and deviations
 of individual atoms from the planes. Atoms used to define the planes are
 preceded with *.
  (Perpendicular contact distances are calculated to the 14 atom
   phenanthroline plane for the C-H...\p bonds. The phenanthrolinium ions
   related by the centers at (0, 1/2, 1/2) overlap at the edges of the N
   containing rings, while the phenanthrolinium ions related by the
   centers at (1/2, 1/2, 1/2) overlap the faces of the N containing rings.

Plane 1:  14 Atom Phenanthronine Plane
        6.580(1) x + 1.570(6) y - 3.774(5) z = 3.856(2)
  *  0.019(2)  C31       * -0.002(2)  C32       * -0.011(2)  C33
  *  0.009(2)  N34       *  0.017(2)  C35       *  0.014(2)  C36
  * -0.034(2)  C37       * -0.036(2)  C38       *  0.017(2)  C39
  *  0.014(2)  C40       * -0.026(2)  N41       * -0.031(2)  C42
  *  0.015(2)  C43       *  0.036(2)  C44
  Rms deviation of fitted atoms =   0.022
 Deviation of the hydrogen bonded to C41
    -0.100 (0.028)  H41N
 Deviation of the C--H...pi bonded hydrogen atoms of the pi-pi stacks
   centers at:   (0, 1/2, 1/2)             (1/2, 1/2, 1/2)
                3.277(3)  H33  2_766      -3.235(8)  H41N 2_666
                3.345(8)  H41N 2_766      -3.366(2)  H43  2_666
```

```
               3.309(3)  H42  2_766      -3.399(2)  H44  2_666

Plane 2:  6 Atom Middle Ring Plane
        6.524(3) x + 1.826(11) y - 3.878(11) z = 3.924(7)
  * -0.007(2)  C35       *  0.015(2)  C36       * -0.007(2)  C37
  * -0.009(2)  C38       *  0.018(2)  C39       * -0.010(2)  C40
     0.020(4)  C31         -0.026(4)  C32         -0.059(4)  C33
    -0.040(3)  N34         -0.074(3)  N41         -0.080(4)  C42
    -0.010(4)  C43          0.036(4)  C44
  Rms deviation of fitted atoms =   0.012

Plane 3:  6 Atom Unprotonated Ring Plane
        6.604(3) x + 1.480(12) y - 3.669(12) z = 3.899(8)
  *  0.007(2)  C31       * -0.001(2)  C32       * -0.006(2)  C33
  *  0.005(2)  N34       *  0.001(2)  C35       * -0.007(2)  C36
    -0.069(4)  C37         -0.079(5)  C38         -0.022(4)  C39
    -0.011(4)  C40         -0.047(4)  N41         -0.059(5)  C42
    -0.027(6)  C43         -0.011(6)  C44
  Rms deviation of fitted atoms =   0.005

Plane 4:  6 Atom Protonated Ring Plane
        6.640(2) x + 1.288(12) y - 3.627(12) z = 3.821(5)
  * -0.013(2)  C39       *  0.013(2)  C40       * -0.002(2)  N41
  * -0.009(2)  C42       *  0.008(2)  C43       *  0.003(2)  C44
     0.001(5)  C31          0.010(6)  C32          0.026(5)  C33
     0.042(4)  N34          0.021(4)  C35         -0.009(4)  C36
    -0.086(4)  C37         -0.092(4)  C38         -0.059(9)  H41N
  Rms deviation of fitted atoms =   0.009

 Interplanar Angles:
                    Phenanthroline  Unprotonated   Protonated
  Middle Ring          1.18(8)       1.65(10)       2.50(10)
  Protonated Ring      1.32(8)       0.90(10)
  Unprotonated Ring    0.55(8)
;
loop_
 _geom_hbond_atom_site_label_D
 _geom_hbond_atom_site_label_H
 _geom_hbond_atom_site_label_A
 _geom_hbond_distance_DH
 _geom_hbond_distance_HA
 _geom_hbond_distance_DA
 _geom_hbond_angle_DHA
 _geom_hbond_site_symmetry_A
 _geom_hbond_publ_flag
O12 H12O O14  0.72(3) 1.86(3) 2.579(2) 177.3(33) 2_656 y
N41 H41N O14  0.79(3) 1.91(3) 2.688(2) 166.3(30) 2_656 y
N41 H41N N34  0.79(3) 2.46(3) 2.737(3) 101.9(24) .     y
C42 H42  O13  0.95    2.40    3.154(3) 136.0     2_656 y
C43 H43  Cl12 0.95    2.74    3.578(3) 147.8     1_554 y
C44 H44  Cl12 0.95    2.86    3.785(3) 165.4     2_666 y
C37 H37  O13  0.95    2.86    3.458(3) 122.5     1_565 y
C38 H38  O11  0.95    2.70    3.596(3) 158.4     2_666 y
C31 H31  Cl11 0.95    2.95    3.578(3) 125.1     2_667 y
C31 H31  Cl11 0.95    3.04    3.619(3) 121.2     1_665 y
C32 H32  Cl11 0.95    3.18    3.691(3) 116.4     2_667 y
C33 H33  O12  0.95    2.74    3.377(3) 125.3     .     y
# END of CIF
```

APPENDIX C

SUPPLEMENTARY MATERIALS FOR

$[Mg(H_2O)_6](NO_3)_2 \cdot 2HMT \cdot 4H_2O$

Table C.1. Derived fractional coordinates[a] and isotropic atomic displacement parameters[b] ($Å^2$) for the hydrogen atoms in $[Mg(H_2O)_6](NO_3)_2 \cdot 2HMT \cdot 4H_2O$.

	x	*y*	*z*	U_{eq}
H1A	0.1653(36)	0.8903(22)	0.445219)	0.051(1)
H1B	0.1014(41)	0.8267(24)	0.41116(20)	0.055(1)
H2A	0.0175(37)	0.7658(23)	0.5565(19)	0.053(1)
H2B	0.0807(38)	0.7009(24)	0.5904(20)	0.057(1)
H3A	0.4256(38)	0.8624(22)	0.5605(19)	0.049(1)
H3B	0.3012(39)	0.8647(24)	0.5926(20)	0.054(1)
H4A	0.3543(36)	0.6083(22)	0.5552(19)	0.047(1)
H4B	0.4233(40)	0.6744(23)	0.5931(19)	0.052(1)
H5A	0.5156(36)	0.7318(22)	0.4395(18)	0.047(1)
H5B	0.4510(37)	0.8009(23)	0.4102(19)	0.052(1)
H6A	0.1042(38)	0.6360(22)	0.4400(19)	0.051(1)
H6B	0.2270(40)	0.6343(24)	0.4038(20)	0.054(1)
H11A	0.3946(37)	0.1533(25)	0.3238(19)	0.055(1)
H11B	0.4358(35)	0.0575(23)	0.3259(18)	0.049(1)
H12A	0.2545(36)	–0.0374(21)	0.3333(17)	0.044(1)
H12B	0.0868(35)	–0.0105(20)	0.3340(17)	0.044(1)
H13A	0.0296(39)	0.1307(22)	0.3269(18)	0.051(1)
H13B	0.1634(38)	0.2010(23)	0.3251(18)	0.056(1)
H14A	0.3383(36)	0.0338(23)	0.4980(19)	0.053(1)
H14B	0.3967(33)	–0.0124(22)	0.4255(18)	0.048(1)

Table C.1. (Continued).

	x	*y*	*z*	U_{eq}
H15A	0.3078(37)	0.2280(22)	0.4169(19)	0.055(1)
H15B	0.2829(36)	0.1725(22)	0.4930(19)	0.052(1)
H16A	0.1043(35)	0.0774(22)	0.4968(19)	0.046(1)
H16B	–0.0004(35)	0.0623(21)	0.4296(18)	0.044(1)
H21A	0.0338(35)	0.4454(22)	0.6774(18)	0.051(1)
H21B	0.0770(36)	0.3484(24)	0.6793(18)	0.049(1)
H22A	0.3919(36)	0.5070(21)	0.6702(17)	0.048(1)
H22B	0.2299(38)	0.5395(22)	0.6710(18)	0.048(1)
H23A	0.3045(38)	0.3005(22)	0.6822(18)	0.051(1)
H23B	0.4321(39)	0.3661(22)	0.6761(18)	0.051(1)
H24A	0.0715(35)	0.5249(22)	0.5748(18)	0.049(1)
H24B	0.1412(35)	0.4776(21)	0.5069(18)	0.044(1)
H25A	0.1842(35)	0.3377(22)	0.5098(19)	0.046(1)
H25B	0.1549(36)	0.2827(23)	0.5789(18)	0.049(1)
H26A	0.4805(35)	0.4390(22)	0.5731(18)	0.048(1)
H26B	0.3756(35)	0.4289(22)	0.5063(19)	0.044(1)
H7A	0.7087(39)	0.4260(24)	0.7172(20)	0.058(1)
H7B	0.7148(39)	0.4922(26)	0.6611(19)	0.058(1)
H8A	0.7647(45)	0.0718(26)	0.2909(20)	0.063(1)
H8B	0.7674(42)	0.0039(26)	0.3399(19)	0.063(1)
H9A	0.0846	0.6285	0.8215	0.070
H9B	–0.0598	0.6216	0.8026	0.070
H9'A	0.1169	0.6338	0.8465	0.070
H9'B	0.0368	0.6421	0.7847	0.070
H10A	0.5485	0.3222	0.2956	0.070
H10B	0.4025	0.3313	0.3091	0.070
H10'A	0.4662	0.3225	0.2856	0.070
H10'B	0.3716	0.3469	0.3380	0.070

[a]Estimated standard deviations of the least significant digits are given in parentheses.
[b]Equivalent isotropic atomic displacement parameters for the atoms refined anisotropically,

$U_{eq} = 1/3 \sum_i \sum_j U_{ij}\, a_i^* a_j^*\, \mathbf{a}_i \cdot \mathbf{a}_j$

Table C.2. Derived anisotropic atomic displacement parameters[a] ($Å^2$) for the hydrogen atoms in $[Mg(H_2O)_6](NO_3)_2 \cdot 2HMT \cdot 4H_2O$.

Atom	*U11*	*U22*	*U33*	*U12*	*U13*	*U23*
H1A	0.045	0.032	0.077	0.001	–0.014	0.013
H1B	0.056	0.047	0.062	0.002	–0.028	0.010
H2A	0.035	0.042	0.080	0.007	0.022	0.005
H2B	0.051	0.055	0.064	0.007	0.028	0.018
H3A	0.032	0.049	0.068	–0.005	–0.003	–0.020
H3B	0.045	0.062	0.055	–0.004	0.006	–0.028
H4A	0.045	0.030	0.067	0.001	–0.008	0.014
H4B	0.059	0.048	0.049	0.002	–0.021	0.011
H5A	0.034	0.040	0.067	0.009	0.019	0.004
H5B	0.048	0.051	0.056	0.009	0.022	0.018
H6A	0.032	0.046	0.075	–0.007	–0.004	–0.021
H6B	0.047	0.060	0.054	–0.006	0.002	–0.029
H11A	0.051	0.051	0.063	–0.007	0.021	–0.003
H11B	0.036	0.054	0.059	–0.003	0.013	–0.010
H12A	0.048	0.035	0.046	–0.005	0.003	–0.005
H12B	0.047	0.042	0.044	–0.006	–0.003	–0.007
H13A	0.046	0.054	0.054	0.011	–0.005	0.010
H13B	0.063	0.043	0.061	0.007	0.010	0.018
H14A	0.049	0.061	0.048	0.009	–0.012	–0.003
H14B	0.037	0.046	0.060	0.012	–0.007	–0.003
H15A	0.054	0.034	0.076	–0.008	0.017	–0.016
H15B	0.048	0.050	0.057	–0.007	0.004	–0.022
H16A	0.043	0.050	0.046	–0.004	0.010	0.000
H16B	0.031	0.045	0.056	–0.002	0.008	–0.001
H21A	0.039	0.054	0.054	0.002	0.013	–0.010
H21B	0.047	0.052	0.048	–0.012	0.010	0.000
H22A	0.050	0.045	0.047	–0.013	–0.013	–0.003
H22B	0.059	0.035	0.048	–0.002	–0.004	–0.007

Table C.2. (Continued).

Atom	*U11*	*U22*	*U33*	*U12*	*U13*	*U23*
H23A	0.065	0.041	0.051	0.006	–0.004	0.015
H23B	0.046	0.055	0.053	0.009	–0.011	0.009
H24A	0.045	0.045	0.057	0.017	–0.008	0.000
H24B	0.046	0.045	0.040	0.005	–0.013	0.004
H25A	0.046	0.042	0.050	–0.001	0.002	–0.009
H25B	0.053	0.035	0.061	–0.005	0.004	–0.004
H26A	0.032	0.055	0.057	–0.001	0.005	0.006
H26B	0.044	0.046	0.044	–0.001	0.010	0.006
H7A	0.062	0.067	0.046	–0.009	0.001	–0.015
H7B	0.062	0.067	0.046	–0.009	0.001	–0.015
H8A	0.084	0.060	0.044	0.008	0.002	–0.012
H8B	0.084	0.060	0.044	0.008	0.002	–0.012
H9A	0.062	0.084	0.065	–0.030	0.024	–0.026
H9B	0.062	0.084	0.065	–0.030	0.024	–0.026
H9'A	0.062	0.084	0.065	–0.030	0.024	–0.026
H9'B	0.062	0.084	0.065	–0.030	0.024	–0.026
H10A	0.061	0.094	0.054	–0.004	–0.007	0.010
H10B	0.061	0.094	0.054	–0.004	–0.007	0.010
H10'A	0.061	0.094	0.054	–0.004	–0.007	0.010
H10'B	0.061	0.094	0.054	–0.004	–0.007	0.010

[a]Estimated standard deviations of the least significant digits are given in parentheses.

APPENDIX D

SUPPLEMENTARY MATERIALS FOR

$[M(H_2O)_6]I_2{\cdot}2HMT{\cdot}4H_2O$, WHERE M = Ni AND Mn

Table D.1. Derived fractional coordinates[a] and isotropic atomic displacement parameters[b] (Å^2) for the hydrogen atoms.

	x	*y*	*z*	U_{eq}
$[Ni(H_2O)_6]I_2{\cdot}2HMT{\cdot}4H_2O$				
H1A	0.6694	0.4337	0.3483	0.039
H1B	0.5223	0.4642	0.2574	0.037
H2A	0.5322	0.6726	0.4007	0.043
H2B	0.5344	0.6950	0.5483	0.046
H3A	0.7719	0.5487	0.5975	0.046
H3B	0.7578	0.4416	0.6532	0.041
H4A	0.1638	0.5478	0.0328	0.149
H4B	0.1331	0.4626	–0.0693	0.149
H5A	0.4579	0.3739	0.0689	0.132
H5B	0.3496	0.4655	0.0717	0.132
HC1A	0.5744	0.9614	0.2084	0.039
HC1B	0.5627	0.9507	0.0579	0.043
HC2A	0.4064	0.8333	–0.0438	0.046
HC2B	0.3124	0.7641	0.0371	0.049
HC3A	0.3290	0.7819	0.2568	0.049
HC3B	0.4380	0.8626	0.3254	0.043
HC4A	0.7489	0.7332	0.0622	0.041
HC4B	0.6676	0.8141	–0.0298	0.040
HC5A	0.6959	0.8436	0.3412	0.039

Table D.1. (Continued).

	x	*y*	*z*	U_{eq}
HC5B	0.7669	0.7506	0.2815	0.044
HC6A	0.6103	0.6319	0.1757	0.049
HC6B	0.4333	0.6435	0.1653	0.051
$[Mn(H_2O)_6]I_2 \cdot 2HMT \cdot 4H_2O$				
H1A	0.6695	0.4297	0.3405	0.049
H1B	0.5279	0.4618	0.2472	0.043
H2A	0.5340	0.6796	0.4019	0.048
H2B	0.5365	0.7001	0.5483	0.053
H3A	0.7803	0.5472	0.6016	0.053
H3B	0.7677	0.4409	0.6560	0.048
H4A	0.1539	0.5459	0.0422	0.161
H4B	0.1264	0.4621	–0.0598	0.161
H5A	0.4621	0.3776	0.0550	0.123
H5B	0.3530	0.4662	0.0648	0.123
HC1A	0.5740	0.9612	0.2074	0.046
HC1B	0.5653	0.9496	0.0590	0.048
HC2A	0.4113	0.8305	–0.0429	0.052
HC2B	0.3173	0.7636	0.0379	0.057
HC3A	0.3305	0.7846	0.2522	0.058
HC3B	0.4362	0.8653	0.3205	0.051
HC4A	0.7471	0.7325	0.0686	0.050
HC4B	0.6688	0.8118	–0.0248	0.047
HC5A	0.6915	0.8465	0.3404	0.047
HC5B	0.7617	0.7533	0.2841	0.052
HC6A	0.6056	0.6341	0.1828	0.058
HC6B	0.4312	0.6479	0.1698	0.059

[a]Estimated standard deviations of the least significant digits are given in parentheses.

[b]Equivalent isotropic atomic displacement parameters for the atoms refined anisotropically,

$U_{eq} = 1/3 \sum_i \sum_j U_{ij} a_i^* a_j^* \mathbf{a}_i \cdot \mathbf{a}_j$

Table D.2. Derived anisotropic atomic displacement parameters[a] ($Å^2$) for the hydrogen atoms.

Atom	*U11*	*U22*	*U33*	*U12*	*U13*	*U23*
$[Ni(H_2O)_6]I_2 \cdot 2HMT \cdot 4H_2O$						
H1A	0.041	0.046	0.030	0.016	0.007	0.002
H1B	0.049	0.036	0.024	0.013	0.002	0.000
H2A	0.066	0.022	0.042	–0.006	0.006	0.008
H2B	0.073	0.018	0.044	–0.006	–0.003	–0.003
H3A	0.029	0.055	0.049	–0.011	–0.007	–0.004
H3B	0.035	0.052	0.034	0.013	–0.008	–0.002
H4A	0.136	0.133	0.169	0.018	–0.016	–0.026
H4B	0.136	0.133	0.169	0.018	–0.016	–0.026
H5A	0.192	0.085	0.095	0.059	–0.074	–0.058
H5B	0.192	0.085	0.095	0.059	–0.074	–0.058
HC1A	0.045	0.027	0.044	0.000	0.005	0.000
HC1B	0.055	0.031	0.042	0.002	0.002	0.013
HC2A	0.043	0.056	0.035	0.004	–0.010	0.005
HC2B	0.031	0.063	0.049	–0.007	–0.004	–0.008
HC3A	0.038	0.061	0.051	–0.013	0.016	–0.005
HC3B	0.040	0.050	0.040	–0.003	0.012	–0.005
HC4A	0.035	0.043	0.046	0.005	0.007	–0.005
HC4B	0.043	0.046	0.032	–0.006	0.009	0.002
HC5A	0.039	0.046	0.030	–0.001	–0.004	0.002
HC5B	0.040	0.047	0.042	0.011	–0.008	0.008
HC6A	0.065	0.026	0.056	0.003	0.005	0.007
HC6B	0.061	0.036	0.056	–0.018	0.013	0.001
$[Mn(H_2O)_6]I_2 \cdot 2HMT \cdot 4H_2O$						
H1A	0.053	0.058	0.037	0.022	0.014	0.003
H1B	0.063	0.039	0.028	0.013	0.007	0.000
H2A	0.076	0.025	0.040	–0.011	0.000	0.007
H2B	0.093	0.022	0.041	–0.006	–0.007	–0.001
H3A	0.034	0.067	0.055	–0.015	–0.009	0.005

Table D.2. (Continued).

Atom	*U11*	*U22*	*U33*	*U12*	*U13*	*U23*
H3B	0.038	0.060	0.044	0.012	–0.008	0.002
H4A	0.140	0.176	0.159	0.023	–0.013	–0.043
H4B	0.140	0.176	0.159	0.023	–0.013	–0.043
H5A	0.174	0.086	0.088	0.051	–0.063	–0.046
H5B	0.174	0.086	0.088	0.051	–0.063	–0.046
HC1A	0.057	0.029	0.051	0.000	0.005	–0.002
HC1B	0.064	0.033	0.048	0.001	0.004	0.013
HC2A	0.050	0.062	0.039	0.004	–0.013	0.005
HC2B	0.034	0.073	0.060	–0.010	–0.009	–0.006
HC3A	0.041	0.074	0.063	–0.012	0.021	–0.002
HC3B	0.050	0.059	0.046	0.002	0.017	–0.006
HC4A	0.041	0.054	0.057	0.013	0.011	–0.006
HC4B	0.051	0.055	0.038	–0.003	0.015	0.001
HC5A	0.047	0.054	0.035	–0.002	–0.008	0.000
HC5B	0.044	0.058	0.050	0.015	–0.012	0.008
HC6A	0.079	0.029	0.064	0.007	0.005	0.008
HC6B	0.072	0.041	0.066	–0.023	0.012	0.003

[a]Estimated standard deviations of the least significant digits are given in parentheses.

APPENDIX E

SUPPLEMENTARY MATERIALS FOR $SP(C_2H_5)_3$

Table E.1. Derived fractional coordinates[a] and isotropic atomic displacement parameters[b] (Å^2) for the hydrogen atoms in $SP(C_2H_5)_3$.

	x	*y*	*z*	U_{eq}
H11A	0.4032	0.7680	–0.2926	0.046
H11B	0.4755	0.7732	–0.1257	0.048
H12A	0.4733	0.9022	–0.1269	0.070
H12B	0.3714	0.8508	–0.0615	0.058
H12C	0.4437	0.8561	0.1054	0.058
H13A	0.2330	0.6379	–0.2735	0.046
H13B	0.2330	0.7038	–0.0942	0.048
H14A	0.1031	0.5736	–0.0880	0.071
H14B	0.1547	0.5214	–0.0438	0.058
H14C	0.1547	0.5873	0.1355	0.058
H15A	0.3556	0.5937	–0.2998	0.046
H15B	0.3056	0.5290	–0.1014	0.048
H16A	0.4407	0.5412	–0.1540	0.070
H16B	0.4876	0.6455	–0.1211	0.057
H16C	0.4376	0.5809	0.0773	0.057
H21A	0.9032	0.7680	–0.2926	0.046
H21B	0.9755	0.7732	–0.1257	0.048
H22A	0.9733	0.9022	–0.1269	0.070
H22B	0.8714	0.8508	–0.0615	0.058
H22C	0.9437	0.8561	0.1054	0.058
H23A	0.7330	0.6379	–0.2735	0.046
H23B	0.7330	0.7038	–0.0942	0.048

Table E.1. (Continued).

	x	*y*	*z*	U_{eq}
H24A	0.6031	0.5736	–0.0880	0.071
H24B	0.6547	0.5214	–0.0438	0.058
H24C	0.6547	0.5873	0.1355	0.058
H25A	0.8556	0.5937	–0.2998	0.046
H25B	0.8056	0.5290	–0.1014	0.048
H26A	0.9407	0.5412	–0.1540	0.070
H26B	0.9876	0.6455	–0.1211	0.057
H26C	0.9376	0.5809	0.0773	0.057
H31A	0.2990	0.2748	–0.0510	0.048
H31B	0.3558	0.2662	–0.2423	0.046
H32A	0.4365	0.3976	–0.0640	0.070
H32B	0.4239	0.3463	0.1594	0.057
H32C	0.4806	0.3376	–0.0319	0.057
H33A	0.4696	0.1950	–0.0291	0.048
H33B	0.4115	0.1490	–0.2401	0.046
H34A	0.4523	0.0571	–0.0758	0.069
H34B	0.4057	0.0604	0.1440	0.056
H34C	0.3476	0.0145	–0.0670	0.057
H35A	0.2259	0.0269	–0.0849	0.048
H35B	0.2352	0.0982	–0.2607	0.046
H36A	0.0975	0.0291	–0.1142	0.070
H36B	0.1381	0.0602	0.1231	0.058
H36C	0.1474	0.1314	–0.0527	0.058
H41A	0.7990	0.2748	–0.0510	0.048
H41B	0.8558	0.2662	–0.2423	0.046
H42A	0.9365	0.3976	–0.0640	0.070
H42B	0.9239	0.3463	0.1594	0.057
H42C	0.9806	0.3376	–0.0319	0.057
H43A	0.9696	0.1950	–0.0291	0.048

Table E.1. (Continued).

	x	*y*	*z*	U_{eq}
H43B	0.9115	0.1490	–0.2401	0.046
H44A	0.9523	0.0571	–0.0758	0.069
H44B	0.9057	0.0604	0.1440	0.056
H44C	0.8476	0.0145	–0.0670	0.057
H45A	0.7259	0.0269	–0.0849	0.048
H45B	0.7352	0.0982	–0.2607	0.046
H46A	0.5975	0.0291	–0.1142	0.070
H46B	0.6381	0.0602	0.1230	0.058
H46C	0.6474	0.1314	–0.0527	0.058
H51A	0.2022	0.7268	0.3743	0.048
H51B	0.1352	0.7320	0.2074	0.046
H52A	0.0711	0.5978	0.3731	0.070
H52B	0.0876	0.6439	0.6054	0.058
H52C	0.0206	0.6492	0.4385	0.058
H53A	0.0292	0.7962	0.4058	0.048
H53B	0.0951	0.8621	0.2265	0.046
H54A	0.0295	0.9264	0.4120	0.071
H54B	0.0674	0.9127	0.6355	0.058
H54C	0.1333	0.9786	0.4562	0.058
H55A	0.2766	0.9710	0.3986	0.048
H55B	0.2619	0.9063	0.2002	0.046
H56A	0.3994	0.9588	0.3460	0.070
H56B	0.3568	0.9191	0.5773	0.057
H56C	0.3421	0.8545	0.3789	0.057
H61A	0.7022	0.7268	0.3743	0.048
H61B	0.6352	0.7320	0.2074	0.046
H62A	0.5711	0.5978	0.3731	0.070
H62B	0.5876	0.6439	0.6054	0.058
H62C	0.5206	0.6492	0.4385	0.058

Table E.1. (Continued).

	x	*y*	*z*	U_{eq}
H63A	0.5292	0.7962	0.4058	0.048
H63B	0.5951	0.8621	0.2265	0.046
H64A	0.5295	0.9264	0.4120	0.071
H64B	0.5674	0.9127	0.6355	0.058
H64C	0.6333	0.9786	0.4562	0.058
H65A	0.7766	0.9710	0.3986	0.048
H65B	0.7619	0.9063	0.2002	0.046
H66A	0.8994	0.9588	0.3460	0.070
H66B	0.8568	0.9191	0.5773	0.057
H66C	0.8421	0.8545	0.3789	0.057
H71A	0.0897	0.2338	0.2577	0.046
H71B	0.0242	0.2252	0.4491	0.048
H72A	0.0389	0.1024	0.4360	0.070
H72B	0.1430	0.1624	0.4681	0.057
H72C	0.0776	0.1537	0.6594	0.057
H73A	0.2625	0.3510	0.2599	0.046
H73B	0.2746	0.3050	0.4709	0.048
H74A	0.3952	0.4429	0.4242	0.069
H74B	0.3332	0.4855	0.4330	0.057
H74C	0.3452	0.4396	0.6440	0.056
H75A	0.1371	0.4018	0.2393	0.046
H75B	0.1990	0.4731	0.4151	0.048
H76A	0.0683	0.4709	0.3858	0.070
H76B	0.0160	0.3686	0.4473	0.058
H76C	0.0779	0.4398	0.6231	0.058
H81A	0.5897	0.2338	0.2577	0.046
H81B	0.5242	0.2252	0.4491	0.048
H82A	0.5389	0.1024	0.4360	0.070
H82B	0.6430	0.1624	0.4681	0.057

Table E.1. (Continued).

	x	*y*	*z*	U_{eq}
H82C	0.5776	0.1537	0.6594	0.057
H83A	0.7625	0.3510	0.2599	0.046
H83B	0.7625	0.3510	0.2599	0.046
H84A	0.8952	0.4429	0.4242	0.069
H84B	0.8332	0.4855	0.4330	0.057
H84C	0.8452	0.4396	0.6440	0.056
H85A	0.6371	0.4018	0.2393	0.046
H85B	0.6990	0.4731	0.4151	0.048
H86A	0.5683	0.4709	0.3858	0.070
H86B	0.5160	0.3686	0.4473	0.058
H86C	0.5779	0.4398	0.6231	0.058

[a]Estimated standard deviations of the least significant digits are given in parentheses.

[b]Equivalent isotropic atomic displacement parameters for the atoms refined anisotropically,

$U_{eq} = 1/3 \sum_i \sum_j U_{ij} a_i^* a_j^* \mathbf{a}_i \cdot \mathbf{a}$

Table E.2. Derived anisotropic atomic displacement parameters[a] ($Å^2$) for the hydrogen atoms of $SP(C_2H_5)_3$.

Atom	*U11*	*U22*	*U33*	*U12*	*U13*	*U23*
H11A	0.053	0.046	0.033	0.021	0.005	0.008
H11B	0.041	0.051	0.040	0.014	0.004	0.003
H12A	0.085	0.039	0.064	0.014	0.004	0.007
H12B	0.084	0.043	0.052	0.035	0.000	0.002
H12C	0.070	0.039	0.051	0.017	–0.004	–0.007
H13A	0.045	0.058	0.034	0.026	–0.008	–0.002
H13B	0.051	0.063	0.041	0.037	–0.002	0.001
H14A	0.038	0.097	0.065	0.026	–0.004	–0.002
H14B	0.042	0.058	0.052	0.008	–0.001	–0.001
H14C	0.040	0.075	0.050	0.022	0.008	0.004
H15A	0.058	0.051	0.033	0.031	0.001	–0.006
H15B	0.064	0.040	0.041	0.027	–0.001	–0.003

Table E.2. (Continued).

Atom	*U11*	*U22*	*U33*	*U12*	*U13*	*U23*
H16A	0.093	0.086	0.063	0.070	0.004	–0.005
H16B	0.054	0.082	0.050	0.046	0.004	–0.001
H16C	0.070	0.073	0.050	0.052	–0.003	0.002
H21A	0.053	0.046	0.033	0.021	0.005	0.008
H21B	0.041	0.051	0.040	0.014	0.004	0.003
H22A	0.085	0.039	0.064	0.014	0.004	0.007
H22B	0.084	0.043	0.052	0.035	0.000	0.002
H22C	0.070	0.039	0.051	0.017	–0.004	–0.007
H23A	0.045	0.058	0.034	0.026	–0.008	–0.002
H23B	0.051	0.063	0.041	0.037	–0.002	0.001
H24A	0.038	0.097	0.065	0.026	–0.004	–0.002
H24B	0.042	0.058	0.052	0.008	–0.001	–0.001
H24C	0.040	0.075	0.050	0.022	0.008	0.004
H25A	0.058	0.051	0.033	0.031	0.001	–0.006
H25B	0.064	0.040	0.041	0.027	–0.001	–0.003
H26A	0.093	0.086	0.063	0.070	0.004	–0.005
H26B	0.054	0.082	0.050	0.046	0.004	–0.001
H26C	0.070	0.073	0.050	0.052	–0.003	0.002
H31A	0.064	0.050	0.041	0.037	–0.001	0.002
H31B	0.058	0.046	0.034	0.026	0.002	0.008
H32A	0.092	0.038	0.064	0.021	0.003	0.006
H32B	0.070	0.039	0.049	0.019	–0.004	–0.007
H32C	0.053	0.045	0.051	0.008	0.002	0.003
H33A	0.040	0.064	0.041	0.027	0.002	0.000
H33B	0.051	0.059	0.034	0.031	0.006	–0.001
H34A	0.087	0.092	0.064	0.070	0.003	–0.003
H34B	0.073	0.067	0.049	0.051	–0.003	0.004
H34C	0.081	0.053	0.050	0.045	0.000	–0.004
H35A	0.051	0.040	0.040	0.014	–0.003	–0.004
H35B	0.047	0.052	0.032	0.021	–0.007	–0.005

Table E.2. (Continued).

Atom	*U11*	*U22*	*U33*	*U12*	*U13*	*U23*
H36A	0.040	0.084	0.064	0.014	–0.009	–0.005
H36B	0.038	0.071	0.051	0.017	0.006	0.003
H36C	0.043	0.083	0.052	0.035	–0.004	–0.001
H41A	0.064	0.050	0.041	0.037	–0.001	0.002
H41B	0.058	0.046	0.034	0.026	0.002	0.008
H42A	0.092	0.038	0.064	0.021	0.003	0.006
H42B	0.070	0.039	0.049	0.019	–0.004	–0.007
H42C	0.053	0.045	0.051	0.008	0.002	0.003
H43A	0.040	0.064	0.041	0.027	0.002	0.000
H43B	0.051	0.059	0.034	0.031	0.006	–0.001
H44A	0.087	0.092	0.064	0.070	0.003	–0.003
H44B	0.073	0.067	0.049	0.051	–0.003	0.004
H44C	0.081	0.053	0.050	0.045	0.000	–0.004
H45A	0.051	0.040	0.040	0.014	–0.003	–0.004
H45B	0.047	0.052	0.032	0.021	–0.007	–0.005
H46A	0.040	0.084	0.064	0.014	–0.009	–0.005
H46B	0.038	0.071	0.051	0.017	0.006	0.003
H46C	0.043	0.083	0.052	0.035	–0.004	–0.001
H51A	0.063	0.051	0.040	0.036	0.001	–0.003
H51B	0.057	0.046	0.033	0.025	–0.003	–0.008
H52A	0.096	0.039	0.064	0.025	–0.003	–0.007
H52B	0.075	0.039	0.051	0.022	0.003	0.007
H52C	0.057	0.043	0.052	0.008	–0.002	–0.002
H53A	0.040	0.063	0.041	0.026	–0.003	–0.001
H53B	0.052	0.058	0.034	0.033	–0.005	0.002
H54A	0.084	0.097	0.065	0.071	–0.003	0.002
H54B	0.070	0.075	0.050	0.052	0.005	–0.004
H54C	0.084	0.058	0.052	0.049	0.000	0.001
H55A	0.050	0.040	0.041	0.014	0.002	0.003
H55B	0.047	0.051	0.033	0.020	0.007	0.006

Table E.2. (Continued).

Atom	*U11*	*U22*	*U33*	*U12*	*U13*	*U23*
H56A	0.039	0.086	0.063	0.016	0.009	0.005
H56B	0.038	0.073	0.050	0.020	–0.005	–0.002
H56C	0.045	0.082	0.050	0.036	0.005	0.001
H61A	0.063	0.051	0.040	0.036	0.001	–0.003
H61B	0.057	0.046	0.033	0.025	–0.003	–0.008
H62A	0.096	0.039	0.064	0.025	–0.003	–0.007
H62B	0.075	0.039	0.051	0.022	0.003	0.007
H62C	0.057	0.043	0.052	0.008	–0.002	–0.002
H63A	0.040	0.063	0.041	0.026	–0.003	–0.001
H63B	0.052	0.058	0.034	0.033	–0.005	0.002
H64A	0.084	0.097	0.065	0.071	–0.003	0.002
H64B	0.070	0.075	0.050	0.052	0.005	–0.004
H64C	0.084	0.058	0.052	0.049	0.000	0.001
H65A	0.050	0.040	0.041	0.014	0.002	0.003
H65B	0.047	0.051	0.033	0.020	0.007	0.006
H66A	0.039	0.086	0.063	0.016	0.009	0.005
H66B	0.038	0.073	0.050	0.020	–0.005	–0.002
H66C	0.045	0.082	0.050	0.036	0.005	0.001
H71A	0.052	0.046	0.034	0.020	–0.006	–0.008
H71B	0.040	0.050	0.041	0.013	–0.003	–0.002
H72A	0.087	0.038	0.064	0.017	–0.003	–0.006
H72B	0.082	0.045	0.051	0.037	0.000	–0.003
H72C	0.072	0.039	0.049	0.021	0.003	0.007
H73A	0.047	0.059	0.034	0.028	0.007	0.001
H73B	0.050	0.064	0.041	0.037	0.002	0.000
H74A	0.038	0.092	0.064	0.022	0.006	0.003
H74B	0.045	0.053	0.050	0.009	0.004	0.004
H74C	0.039	0.067	0.049	0.017	–0.006	–0.004
H75A	0.057	0.052	0.032	0.031	–0.002	0.005
H75B	0.063	0.040	0.040	0.026	0.001	0.004

Table E.2. (Continued).

Atom	*U11*	*U22*	*U33*	*U12*	*U13*	*U23*
H76A	0.096	0.084	0.064	0.070	–0.004	0.005
H76B	0.057	0.083	0.052	0.049	–0.003	0.001
H76C	0.075	0.071	0.051	0.054	0.002	–0.003
H81A	0.052	0.046	0.034	0.020	–0.006	–0.008
H81B	0.040	0.050	0.041	0.013	–0.003	–0.002
H82A	0.087	0.038	0.064	0.017	–0.003	–0.006
H82B	0.082	0.045	0.051	0.037	0.000	–0.003
H82C	0.072	0.039	0.049	0.021	0.003	0.007
H83A	0.047	0.059	0.034	0.028	0.007	0.001
H83B	0.050	0.064	0.041	0.037	0.002	0.000
H84A	0.038	0.092	0.064	0.022	0.006	0.003
H84B	0.045	0.053	0.050	0.009	0.004	0.004
H84C	0.039	0.067	0.049	0.017	–0.006	–0.004
H85A	0.057	0.052	0.032	0.031	–0.002	0.005
H85B	0.063	0.040	0.040	0.026	0.001	0.004
H86A	0.096	0.084	0.064	0.070	–0.004	0.005
H86B	0.057	0.083	0.052	0.049	–0.003	0.001
H86C	0.075	0.071	0.051	0.054	0.002	–0.003

[a]Estimated standard deviations of the least significant digits are given in parentheses.

APPENDIX F

SUPPLEMENTARY MATERIALS FOR

$\{[Cu(bipy)]_2(SO_4)\cdot TPA\}_n$

Table F.1. Derived fractional coordinates[a] and isotropic atomic displacement parameters[b] (Å^2) for the hydrogen atoms in $\{[Cu(bipy)]_2(SO_4)\cdot TPA\}_n$.

	x	*y*	*z*	U_{eq}
H1	0.7724	0.2098	–0.5491	0.099
H2	0.7245	0.1992	–0.4375	0.092
H4	0.7404	0.0839	–0.4717	0.101
H5	0.7880	0.0961	–0.5826	0.119
H6	0.6326	0.0589	–0.2855	0.104
H7	0.6932	0.0725	–0.3864	0.097
H9	0.6776	0.1882	–0.3383	0.094
H10	0.6176	0.1710	–0.2391	0.096
H11	0.5296	0.0476	–0.0471	0.075
H12	0.4783	0.0563	0.0622	0.070
H14	0.4873	0.1721	0.0296	0.088
H15	0.5384	0.1619	–0.0789	0.098
H16	0.3792	0.1918	0.2211	0.080
H17	0.4385	0.1816	0.1175	0.083
H19	0.4311	0.0647	0.1591	0.069
H20	0.3721	0.0786	0.2613	0.066
H21	0.2692	0.1954	0.4484	0.087
H22	0.2235	0.1864	0.5624	0.095

Table F.1. (Continued).

	x	*y*	*z*	U_{eq}
H24	0.2438	0.0707	0.5381	0.100
H25	0.2891	0.0813	0.4247	0.100
H26	0.1368	0.0487	0.7273	0.119
H27	0.1976	0.0605	0.6258	0.106
H29	0.1776	0.1770	0.6620	0.104
H30	0.1175	0.1615	0.7622	0.110
H31	0.0127	0.0442	0.9545	0.108
H32	–0.0378	0.0578	1.0625	0.102
H34	–0.0049	0.1718	1.0310	0.136
H35	0.0451	0.1566	0.9237	0.147
H36	–0.1113	0.2014	1.2190	0.132
H37	–0.0555	0.1857	1.1146	0.133
H39	–0.0792	0.0708	1.1633	0.099
H40	–0.1342	0.0900	1.2661	0.093
H43	0.3813	0.0082	0.0378	0.077
H44	0.3242	0.0226	0.1461	0.082
H46	0.1256	0.0034	–0.0320	0.095
H47	0.1827	–0.0110	–0.1403	0.104
H51	0.1352	0.2500	0.5700	0.045
H52	0.0600	0.2353	0.6586	0.074
H54	–0.1199	0.2481	0.4467	0.031
H55	–0.0447	0.2628	0.3582	0.040
H11O	0.4050	0.0162	–0.0324	0.162
H13O	0.0773	0.0133	0.0488	0.148
H15O	0.1581	0.2255	0.4462	0.043
H17O	–0.1709	0.2436	0.5497	0.105

[a]Estimated standard deviations of the least significant digits are given in parentheses.

[b]Equivalent isotropic atomic displacement parameters for the atoms refined anisotropically,

$U_{eq} = 1/3 \sum_i \sum_j U_{ij}\, a_i^* a_j^*\, \mathbf{a}_i \cdot \mathbf{a}_j$

Table F.2. Derived anisotropic atomic displacement parameters[a] ($Å^2$) for the hydrogen atoms of $\{[Cu(bipy)]_2(SO_4)\cdot TPA\}_n$.

Atom	*U11*	*U22*	*U33*	*U12*	*U13*	*U23*
H1	0.167	0.061	0.112	–0.023	0.107	0.009
H2	0.178	0.032	0.114	–0.024	0.115	–0.010
H4	0.192	0.038	0.129	0.011	0.135	–0.002
H5	0.210	0.076	0.135	0.005	0.149	–0.013
H6	0.195	0.042	0.128	–0.018	0.128	0.004
H7	0.191	0.027	0.128	0.001	0.131	0.001
H9	0.187	0.031	0.115	–0.022	0.123	–0.022
H10	0.174	0.056	0.109	–0.006	0.118	–0.018
H11	0.128	0.046	0.088	0.011	0.086	0.007
H12	0.124	0.038	0.084	0.011	0.083	0.011
H14	0.164	0.039	0.109	0.002	0.115	0.011
H15	0.183	0.049	0.118	0.004	0.129	0.013
H16	0.151	0.034	0.099	0.013	0.103	0.016
H17	0.157	0.034	0.104	0.006	0.109	0.013
H19	0.124	0.034	0.083	0.011	0.083	0.014
H20	0.116	0.033	0.080	0.005	0.078	0.011
H21	0.175	0.023	0.114	0.007	0.121	0.003
H22	0.191	0.029	0.119	–0.003	0.131	–0.011
H24	0.199	0.027	0.133	0.017	0.140	0.015
H25	0.206	0.025	0.132	0.007	0.144	–0.001
H26	0.210	0.070	0.137	–0.008	0.142	0.019
H27	0.203	0.040	0.135	0.010	0.141	0.019
H29	0.201	0.049	0.123	–0.006	0.139	–0.017
H30	0.184	0.085	0.116	0.006	0.129	–0.008

Table F.2. (Continued).

Atom	*U11*	*U22*	*U33*	*U12*	*U13*	*U23*
H31	0.156	0.099	0.118	–0.016	0.114	–0.008
H32	0.152	0.087	0.115	–0.016	0.112	–0.003
H34	0.243	0.085	0.153	0.017	0.174	0.031
H35	0.263	0.098	0.162	0.022	0.188	0.034
H36	0.240	0.081	0.146	0.036	0.166	0.041
H37	0.242	0.082	0.148	0.030	0.169	0.039
H39	0.152	0.080	0.113	–0.009	0.112	0.006
H40	0.136	0.082	0.104	–0.013	0.101	0.005
H43	0.095	0.068	0.088	0.008	0.058	0.004
H44	0.098	0.082	0.087	0.004	0.057	–0.006
H46	0.096	0.116	0.093	–0.001	0.058	–0.012
H47	0.102	0.138	0.093	–0.005	0.058	–0.024
H51	0.026	0.074	0.036	0.001	0.011	–0.009
H52	0.052	0.152	0.020	–0.010	0.014	–0.001
H54	0.023	0.035	0.044	0.006	0.022	–0.002
H55	0.030	0.060	0.033	0.009	0.016	0.019
H11O	0.116	0.274	0.129	–0.058	0.088	–0.083
H13O	0.104	0.265	0.098	–0.028	0.065	–0.016
H15O	0.029	0.048	0.068	0.009	0.033	–0.002
H17O	0.060	0.196	0.076	0.038	0.047	–0.039

[a]Estimated standard deviations of the least significant digits are given in parentheses.

APPENDIX G

SUPPLEMENTARY MATERIALS FOR $[Ag(bipy)NO_3]_n$

G.1 Reflection data processing using EvalCCD

EvalCCD extracts intensity information using .rmat files to define the centers of possible shoeboxes. Each .rmat file describes the orientation of **a***, **b***, **c*** for the reduced cell of a particular twin component. An .rmat file can be generated using a Phi/Chi procedure available in EvalCCD (Duisenberg, Hooft, Schreurs & Kroon, 2000). Alternatively the .rmat file can be generated using the NDIRAX program. Having found the .rmat file for one twin component an .rmat file is found for another twin component using the non-fitting reflections. A known twin rule can be imposed to relate twin components exactly implying the dimensions of the two cells are equal.

The standard strategy for data collection on the Nonius KappaCCD results in scan sets for different sweeps through diffraction space. Each scan set produces its own .rmat file which is named rotindex.rmat. Each successive file overwrites any previous file. The .rmat file for the first scan set is actually the best determined one. In general this scan sets covers the biggest angular range and has as many reflections as possible per frame. This gives an optimum resolution of spots, including those from twinned crystals if spot splitting is along a reciprocal space direction associated with a short reciprocal space vector (long axial length). The .rmat file evaluated gives the projection of the reciprocal axes of a primitive reduced cell onto three orthonormal reference axes. However the relationship between different .rmat files for different

twin components, different scan sets and different temperatures is not always obvious for a crystal with a centred lattice. The reciprocal lattice of the primitive reduced cell could equally well be in one of four 222 symmetry related orientations when compared to a face centre cell with reciprocal space vectors $\mathbf{a}_o^*$, $\mathbf{b}_o^*$, $\mathbf{c}_o^*$; $\mathbf{a}_o^* > \mathbf{b}_o^* > \mathbf{c}_o^*$ reciprocal lattice cell option can be expressed as $h_o\mathbf{a}_o^* + k_o\mathbf{b}_o^* + l_o\mathbf{c}_o^*$ where h_o, k_o, l_o are −1,1,1; −1,−1,1; 0,0,2 or 1,−1,1; 1,1,1; 0,0,2 or 1,1,−1; 1,−1,−1; 0,0,−2 or −1,−1,−1; −1,1,−1; 0,0,−2

The choice is somewhat arbitrary and is a consequence of the angles α_o, β_o, γ_o of the orthorhombic cell not quite being 90° because of experimental error. In the *C*-centred cell the orthorhombic parent cell has $\beta_o \neq 90°$ systematically so only two options for the .rmat file exist, but there are also two options for each twin component. This creates problems for an analytic absorption correction as faces have to be reindexed. However, for our crystal, the empirical program Sortav (Blessing, 1987) could be used and only requires a knowledge of the minimum crystal dimension since it uses data correlation to apply an absorption correction. However it is still advisable to get all scan sets off using the same .rmat file to avoid problems. The diffraction patterns could be described as coming from a twinned *F12/d1* structure but automated procedures of EvalCCD determined *h*, *k*, *l* values for a *C*-centred structure, namely *C12/c1* which is simply a different setting of *F12/d1*.

200 K

Using NDIRAX on the first scan set produced the orthorhombic unit cell *a* = 12.8226(4) Å, *b* = 9.9373(3) Å, *c* = 34.4498(10) Å. Absorption corrections were carried out using Sortav with a minimum distance in the crystal of 0.20 mm to produce a merged set of reflections for *F*-centered orthorhombic symmetry.

100 K

The two components of the twinned monoclinic crystal exist in an approximately 3:1 ratio. The .rmat file for the major component was obtained using NDIRAX. Initially the .rmat file for the second component was obtained from the reflections that did not fit the twin component and established the twin rule. The .rmat file that was subsequently used for the second component was obtained by a 180° rotation about **c*** of the reciprocal lattice cell of the first twin component.

The file final.nanny.sum detailed the two .rmat files. The monoclinic unit cell has a = 12.7506(14) Å, b = 9.8596(11) Å, c = 18.3794(21) Å, β = 109.980 (7) °. This makes the spot splitting along **c***, equal to −0.01493h**c*** (*vida supra*). The intensity of each twin pair of reflections was obtained as the sum of the two components. If we had indeed obtained resolved components of the twin we could have added them together. However by setting the boxes large enough and using appropriate resolution parameters (Split overlap fraction 0.1, Sum overlap fraction 0.7 and Split peak quality ratio 1000) only reflections with a split overlap fraction of < 0.1 are resolved into two components and there were none of these. These parameters were default settings of the program.

The Sortav program can operate using a file that contains the *h, k, l* indexes of the first twin component, the total intensity and its standard error. The file has attached direction cosines l_1, l_2, m_1, m_2, n_1, n_2 where l_1, m_1, n_1 are the cosines of the angles that the ingoing beam (direction sense from the crystal to the X-ray source) makes with the reciprocal lattice directions of the first twin component l_2, m_2, n_2 are the cosines of the angles that the outgoing beam (direction sense from the crystal to the detector) makes with the same reciprocal lattice directions.

i.e. $-\mathbf{H}_{in} = l_1a^*\mathbf{a} + m_1b^*\mathbf{b} + n_1c^*\mathbf{c}$, $\mathbf{H}_{out} = l_2a^*\mathbf{a} + m_2b^*\mathbf{b} + n_2c^*\mathbf{c}$

$2\sin\beta = |(l_2+l_1)\, a^*\mathbf{a} + (m_2+m_1)\, b^*\mathbf{b} + (n_2+n_1)\, c^*\mathbf{c}|$. Note $\mathbf{H}_{out}.\mathbf{a}^*/a^* = l_2$, *etc*.

The magnitude of $\mathbf{H}_{out} = 1 = l_2a^*a^2 + m_2b^*b^2 + n_2c^*c^2 + 2l_2m_2a^*b^*ab\cos\beta$

$$+ 2l_2n_2a^*c^*ac\cos\beta + 2m_2n_2b^*c^*bc\cos\alpha$$

An initial solution of a twinned crystal often requires an allocation of intensity between the overlapping components of a twin. If the twin ratio is far away from 1:1, this can be done by using pseudo equivalent reflections related by the twin rule. If I_a and I_b are values of components per unit cell then twin rule related reflection pairs have intensity $I_1 = aI_a+bI_b$ and $I_2 = bI_a+aI_b$ where $a+b = 1$. Consequently $I_a+I_b = I_1+I_2$ is well determined but $I_a-I_b = (I_1-I_2)/(a-b)$ is not as well determined. The fact that I_1, I_2, I_a and I_b are all ≥ 0 limits the range possible for $a-b$, *i.e* $|a-b|$ is greater than the minimum value of $|(I_1-I_2)/(I_1+I_2)|$ which would correspond to either I_a or I_b, being zero. For our structure an initial model of the twinned crystal can be obtained by ordering the known disordered structure and the twin ratio could be refined as part of the structure refinement.

Table G.1. Derived fractional coordinates[a] and isotropic atomic displacement parameters[b] (Å^2) for the hydrogen atoms in [Ag(bipy)NO_3]$_n$.

	x	*y*	*z*	U_{eq}
100 K				
H2	0.2017	0.3657	0.4429	0.022
H3	0.2608	0.5291	0.5437	0.021
H5	0.1825	0.8292	0.3750	0.022
H6	0.1224	0.6564	0.2797	0.025
H2'	0.0213	0.3667	0.0863	0.020
H3'	–0.0264	0.2288	–0.0261	0.020
H5'	0.0562	–0.1085	0.1179	0.022
H6'	0.0982	0.0403	0.2259	0.027
200 K				
H2	0.0238	0.1281	0.2184	0.039
H3	0.0107	–0.0281	0.2700	0.040
H5	0.0006	–0.3334	0.1879	0.041
H6	0.0140	–0.1671	0.1388	0.045
H2'	0.0191	0.1305	0.0395	0.036
H3'	0.0051	0.2732	–0.0152	0.038
H5'	0.0068	0.5991	0.0601	0.042
H6'	0.0209	0.4456	0.1125	0.048

[a]Estimated standard deviations of the least significant digits are given in parentheses.

[b]Equivalent isotropic atomic displacement parameters for the atoms refined anisotropically, $U_{eq} = 1/3 \sum_i \sum_j U_{ij} a_i^* a_j^* \mathbf{a}_i \cdot \mathbf{a}_j$

Table G.2. Derived anisotropic atomic displacement parameters[a] ($Å^2$) for the hydrogen atoms of $[Ag(bipy)NO_3]_n$.

Atom	*U11*	*U22*	*U33*	*U12*	*U13*	*U23*
100 K						
H2	0.027	0.017	0.022	–0.003	0.010	–0.002
H3	0.030	0.017	0.017	–0.002	0.008	0.001
H5	0.031	0.019	0.014	–0.001	0.006	0.001
H6	0.033	0.024	0.015	0.000	0.005	–0.002
H2'	0.016	0.017	0.024	0.000	0.004	–0.011
H3'	0.023	0.016	0.020	0.000	0.004	–0.008
H5'	0.029	0.018	0.017	0.000	0.004	–0.007
H6'	0.038	0.024	0.017	0.000	0.005	–0.009
200 K						
H2	0.064	0.030	0.022	–0.006	–0.007	0.008
H3	0.067	0.030	0.021	–0.005	–0.006	0.007
H5	0.073	0.030	0.021	–0.002	–0.004	0.007
H6	0.083	0.030	0.021	0.002	–0.001	0.008
H2'	0.049	0.025	0.035	0.006	0.007	0.009
H3'	0.057	0.024	0.034	0.004	0.006	0.008
H5'	0.068	0.024	0.034	0.002	0.004	0.008
H6'	0.086	0.025	0.034	–0.003	0.000	0.009

[a]Estimated standard deviations of the least significant digits are given in parentheses.

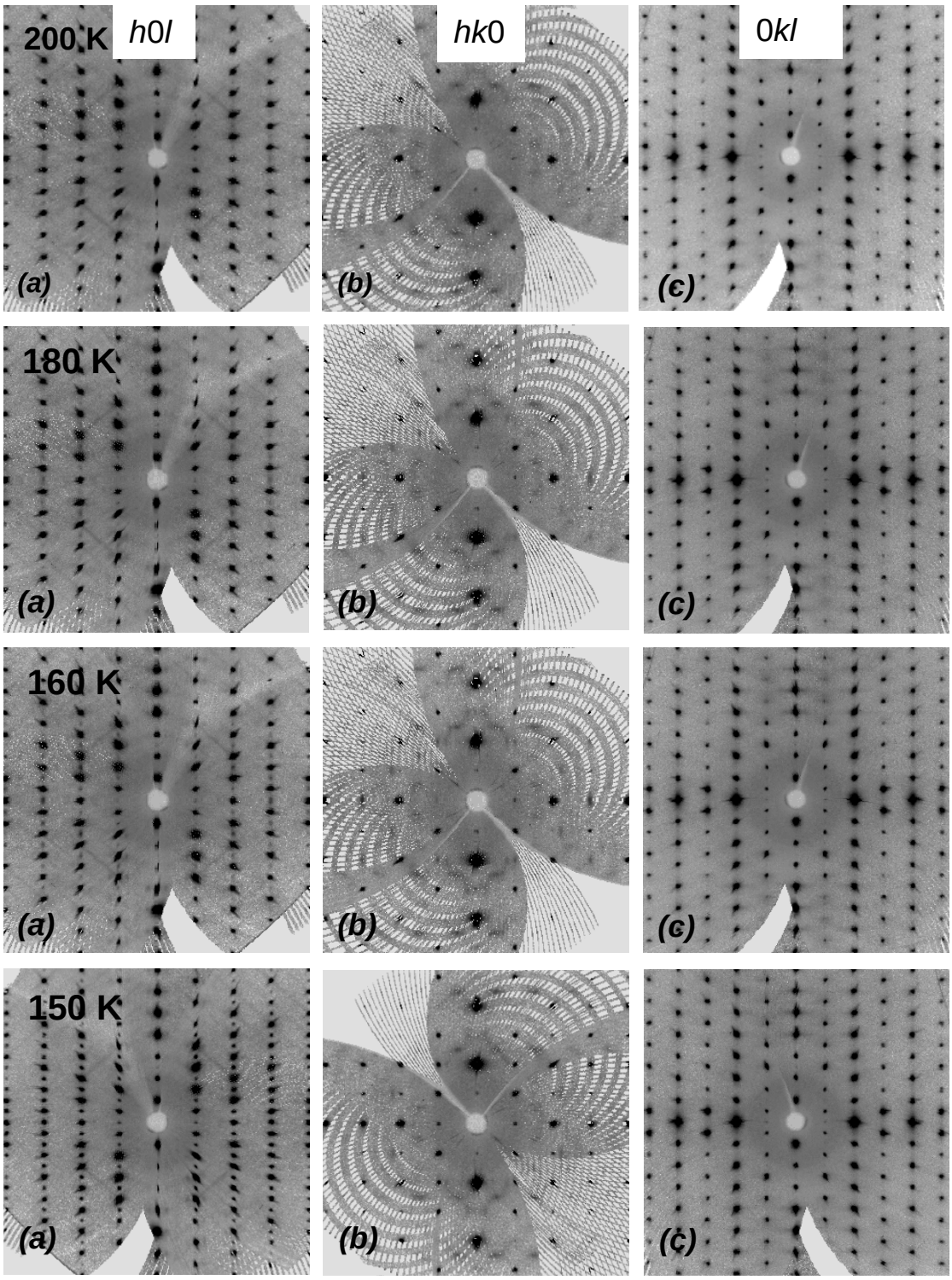

Figure G.1. Series of synthetic precession photographs of $[Ag(bipy)NO_3)]_n$. The cell at 140 K is a 180° rotation about **b** and 150 K data is a 180° rotation about **c*** relative to the other data sets.

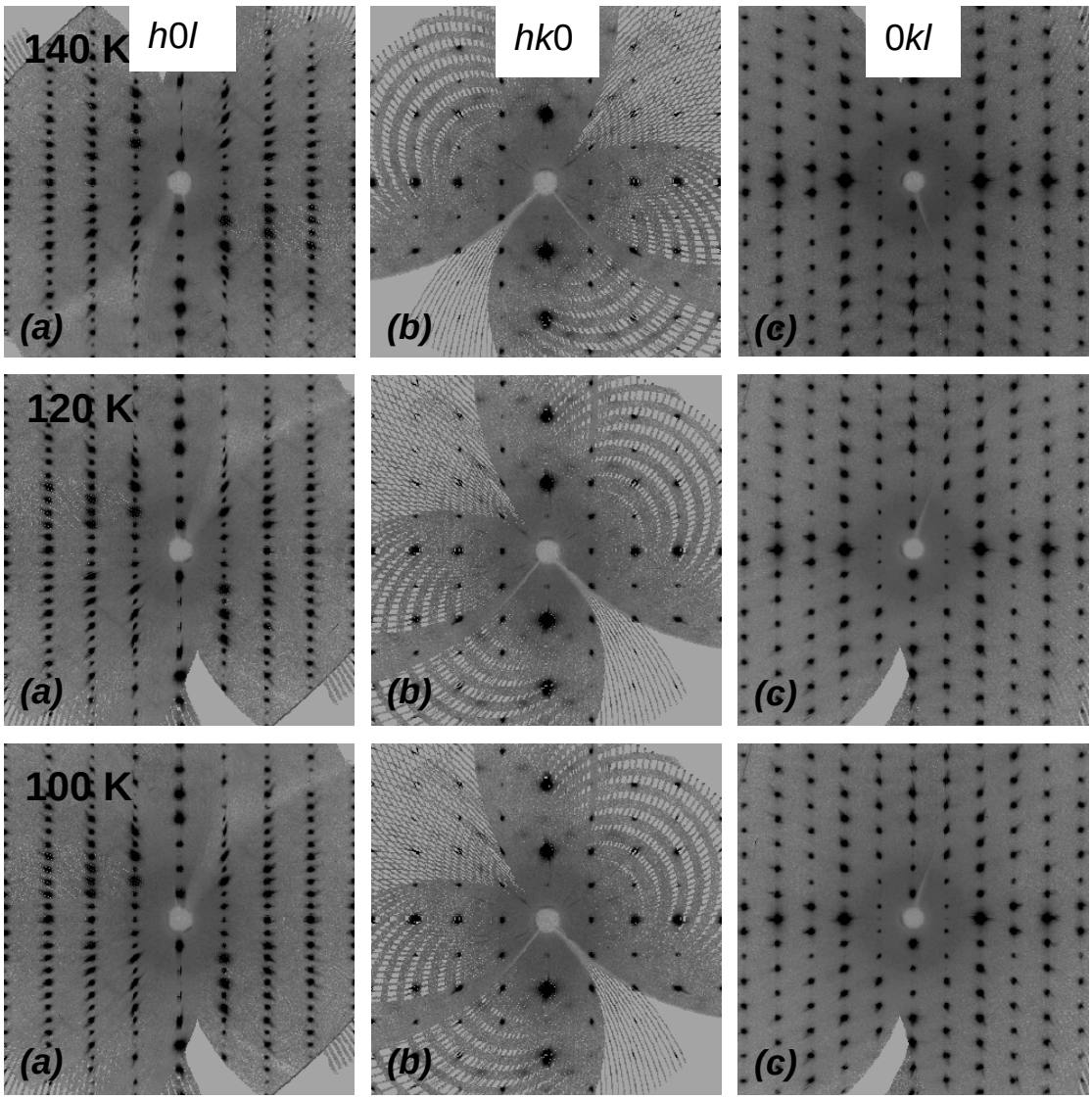

Figure G.1. (Continued).

```
##############################################################################
###    CIF submission form for molecular structure report (Acta Cryst. B)  ###
###                                          Version: 2.0.2  (6 July 1998)  ###
##############################################################################

#==============================================================================
data_global
#==============================================================================
# SUBMISSION DETAILS

_publ_contact_author_name            'Kenneth J. Haller'
_publ_contact_author_address
;
School of Chemistry
Institute of Science
Suranaree University of Technology
Nahkon Ratchasima 30000
Thailand
;
_publ_contact_author_email           'haller@ccs.sut.ac.th'
_publ_contact_author_fax             '+66-44-224-185'
_publ_contact_author_phone           '+66-44-224-303'

_publ_contact_letter
;
School of Chemistry
Institute of Science
Suranaree University of Technology
Nahkon Ratchasima 30000
Thailand
;

_publ_requested_journal              ?
_publ_requested_category             ?

#==============================================================================

# TITLE AND AUTHOR LIST

_publ_section_title
;
The Ordered-Disordered Phase Transition of Polymeric Ag(bipy)NO~3~
;
_publ_section_title_footnote
; ?
;

# The loop structure below should contain the names and addresses of all
# authors, in the required order of publication. Repeat as necessary.

loop_
          _publ_author_name
      _publ_author_footnote
          _publ_author_address
'Somphon, Weenawan'
; # footnote
;
;
School of Chemistry
Institute of Science
Suranaree University of Technology
Nahkon Ratchasima 30000
Thailand
;
'Haller, Kenneth J.'
; # footnote
;
;
School of Chemistry
Institute of Science
Suranaree University of Technology
Nahkon Ratchasima 30000
Thailand
;
'Rae A. David'
; # footnote
;
;
Research of Chemistry
The Australian National University
Canberra
ACT 0200
Australia
#==============================================================================

# If more than one structure is reported, the remaining sections should be
# completed per structure. For each data set, replace the '?' in the
# data_? line below by a unique identifier.

data_100K
#==============================================================================
# CHEMICAL DATA

_chemical_name_systematic
;
catena-((\m~2~-4,4'-Bipyridine)-silver(I) nitrate)
```

```
;
_chemical_name_common                ?
_chemical_formula_moiety             'C10 H8 Ag N2, N O3'
_chemical_formula_sum                'C10 H8 Ag N3 O3'
_chemical_formula_structural         ?
_chemical_formula_analytical         ?
_chemical_formula_iupac              ?
_chemical_formula_weight             326.062
_chemical_melting_point              ?

#==============================================================================

# CRYSTAL DATA

_symmetry_cell_setting               monoclinic
_symmetry_space_group_name_H-M       'C 2/c'
_symmetry_space_group_name_Hall      '-C 2yc'

loop_
        _symmetry_equiv_pos_as_xyz
       'x,y,z'
      '-x,y,1/2-z'
       '-x,-y,-z'
       'x,-y,1/2+z'
       '1/2+x,1/2+y,z'
       '1/2-x,1/2+y,1/2-z'
       '1/2-x,1/2-y,-z'
       '1/2+x,1/2-y,1/2+z'
_cell_length_a                       12.7506(14)
_cell_length_b                       9.8596(11)
_cell_length_c                       18.3794(21)
_cell_angle_alpha                    90
_cell_angle_beta                     109.980(7)
_cell_angle_gamma                    90
_cell_volume                         2171.5(4)
_cell_formula_units_Z                8
_cell_measurement_reflns_used        28278
_cell_measurement_theta_min          3.16
_cell_measurement_theta_max          27.49
_cell_measurement_temperature        100(1)

_exptl_crystal_description           block
_exptl_crystal_colour                colorless
_exptl_crystal_size_max              0.34
_exptl_crystal_size_mid              0.32
_exptl_crystal_size_min              0.30
_exptl_crystal_size_rad              ?
_exptl_crystal_density_diffrn        1.995
_exptl_crystal_density_meas          ?
_exptl_crystal_density_method        'not measured'
_exptl_crystal_F_000                 1280
_exptl_absorpt_coefficient_mu        1.86
_exptl_absorpt_correction_type       multi-scan
_exptl_absorpt_process_details       '(SORTAV; Blessing, 1995)'
_exptl_absorpt_correction_T_min      0.530
_exptl_absorpt_correction_T_max      0.570
#==============================================================================
# EXPERIMENTAL DATA

_exptl_special_details
;
Twinned monoclinic crystal. The intensity of each twin
pair of reflections was obtained as the sum of the two components
;
_diffrn_ambient_temperature          100(1)
_diffrn_radiation_type               MoK\a
_diffrn_radiation_wavelength         0.71073
_diffrn_radiation_source             'fine-focus sealed tube'

_diffrn_radiation_monochromator      graphite
_diffrn_measurement_device_type      'Nonius KappaCCD'
_diffrn_measurement_method           '\f scans, and \w scans with \k offsets'
_diffrn_detector_area_resol_mean     ?

_diffrn_reflns_number                28278
_diffrn_reflns_av_R_equivalents      0.039
_diffrn_reflns_av_sigmaI/netI        ?
_diffrn_reflns_theta_min             3.15
_diffrn_reflns_theta_max             27.49
_diffrn_reflns_theta_full            27.49
_diffrn_measured_fraction_theta_max  0.997
_diffrn_measured_fraction_theta_full 0.997
_diffrn_reflns_limit_h_min           -16
_diffrn_reflns_limit_h_max           16
_diffrn_reflns_limit_k_min           -11
_diffrn_reflns_limit_k_max           12
_diffrn_reflns_limit_l_min           -23
_diffrn_reflns_limit_l_max           23
_diffrn_reflns_reduction_process     ?

_diffrn_standards_number             ?
_diffrn_standards_interval_count     ?
_diffrn_standards_interval_time      ?
_diffrn_standards_decay_%            ?
loop_
        _diffrn_standard_refln_index_h
        _diffrn_standard_refln_index_k
```

```
        _diffrn_standard_refln_index_l
#===============================================================================
# REFINEMENT DATA

_refine_special_details
; ?
;
_reflns_number_total                2486
_reflns_number_gt                   2350
_reflns_threshold_expression        'I>3\s(I)'

_refine_ls_structure_factor_coef    F

_refine_ls_matrix_type              full
_refine_ls_R_factor_all             0.0238
_refine_ls_R_factor_gt              0.0207
_refine_ls_wR_factor_all            0.0320
_refine_ls_wR_factor_ref            0.0302
_refine_ls_goodness_of_fit_all      1.324
_refine_ls_goodness_of_fit_ref      1.289
_refine_ls_restrained_S_all         ?
_refine_ls_restrained_S_obs         ?
_refine_ls_number_reflns            2350
_refine_ls_number_parameters        84
_refine_ls_number_restraints        ?
_refine_ls_number_constraints       ?
_refine_ls_hydrogen_treatment       noref
_refine_ls_weighting_scheme         calc
_refine_ls_weighting_details
'calc w=1/(\s^2^(F)+0.0004F^2^)'
_refine_ls_shift/su_max             0.04
_refine_ls_shift/su_mean            ?
_refine_diff_density_max            0.650
_refine_diff_density_min            -0.429
_refine_ls_extinction_method        none
_refine_ls_extinction_coef          ?
_refine_ls_abs_structure_details    ?
_refine_ls_abs_structure_Flack      ?
_refine_ls_abs_structure_Rogers     ?

loop_
     _atom_type_symbol
     _atom_type_description
     _atom_type_scat_dispersion_real
     _atom_type_scat_dispersion_imag
     _atom_type_scat_source
    'C' 'C' 0.0033 0.0016
                        'International Tables Vol C Tables 4.2.6.8 and 6.1.1.4'
    'H' 'H' 0.0000 0.0000
                        'International Tables Vol C Tables 4.2.6.8 and 6.1.1.4'
    'N' 'N' 0.0061 0.0033
                        'International Tables Vol C Tables 4.2.6.8 and 6.1.1.4'
    'O' 'O' 0.0106 0.0060
                        'International Tables Vol C Tables 4.2.6.8 and 6.1.1.4'
    'Ag' 'Ag' -0.8971 1.1015
                        'International Tables Vol C Tables 4.2.6.8 and 6.1.1.4'
_computing_data_collection          'COLLECT (Nonius, 1998)'
_computing_cell_refinement          'DIRAX (Duisenberg, 1992)'
_computing_data_reduction           'EVAL14 (Duisenberg et al., 2003 )'
_computing_structure_solution       'SIR97 (Altomare et al., 1999)'
_computing_structure_refinement     'RAELS (Rae, 2000)'
_computing_molecular_graphics
         'ORTEP-III (Burnett & Johnson, 1996; Farrugia, 1997)'
_computing_publication_material      ?
#===============================================================================
# ATOMIC COORDINATES AND DISPLACEMENT PARAMETERS

loop_
_atom_site_label
_atom_site_fract_x
_atom_site_fract_y
_atom_site_fract_z
_atom_site_occupancy
_atom_site_U_iso_or_equiv
_atom_site_refinement_flags
_atom_site_thermal_displace_type
_atom_site_calc_flag
_atom_site_calc_attached_atom
Ag       0.12065(2)   0.35147(2)   0.26167(1)    1.0  0.0202(1) . Uani d ?
N1        0.1587(2)    0.4975(2)    0.3539(1)    1.0   0.018(1) . Uani d ?
C2        0.1977(2)    0.4640(2)    0.4289(1)    1.0   0.018(1) . Uani d ?
C3        0.2329(2)    0.5589(2)    0.4883(1)    1.0   0.017(1) . Uani d ?
C4        0.2288(2)    0.6968(2)    0.4695(1)    1.0   0.015(1) . Uani d ?
C5        0.1873(2)    0.7318(2)    0.3910(1)    1.0   0.018(1) . Uani d ?
C6        0.1528(2)    0.6300(2)    0.3355(2)    1.0   0.019(1) . Uani d ?
N1'       0.0639(2)    0.2157(2)    0.1645(1)    1.0   0.018(1) . Uani d ?
C2'       0.0284(2)    0.2660(2)    0.0928(1)    1.0   0.017(1) . Uani d ?
C3'       0.0006(2)    0.1862(2)    0.0264(1)    1.0   0.017(1) . Uani d ?
C4'       0.0113(2)    0.0452(2)    0.0347(1)    1.0   0.015(1) . Uani d ?
C5'       0.0479(2)   -0.0083(2)    0.1096(1)    1.0   0.019(1) . Uani d ?
C6'       0.0728(2)    0.0795(2)    0.1726(2)    1.0   0.021(1) . Uani d ?
N2        0.3192(2)    0.1018(2)    0.3518(2)    1.0   0.021(1) . Uani d ?
O1        0.2754(2)   -0.0081(2)    0.3237(1)    1.0   0.027(1) . Uani d ?
O2        0.4199(2)    0.1222(3)    0.3597(2)    1.0   0.039(1) . Uani d ?
O3        0.2652(2)    0.1888(3)    0.3724(2)    1.0   0.043(2) . Uani d ?
H2        0.2017       0.3657       0.4429       1.0   0.022    . Uani c ?
H3        0.2608       0.5291       0.5437       1.0   0.021    . Uani c ?
```

```
H5         0.1825       0.8292       0.3750       1.0   0.022    . Uani c ?
H6         0.1224       0.6564       0.2797       1.0   0.025    . Uani c ?
H2'        0.0213       0.3667       0.0863       1.0   0.020    . Uani c ?
H3'     -  0.0264       0.2288      -0.0261       1.0   0.020    . Uani c ?
H5'        0.0562      -0.1085       0.1179       1.0   0.022    . Uani c ?
H6'        0.0982       0.0403       0.2259       1.0   0.027    . Uani c ?

loop_
_atom_site_aniso_label
_atom_site_aniso_U_11
_atom_site_aniso_U_22
_atom_site_aniso_U_33
_atom_site_aniso_U_12
_atom_site_aniso_U_13
_atom_site_aniso_U_23
Ag        0.0177(1)  0.0235(1)  0.0185(1) -0.0029(1)  0.0048(1) -0.0138(1)
N1         0.016(1)   0.020(1)   0.018(1)  -0.002(1)   0.007(1)  -0.004(1)
C2         0.019(1)   0.017(1)   0.019(1)  -0.003(1)   0.008(1)  -0.002(1)
C3         0.020(1)   0.016(1)   0.016(1)  -0.002(1)   0.008(1)   0.000(1)
C4         0.016(1)   0.0164(4)  0.014(1)  -0.002(1)   0.007(1)   0.000(1)
C5         0.022(1)   0.0182(3)  0.014(1)  -0.001(1)   0.006(1)   0.000(1)
C6         0.022(1)   0.0208(5)  0.015(1)  -0.001(1)   0.006(1)  -0.002(1)
N1'        0.014(1)   0.020(1)   0.019(1)  -0.001(1)   0.004(0)  -0.011(1)
C2'        0.013(1)   0.017(1)   0.021(1)  -0.001(1)   0.004(1)  -0.010(1)
C3'        0.014(1)   0.016(1)   0.019(1)  -0.000(1)   0.004(1)  -0.009(1)
C4'        0.012(1)   0.016(1)   0.017(1)  -0.001(1)   0.004(1)  -0.008(1)
C5'        0.020(1)   0.017(1)   0.017(1)   0.000(1)   0.004(1)  -0.008(1)
C6'        0.023(1)   0.020(1)   0.017(1)  -0.001(1)   0.005(1)  -0.009(1)
N2         0.027(2)   0.015(1)   0.021(1)   0.004(1)   0.008(1)   0.002(1)
O1         0.039(3)   0.022(1)   0.022(1)  -0.006(1)   0.011(1)   0.000(1)
O2         0.033(2)   0.053(2)   0.033(1)  -0.014(1)   0.013(1)  -0.009(1)
O3         0.055(2)   0.037(2)   0.033(2)   0.024(1)   0.013(1)  -0.004(1)
H2         0.027      0.017      0.022     -0.003      0.010     -0.002
H3         0.030      0.017      0.017     -0.002      0.008      0.001
H5         0.031      0.019      0.014     -0.001      0.006      0.001
H6         0.033      0.024      0.015      0.000      0.005     -0.002
H2'        0.016      0.017      0.024      0.000      0.004     -0.011
H3'        0.023      0.016      0.020      0.000      0.004     -0.008
H5'        0.029      0.018      0.017      0.000      0.004     -0.007
H6'        0.038      0.024      0.017      0.000      0.005     -0.009
#===============================================================================
# MOLECULAR GEOMETRY

_geom_special_details
;
Weak noncovalent interactions to the C atoms of the bipyridine on the polymer
chains, C(\d^+^)...O(\d^-^) dipole-dipole interaction;
C6   O2  3.151(3)  .  5_455
C2'   O1   3.309(3)  .  6_555
;

 loop_
_geom_bond_atom_site_label_1
_geom_bond_atom_site_label_2
_geom_bond_distance
_geom_bond_site_symmetry_1
_geom_bond_site_symmetry_2
_geom_bond_publ_flag
Ag         Ag         2.9578(5)   . 2_555  yes
Ag         N1         2.150(1)    .  .  yes
Ag         N1'        2.150(1)    .  .  yes
Ag         O1         2.749(2)    . 6_555  yes
Ag         O3         2.747(2)    .  .  yes
N1         C2         1.337(3)    .  .  yes
N1         C6         1.345(3)    .  .  yes
C2         C3         1.391(3)    .  .  yes
C3         C4         1.400(3)    .  .  yes
C4         C4         1.496(4)    . 7_566  yes
C4         C5         1.399(3)    .  .  yes
C5         C6         1.391(3)    .  .  yes
N1'        C2'        1.334(3)    .  .  yes
N1'        C6'        1.351(3)    .  .  yes
C2'        C3'        1.391(3)    .  .  yes
C3'        C4'        1.400(3)    .  .  yes
C4'        C4'        1.501(4)    . 3_555  yes
C4'        C5'        1.397(3)    .  .  yes
C5'        C6'        1.393(3)    .  .  yes
N2         O1         1.246(3)    .  .  yes
N2         O2         1.258(4)    .  .  yes
N2         O3         1.238(3)    .  .  yes
C2        H2        1.00    .  .  no
C3        H3        1.00    .  .  no
C5        H5        1.00    .  .  no
C6        H6        1.00    .  .  no
C2'       H2'       1.00    .  .  no
C3'       H3'       1.00    .  .  no
C5'       H5'       1.00    .  .  no
C6'       H6'       1.00    .  .  no

loop_
_geom_angle_atom_site_label_1
_geom_angle_atom_site_label_2
_geom_angle_atom_site_label_3
_geom_angle
_geom_angle_site_symmetry_1
_geom_angle_site_symmetry_2
_geom_angle_site_symmetry_3
```

```
_geom_angle_publ_flag
Ag         Ag         N1          93.3(1)  2_555  .  .  yes
Ag         Ag         N1'         80.9(1)  2_555  .  .  yes
Ag         Ag         O1         126.7(0)  2_555  . 6_555  yes
Ag         Ag         O3         120.6(1)  2_555  .  .  yes
N1         Ag         N1'        173.4(1)   .  .  .  yes
N1         Ag         O1          95.2(1)   .  . 6_555  yes
N1         Ag         O3          83.9(1)   .  .  .  yes
N1'        Ag         O1          86.0(1)   .  . 6_555  yes
N1'        Ag         O3         101.7(1)   .  .  .  yes
O1         Ag         O3         112.6(1)  6_555  .  .  yes
Ag         N1         C2         123.5(2)   .  .  .  yes
Ag         N1         C6         118.3(2)   .  .  .  yes
C2         N1         C6         117.9(2)   .  .  .  yes
N1         C2         C3         123.4(2)   .  .  .  yes
C2         C3         C4         118.9(2)   .  .  .  yes
C3         C4         C4         121.5(2)   .  . 7_566  yes
C3         C4         C5         117.7(2)   .  .  .  yes
C4         C4         C5         120.8(2)  7_566  .  .  yes
C4         C5         C6         119.4(2)   .  .  .  yes
N1         C6         C5         122.7(2)   .  .  .  yes
Ag         N1'        C2'        119.6(1)   .  .  .  yes
Ag         N1'        C6'        122.4(1)   .  .  .  yes
C2'        N1'        C6'        117.8(2)   .  .  .  yes
N1'        C2'        C3'        123.6(2)   .  .  .  yes
C2'        C3'        C4'        118.7(2)   .  .  .  yes
C3'        C4'        C4'        121.0(2)   .  . 3_555  yes
C3'        C4'        C5'        118.0(2)   .  .  .  yes
C4'        C4'        C5'        121.0(2)  3_555  .  .  yes
C4'        C5'        C6'        119.2(2)   .  .  .  yes
N1'        C6'        C5'        122.7(2)   .  .  .  yes
O1         N2         O2         118.8(2)   .  .  .  yes
O1         N2         O3         120.8(3)   .  .  .  yes
O2         N2         O3         120.4(3)   .  .  .  yes
N1        C2        H2        118.24   .  .  .  no
C3        C2        H2        118.42  .  .  .  no
C2        C3        H3        120.55 .  .  .  no
C4        C3        H3        120.44   .  .  .  no
C4        C5        H5        120.23  .  .  .  no
C6        C5        H5        120.33 .  .  .  no
C5        C6        H6        118.64   .  .  .  no
N1        C6        H6        118.68  .  .  .  no
N1'       C2'       H2'       118.24   .  .  .  no
C3'       C2'       H2'       118.07  .  .  .  no
C2'       C3'       H3'       120.62 .  .  .  no
C4'       C3'       H3'       120.73   .  .  .  no
C4'       C5'       H5'       120.38  .  .  .  no
C6'       C5'       H5'       120.34 .  .  .  no
C5'       C6'       H6'       118.71   .  .  .  no
N1'       C6'       H6'       118.65  .  .  .  no

 loop_
_geom_hbond_atom_site_label_D
_geom_hbond_atom_site_label_H
_geom_hbond_atom_site_label_A
_geom_hbond_site_symmetry_D
_geom_hbond_site_symmetry_H
_geom_hbond_site_symmetry_A
_geom_hbond_distance_DH
_geom_hbond_distance_HA
_geom_hbond_distance_DA
_geom_hbond_angle_DHA
C3 H3 O1 . . 7_556 1.00 2.64 3.529(3) 148.1
C5 H5 O1 . . 1_565 1.00 2.37 3.212(3) 141.0
C6' H6' O1 . . . 1.00 2.41 3.198(3) 135.6
C6 H6 O2 . . 6_555 1.00 2.45 3.386(3) 154.9
C3' H3' O2 . . 8_454 1.00 2.46 3.444(3) 168.1
C2 H2 O3 . . . 1.00 2.47 3.130(3) 123.2

data_200K
#==============================================================================
# CHEMICAL DATA

_chemical_name_systematic
;
catena-((\m~2~-4,4'-Bipyridine)-silver(I) nitrate)
;
_chemical_name_common                 ?
_chemical_formula_moiety              'C10 H8 Ag N2, N O3'
_chemical_formula_sum                 'C10 H8 Ag N3 O3'
_chemical_formula_structural          ?
_chemical_formula_analytical          ?
_chemical_formula_iupac               ?
_chemical_formula_weight              326.062
_chemical_melting_point               ?

#==============================================================================

# CRYSTAL DATA

_symmetry_cell_setting                orthorhombic
_symmetry_space_group_name_H-M        'F d d d'
_symmetry_space_group_name_Hall       '-F 2uv 2vw'

    loop_
        _symmetry_equiv_pos_as_xyz
       'x,y,z'
```

```
       'x,1/4-y,1/4-z'
       '1/4-x,y,1/4-z'
       '1/4-x,1/4-y,z'
       '-x,-y,-z'
       '-x,1/4+y,1/4+z'
       '1/4+x,-y,1/4+z'
       '1/4+x,1/4+y,-z'
       'x,1/2+y,1/2+z'
       'x,3/4-y,3/4-z'
       '1/4-x,1/2+y,3/4-z'
       '1/4-x,3/4-y,1/2+z'
       '-x,1/2-y,1/2-z'
       '-x,3/4+y,3/4+z'
       '1/4+x,1/2-y,3/4+z'
       '1/4+x,3/4+y,1/2-z'
       '1/2+x,y,1/2+z'
       '1/2+x,1/4-y,3/4-z'
       '3/4-x,y,3/4-z'
       '3/4-x,1/4-y,1/2+z'
       '1/2-x,-y,1/2-z'
       '1/2-x,1/4+y,3/4+z'
       '3/4+x,-y,3/4+z'
       '3/4+x,1/4+y,1/2-z'
       '1/2+x,1/2+y,z'
       '1/2+x,3/4-y,1/4-z'
       '3/4-x,1/2+y,1/4-z'
       '3/4-x,3/4-y,z'
       '1/2-x,1/2-y,-z'
       '1/2-x,3/4+y,1/4+z'
       '3/4+x,1/2-y,1/4+z'
       '3/4+x,3/4+y,-z'
_cell_length_a                      12.8226(4)
_cell_length_b                      9.9373(3)
_cell_length_c                      34.4498(10)
_cell_angle_alpha                   90
_cell_angle_beta                    90
_cell_angle_gamma                   90
_cell_volume                        4389.7(2)
_cell_formula_units_Z               16
_cell_measurement_reflns_used       14031
_cell_measurement_theta_min         3.15
_cell_measurement_theta_max         27.49
_cell_measurement_temperature       200(1)

_exptl_crystal_description          block
_exptl_crystal_colour               colorless
_exptl_crystal_size_max             0.34
_exptl_crystal_size_mid             0.32
_exptl_crystal_size_min             0.30
_exptl_crystal_size_rad             ?
_exptl_crystal_density_diffrn       1.974
_exptl_crystal_density_meas        ?
_exptl_crystal_density_method       'not measured'
_exptl_crystal_F_000                2560
_exptl_absorpt_coefficient_mu       1.84
_exptl_absorpt_correction_type      multi-scan
_exptl_absorpt_process_details      '(SORTAV; Blessing, 1995)'
_exptl_absorpt_correction_T_min     0.530
_exptl_absorpt_correction_T_max     0.570
#==============================================================================
# EXPERIMENTAL DATA

_exptl_special_details
;
Crystal twinned to appear monoclinic.
;

_diffrn_ambient_temperature         200(1)
_diffrn_radiation_type              MoK\a
_diffrn_radiation_wavelength        0.71073
_diffrn_radiation_source            'fine-focus sealed tube'

_diffrn_radiation_monochromator     graphite
_diffrn_measurement_device_type     'KappaCCD'
_diffrn_measurement_method          'CCD'
_diffrn_detector_area_resol_mean    ?

_diffrn_reflns_number               14031
_diffrn_reflns_av_R_equivalents     0.048
_diffrn_reflns_av_sigmaI/netI       ?
_diffrn_reflns_theta_min            3.15
_diffrn_reflns_theta_max            27.49
_diffrn_reflns_theta_full           27.49
_diffrn_measured_fraction_theta_max 0.999
_diffrn_measured_fraction_theta_full 0.999
_diffrn_reflns_limit_h_min          -16
_diffrn_reflns_limit_h_max          16
_diffrn_reflns_limit_k_min          -11
_diffrn_reflns_limit_k_max          12
_diffrn_reflns_limit_l_min          -44
_diffrn_reflns_limit_l_max          43
_diffrn_reflns_reduction_process    ?

_diffrn_standards_number            ?
_diffrn_standards_interval_count    ?
_diffrn_standards_interval_time     ?
_diffrn_standards_decay_%           ?
```

```
loop_
        _diffrn_standard_refln_index_h
        _diffrn_standard_refln_index_k
        _diffrn_standard_refln_index_l
#===============================================================================
# REFINEMENT DATA

_refine_special_details
;
An additional parameterization of the Ag atom as an isolated anisotropic atom
constrained by its site symmetry was therefore included. The NO~3~^-^ ion was
refined using a TLX model with only two principal libration axes nonzero
;

_reflns_number_total                1270
_reflns_number_gt                   1004
_reflns_threshold_expression        'I>3\s(I)'

_refine_ls_structure_factor_coef    F

_refine_ls_matrix_type              full
_refine_ls_R_factor_all             0.0442
_refine_ls_R_factor_gt              0.0280
_refine_ls_wR_factor_all            0.0663
_refine_ls_wR_factor_ref            0.0468
_refine_ls_goodness_of_fit_all      1.666
_refine_ls_goodness_of_fit_ref      1.316
_refine_ls_restrained_S_all         ?
_refine_ls_restrained_S_obs         ?
_refine_ls_number_reflns            1004
_refine_ls_number_parameters        63
_refine_ls_number_restraints        ?
_refine_ls_number_constraints       ?
_refine_ls_hydrogen_treatment       noref
_refine_ls_weighting_scheme         calc
_refine_ls_weighting_details
'calc w=1/(\s^2^(F)+0.0009F^2^)'
_refine_ls_shift/su_max             0.04
_refine_ls_shift/su_mean            ?
_refine_diff_density_max            0.502
_refine_diff_density_min            -0.429
_refine_ls_extinction_method        none
_refine_ls_extinction_coef          ?
_refine_ls_abs_structure_details    ?
_refine_ls_abs_structure_Flack      ?
_refine_ls_abs_structure_Rogers     ?

 loop_
    _atom_type_symbol
    _atom_type_description
    _atom_type_scat_dispersion_real
    _atom_type_scat_dispersion_imag
    _atom_type_scat_source
   'C' 'C' 0.0033 0.0016
                        'International Tables Vol C Tables 4.2.6.8 and 6.1.1.4'
   'H' 'H' 0.0000 0.0000
                        'International Tables Vol C Tables 4.2.6.8 and 6.1.1.4'
   'N' 'N' 0.0061 0.0033
                        'International Tables Vol C Tables 4.2.6.8 and 6.1.1.4'
   'O' 'O' 0.0106 0.0060
                        'International Tables Vol C Tables 4.2.6.8 and 6.1.1.4'
   'Ag' 'Ag' -0.8971 1.1015
                        'International Tables Vol C Tables 4.2.6.8 and 6.1.1.4'
_computing_data_collection          'COLLECT (Nonius, 1998)'
_computing_cell_refinement          'DIRAX (Duisenberg, 1992)'
_computing_data_reduction           'EVAL14 (Duisenberg et al., 2003)'
_computing_structure_solution       'SIR97 (Altomare et al., 1999)'
_computing_structure_refinement     'RAELS (Rae, 2000)'
_computing_molecular_graphics
         'ORTEP-III (Burnett & Johnson, 1996; Farrugia, 1997)'
_computing_publication_material     '?'
#===============================================================================
# ATOMIC COORDINATES AND DISPLACEMENT PARAMETERS

loop_
_atom_site_label
_atom_site_fract_x
_atom_site_fract_y
_atom_site_fract_z
_atom_site_occupancy
_atom_site_U_iso_or_equiv
_atom_site_refinement_flags
_atom_site_thermal_displace_type
_atom_site_calc_flag
_atom_site_calc_attached_atom
Ag         0.0103(1)    0.1344(2)    0.1273(1)    0.5  0.040(1) . Uani d ?
N1         0.0199(6)   -0.0067(4)    0.1747(1)    0.5  0.029(1) . Uani d ?
C2         0.0188(7)    0.0301(4)    0.2121(1)    0.5  0.031(1) . Uani d ?
C3         0.0112(6)   -0.0605(3)    0.2425(1)    0.5  0.031(1) . Uani d ?
C4         0.0042(1)   -0.1992(2)    0.2341(1)    0.5  0.026(1) . Uani d ?
C5         0.0054(5)   -0.2362(4)    0.1953(1)    0.5  0.032(1) . Uani d ?
C6         0.0133(6)   -0.1381(4)    0.1666(1)    0.5  0.034(1) . Uani d ?
N1'        0.0211(6)    0.2762(4)    0.0802(1)    0.5  0.030(1) . Uani d ?
C2'        0.0165(7)    0.2300(4)    0.0437(1)    0.5  0.030(1) . Uani d ?
C3'        0.0082(6)    0.3126(3)    0.0115(1)    0.5  0.030(1) . Uani d ?
C4'        0.0044(1)    0.4533(2)    0.0169(1)    0.5  0.026(1) . Uani d ?
C5'        0.0093(5)    0.5002(4)    0.0548(1)    0.5  0.033(1) . Uani d ?
```

```
C6'        0.0175(6)    0.4096(4)    0.0854(1)    0.5  0.036(1) . Uani d ?
N2        -0.1375(5)    0.3890(6)    0.1748(1)    0.5  0.034(3) . Uani d ?
O1        -0.1001(5)    0.4942(6)    0.1637(2)    0.5  0.053(2) . Uani d ?
O2        -0.2322(5)    0.3778(6)    0.1793(2)    0.5  0.060(4) . Uani d ?
O3        -0.0813(8)    0.2905(9)    0.1820(2)    0.5  0.102(5) . Uani d ?
H2       0.0238       0.1281       0.2184       0.5  0.039    . Uani c ?
H3       0.0107      -0.0281       0.2700       0.5  0.040    . Uani c ?
H5       0.0006      -0.3334       0.1879       0.5  0.041    . Uani c ?
H6       0.0140      -0.1671       0.1388       0.5  0.045    . Uani c ?
H2'      0.0191       0.1305       0.0395       0.5  0.036    . Uani c ?
H3'      0.0051       0.2732      -0.0152       0.5  0.038    . Uani c ?
H5'      0.0068       0.5991       0.0601       0.5  0.042    . Uani c ?
H6'      0.0209       0.4456       0.1125       0.5  0.048    . Uani c ?

loop_
_atom_site_aniso_label
_atom_site_aniso_U_11
_atom_site_aniso_U_22
_atom_site_aniso_U_33
_atom_site_aniso_U_12
_atom_site_aniso_U_13
_atom_site_aniso_U_23
Ag         0.043(1)   0.042(1)   0.036(1)   0.007(1)   0.006(1)   0.024(1)
N1         0.035(1)   0.030(1)   0.022(1)  -0.002(1)  -0.002(1)   0.008(1)
C2         0.041(1)   0.030(1)   0.022(1)  -0.004(1)  -0.005(1)   0.008(1)
C3         0.041(1)   0.030(1)   0.021(1)  -0.004(1)  -0.005(1)   0.007(1)
C4         0.028(1)   0.030(1)   0.021(1)  -0.003(1)  -0.004(1)   0.007(1)
C5         0.045(1)   0.030(1)   0.021(1)  -0.002(1)  -0.003(1)   0.007(1)
C6         0.050(1)   0.030(1)   0.021(1)   0.000(1)  -0.002(1)   0.008(1)
N1'        0.030(1)   0.025(1)   0.034(1)   0.001(1)   0.003(1)   0.009(1)
C2'        0.030(1)   0.025(1)   0.034(1)   0.004(1)   0.005(1)   0.009(1)
C3'        0.031(1)   0.024(1)   0.034(1)   0.004(1)   0.006(1)   0.008(1)
C4'        0.021(1)   0.024(1)   0.034(1)   0.003(1)   0.005(1)   0.008(1)
C5'        0.040(1)   0.024(1)   0.034(1)   0.002(1)   0.004(1)   0.009(1)
C6'        0.048(2)   0.025(1)   0.034(1)   0.000(1)   0.002(1)   0.009(1)
N2         0.050(6)   0.030(3)   0.023(2)   0.012(2)  -0.002(2)   0.002(2)
O1         0.073(6)   0.048(3)   0.038(3)  -0.013(2)   0.002(2)   0.002(2)
O2         0.052(5)   0.071(3)   0.059(4)  -0.006(2)  -0.005(3)   0.015(2)
O3         0.117(8)   0.088(4)   0.103(6)   0.073(5)   0.035(5)   0.048(5)
H2         0.064      0.030      0.022     -0.006     -0.007      0.008
H3         0.067      0.030      0.021     -0.005     -0.006      0.007
H5         0.073      0.030      0.021     -0.002     -0.004      0.007
H6         0.083      0.030      0.021      0.002     -0.001      0.008
H2'        0.049      0.025      0.035      0.006      0.007      0.009
H3'        0.057      0.024      0.034      0.004      0.006      0.008
H5'        0.068      0.024      0.034      0.002      0.004      0.008
H6'        0.086      0.025      0.034     -0.003      0.000      0.009
#===============================================================================
# MOLECULAR GEOMETRY

_geom_special_details               ?

loop_
_geom_bond_atom_site_label_1
_geom_bond_atom_site_label_2
_geom_bond_distance
_geom_bond_site_symmetry_1
_geom_bond_site_symmetry_2
_geom_bond_publ_flag
Ag         Ag         2.946(1)   . 3_555  yes
Ag         N1         2.154(3)   .  .  yes
Ag         N1'        2.155(3)   .  .  yes
Ag         O1         2.855(6)   . 27_445  yes
Ag         O3         2.708(7)   .  .  yes
Ag         O1         2.691(6)   . 28_455  yes
Ag         O2         2.987(6)   . 28_455  yes
Ag         O3         2.928(7)   . 2_555  yes
N1         C2         1.340(4)   .  .  yes
N1         C6         1.338(5)   .  .  yes
C2         C3         1.384(4)   .  .  yes
C3         C4         1.410(4)   .  .  yes
C4         C4         1.492(6)   . 13_545  yes
C4         C5         1.388(4)   .  .  yes
C5         C6         1.392(5)   .  .  yes
N1'        C2'        1.340(4)   .  .  yes
N1'        C6'        1.338(5)   .  .  yes
C2'        C3'        1.384(4)   .  .  yes
C3'        C4'        1.410(4)   .  .  yes
C4'        C4'        1.492(6)   . 5_565  yes
C4'        C5'        1.388(4)   .  .  yes
C5'        C6'        1.392(5)   .  .  yes
N2         O1         1.212(8)   .  .  yes
N2         O2         1.229(9)   .  .  yes
N2         O3         1.240(9)   .  .  yes
C2        H2        1.00   .  .  no
C3        H3        1.00   .  .  no
C5        H5        1.00   .  .  no
C6        H6        1.00   .  .  no
C2'       H2'       1.00   .  .  no
C3'       H3'       1.00   .  .  no
C5'       H5'       1.00   .  .  no
C6'       H6'       1.00   .  .  no

loop_
_geom_angle_atom_site_label_1
_geom_angle_atom_site_label_2
_geom_angle_atom_site_label_3
```

```
_geom_angle
_geom_angle_site_symmetry_1
_geom_angle_site_symmetry_2
_geom_angle_site_symmetry_3
_geom_angle_publ_flag
Ag         Ag         N1          89.1(2)  3_555  .  .  yes
Ag         Ag         N1'         84.0(2)  3_555  .  .  yes
Ag         Ag         O1         133.7(1)  3_555  . 27_445  yes
Ag         Ag         O3         118.1(3)  3_555  .  .  yes
N1         Ag         N1'        173.0(1)   .  .  .  yes
N1         Ag         O1          95.6(2)   .  . 27_445  yes
N1         Ag         O3          82.6(2)   .  .  .  yes
N1         Ag         O3          99.5(2)   .  . 2_555  yes
N1'        Ag         O1          89.6(2)   .  . 27_445  yes
N1'        Ag         O3         100.2(2)   .  .  .  yes
O1         Ag         O3         108.2(3)  27_445  .  .  yes
Ag         N1         C2         123.4(2)   .  .  .  yes
Ag         N1         C6         118.3(3)   .  .  .  yes
C2         N1         C6         117.7(3)   .  .  .  yes
N1         C2         C3         123.5(3)   .  .  .  yes
C2         C3         C4         119.1(3)   .  .  .  yes
C3         C4         C4         121.1(2)   .  . 13_545  yes
C3         C4         C5         117.1(3)   .  .  .  yes
C4         C4         C5         121.8(2)  13_545  .  .  yes
C4         C5         C6         119.9(3)   .  .  .  yes
N1         C6         C5         122.8(3)   .  .  .  yes
Ag         N1'        C2'        118.7(3)   .  .  .  yes
Ag         N1'        C6'        123.0(3)   .  .  .  yes
C2'        N1'        C6'        117.7(3)   .  .  .  yes
N1'        C2'        C3'        123.5(3)   .  .  .  yes
C2'        C3'        C4'        119.1(3)   .  .  .  yes
C3'        C4'        C4'        121.1(2)   .  . 5_565  yes
C3'        C4'        C5'        117.1(3)   .  .  .  yes
C4'        C4'        C5'        121.8(2)  5_565  .  .  yes
C4'        C5'        C6'        119.9(3)   .  .  .  yes
N1'        C6'        C5'        122.8(3)   .  .  .  yes
O1         N2         O2         120.5(6)   .  .  .  yes
O1         N2         O3         120.9(8)   .  .  .  yes
O2         N2         O3         118.6(7)   .  .  .  yes
N1        C2        H2        118.30   .  .  .  no
C3        C2        H2        118.28   .  .  .  no
C2        C3        H3        120.49   .  .  .  no
C4        C3        H3        120.53   .  .  .  no
C4        C5        H5        120.05   .  .  .  no
C6        C5        H5        119.96   .  .  .  no
C5        C6        H6        118.62   .  .  .  no
N1        C6        H6        118.71   .  .  .  no
N1'       C2'       H2'       118.24   .  .  .  no
C3'       C2'       H2'       118.23   .  .  .  no
C2'       C3'       H3'       120.52   .  .  .  no
C4'       C3'       H3'       120.50   .  .  .  no
C4'       C5'       H5'       120.02   .  .  .  no
C6'       C5'       H5'       120.02   .  .  .  no
C5'       C6'       H6'       118.63   .  .  .  no
N1'       C6'       H6'       118.52   .  .  .  no
```

APPENDIX H

SUBMITTED ABSTRACTS AND PRESENTATIONS

International Presentation:

1. Somphon, W., Haller, K. J., and Rae, A. D. (2004). The Order-Disorder Transition at 150 of Polymeric $Ag(bipy)NO_3$. The Sixth Conference of the Asian Crystallographic Association (AsCA'04), Hong Kong, China, 27-30 June 2004.

2. Somphon, W. and Haller, K. J. (2003). Supramolecular Structure of $[Cd_2(bpa)_3(NO_3)_4]_n$, bpa = 1,2-bis(4-bipyridyl)ethane. 10^{th} Asian Chemical Congress (10-ACC), Hanoi, Vietnam, 21-24 October 2003.

3. Somphon, W., Haller, K. J., and Ng, S. W. (2002) Supramolecular Structure of 1,10-Phenanthrolin-1-ium Cation with A Tin(IV) Anion. XIXth Congress and Assembly of International Union of Crystallography, Geneva, Switzerland, 6-15 August 2002.

4. Somphon, W., Haller, K. J., and Rae, A. D. (2001). The Multiply Twinned Modulated Structure of Triethyl Phosphine Sulfide. IV Meeting of Asian Crystallographic Association (AsCa'01), Bangalore, India, 18-20 November 2001.

5. Haller, K. J., Somphon, W., Rae, A. D., and Williams, I. D. (2001). The Modulated Structure of Copper-(4,4'-Bipyridyl)-Sulfate Coordination Polymer Cocrystallised with Teraphthalic acid. IV Meeting of Asian Crystallographic Association (AsCa'01), Bangalore, India, 18-20 November 2001.

National Presentation:

1. Somphon, W. and Haller, K. J. (2004). Isomorphism and Twinning in $[M(H_2O)_6]I_2.2(HMT).4H_2O$; M = Ni^{2+}, Mn^{2+} and HMT = Hexamethylenetetramine. The 4th National Symposium on Graduate Research, Chaing Mai, Thailand, 10-11 August, 2004.

2. Somphon, W., Haller, K. J., and Rae, A. D. (2004). The Ordered Twin to Disordered Phase Transition in Modulated $[Ag(bipy)NO_3]_n$. RGJ-Ph.D. Congress V, ChonBuri, Thailand, 23-25 April 2004.

3. Somphon, W., Haller, K. J., Rae, A. D., and Williams, I. D. (2002). The Commensurately Modulated Structure of Copper-(4,4'-Bipyridyl)-Sulfate Coordination Polymer Cocrystallised with Teraphthalic acid. The 28th Congress on Science and Technology of Thailand, Bangkok, Thailand, 24-26 October 2002.

4. Somphon, W. and Haller, K. J. (2002). Recognizing and Modeling Problems in Nonroutine X-Ray Crystal Structures. The3rd National Symposium on Graduate Research, Nakhon Ratchasima, Thailand, 18-19 July 2002.

5. Somphon, W. and Haller, K. J. (2002). Redetermination of Triethyl Phosphine Sulfide: A Commensurately Modulated Structure. RGJ-Ph.D. Congress III, Chonburi, Thailand, 25-27 April 2002.

6. Somphon, W. and Haller, K. J. (2001). X-Ray Structure of the 1,10-Phenanthrolin-1-ium in a Supramolecular Structure. RGJ-Ph.D. Congress II, Chonburi, Thailand, 20-22 April 2001.

7. Somphon, W. and Haller, K. J. (2000). Crystal Structure of a 1:1 Tin Complex Phenanthroline System. The 26th Congress on Science and Technology of Thailand, Bangkok, Thailand, 18-20 October 2000.

CURRICULUM VITAE

WEENAWAN SOMPHON

Citizenship: Thai

Marital Status: Single

Date of Birth: April, 2 1974, Chanthaburi, THAILAND

EDUCATION:

1995-1998 B.Sc., Chemistry, Ramkhamhaeng University, Bangkok, Thailand

SCHOLARSHIPS, GRANTS, AWARDS, PRIZES:

Scholarship: The Royal Golden Jubilee Scholarship, Ph.D. (Thailand).

Grant : The Basic Research Grant (Thailand).

Awards : 1) Young Scientist Financial Support Award from Asian Crystallographic Association Meeting, AsCA'01 at Bangalore, India (2001).

2) A student Bursary Award from the XIX IUCr Congress and Assembly of International Union of Crystallography (2002).

3) Young Scientist Financial Support Award from Asian Crystallographic Association Meeting, AsCA'04 at Hong Kong, China (2004).

Prize: The Oxford Cryosystems Low Temperature Prize from Asian Crystallographic Association Meeting, AsCA'04 at Hong Kong, China.

PUBLICATIONS:

1. Somphon, W., Haller, K. J., and Ng, S. W. (2002). Supramolecular Structure of 1,10-Phenanthrolin-1-ium Cation with A Tin(IV) Anion. *Acta Cryst.* A**58**, C314.